FLOWERING REGULATORS AND INTERCELLULAR SA CONTRIBUTE TO ARR

FLOWERING-TIME REGULATORS AND INTERCELLULAR SALICYLIC ACID CONTRIBUTE TO AGE-RELATED RESISTANCE IN *ARABIDOPSIS THALIANA*

By DANIEL CULLEN WILSON, B.Sc.

A Thesis Submitted to the School of Graduate Studies in Partial Fulfilment of the Requirements for the Degree Doctor of Philosophy

McMaster University DOCTOR OF PHILOSOPHY (2017) Hamilton, Ontario (Biology)

TITLE: Flowering-time regulators and intercellular salicylic acid contribute to age-related resistance in *Arabidopsis thaliana*

AUTHOR: Daniel C. Wilson, B.Sc. (McMaster University)

SUPERVISOR: Dr. Robin K. Cameron

NUMBER OF PAGES: xvi, 171

Abstract

Some plants become more resistant to pathogens as they age, a phenomenon known as Age-Related-Resistance (ARR). In this thesis, the *Arabidopsis thaliana*-*Pseudomonas syringae* pathosystem was used to explore: i) the association between ARR and the transition to flowering, and ii) the idea that salicylic acid (SA) acts directly on pathogens in the intercellular space during ARR. The ARR phenotypes of flowering-time mutants and wild-type plants induced to flower early by transient exposure to long days suggest that flowering is neither required nor sufficient for ARR, and is not the developmental cue for ARR. Two MADS-domain transcription factors were identified that appear to play distinct roles in the regulation of flowering time and ARR. Specifically, SVP (SHORT VEGETATIVE PHASE) is required for ARR and contributes to intercellular SA accumulation, a key aspect of ARR. Mutant and overexpression analyses suggest that the role of SVP during ARR is to repress SOC1 (SUPPRESSOR OF OVEREXPRESSION OF CO 1), which contributes negatively to ARR, upstream of intercellular SA accumulation. Assessing the in vitro antimicrobial activity of SA under biologically relevant conditions, and estimating the concentration of intercellular SA during ARR, provided convincing evidence that SA acts as an antimicrobial agent in the intercellular space during ARR. Moreover, the results of in vitro biofilm assays and biofilm visualization in the intercellular space suggest that SA also plays a role in reducing *P. syringae* biofilm formation during ARR. Lastly, I present evidence that intercellular SA also plays a role during pattern- and effector-

triggered immunity in young plants. Altogether this work highlights the complex interplay between disease resistance and development, and reveals the potential for direct effects of SA on phytopathogens in vivo. This fundamental knowledge will be useful for the management of existing crops and the development of new disease-resistant varieties.

Acknowledgements

Many thanks to my supervisor Dr. Robin Cameron for the years of mentorship and providing an environment that challenged me to improve as a researcher without forgetting all the other things in life. Also for motivating me (by example) to bike to work every day, even in the most inclement of weather – you are one of the toughest people I know.

Thanks to my committee members for providing constructive criticism and support. Especially Dr. Elizabeth Weretilnyk for her insightful comments and sense of humor, and Dr. David Liscombe for his infectious enthusiasm and words of encouragement. For research collaboration, thanks to Drs. Elizabeth Weretilnyk and Brian Golding for working with us on the whole-genome sequencing project, and Dr. David Liscombe for hosting and helping me in his lab at Vineland.

Thanks to all the members of the Cameron lab, whom I spent so much time with that they eventually started to feel like some kind of weird second family. This was especially true of Marisa, May, Phil, and Marc - you all brought something unique to the group and made the lab an interesting and fun place. Later on Christine provided much-appreciated companionship, both in the lab and in the garden, although she didn't make for a very challenging backgammon opponent ... we'll keep working on that!

My friends and family deserve huge thanks for all their encouragement and support over the years, especially my Mom, who didn't call me once for fear of bothering me, but would talk for hours any time I got around to calling her. Brian who made a great squash and disc-golf opponent, and an even better award-winning co-brewer. Billie, who was a caring friend and tolerated our brewing operation and other exploits. And Braden, whose visits to Hamilton (and mine to Newcastle) were too few, but always looked forward to.

Sarah comes last but not least. In the interest of brevity, suffice it to say that she is the best companion I could have hoped for throughout all these years, which stretch back even further than my time here at McMaster. I love you Sarah, and could never thank you enough for all that you have done for me.

Table of contents

List of figures

List of tables

Abbreviations

µM	micromolar
µm	micrometer
µl	microliter
AHL	*N*-acyl homoserine lactone
ANOVA	analysis of variance
AP1	apetala 1
ARR	age-related resistance
Avr	avirulence
BAK1	BRI1-associated receptor kinase
BLAST	basic local alignment search tool
BSMT1	benzoic acid/salicylic acid carboxyl methyltransferase
CBF	CRT/DRE-binding factors
CBP60g	calmodulin-binding protein 60 g
CDPK	calcium-dependent protein kinase
CFU	colony-forming units
ChIP	chromatin immunoprecipitation
CO	constans
COI1	coronatine insensitive 1
Col-0	Columbia-0
COR	coronatine
DAMP	danger-associated molecular pattern
DEL1	DP-E2F-like 1
DHBA	dihydroxybenzoic acid
DNA	deoxyribonucleic acid
DPI	days post-inoculation
F2 generation	second filial generation
FLS2	flagellin-sensing 2
FT	flowering locus T
FUL	fruitful
GA	gibberellic acid
EDS	enhanced disease susceptibility
ELM1	EDS5-like MATE transporter
ETI	effector-triggered immunity
FLC	flowering locus C
FRI	frigida
GFP	green fluorescence protein
HIM	*hrp*-inducing minimal medium
HPI	hours post-inoculation
HR	hypersensitive response
HRP	hypersensitive response and pathogenicity
HSD	honestly significant difference

IAP1	important for age-related resistance protein 1
ICS	isochorismate synthase
IWF	intercellular washing fluid
J3	DNAJ homolog 3
JA	jasmonic acid-isoleucine
JAZ	jasmonate-zim-domain proteins
KB	King's B medium
LFY	leafy
MADS	MCM1, AG, DEF, SRF
MAMP	microbe-associated molecular pattern
MAPK	mitogen-activated protein kinase
MATE	multi-drug and toxin extrusion
MeSA	methyl salicylic acid
miR	microRNA
mM	millimolar
mRNA	messenger ribonucleic acid
MYC2	myelocytomatosis viral oncogene homolog 2
NAC	NAM, ATAF1,2, CUC2
NDR1	non-race-specific disease resistance 1
NLR	nucleotide-binding leucine-rich repeat
NPR	non-expressor of pathogenesis-related genes
OD	optical density
PAD4	phytoalexin deficient 4
PAL	phenylalanine ammonia lyase
PPH	pheophytinase
PR1	pathogenesis-related 1
PRR	pattern recognition receptor
Pst	*Pseudomonas syringae* pv. *tomato*
PTI	pattern-triggered immunity
pv	pathovar
qRT-PCR	quantitative reverse transcription polymerase chain reaction
R protein	resistance protein
RIN4	RPM1-interacting protein 4
RPM1	resistance to *Pseudomonas syringae* pv. *maculicola* 1
RPP31	resistance to *Peronospora parasitica* 1
RPS2	resistance to *Pseudomonas syringae* 2
SA	salicylic acid
SAG	salicylic acid *O*-*β*-glucoside
SAG13	senescence-associated gene 13
SAR	systemic acquired resistance
SARD1	systemic acquired resistance-deficient 1
SCF	SKP1, CULLIN, F-BOX
Sf-2	San Feliu-2

SID2	salicylic acid induction-deficient 2
SOC1	suppressor of overexpression of constans 1
SPL	squamosa promoter binding protein-like
SVP	short vegetative phase
TBF1	TL1-binding factor 1
TFL1	terminal flower 1
TGA	TGACG sequence-specific binding protein
TMV	tobacco mosaic virus
UGT	uridine diphosphate-dependent glycosyltransferase
WHY1	whirly 1
WPG	weeks post-germination
Ws	Wassilewskija

Chapter 1 – Introduction

PREFACE

This thesis consists of an introduction chapter followed by two chapters of previously published research (Chapters 2 and 3) and Chapter 4, which consists of research prepared for submission to Molecular Plant-Microbe Interactions. Each research chapter begins with a description of the main findings and author contributions. These chapters have self-contained introductions, methods, discussions, and references, and there is substantial overlap between the chapters with respect to some of these sections. There is also overlap between this introduction chapter and the introductions of the research chapters. The references list for this thesis follows the discussion chapter and contains works cited in the introduction and discussion chapters.

1.1 Plant responses to the environment

The ability of plants to survive in nearly every environment on Earth is astounding, especially given that in most respects, plants are immobile. Dispersal of seeds or spores allows for movement on the timescale of generations, and vegetative growth allows plant roots and shoots to explore the environment on the timescale of individual lifespans. Individuals, however, cannot move from

place to place in order to escape environmental stress – and plants face numerous stresses, both abiotic (e.g., light, water, temperature, and mineral extremes) and biotic (e.g., other plants, herbivores, and pathogens). As a result, plants have evolved complex signaling networks to sense and respond to these stresses.

1.2 Plant responses to pathogens

Microbial pathogens (e.g., bacteria, fungi, and oomycetes) are the most significant biotic stress experienced by plants based on yield losses for six of the world's major crops (Oerke, 2006). While the focus is often on food crops, plants provide many other resources such as lumber, textiles, and chemicals. They are also major components of natural and artificial landscapes, and provide essential ecosystem services (de Groot et al., 2002; Nabors, 2004). Fundamental knowledge of plant-pathogen interactions forms the basis of strategies to combat plant disease, from the development of effective crop-management practices, to the generation of disease-resistant varieties through breeding programs or more direct forms of genetic modification.

Pathogenic or disease-causing microbes are those that multiply and/or grow at the expense of the plant. Successful pathogens are able to invade and colonize plant tissues, obtain nutrients, and evade or suppress the plant immune response. They usually interfere with essential functions in the plant, cause

disease symptoms, inhibit growth and/or reproduction, and sometimes cause death of the infected tissue or entire plant (Agrios, 2005). The ability of most pathogens to enter or multiply within plant tissues is restricted by constitutive physical and chemical barriers such as the waxy cuticle and antimicrobial compounds (Senthil-Kumar and Mysore, 2013). Other disease-resistance mechanisms are activated only in the presence of pathogens. These so-called induced disease-resistance responses are traditionally classified according to the type of pathogen signature that triggers them, either microbe-associated molecular patterns (MAMPs) or effector proteins (described in sections 1.2.2 and 1.2.4, respectively). Some pathogens are able to surpass constitutive defenses, for example, entering through natural openings such as stomata (Melotto et al., 2008) and degrading or extruding antimicrobials (Lewis and Ausubel, 2006). Some pathogens can also suppress induced disease-resistance responses, as discussed in the sections below.

1.2.1 The *Arabidopsis thaliana-Pseudomonas syringae* pathosystem

The gram-negative bacterium *Pseudomonas syringae* is an economically important phytopathogen, causing disease on a wide variety of host plants (Mansfield et al., 2012). For example, bacterial canker caused by *P. syringae* pv. *actinidiae*, has been devastating the kiwifruit industry for the past ten years or so, although recovery is now on the horizon thanks to improved management practices and introduction of a resistant hybrid variety (Lee-Jones, 2016).

Interestingly, *P. syringae* is perhaps best known for its ability to infect a small flowering plant of no direct economic importance. This observation, published in landmark studies by Whalen et al. (1991) and Dong et al. (1991), led to the wide-spread use of the *Arabidopsis thaliana-P. syringae* pathosystem for research on plant-pathogen interactions. Since then, this pathosystem has greatly facilitated our understanding of pathogen virulence strategies and host resistance mechanisms.

P. syringae typically inhabits the aboveground organs of plants, mainly the leaves. The disease cycle begins with an epiphytic phase of growth or survival on the leaf surface, followed by invasion of the intercellular space, often through stomata. In a susceptible host, *P. syringae* can multiply extensively in the intercellular space and cause disease (Xin and He, 2013). *P. syringae* obtains nutrients from living host cells at early stages of the infection (biotrophy), and from dead cells at later stages (necrotrophy), and is therefore classified as a hemi-biotroph (Glazebrook et al., 2005; Xin and He, 2013). Unless otherwise specified, the information given in subsequent sections pertains to the *A. thaliana-P. syringae* pathosystem, although many of the concepts are also applicable to other plant-pathogen interactions.

1.2.2 Pattern-triggered resistance

Plants have a large number of plasma membrane-associated receptor-like kinases and receptor-like proteins, many of which function as pattern recognition receptors (PRRs) (Jones and Dangl, 2006). These PRRs recognize MAMPs such as bacterial flagellin and elongation factor Tu (Bauer et al., 2001; Chinchilla et al., 2006; Gómez-Gómez and Boller, 2000; Zipfel et al., 2006). Ligand binding by their extracellular domains typically leads to the formation of multimeric receptor complexes and activation of receptor complex components by auto- and trans-phosphorylation of the intracellular kinase domains. While the link between receptor activation and downstream signaling events is not yet clear, the latter proceeds in part through mitogen-activated protein kinases (MAPKs) and calcium-dependent protein kinases (CDPKs), ultimately leading to the transcriptional reprogramming of hundreds of genes. The resulting cellular defense mechanisms are collectively referred to as pattern-triggered immunity (PTI), and include cell wall modifications and production of antimicrobial compounds (Bigeard et al., 2015; Macho and Zipfel, 2014; Wu and Zhou, 2013). One of the best-characterized PRRs is FLS2 (FLAGELLIN SENSING 2), which binds the flg22 peptide of bacterial flagellin (Chinchilla et al., 2006; Sun et al., 2013). Binding of flg22 to FLS2 triggers rapid dimerization with the coreceptor BAK1 (BRI1-ASSOCIATED RECEPTOR KINASE), followed by phosphorylation of these and other members of the receptor complex, activating them for initiation

of downstream signaling, presumably through MAPKs and CDPKs (Chinchilla et al., 2007; Schulze et al., 2010; Sun et al., 2013).

1.2.3 Effector-triggered susceptibility

Some pathogens are able to circumvent PTI through the use of effector proteins (Jones and Dangl, 2006). Many bacterial pathogens deliver effectors into plant cells via a type III secretion system, where the effectors then interact with a variety of host targets to suppress disease-resistance responses (Dou and Zhou, 2012; Hogenhout et al., 2009; Xin and He, 2013). For example, the *P. syringae* AvrRpt2 effector is a cysteine protease that cleaves several host proteins, and at least some of these proteins play important roles during PTI (Axtell et al., 2003; Belkhadir et al., 2004; Chisholm et al., 2005; Kim et al., 2005). One such protein, RIN4 (RPM1-INTERACTING PROTEIN 4), is normally tethered to the plasma membrane, but cleavage by AvrRpt2 releases fragments that act as negative regulators of PTI (Afzal et al., 2011).

Pathogens also produce small molecules or toxins that function in the suppression of disease resistance. For example, some strains of *P. syringae* produce coronatine (COR), a mimic of the phytohormone jasmonic acid-isoleucine (JA). The JA receptor COI1 (CORONATINE INSENSITIVE 1) is part of the SKP1 CULLIN F-BOX $(SCF)^{COI1}$ ubiquitin ligase, which is involved in proteasome-mediated protein degradation. Binding of either JA or COR facilitates

the interaction of COI1 with members of the JAZ (JASMONATE-ZIM DOMAIN) family of transcriptional repressors. The subsequent degradation of JAZ proteins de-represses transcription factors such as MYC2 (MYELOCYTOMATOSIS VIRAL ONCOGENE HOMOLOG 2), which go on to upregulate a variety of JA-responsive genes (Geng et al., 2014; Xin and He, 2013). Activation of JA signaling by COR is beneficial to *P. syringae* since JA signaling is associated with defense against necrotrophic pathogens and herbivores, and is antagonistic to salicylic acid (SA) signaling (discussed in section 1.2.5), which is associated with defense against biotrophs and hemi-biotrophs (Glazebrook, 2005). The mechanistic basis of this antagonism became clearer when Zheng et al. (2012) discovered that MYC2 directly activates the expression of three functionally redundant *NAC* (*NAM ATAF1,2 CUC2*)-family genes, *NAC072*, *NAC055*, and *NAC019*. These genes encode transcription factors that directly repress the SA biosynthesis gene *ICS1 (ISOCHORISMATE SYNTHASE 1)*, and activate the SA metabolism gene *BSMT1 (BENZOIC ACID/SALICYLIC ACID CARBOXYL METHYLTRANSFERASE 1)*. The combined action of these events results in decreased SA accumulation and enhanced disease susceptibility (Figure 1.1).

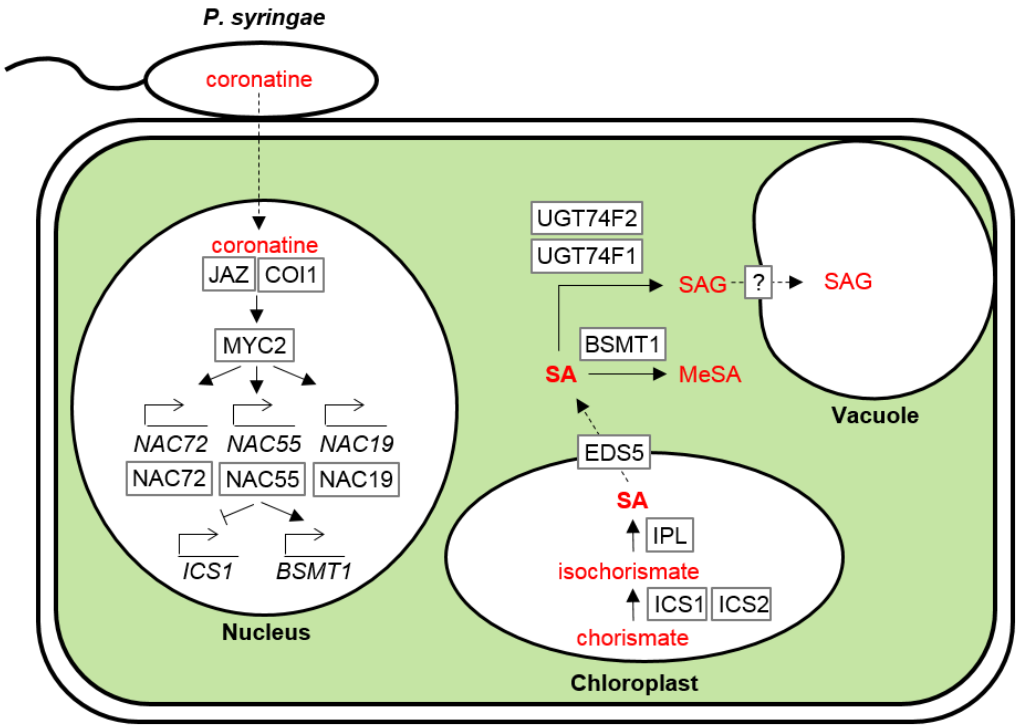

Figure 1.1 – Biosynthesis and metabolism of SA, and coronatine-mediated suppression of SA accumulation in *Arabidopsis*. In the nucleus, binding of the diffusible phytotoxin coronatine to the JA receptor complex (which includes COI1) fascilitates proteasome-mediated degradation of JAZ repressor proteins. JAZ degredation de-represses MYC2 which activates three *NAC* genes whose products activate *BSMT1* and repress *ICS1*. In the chloroplasts chorismate is converted to isochorismate, mainly via ICS1, and isochorismate is subsequently converted to SA by hypothetical IPL. SA is transported to the cytoplasm by the MATE-family protein EDS5 where it is then converted to a number of conjugates including MeSA by BMST1, and SAG by UGTs (mainly UGT74F1). SAG is transported to the vacuole by an unknown transporter, presumably for storage of this inactive SA conjugate. Proteins are surrounded by grey boxes, genes are in italics underneath promoter symbols, and chemical compounds are shown in red. Dashed lines indicate translocation of compounds. See the text for additional details and references. Abbreviations: BSMT1, benzoic acid/salicylic acid carboxyl methyltransferase 1; COI1, coronatine insensitive 1; EDS5, enhanced disease susceptibility 5; ICS, isochorismate synthase; IPL, isochorismate pyruvate lyase; JA, jasmonic acid-isoleucine; JAZ, jasmonate-zim-domain; MeSA, methyl salicylic acid; MYC2, myelocytomatosis viral oncogene homolog 2; NAC, NAM/ATAF1,2/CUC2; SA, salicylic acid; SAG, salicylic acid *O*-*β*-glucoside; UGT, uridine diphosphate-dependent glycosyltransferase.

1.2.4 Effector-triggered resistance

Plants also possess receptors known as Resistance (R) proteins, of which many are intracellular and of the NLR class (nucleotide-binding leucine-rich repeat) (Dodds and Rathjen, 2010; Jones and Dangl, 2006). R proteins recognize pathogen effectors, and while some do so directly, others do so indirectly by sensing the modifications that effectors make to their host targets. Upon effector recognition, R proteins become activated and initiate signaling for a disease-resistance response termed ETI (effector-triggered immunity) (Jones and Dangl, 2006). ETI shares many characteristics with the PTI response, although ETI is typically faster and stronger, probably because effectors are more likely than MAMPs to indicate the presence of pathogenic versus non-pathogenic microbes (Cui et al., 2015; Gassmann and Bhattacharjee, 2012). Continuing with the AvrRpt2 example, in response to AvrRpt2-mediated cleavage of RIN4, the R protein RPS2 (RESISTANCE TO PSEUDOMONAS SYRINGAE 2) becomes activated and initiates an ETI response (Axtell et al., 2003; Axtell and Staskawicz, 2003; Mackey et al., 2003).

Another difference between PTI and ETI is that unlike PTI, ETI is often associated with a form of cell death known as the hypersensitive response (HR). The HR is thought to prevent the growth of biotrophic or hemi-biotrophic pathogens such as *P. syringae*, which rely on living host cells to obtain nutrients for at least part of their life cycle (Glazebrook, 2005). However, this interpretation is inconsistent with some instances of ETI, where the HR can either be

genetically separated from the restriction of pathogen growth, or does not occur in the first place. For example, both Col-0 (Columbia-0) and Ws-0 (Wassilewskija-0) accessions are similarly resistant to *P. syringae* pv. *tomato* (*Pst*) carrying the HopPsyA effector protein, but in Col-0, resistance occurs in the absence of an HR (Gassmann, 2005). In the F2 generation of a Col-0 x Ws-0 cross, the HR phenotype segregated in a pattern consistent with its control by a single recessive locus that has yet to be identified. These types of observations have led to the more recent suggestion that rather than being a cause of resistance, the HR may instead be the result of a highly activated host immune system, where cell death results from a build-up of toxic defense compounds (Cui et al., 2015; Coll et al., 2011; Luis et al., 2008).

As our knowledge of plant disease resistance has increased, the line between PTI and ETI has started to blur. In addition to MAMPs and effectors, damage-associated molecular patterns (DAMPs) can also trigger resistance responses. DAMPs are host-derived molecules formed or released as a result of pathogen activity, for example, oligogalacturonides released from the plant cell wall by pathogen cell-wall-degrading enzymes (Boller and Felix, 2009; Wu, 2013). While DAMPs are conceptually indistinct from host targets that have been modified by effectors, many DAMPS are recognized by PRR-type proteins (Boller and Felix, 2009). Indeed, the disease-resistance responses discussed so far are increasingly viewed as a similar set of defense mechanisms elicited by a diverse array of non-host or modified host molecules. The timing and intensity of the

response may differ depending on the stimulus (i.e., depending on which particular receptors and downstream signaling networks are activated), but the output is qualitatively similar (Boller and Felix, 2009; Cui et al., 2015).

1.2.5 Salicylic acid

SA (2-hydroxybenzoic acid) is a phytohormone that influences a wide variety of plant processes including developmental events from germination to senescence (Vicente and Plasencia, 2011), and responses to abiotic stresses such as drought, cold, and heavy metals (Khan et al., 2015). SA also plays a key role in plant responses to pathogens (Vlot et al., 2009). Indeed, many plants accumulate SA in response to pathogens, including tomato, pepper, tobacco, cucumber, and *Arabidopsis* (Dempsey and Klessig, 2017; Dempsey et al., 2011; Vlot et al., 2009). The following subsections outline the biosynthesis and metabolism of SA, and its role in disease resistance. While there are some differences between plant species in these respects, the main focus will be on *Arabidopsis.*

1.2.5.1 Salicylic acid biosynthesis and metabolism

In plants, SA biosynthesis proceeds through two pathways that branch from chorismate. In one, chorismate is converted to SA in multi-step process involving PAL (PHENYLALANINE AMMONIA LYASE) enzymes, and in the other, chorismate is converted to SA via an isochorismate intermediate (Dempsey et al.,

2011; Vlot et al., 2009). In *Arabidopsis,* SA is produced in response to pathogens including *P. syringae*, mostly through the isochorismate pathway (Fig. 1.1; Nawrath and Mètraux, 1999; Wildermuth et al., 2001). *Arabidopsis* has two ICS enzymes, ICS1 and ICS2, but ICS1 is the major contributor to SA biosynthesis. In fact, ICS2-mediated SA biosynthesis is only detectable in the absence of ICS1, and even then, is quite limited (Garcion et al., 2008). Isochorismate is presumably converted to SA by ISOCHORISMATE PYRUVATE LYASE (IPL), which is yet to be identified (Dempsey et al., 2011). *ICS1* expression is pathogen-inducible (Wildermuth et al., 2001) and although the signaling events linking pathogen recognition to SA biosynthesis are not well understood, some of the key players have been identified. These include EDS1 (ENHANCED DISEASE SUSCEPTIBILITY 1), PAD4 (PHYTOALEXIN-DEFICIENT 4), and NDR1 (NON-RACE-SPECIFIC DISEASE RESISTANCE 1). Although their exact functions are still unclear, these proteins are thought to participate in signaling downstream of PRR and R protein activation, and upstream of SA biosynthesis. Indeed, they have been shown to associate with various PRRs and R proteins, and are required for *ICS1* expression and SA accumulation in response to various pathogens (Dempsey and Klessig, 2017; Dempsey et al., 2011; Gassmann and Bhattacharjee, 2012; Janda and Ruelland, 2015; Vlot et al., 2009). Several transcription factors that directly regulate *ICS1* expression have also been identified, including partially redundant SARD1 (SAR-DEFICIENT 1) and CBP60g (CALMODULIN-BINDING PROTEIN 60 g), which are required for activation of

ICS1 expression and SA biosynthesis in response to *P. syringae* (Wang et al., 2011; Zhang et al., 2010).

ICS1-mediated SA biosynthesis occurs in chloroplasts (Fragnière et al., 2011; Garcion et al., 2008; Strawn et al., 2008) and SA is transported to the cytoplasm by the multi-drug and toxin extrusion (MATE)-family transporter EDS5 (Serrano et al., 2013; Figure 1.1). SA is subsequently converted to a number of conjugates, including SAG (SA *O-β*-glucoside) by the uridine diphosphate-dependent SA glycosyltransferases (UGTs) UGT74F1 and UGT74F2, with the former being the major contributor (Dean and Delaney, 2008; Lim et al., 2002; Song, 2006). Earlier studies on tobacco and soybean suggest that SAG is formed in the cytoplasm then transported into the vacuole (Dean et al., 2005; Dean and Mills, 2004; Dean et al., 2003). The formation and vacuolar storage of SAG is thought to prevent the toxic effects associated with high levels of free SA. Other SA derivatives include methyl SA (MeSA) and dihydroxybenzoic acid (DHBA), which may be detoxified storage forms of SA, similar to SAG, or play roles in disease resistance that are distinct from the roles of SA (Dempsey et al., 2011; Vlot et al., 2009).

1.2.5.2 Salicylic acid as a signal for defense-gene expression

SA acts as a signal for defense-gene expression, largely through the transcriptional coregulator NPR1 (NON-EXPRESSOR OF PR GENES 1) (Janda and Ruelland, 2015; Vlot et al., 2009). NPR1 normally exists as a cytosolic

oligomer, but upon SA accumulation, changes in cellular redox status lead to NPR1 monomerization and subsequent translocation to the nucleus. In the nucleus, NPR1 interacts with TGA (TGACG SEQUENCE-SPECIFIC BINDING PROTEIN) transcription factors to activate defense-related genes including *PR1* (*PATHOGENESIS-RELATED 1*), the archetypal marker gene for SA signaling (Janda and Ruelland, 2015; Vlot et al., 2009). Interestingly, some evidence suggests that NPR1 functions as an SA receptor (Wu et al., 2012). The authors of this study propose a model where NPR1 monomerization requires both reducing conditions and an SA-mediated conformational change. This conformational change also appears to be important for the activity of NPR1 as a transcriptional coactivator. Around the same time, another group proposed that two NPR1 paralogs act as SA receptors (Fu et al., 2012). In their model, NPR3 and NPR4 bind SA with different affinities and control the proteasome-mediated degradation of NPR1, which is important for a properly regulated disease-resistance response. In addition, several other SA-binding proteins could be considered to be SA receptors (Klessig et al., 2016; Janda and Ruelland, 2015; Vlot et al., 2009). Which proteins constitute “true” SA receptors is still up for debate, although it seems likely that SA is perceived on multiple levels. As eluded to above, not all SA signaling is NPR1-dependent. For example, the transcription factor WHY1 (WHIRLY 1) is required for SA-induced *PR1* expression, and WHY1 binds DNA in an SA-dependent but NPR1-independent manner (Desveaux et al., 2004).

Compared to wild type, mutants or transgenic plants that are unable to accumulate SA exhibit enhanced disease susceptibility to pathogens such as *P. syringae*. For example, *sid2* (*salicylic acid induction-deficient 2*)/*ics1* and *eds5* mutants support enhanced growth of *P. syringae* strains that trigger PTI or ETI responses (Delaney et al., 1994; Nawrath and Mètraux, 1999; Tsuda et al., 2008; Tsuda et al., 2009). Although the chloroplast SA transporter EDS5 is not directly involved in SA biosynthesis, *eds5* mutants still fail to accumulate SA, probably because a build-up of SA in the chloroplasts exerts negative feedback on SA biosynthesis (Serrano al., 2013). The SA signaling mutants *npr1* and *why1* are also defective for PTI and ETI (Cao et al., 1994; Delaney et al., 1995; Desveaux et al., 2004; Glazebrook et al., 1996; Shah et al., 1997). Therefore, SA is an important component of PTI and ETI, and appears to act as a signal for defense-gene expression during these disease-resistance responses.

SAG is considered to be biologically inactive in terms of contributing to disease resistance since it fails to activate *PR1* expression in tobacco (Hennig et al., 1993). Similarly, 2,3-DHBA and MeSA induce little expression of *PR1* in *Arabidopsis* (Bartsch et al., 2010; Koo et al., 2007; Song et al., 2008). Moreover, transgenic plants that hyperaccumulate 2,3-DHBA or MeSA display enhanced susceptibility to *P. syringae*, presumably because they accumulate very little SA (Koo et al., 2007; Liu et al., 2010; Song et al., 2008; Zhang et al., 2015). Therefore, current evidence suggests that DHBA and MeSA do not contribute to defense against *P. syringae*, with the exception that MeSA is involved in systemic

defense signaling during Systemic Acquired Resistance (SAR) (Dempsey et al., 2011; Vlot et al., 2009).

1.2.6 Age-related resistance

Much of our knowledge of plant disease resistance comes from experiments on young plants, and in some studies plant age is not considered or reported at all. We should be concerned about these omissions because disease resistance has been observed to change throughout the course of development in a wide variety of crop plants (Develey-Rivière and Galiana, 2007; Whalen, 2005). Specifically, resistance often increases with age, a phenomenon typically referred to as Age-Related Resistance (ARR). Relatively little is known about this type of plant disease resistance, although the mechanisms have been investigated in a few cases.

Upon the transition to flowering, tobacco plants exhibit enhanced resistance to the oomycete *Phytopthora parasitica* (Hugot et al., 1999). This resistance is characterized by a reduction in the number of leaves showing disease symptoms, and reduced hyphal spreading on leaves that do show disease symptoms. Resistance in flowering plants is associated with SA-independent antimicrobial activity in the intercellular space, and the SA-dependent presence of PR1 protein in the intercellular space (Hugot et al., 1999), although silencing *PR1* genes did not compromise resistance (Rivière et al., 2008). Both antimicrobial activity and

PR1 protein were present in the intercellular space of healthy plants (Hugot et al., 1999), suggesting that the resistance mechanisms associated with tobacco ARR to *P. parasitica* are constitutive rather than pathogen-induced. ARR has been associated with an age-dependent accumulation of antimicrobial compounds in other cases as well, including soybean ARR to *Phytophthora megasperma* (glyceollin; Battacharyya and Ward, 1986), pepper ARR to *Phytophthora capsici* (capsidiol; Hwang, 1995), and cotton ARR to *Rhizoctonia solani* (terpenoids; Hunter 1978). In these cases accumulation of antimicrobial compounds occurs either in the absence of pathogens (i.e., constitutively), in response to pathogens, or a combination of both.

ARR can either be broad-spectrum or specific to a particular pathogen species or strain. Moreover, some plants appear to possess multiple, distinct ARR responses (Develey-Rivière and Galiana, 2007; Whalen, 2005). For example, in tomato, the R protein CF9-B confers resistance to *Cladosporum fulvum* carrying the Avr9B effector protein, but only in mature plants (Panter et al., 2002). The regulatory mechanism for this ARR response is unknown, although differential expression of *CF9-B* in young and mature plants was ruled out (Panter et al., 2002). In addition to developmentally regulated ETI, tomato exhibits a broad-spectrum ARR response to *C. fulvum* and *Clavibacter michiganensis* (Panter et al., 2002; Sharabani et al., 2013).

ARR in the *Arabidopsis-Pseudomonas* pathosystem was first described by Kus et al. (2002), who found that mature plants inoculated with *Pst* supported less

bacterial growth and developed fewer disease symptoms compared to young plants. *Arabidopsis* ARR is also effective against *P. syringae* pv. *maculicola* and the obligate biotroph and oomycete *Hyaloperonospora arabidopsidis* (formerly *Peronospora parasitica*), but is not effective against the necrotrophic pathogens *Erwinia carotovora* and *Botrytis cinerea* (Kus et al., 2002; Rusterucci et al., 2005). McDowell et al. (2005) have described a distinct ARR response in *Arabidopsis,* where older plants display enhanced resistance to the Emco5 strain of *H. arabidopsidis.* This appears to be an instance of developmentally regulated ETI since the resistance phenotype is associated with an HR, isn't observed in response to other strains of *H. arabidopsidis*, and maps to a single locus, the putative R gene *RPP31 (RESISTANCE TO PERONOSPORA PARASITICA 31)*, which has not yet been identified (McDowell et al., 2005). Subsequent discussion of ARR and the work presented in this thesis pertains to the broad-spectrum ARR response described by Kus et al. (2002) in the *Arabidopsis-Pseudomonas* pathosystem.

SA is required for ARR to *P. syringae*, since mutants and transgenics that are unable to accumulate SA (*sid2-1, eds5-3, eds1-1, pad4-1,* and *NahG*) are ARR-defective (Cameron and Zaton, 2004; Carviel et al., 2009; Kus et al., 2002). Interestingly, SA signaling does not appear to be required for ARR, since *npr1-1* mutants are ARR-competent, and pathogen-responsive SA-dependent *PR1* expression is reduced in mature plants relative to young plants (Kus et al., 2002; Rusterucci et al., 2005). Instead, early studies on ARR hinted at a different role

for SA, namely that of an antimicrobial agent. This idea arose from the observation that intercellular washing fluids (IWFs) collected from mature plants inoculated with *Pst* possessed antibacterial activity that was not present in corresponding IWFs from young plants or mature mock-inoculated plants (Cameron and Zaton, 2004; Kus et al., 2002). Moreover, antibacterial activity was absent in IWFs from mature *NahG* plants (transgenics expressing a bacterial salicylate hydroxylase), suggesting that SA accumulation is required for the antibacterial activity observed in mature wild-type plants. Further investigation revealed that SA accumulated in IWFs from mature plants but not young plants following inoculation with *Pst* (Cameron and Zaton, 2004). Addition of exogenous SA to the intercellular space rescued the ARR defect of SA biosynthesis mutant *sid2-1,* but not SA-degrading *NahG* plants. Conversely, addition of salicylate hydroxylase to the intercellular space impaired the ARR response of wild-type plants (Cameron and Zaton, 2004). Together these data suggest that SA accumulation in the intercellular space is an important aspect of the ARR response, and along with the numerous observations of SA's in vitro antimicrobial effects on a variety of plant pathogens (Amborabé et al., 2002; Brown 2007; Cameron and Zaton, 2004; El-Mougy, 2002; Georgiou et al., 2000; Martín et al., 2010; Prithiviraj et al., 1997; Lowe-Power et al., 2016; Yuan et al., 2007), suggest that SA acts as an antimicrobial agent.

Both forward and reverse genetic screens have identified genes potentially involved in ARR, including a microarray experiment comparing mature plants that

were inoculated with *Pst* to mature plants that were mock inoculated (Carviel et al., 2009). One of the most highly upregulated genes in plants inoculated with *Pst* was *NAC055*, and subsequent experiments showed that *nac055* mutants were partially ARR-defective. This partial defect could be due to functional redundancy with at least two similar genes, *NAC072* and *NAC019* (Al-Daoud and Cameron, 2011), although this hypothesis remains to be tested. Carviel et al. (2009) also performed a forward genetic screen for ARR-defective mutants and identified *iap1-1* (*important for ARR protein 1-1*), a mutant unable to accumulate both intracellular and intercellular SA in response to *Pst.* The causal mutation was localized to the long arm of chromosome 4 through map-based cloning.

In some cases, ARR is associated with the age of individual organs. In other cases, including *Arabidopsis* ARR to *P. syringae*, it is the age of the entire plant that is important. For example, on mature plants, young leaves are not more susceptible than older leaves. Similarly, a young leaf on a young plant is more susceptible than a young leaf on a mature plant (Kus et al., 2002). In most cases, ARR onset is associated with developmental transitions such as the transition to flowering or senescence (Develey-Rivière and Galiana, 2007; Whalen, 2005). *Arabidopsis* ARR is not associated with visible signs of senescence or expression of the senescence marker gene *SAG13* (*SENESCENCE ASSOCIATED GENE 13*; Kus et al., 2002), however, it is associated with the transition to flowering. In both short- and long-day-grown plants (9- and 16-hour days, respectively), ARR onset occurs at the same time as, or just before the majority of plants produce

visible inflorescence stems (Rusterucci et al., 2005). This observation suggests that the transition to flowering could be the cue for ARR competence.

1.3 Regulation of flowering time

The transition to flowering is a highly regulated process governed by complex signaling networks that integrate environmental and endogenous information such as photoperiod (daylength) and age. In response to inductive cues (e.g., long days and increasing age) the combined upregulation of floral activators and downregulation of floral repressors results in upregulation of floral meristem identity genes in the shoot apical meristem. This causes the meristem to switch from a vegetative meristem, which produces leaves, to an inflorescence meristem, which produces flowers (Amasino, 2010; Andrés and Coupland, 2012; Fornara et al., 2010). The photoperiod pathway will be the main focus here because photoperiod-induced flowering is an important concept in Chapter 2, and also involves many of the genes that are key players in Chapters 2 and 4.

In many plants, including *Arabidopsis*, long days induce flowering (Figure 1.2A). Daylength is sensed in the leaves, where a combination of transcriptional and post-translational regulation causes the transcription factor CO (CONSTANS) to accumulate in phloem companion cells specifically during long days. CO activates *FT* (*FLOWERING LOCUS T*) expression, and FT protein enters sieve elements to move via the phloem to the meristem where it partners with the

transcription factor FD (full name, not an abbreviation). The FT-FD complex then initiates flowering by activating expression of the floral meristem identity gene *AP1 (APETALA 1)* and the floral activator *SOC1* (*SUPPRESSOR OF OVEREXPRESSION OF CO 1*). SOC1 is a MADS (MCM1, AG, DEF, SRF)-domain transcription factor, and activates expression of a second floral meristem identity gene, *LFY* (*LEAFY*) (Amasino, 2010; Andrés and Coupland, 2012; Fornara et al., 2010).

Endogenous cues also mediate flowering, specifically the gibberellic acid (GA) and ageing pathways are thought to be responsible for the eventual transition to flowering that occurs in short days (Figure 1.2B). The ageing pathway is regulated primarily by the microRNA *miR156*. Expression of *miR156* decreases throughout development, resulting in the gradual de-repression of several *SPL* (*SQUAMOSA PROMOTER BINDING PROTEIN-LIKE*) genes that encode transcription factors that act as positive regulators of flowering (Hyun et al., 2017). GA is also a positive regulator of flowering (Wilson et al., 1992) and increased GA levels in the meristem correspond to the floral transition (Eriksson et al., 2006). Hyun et al. (2016) recently showed that SPL15 integrates signals from the ageing and GA pathways. Reduced levels of *miR156* and increased levels of GA activate SPL15 (at the mRNA and protein level, respectively). SPL15 then participates in a complex with SOC1 to upregulate the expression of floral meristem identity genes, indirectly through other floral activators not discussed here (*FUL* and *miR172b*).

An important aspect of flowering-time control is the negative regulation of floral activators so that flowering does not occur in the absence of inductive cues. This role is filled by floral repressors such as the MADS-domain transcription factor SVP (SHORT VEGETATIVE PHASE; Hartmann et al., 2000). SVP delays flowering by directly repressing expression of floral activators such as *FT* and *SOC1* (Gregis et al., 2013; Lee et al., 2007; Li et al., 2008). SVP acts in multiple tissues to delay flowering. In the leaves SVP represses *FT* expression, and in the meristem it represses *SOC1* expression (Andrés et al., 2014). SVP also represses *SOC1* expression in leaves, however, the biological significance of this is unclear since it is not known how or whether SOC1 in the leaves contributes to flowering-time regulation (Lee and Lee, 2010; Searle et al., 2006). *SOC1* is not expressed in the meristem of vegetative plants due to repression by SVP, however, exposure to long days results in the activation of *SOC1* expression and a concomitant repression of *SVP* expression in the meristem (Jang et al., 2009). Interestingly, *SOC1* mRNA levels increase in the meristem before *SVP* mRNA has disappeared, suggesting that the FT-FD complex can overwhelm the repressive effect of SVP (Jang et al., 2009). Moreover, SOC1 appears to positively regulate its own expression, both directly, by interacting with its own promoter (Tao et al., 2009; Immink et al., 2012), and indirectly, by interacting with the *SVP* promoter to repress *SVP* expression (Andres et al., 2014; Immink et al., 2012). The temporal expression of *FT* and *SVP* has not been studied in leaves specifically, however, activation of *FT* expression by CO occurs even in *SVP*

overexpressors when they are exposed to long days (Li et al., 2008; Yoshida et al., 2009). Again, this suggests that in the presence of inductive cues, floral activators (in this case CO) are able to overwhelm the repressive effect of SVP. Moreover, inductive cues such as long days and GA upregulate expression of *J3* (*DNAJ HOMOLOG 3*), which encodes a protein that interacts with SVP protein and reduces the ability of SVP to interact with the regulatory regions of *FT* and *SOC1* DNA (Shen et al., 2011).

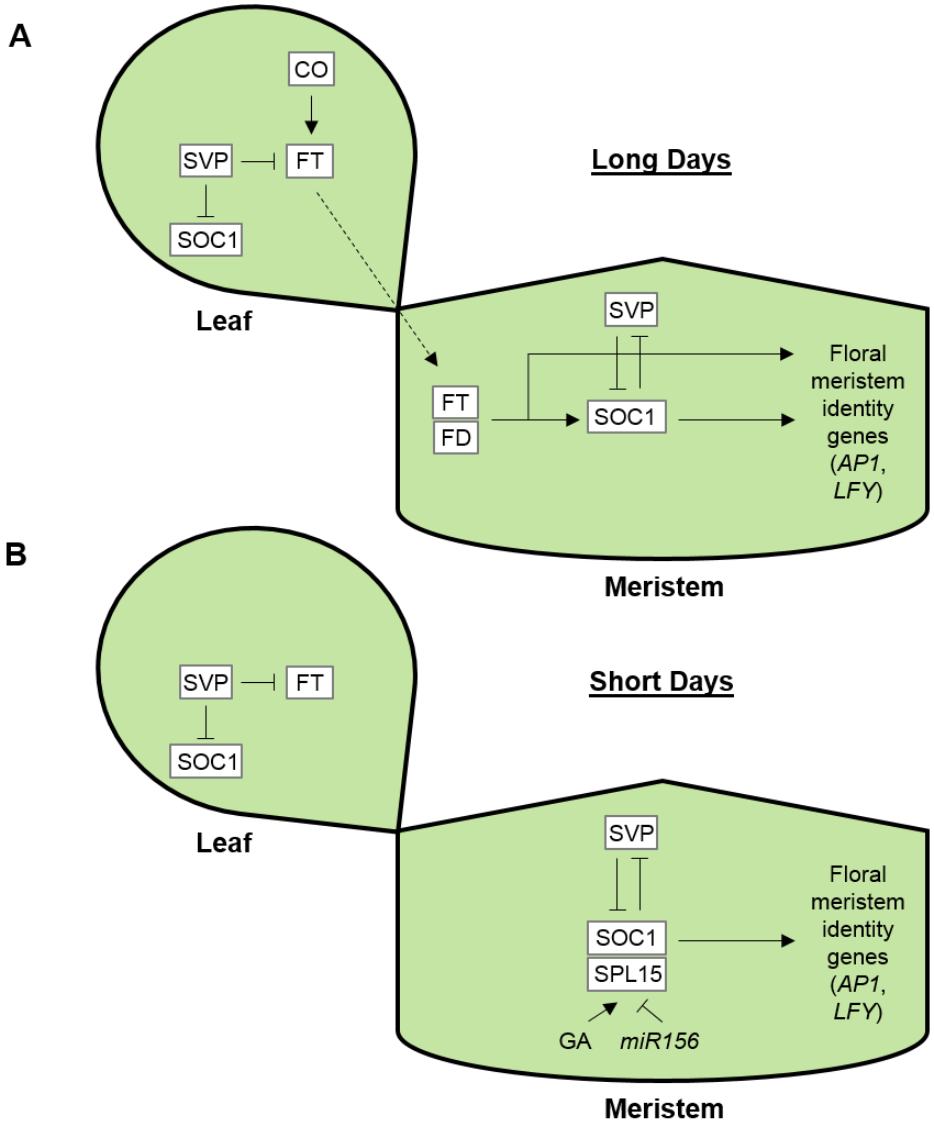

Figure 1.2 – Simplified schematic of the regulation of flowering time in *Arabidopsis*. **A)** In long days CO accumulates in the phloem companion cells of the leaf, activates *FT* expression, and FT protein moves to the meristem. In the meristem FT interacts with FD to activate *AP1* and *SOC1* expression. SOC1 represses *SVP* expression and activates *LFY* expression. **B)** In short days GA accumulates and *miR156* levels decrease with age. This upregulates SPL15 which interacts with SOC1 to activate the expression of floral meristem identity genes. In the absence of inductive cues the floral repressor SVP delays flowering mainly by repressing *FT* expression in the leaves and *SOC1* expression in the meristem. Inductive cues (increased day length or age) overwhelm the repressive effect of SVP. See the text for additional details and references. Abbreviations: AP1, apetala; CO, constans; FT, flowering locus T; GA, gibberellic acid; LFY, leafy; miR156a, microRNA 156a; SOC1, suppressor of overexpression of constans, SPL15, squamosa promoter binding-like 15; SVP, short vegetative phase. FD is a full name.

1.4 Hypotheses and objectives

Chapter 2 – The floral transition is not the developmental switch that confers competence for the Arabidopsis Age-Related Resistance response to Pseudomonas syringae pv. tomato

Hypotheses:

1) The transition to flowering is the developmental cue for ARR competence.
2) ARR in long-day-grown plants is SA-dependent.

Objectives:

1) Determine the ARR phenotypes of early- and late-flowering mutants, as well as wild-type plants that have been induced to flower early by transient exposure to long days.
2) Determine the ARR phenotypes of long-day-grown SA-deficient mutants.

Chapter 3 – Investigation of intercellular salicylic acid accumulation during compatible and incompatible Arabidopsis-Pseudomonas syringae interactions using a fast neutron-generated mutant allele of EDS5 identified by genetic mapping and whole-genome sequencing

Hypotheses:

1) The *IAP1* gene encodes a protein that is important for ARR.
2) Intercellular SA accumulation occurs during PTI and ETI.

Objectives:

1) Identify the causal mutation in the *iap1-1* mutant by map-based cloning and whole-genome sequencing, and confirm the results by Sanger sequencing and complementation testing.
2) Assess intracellular and intercellular SA accumulation in young plants responding to strains of *Pst* that trigger PTI or ETI.

Chapter 4 – Age-Related Resistance in Arabidopsis thaliana involves the MADS-domain transcription factor SHORT VEGETATIVE PHASE and direct action of salicylic acid on Pseudomonas syringae

Hypotheses:

1) SVP is required for SA accumulation during ARR.
2) SOC1 is a downstream target of SVP and a negative regulator of ARR.
3) SA acts directly on *Pst* as an antibacterial and antibiofilm agent in the intercellular space during ARR.

Objectives:

1) Determine whether *svp* mutants have reduced SA accumulation compared to wild type after inoculation with *Pst.*
2) Perform double mutant analysis with SVP and SOC1 and test the ARR phenotype of *SOC1* overexpressors.

3) A) Assess the in vitro antibacterial and antibiofilm activity of SA under biologically relevant conditions.

   B) Determine the in vivo concentration of SA during ARR.

   C) Monitor *Pst* biofilm formation in plants that are competent, incompetent, or defective for ARR.

1.5 Research contributions not otherwise discussed

In addition to the local disease-resistance responses described above, plants have systemic responses whereby infected tissues communicate with distant, uninfected tissues, priming them for enhanced resistance to future infection (Fu and Dong, 2013). One of these, SAR, involves the propagation of phloem-mobile signals, that move from infected leaves to distant leaves to establish a state of long-lasting, broad-spectrum disease resistance. During my Ph.D. I contributed to several SAR projects which resulted in a number of publications on which I am a co-author (Carella et al., 2017; Carella et al., 2016ab; Carella et al., 2015a). I also coauthored a perspective article for the *Frontiers in Plant Science* special research topic “Salicylic Acid Signaling Networks” (Carella et al., 2015b) in which we discuss the different roles of SA in young and mature plants. In addition, we present original data suggesting that WHY1 (described in section 1.2.5.2) is not required for ARR, providing further evidence that SA doesn't play a signaling role during ARR.

Chapter 2 – The floral transition is not the developmental switch that confers competence for the *Arabidopsis* Age-Related Resistance response to *Pseudomonas syringae* pv. *tomato*

PREFACE

This chapter consists of a published research article in which the association between ARR and the transition to flowering was investigated by assessing the ARR phenotypes of flowering-time mutants and wild-type plants that were induced to flower early by transient exposure to long days. This study provides evidence that flowering is neither required nor sufficient for ARR and also reveals that the flowering-time regulator SVP is required for ARR. The requirement of SA accumulation for ARR in long-day-grown plants was assessed by ARR assays of SA-deficient mutants. Their ARR-defective phenotypes suggest that SA accumulation is required for ARR in both short and long days.

Author contributions

DW, PC, and MI performed the experiments. DW and RC wrote the manuscript with assistance from the other authors. All authors contributed to the conception and design of experiments.

Citation and copyright information

Citation: Wilson, D.C., Carella, P., Isaacs, M., Cameron, R.K. (2013). The floral transition is not the developmental switch that confers competence for the

Arabidopsis Age-Related Resistance response to *Pseudomonas syringae* pv. *tomato*. Plant Molecular Biology, 83: 235-246. DOI: 10.1007/s11103-013-0083-7.

Plant Mol Biol (2013) 83:235–246
DOI 10.1007/s11103-013-0083-7

The floral transition is not the developmental switch that confers competence for the *Arabidopsis* age-related resistance response to *Pseudomonas syringae* pv. *tomato*

Daniel C. Wilson · Philip Carella · Marisa Isaacs · Robin K. Cameron

Received: 30 October 2012 / Accepted: 27 May 2013 / Published online: 31 May 2013

Abstract Age-related resistance (ARR) is a plant defense response characterized by enhanced resistance to certain pathogens in mature plants relative to young plants. In *Arabidopsis thaliana* the transition to flowering is associated with ARR competence, suggesting that this developmental event is the switch that initiates ARR competence in mature plants (Rusterucci et al. in Physiol Mol Plant Pathol 66:222–231, 2005). The association of ARR and the floral transition was examined using flowering-time mutants and photoperiod-induced flowering to separate flowering from other developmental events that occur as plants age. Under short-day conditions, late-flowering plant lines *ld-1* (*luminidependens-1*), *soc1-2* (*suppressor of overexpression of co 1-2*), and *FRI*$^{+}$ (*FRIGIDA*) displayed ARR before the transition to flowering occurred. Early-flowering *svp-31*, *svp-32* (*short vegetative phase*), and Ws-2 were ARR-defective, whereas early-flowering *tfl1-14* (*terminal flower 1-14*) displayed ARR at the same time as Col-0. While *svp-31*, *svp-32* and Ws-2 produced few rosette leaves, *tfl1-14* produced a rosette leaf number similar to Col-0, suggesting that the development of a minimum number of rosette leaves is necessary to initiate ARR competence under short-day conditions. Photoperiod-induced transient expression of *FT* (*FLOWERING LOCUS T*) caused precocious flowering in short-day-grown Col-0 but this was not associated with ARR competence. Under long-day conditions *co-9* (*constans-9*) mutants did not flower but displayed an ARR response at the same time as Col-0. This study suggests that SVP is required for the ARR response and that the floral transition is not the developmental event that regulates ARR competence.

Keywords *Arabidopsis* · *Pseudomonas syringae* · Age-related resistance · Developmental resistance · Flowering · Photoperiod

Daniel C. Wilson, Philip Carella and Marisa Isaacs contributed equally to this work.

Electronic supplementary material The online version of this article (doi:10.1007/s11103-013-0083-7) contains supplementary material, which is available to authorized users.

D. C. Wilson · P. Carella · M. Isaacs · R. K. Cameron (✉)
Department of Biology, McMaster University, 1280 Main St West, Hamilton, ON L8S 4L8, Canada
e-mail: rcamero@mcmaster.ca

Introduction

The outcome of a plant-pathogen interaction often depends on the developmental stage of the plant (Agrios 2005). Under short-day conditions (9 h light), young (3- to 4-week-old) *Arabidopsis* are susceptible to the bacterial pathogen *Pseudomonas syringae* pv. *tomato* (*Pst*), as indicated by the presence of disease symptoms and high *in planta* bacterial growth. In contrast, mature plants (>5 weeks old) are typically asymptomatic and show a 10- to 100-fold reduction in bacterial growth (Kus et al. 2002). *Arabidopsis* age-related resistance (ARR) also confers protection against the oomycete *Hyaloperonospora arabidopsidis* (Rusterucci et al. 2005). ARR has been observed in many plant species and the mechanisms involved appear to differ widely (Reviewed in Develey-Rivière and Galiana 2007; Whalen 2005). For example, tobacco (*Nicotiana tabacum*) develops enhanced resistance to *Phytopthora parasitica* during the transition to flowering. Enhanced resistance in reproductive-stage tobacco plants is associated with PATHOGENESIS-RELATED 1 (PR1) accumulation and cytotoxic activity in the apoplast (Hugot et al.

1999). In rice (*Oryza sativa*), the onset of developmentally regulated resistance to *Xanthomonas oryzae* pv. *oryzae* occurs during the vegetative phase (Mazzola et al. 1994). In part this involves the interaction of the rice *Xa-21* resistance gene product with the *X. oryzae* Ax21 effector (Lee et al. 2009; Mazzola et al. 1994).

Arabidopsis salicylic acid (SA) accumulation mutants such as *sid2* (*salicylic acid induction deficient 2*), *eds1* (*enhanced disease susceptibility 1*), *eds5/sid1*, and *pad4* (*phytoalexin deficient 4*) are defective for the ARR response (Cameron and Zaton 2004; Carviel et al. 2009; Kus et al. 2002) indicating that SA accumulation is important during ARR. In addition, the ARR-defective *iap1-1* (*important for the ARR pathway 1-1*) mutant accumulates little SA in response to *Pst* (Carviel et al. 2009). The role of SA in defense signaling is well-documented (Reviewed in Vlot et al. 2009), however, the SA-signaling mutant *npr1-1* (*non-expressor of PR1*) shows a wild-type ARR response suggesting that SA may not play a conventional defense-signaling role during ARR (Kus et al. 2002). Moreover, in plants undergoing an ARR response SA accumulates in the intercellular space of leaves (Cameron and Zaton 2004). Based on these data we propose that SA acts as an antimicrobial agent during ARR. Consistent with this hypothesis, it was shown that intercellular washing fluids of mature plants undergoing ARR, as well as purified SA, have an antimicrobial effect on *Pst* in vitro (Cameron and Zaton 2004).

As a facultative long-day plant, *Arabidopsis* flowers later in short days than in long days (Gregory and Hussey 1953). We previously observed that in both short- and long-day-grown Col-0, ARR onset is associated with the floral transition at approximately 6 weeks post-germination (wpg) in short days and four wpg in long days (Rusterucci et al. 2005). Several studies indicate that regulatory elements are shared between disease resistance and flowering pathways in *Arabidopsis*, including SA, which in addition to its role in disease resistance, also plays a role in flowering-time control (Reviewed in Rivas-San Vicente and Plasencia 2011). For example, evidence suggests that the SUMO and ubiquitin E3 ligases SIZ1 and PUB13 modify proteins that affect SA-related defense responses and flowering-time (Jin et al. 2008; Lee et al. 2006; Liu et al. 2012). Moreover, Wang et al. (2011) found that the putative acetylornithine transaminase encoded by *WIN3* acts together with other SA regulatory proteins such as NPR1 to control cell death, disease resistance, and flowering time. SA accumulation mutants such as *sid2* have been observed to flower later than wild type and also produce greater rosette leaf biomass and seed yield (Abreu and Munné-Bosch 2009; Martínez et al. 2004). However, this has not been observed for the ARR-defective and SA accumulation-deficient mutant *iap1-1* (Carviel et al. 2009).

The timing of the floral transition is highly regulated and is controlled by several major pathways that respond to environmental and endogenous stimuli. These pathways converge on a group of integrator genes that regulate the floral meristem-identity genes responsible for floral organ development at the shoot apical meristem (SAM). Figure 1 is a schematic diagram of flowering-time regulation in *Arabidopsis* that is limited to the flowering-time genes that are relevant to this study. Environmental cues that affect flowering include day length (photoperiod pathway), prolonged periods of cold (vernalization pathway), and ambient temperature. Other pathways respond to endogenous stimuli, for example, the autonomous, gibberellin, and ageing pathways (Reviewed in Amasino 2010; Simpson and Dean 2002).

FLOWERING LOCUS T (FT) is a floral integrator that links day-length perception in the leaves to floral induction at the SAM. During long days, the CONSTANS (CO) transcription factor accumulates in the phloem companion cells of leaves and upregulates *FT* transcription (An et al. 2004; Ayre and Turgeon 2004; Suárez-López et al. 2001; Yanovsky and Kay 2002). FT moves from the leaves via the phloem to the SAM (Corbesier et al. 2007; Jaeger and Wigge 2007) where it upregulates another floral integrator *SUPRESSOR OF OVEREXPRESSION OF CO 1* (*SOC1*) (Michaels et al. 2005; Yoo et al. 2005) and the floral meristem-identity gene *APETALA 1* (*AP1*) (Abe et al. 2005; Wigge et al. 2005). *SOC1* participates in a positive feedback loop with *AGAMOUS-LIKE 24* (*AGL24*) to upregulate the *LEAFY* (*LFY*) floral meristem identity gene (Lee et al. 2008; Liu et al. 2008).

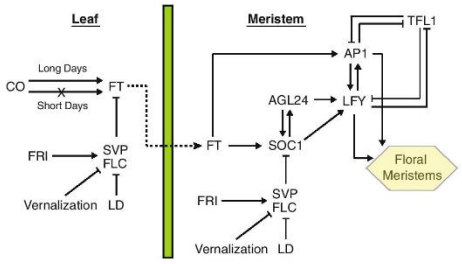

Fig. 1 Simplified representation of flowering-time regulation adapted from Amasino (2010) and Fornara et al. (2010). The FLC-SVP complex represses *FT* in the leaf and *SOC1* in the meristem and is regulated by FRI, vernalization, and the components of the autonomous pathway (e.g., LD). In short days *FT* expression remains low, whereas in long days *FT* is upregulated by CO and FT protein moves via the phloem (*dashed line*) from the leaf to the shoot apical meristem where it directly upregulates *SOC1* and *AP1*. SOC1 upregulates *AGL24* and *LFY*. LFY and AP1 are responsible for the production of floral meristems and are repressed by TFL1

Plant Mol Biol (2013) 83:235–246

AP1 and *LFY* are involved in the production of floral meristems (Weigel et al. 1992, Irish and Sussex 1990) and are repressed by TERMINAL FLOWER 1 (TFL1), which is responsible for maintenance of the indeterminate inflorescence meristem (Alvarez et al. 1992; Liljegren et al. 1999; Schultz and Haughn 1993; Shannon and Meeks-Wagner 1991; Shannon and Meeks-Wagner 1993). Evidently, TFL1 also represses flowering in vegetative plants since *tlf1* mutants flower early compared to wild type (Schultz and Haughn 1993; Shannon and Meeks-Wagner 1991). FT and SOC1 also incorporate signals from the vernalization and autonomous flowering pathways. *Arabidopsis* accessions possessing a dominant *FRIGIDA* (*FRI*) allele usually require a vernalization treatment before they become competent to flower (Lee and Amasino 1995; Lee et al. 1993). FRI confers a vernalization requirement by upregulating the floral repressor and MADS-box transcription factor *FLOWERING LOCUS C* (*FLC*) (Michaels and Amasino 1999). FLC forms a high-molecular-weight complex with another MADS-box transcription factor SHORT VEGETATIVE PHASE (SVP), and represses flowering by directly binding to regulatory regions of *FT* and *SOC1* in both leaf and SAM tissue (Helliwell et al. 2006; Lee et al. 2007; Li et al. 2008; Searle et al. 2006). Vernalization confers reproductive competence by derepressing *SOC1* and *FT* through epigenetic silencing of *FLC* (Bastow et al. 2004). Autonomous pathway mutants such as *ld-1* (*luminidependens-1*) are late flowering and exhibit increased expression of *FLC* and *SVP*, suggesting that the autonomous pathway is responsible for controlling the levels of FLC and SVP (Li et al. 2008; Michaels and Amasino 1999; Michaels and Amasino 2001; Sheldon et al. 1999).

The aim of this study is to determine whether the floral transition plays a role in regulating ARR competence. To do this we asked whether the association between flowering and ARR is maintained in flowering-time mutants. To examine the role of photoperiod-induced flowering in ARR onset we separated photoperiod-induced flowering from long-day growth conditions. Our results suggest that in both short- and long-day conditions, flowering is not the developmental cue that initiates ARR competence. We present evidence that *SVP* is required for ARR and propose that in short-day conditions the development of a minimum number of rosette leaves is necessary to initiate ARR competence.

Materials and methods

Plant material and growth conditions

Wild-type Columbia (Col-0) and Wassilewskija (Ws-2) accessions were used. All mutants used in this study were in the Columbia background. Mutants that were previously confirmed to be ARR-defective were *sid2-1* (C. Nawrath, University of Fribourg, Fribourg, Switzerland) and *iap1-1* (described in Carviel et al. 2009). Flowering-time mutants *ld-1* (CS3127), *svp-31* (SALK_026551C), and *tfl1-14* (CS6238) were obtained from the Arabidopsis Biological Resource Centre, Ohio State University, Columbus OH, USA (Alonso et al. 2003). *co-9*, *ft-10*, FRI^{+}, and FRI^{+} *flc-3* were supplied by R. Amasino (University of Wisconsin-Madison, WI, USA). *soc1-2* was supplied by I. Lee (Seoul National University, Seoul, Korea). *35S:miR156* was obtained from S. Poethig (University of Pennsylvania, PA, USA). *svp-32* (SALK_072930) was obtained from J. H. Ahn (Korea University, Seoul, Korea; Lee et al. 2007). Seeds were surface-sterilized and stratified at 4 °C for 2 days before sowing on MS media where they germinated under constant light at 22 °C. Seedlings were transplanted to soil (Sunshine Mix #1) hydrated with 1 g L^{-1} 20–20–20 all-purpose fertilizer approximately 1 week later. Plants were grown in short days unless otherwise specified. Short days consisted of 9 h light, and long days consisted of 16 h light. Light intensity was maintained at approximately 150 μE m^{-2} s^{-1} and temperature at 23 °C. Short-day growth chambers had added humidity (75–85 % relative humidity) whereas the long-day chamber did not (50–70 % relative humidity). Rosette leaves that were large enough to be resolved without magnification were scored to determine rosette leaf number.

Bacterial growth, inoculation, and quantification

Virulent *P. syringae* pv. *tomato* (*Pst*) strain DC3000 (pVSP61) was used in all experiments (A. Bent, University of Wisconsin-Madison, WI, USA). Bacteria were cultured in King's B media with shaking at room temperature to exponential phase ($OD_{600} = 0.2–0.6$) and then diluted to 10^6 colony forming units ml^{-1} in 10 mM $MgCl_2$. Inoculum was pressure-infiltrated into the abaxial side of leaves using a needle-less syringe. Isolation and quantification of *Pst* at 3 days post-inoculation was performed as described previously (Kus et al. 2002).

Analysis of gene expression by RT-PCR

Leaf tissue was harvested in the evening (end of photoperiod), flash-frozen in liquid nitrogen, and stored at −80 °C until further use. RNA was isolated using Sigma TRI Reagent according to the manufacturer's instructions. Residual DNA was degraded using TURBO DNase (Life Technologies) prior to RNA quantification. First-strand cDNA synthesis was carried out using SuperScript III reverse transcriptase (Life Technologies). PCR primers used to amplify *FT* transcripts were: 5′-TAAGCAGAGTTGTT

GGAGACG and 5′-TCTAAAGTCTTCTTCCTCCGCAG (Jang et al. 2009). Primers used to amplify *ACTIN1* transcripts were: 5′-GGCGATGAAGCTCAATCCAAACG and 5′-GGTCACGACCAGCAAGATCAAGACG. Twenty-eight PCR cycles were used for both *FT* and *ACTIN1*.

Statistical analysis

Statistically significant differences in bacterial densities and average rosette leaf numbers were determined by ANOVA. To account for unequal variance in the means the bacterial density data were transformed prior to analysis (log or square root transformation). Tukey's HSD post hoc test was used for pair-wise comparisons ($p < 0.01$). All tests were performed using IBM SPSS Statistics 20.

Results

ARR onset does not coincide with the floral transition in early- and late-flowering plant lines

If the transition to flowering acts as a developmental cue to initiate ARR competence, we should observe delayed ARR onset in late-flowering mutants and early ARR onset in early-flowering mutants. To test this hypothesis, wild-type Col-0, early-flowering *svp-31* (Hartmann et al. 2000), late-flowering *ld-1* (Rèdei 1962), and the early-flowering Ws-2 accession (Giakountis et al. 2010) were analyzed. *In planta* bacterial levels were monitored from 3 to 9 weeks post germination (wpg) by inoculating with virulent *Pst* (10^6 cfu ml^{-1}) followed by isolation and quantification of *in planta* bacteria 3 days later. The transition to flowering was approximated by counting the percentage of plants with visible inflorescence stems each week. In this experiment Col-0 flowered earlier than typically observed when grown under short-day conditions, such that 48 % of plants had visible inflorescence stems at four wpg, 71 % at five wpg, and 76 % at six wpg (Fig. 2a), instead of 0 % at 4 wpg, 5 % at 5 wpg and 33 % at 6 wpg (Fig. 2b). A power outage that interrupted the photoperiod regimen in week 3 exposed the plants to a displaced short day. Displaced short days have been shown to cause early flowering in *Arabidopsis* (Corbesier et al. 1996). While *ld-1* did not produce inflorescence stems during the experiment, 95 % of *svp-31* produced inflorescence stems by three wpg. Ws-2 also made the transition to flowering earlier than Col-0, with 58 % of plants showing inflorescence stems at three wpg, and 95 % at four wpg.

Col-0 became increasingly resistant to *Pst* between three and six wpg (Fig. 2a). Young (three wpg) plants supported high levels of *Pst* (2.3×10^7 cfu ld^{-1}), while 4- and 5-week-old plants supported modestly reduced levels (7.4×10^6 and 4.1×10^6 cfu ld^{-1}) and mature plants (six to nine wpg) supported low levels of *Pst* ($<4.0 \times 10^5$ cfu ld^{-1}). There was a 60-fold decrease in *Pst* between 3- and 6-week-old plants, indicating that Col-0 was fully ARR-competent at six wpg. Late-flowering *ld-1* supported *Pst* levels similar to Col-0 between three and five wpg. At six wpg *ld-1 Pst* levels dropped to 1.5×10^6 cfu ld^{-1} (22-fold less than at three wpg) indicative of moderate ARR. At seven, eight, and nine wpg *ld-1* displayed a robust ARR response (97-fold reduction in *Pst* levels between three and seven wpg). Early-flowering *svp-31* supported high *Pst* densities ($>1.0 \times 10^7$ cfu ld^{-1}) from three to six wpg, remaining ARR-incompetent. At seven wpg, older *svp-31* leaves began to senesce as indicated by yellowing and necrosis, therefore these plants were not tested beyond six wpg. A second mutant allele, *svp-32*, also flowered early and was found to be ARR-defective (Fig. S2). The early-flowering Ws-2 accession also supported high *Pst* densities ($>7.0 \times 10^6$ cfu ld^{-1}) at all ages.

Although somewhat delayed compared to Col-0, the *ld-1* mutant displayed a robust ARR response even in the absence of flowering, suggesting that the floral transition is not required for ARR competence. In addition, early-flowering does not elicit an early ARR response since *svp-31*, *svp-32* and Ws-2 flowered early but did not display ARR at the time of the floral transition or at any time thereafter. Therefore, the floral transition does not appear to act as a developmental cue for ARR competence.

Photoperiod-induced flowering does not elicit ARR competence

To support the hypothesis that the floral transition does not confer ARR competence we used short day/long day shift experiments to elicit precocious flowering in young, short-day-grown Col-0 followed by an assay for ARR competence. Brief exposure of short-day-grown plants to inductive (long-day) photoperiods activates the photoperiod pathway and initiates the transition to flowering (Corbesier et al. 2007; Imaizumi et al. 2003). Eliciting early flowering in wild-type plants has the advantage of avoiding possible pleiotropic effects of mutations in flowering-time genes. Col-0 was grown under three different photoperiod regimens and tested for ARR competence at four wpg. Photoperiod regimens consisted of either short days, long days, or short days plus three long days followed by return to short days (Fig. 3a). All long-day-grown Col-0 had visible inflorescence stems at four wpg, whereas short-day-grown and photoperiod-induced short-day-grown Col-0 did not. To determine whether photoperiod-induced short-day-grown plants had made the transition to flowering, RT-PCR was used to measure *FT* expression in leaf tissue taken at time points spanning the induction period (Fig. 3b). *FT*

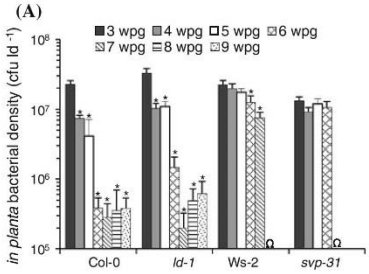

Percent Inflorescence Stems				
	Col-0	*ld-1*	Ws-2	*svp-31*
3 wpg	6	0	58	95
4 wpg	48	0	95	100
5 wpg	71	0	100	100
6 wpg	76	0	100	100
7 wpg	100	0	100	Ω
8 wpg	100	0	Ω	Ω
9 wpg	100	0	Ω	Ω

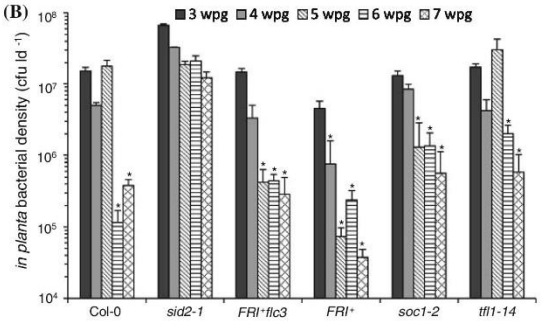

Percent Inflorescence Stems						
	Col-0	*sid2-1*	*FRI⁺ flc3*	*FRI⁺*	*soc1-2*	*tfl1-14*
3 wpg	0	0	0	0	0	100
4 wpg	0	4	2	0	0	100
5 wpg	5	5	2	0	0	100
6 wpg	33	30	33	0	0	100
7 wpg	100	100	89	0	0	100

Fig. 2 ARR responses of various flowering-time mutants. **a** Col-0, *ld-1*, Ws-2 and *svp-31* were grown in short days and tested for ARR each week between three and nine wpg. Plants were inoculated with 10^6 cfu ml^{-1} virulent *Pst* (DC3000) and bacterial levels were quantified 3 days later. Data are presented as the mean of three biological replicates. *Error bars* indicate standard deviation. *Asterisk* denotes significant differences relative to three wpg plants of the same genotype according to Tukey's HSD ($p < 0.01$). Each week at least 12 plants of each genotype were assessed for visible inflorescence stems. *Values* represent the percentage of plants with visible inflorescence stems. Ω indicates the onset of senescence at which point further testing was not possible. Each genotype was tested at least three times with similar results **b** Col-0, *sid2-1*, *FRI⁺ flc-3*, *FRI⁺*, *soc1-2*, and *tfl1-14* were grown in short days and tested for ARR each week between three and seven wpg. Plants were inoculated with 10^6 cfu ml^{-1} virulent *Pst* (DC3000) and bacterial levels were quantified 3 days later. Data are presented as the mean of three biological replicates. *Error bars* indicate standard deviation. *Asterisk* denotes significant differences relative to three wpg plants of the same genotype according to Tukey's HSD ($p < 0.01$). Each week at least 12 plants of each genotype were assessed for visible inflorescence stems. *Values* represent the percentage of plants with visible inflorescence stems. This experiment was performed twice with similar results

expression was detected in the leaves of photoperiod-induced short-day-grown Col-0 at the end of the third long day, indicating that the photoperiod pathway had been activated. *FT* expression was consistently detected in the leaves of long-day-grown Col-0 and was not detected in short-day-grown plants.

Consistent with previous experiments (Rusterucci et al. 2005), at four wpg long-day-grown Col-0 supported few disease symptoms and low bacterial levels whereas short-day-grown Col-0 was susceptible, supporting 125-fold higher *Pst* levels than long-day-grown plants (Fig. 4). This indicates that long-day-grown Col-0 was ARR-competent at four wpg whereas short-day-grown plants were not. Photoperiod-induced short-day-grown Col-0 supported high *Pst* densities at four wpg (1.2×10^7 cfu ld^{-1}), similar to short-day-grown Col-0 (1.4×10^7 cfu ld^{-1}), therefore

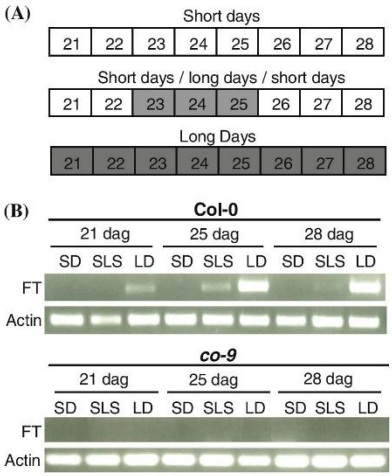

Fig. 3 Short-day-grown plants express *FT* after exposure to three long days. **a** Schematic representation of the three photoperiod regimens. *White bars* indicate short days (9 h light), *dark bars* indicates long days (16 h light). *Numbers* indicate days after-germination. **b** *FT* and *ACTIN* expression measured by RT-PCR in leaf tissue of Col-0 and *co-9* plants grown in short days (SD), short days/long days/short days (SLS), or long days (LD). Tissue was collected in the evening on 21, 25, and 28 days after-germination (dag)

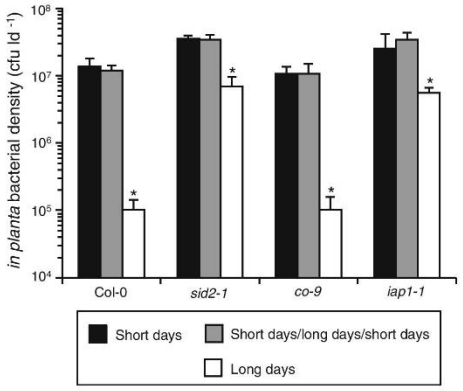

Fig. 4 Photoperiod-induced flowering does not elicit ARR. Col-0, *sid2-1*, *co-9*, and *iap1-1* were grown in short days, short days/long days/short days, or long days and were inoculated with 10^6 cfu ml^{-1} virulent *Pst* (DC3000) at four wpg. Bacterial levels were quantified 3 days later and are presented as the mean of three biological replicates. *Error bars* indicate standard deviation. *Asterisk* indicates significant differences as determined by ANOVA (Tukey's HSD, $p < 0.01$). This experiment was performed twice with similar results

these plants were not competent for ARR at four wpg. This confirms our previous conclusion that the floral transition does not confer ARR competence.

CONSTANS is not required for ARR in long days

Since ARR onset occurs earlier in long-day conditions we wanted to determine whether the transition to flowering, or a different developmental event accelerated in long days, elicits ARR competence. For example, the vegetative phase change from juvenile to adult vegetative stages occurs earlier in long-day-grown plants (Chien and Sussex 1996; Willmann and Poethig 2005) and could be associated with ARR competence. To separate flowering from other developmental changes that might act as a switch for ARR-competence in long days we tested *co* mutants which flower late in long days (Koornneef et al. 1991; Putterill et al. 1995) because *FT* is no longer up-regulated by CO in a photoperiod-dependent manner (Kardailsky et al. 1999; Kobayashi et al. 1999; Samach et al. 2000). If the transition to flowering is the cue for ARR competence in long days, then long-day-grown *co* mutants should have delayed ARR compared to Col-0 (ARR at four wpg). To test this hypothesis the *co-9* mutant was grown in three different photoperiod regimens and tested for ARR competence at four wpg as described previously. In all three photoperiod regimens *co-9* lacked inflorescence stems and detectable *FT* expression throughout the experiment (Fig. 3b), indicating that the photoperiod pathway was not activated. Short-day-grown and photoperiod-induced short-day-grown *co-9* supported high *Pst* levels (1.1×10^7 cfu ld^{-1}), whereas long-day-grown *co-9* supported low levels of *Pst* (1.0×10^5 cfu ld^{-1}; Fig. 4). A 110-fold decrease in *Pst* levels in long-day-grown compared to short-day-grown *co-9* is indicative of a robust ARR response in long-day-grown plants. In long-day-grown *co-9* mutants ARR occurs in the absence of flowering, demonstrating that photoperiod-induced flowering is not required for the establishment of ARR competence in long-day conditions.

ARR competence is associated with leaf number in short-day conditions

Our original hypothesis that the floral transition is the developmental cue for ARR competence was not supported, therefore other developmental events that might act as a switch to initiate ARR-competence were considered. The early-flowering plant lines (*svp-31*, *svp-32*, and Ws-2) were ARR-defective and produced few rosette leaves (Table 1; Figs. S1 and S2). The SAM switches from production of vegetative to reproductive structures during the transition to flowering, therefore the timing of the floral

Plant Mol Biol (2013) 83:235–246

Table 1 ARR onset and leaf number of short-day-grown plants

	Flowering-time phenotype[a]	ARR onset	Average rosette leaves[c] at ARR onset
ARR-competent plant lines			
Col-0	Wild-type	6 wpg	33.9 ± 2.8
FRI^{+} *flc-3*	Wild-type	5 wpg	26.4 ± 2.8[b]
FRI^{+}	Late	5 wpg	27.2 ± 1.3[b]
ld-1	Late	6 wpg	32.7 ± 2.6
soc1-2	Late	5 wpg	27.0 ± 2.1[b]
tfl1-14	Early	6 wpg	28.3 ± 1.7
ARR-defective plant lines			
Ws-2	Early	na	22.8 ± 4.3[c,d]
svp-31	Early	na	21.7 ± 3.8[c,d]

ARR onset and leaf number for experiment presented in Fig. 2a, b. Average rosette leaves for Col-0 from experiment in Fig. 2b

[a] Relative to wild-type Col-0

[b] Rosette leaf number is presented as the average ± standard deviation (n = 9)

[c] Significantly different from Col-0 (ANOVA, Tukey's HSD, $p < 0.01$)

[d] For ARR-defective plant lines the maximum average rosette leaf number is presented

transition affects vegetative growth (rosette leaf number) such that early-flowering plant lines produce fewer rosette leaves than wild type (Hempel and Feldman 1994; Koornneef et al. 1991). It has been suggested that the timing of some developmental events may be influenced by rosette leaf number (McDaniel et al. 1992; Poethig 1990; Schultz and Haughn 1993) and given that the early-flowering plant lines examined thus far produced few rosette leaves and were ARR-defective, we hypothesized that the development of a minimum number of rosette leaves might initiate ARR competence. To assess whether ARR competence is associated with leaf number we analyzed the early-flowering *tfl1-14* mutant (Schultz and Haughn 1993) because it produced more rosette leaves than *svp-31*, *svp-32*, and Ws-2 (Table 1; Figs. S1 and S2). In these experiments plants were assessed for ARR competence and average rosette leaf number between three and seven wpg.

Col-0 made the transition to flowering between six and seven wpg (33 and 100 % inflorescence stems, respectively) and supported high *Pst* densities ($\geq 5.0 \times 10^6$ cfu ld^{-1}) between three and five wpg (Fig. 2b). At six wpg *Pst* levels dropped to 1.2×10^5 cfu ld^{-1}, a 131-fold reduction compared to 3-week-old plants, indicative of a robust ARR response. Col-0 had a rosette leaf number of 33.9 ± 2.8 at six wpg (Table 1) for the experiment presented in Fig. 2b. Moreover, in five independent experiments, Col-0 produced an average of 34.7 ± 3.4 rosette leaves at ARR onset (6 wpg), making it possible to compare leaf number across experiments (Tables 1, 2). ARR-defective *sid2-1* supported high bacterial densities at all ages ($>1.0 \times 10^7$ cfu ld^{-1}) and flowered at approximately the same time as Col-0 (30 and 100 % inflorescence stems at six and seven wpg respectively). At all ages *sid2-1* had a rosette leaf number similar to Col-0 (Fig. S1). This suggests that *sid2-1* is developmentally similar to Col-0 in terms of leaf number and is consistent with previous work suggesting that the *sid2-1* ARR defect is due solely to its inability to accumulate SA (Cameron and Zaton 2004). The transition to flowering occurred prior to three wpg in *tfl1-14*, as 100 % of plants had inflorescence stems by this time (Fig. 2b). *tfl1-14* supported high *Pst* levels at three and five wpg ($>1 \times 10^7$ cfu ld^{-1}) and a statistically insignificant decline at four wpg (4.2×10^6 cfu ld^{-1}). At six wpg *Pst* levels in *tfl1-14* were reduced to 2.0×10^6 cfu ld^{-1}, characteristic of a modest ARR response (9-fold reduction in *Pst* levels relative to three wpg). A more robust ARR response was observed at seven wpg (30-fold reduction in *Pst* levels compared to three wpg). This indicates that ARR occurs in the early-flowering *tfl1-14* mutant. At six wpg *tfl1-14* had a rosette leaf number of 28.3 ± 1.7, not significantly different from Col-0 (Table 1). The ARR-defective early-flowering plant lines *svp-31* and Ws-2 had rosette leaf numbers of 21.7 ± 3.8 and 20.9 ± 6.3 respectively at six wpg; significantly less than *tfl1-14* or Col-0. These results suggest that development of a minimum number of rosette leaves is necessary to initiate ARR competence in short-day-grown plants.

The *ld-1* mutant displayed ARR in the absence of flowering, however, the ARR response was somewhat delayed compared to that of Col-0 (Fig. 2a). To test whether ARR is delayed in the absence of flowering, and to determine whether this could be explained in terms of leaf number, we analyzed two additional late-flowering lines; the *soc1-2* mutant (Borner et al. 2000) and a *FRI*$^{+}$ Col-0

Table 2 ARR in 4-week-old Col-0 and *co-9* grown in different photoperiod regimens

	Photoperiod[a]	Floral transition[c]	ARR response[c]	Average rosette leaves[b,c]
Col-0	SD	–	–	23.1 ± 1.7
	SLS	+	–	24.3 ± 2.3
	LD	+	+	17.4 ± 2.0
co-9	SD	–	–	24.6 ± 2.0
	SLS	–	–	24.7 ± 1.5
	LD	–	+	29.1 ± 2.8

ARR response and leaf number for experiment presented in Fig. 4

[a] Short days (SD), long days (LD), or short days/long days/short days (SLS)

[b] Rosette leaf number is presented as the average ± standard deviation (n = 18)

[c] Measurements were taken at 4 weeks post-germination

line hereafter referred to as *FRI*$^+$ (Lee and Amasino 1995). *SOC1* integrates signals from multiple flowering pathways, therefore *soc1-2* mutants flower later than wild type (Borner et al. 2000). Wild-type Col-0 has recessive alleles of the *FRI* gene and as a result, flowers without vernalization (Johanson et al. 2000; Lee and Amasino 1995). A dominant *FRI* allele introgressed into the Col-0 background severely delays flowering in the absence of vernalization due to upregulation of the floral repressor *FLC* (Lee and Amasino 1995). *FRI*$^+$ and *soc1-2* were chosen primarily for their late-flowering phenotypes. Also, to our knowledge there is no evidence that they exhibit developmental phenotypes aside from late flowering (see discussion on *ld-1*), however, we also tested a *FRI*$^+$ *flc-3* line which flowers at the same time as wild-type Col-0 (Michaels and Amasino 1999) and therefore serves as a control for potential pleiotropic effects of the dominant *FRI* allele. For example, if *FRI*$^+$ had an ARR defect that was caused by its late-flowering phenotype, this defect should not be observed in *FRI*$^+$ *flc-3* which flowers at the same time as wild type. However, if *FRI*$^+$ had an ARR defect for a reason other than late flowering, then *FRI*$^+$ *flc-3* should display that same defect. As expected, neither *soc1-2* nor *FRI*$^+$ flowered during our experiments while *FRI*$^+$ *flc-3* flowered at approximately the same time as Col-0 (Fig. 2b). *soc1-2* supported high *Pst* levels at three and four wpg (>8.0×10^6 cfu ld^{-1}), intermediate levels at five and six wpg (1.4×10^6 cfu ld^{-1}) and lower levels at seven wpg (5.7×10^5 cfu ld^{-1}; Fig. 2b). At five and six wpg there was a 10-fold reduction in *Pst* levels compared to three wpg, indicative of a moderate ARR response in *soc1-2*. By seven wpg this difference had increased to 23-fold lower levels of *Pst* compared to three wpg. s*oc1-2* had a rosette leaf number of 27.0 ± 2.1 at the time of ARR onset (Table 1). *FRI*$^+$ supported relatively high *Pst* levels at three wpg (4.5×10^6 cfu ld^{-1}), intermediate levels at four wpg (7.7×10^5 cfu ld^{-1}) and low levels between five and seven wpg (<1.2×10^5 cfu ld^{-1}; Fig. 2b). There was a 63-fold decrease in *Pst* levels between three and five wpg, indicative of a robust and early ARR response. *FRI*$^+$ had a rosette leaf number of 27.2 ± 1.3 at the time of ARR onset (Table 1). Bacterial levels in *FRI*$^+$ *flc-3* were similar to those of *FRI*$^+$ and ARR was also first observed at five wpg (35-fold reduction in *Pst* relative to three wpg; Fig. 2b). *FRI*$^+$ *flc-3* produced a similar rosette leaf number to *FRI* + at the time of ARR onset (Table 1). Neither *FRI*$^+$ nor *soc1-2* flowered during the experiment, but both displayed ARR, further supporting the conclusion that flowering is not necessary for ARR competence. The rosette leaf number of *FRI* + and *soc1-2* at the time of ARR onset was significantly lower than Col-0 but still higher than the maximum reached by the ARR-defective plant lines *svp-31*, *svp-32*, and Ws-2 (Table 1, Fig. S2). The observation that one late-flowering mutant (*ld-1*) had delayed ARR while two other late-flowering plant lines (*FRI*$^+$, *soc1-2*) and a wild-type flowering-time plant line (*FRI*$^+$ *flc-3*) had early ARR indicates that the timing of ARR onset varies between plant lines independently of the timing of the floral transition. Altogether the leaf number data presented in Table 1 is consistent with the hypothesis that development of a minimum number of rosette leaves is required for ARR competence in short-day-grown plants.

To determine whether our hypothesis of a minimum rosette leaf number requirement also applies to long-day-grown plants we analyzed rosette leaf number data collected during the short day/long day shift experiments described above. 4-week-old short-day-grown and photoperiod-induced short-day-grown Col-0 and *co-9* had low rosette leaf numbers (between 23 and 25; Table 2) and were ARR-incompetent at this time. This is consistent with our observations that short-day-grown plants remain ARR-incompetent until the production of approximately 30 rosette leaves (Table 1). At four wpg, short-day-grown and photoperiod-induced short-day-grown plants were either vegetative or just beginning the transition to flowering. In contrast, long-day-grown Col-0 made the transition to flowering at approximately three wpg (100 % of plants had inflorescence stems) and therefore had developed fewer rosette leaves (17.4 ± 2.0) than short-day-grown plants at four wpg. The observation that long-day-grown Col-0 was ARR-competent with so few rosette leaves is not consistent with the leaf number-ARR competence relationship observed for short-day-grown plants. This could indicate that the leaf number threshold for ARR competence is lower for plants grown in long days or alternatively, that ARR competence is regulated by a different mechanism in long-day-grown plants.

IAP1 and *SID2* are required for ARR in long days

IAP1 and *SID2* are important components of the ARR response that occurs in short-day-grown plants (Carviel et al. 2009; Kus et al. 2002). Plants grown in long days display a similar but earlier ARR response (Rusterucci et al. 2005). To obtain clues as to whether the ARR pathway in short-day-grown plants shares components with the ARR pathway in long-day-grown plants, two mutants that are known to be ARR-defective in short-day conditions, *iap1-1* and *sid2-1*, were examined in three different photoperiod regimens as described previously. Short-day-grown and photoperiod-induced short-day-grown *iap1-1* and *sid2-1* all supported high levels of *Pst* (>1.0×10^7 cfu ml^{-1}) similar to Col-0 (Fig. 4). Long-day-grown *iap1-1* and *sid2-1* both supported lower *Pst* densities compared to their short-day-grown counterparts (5-fold reduction), however, these plants were still susceptible as indicated by

Plant Mol Biol (2013) 83:235–246

high *Pst* levels (50- to 70-fold higher than long-day-grown Col-0) and characteristic disease symptoms (data not shown), indicative of a defective ARR response. The lower *Pst* levels in long-day-grown plants were probably due to lower humidity in the long-day chamber (60 %) compared to the short-day chamber (80 %), since high humidity enhances *in planta Pst* growth (Agrios 2005). Both *iap1-1* and *sid2-1* had a similar rosette leaf number to Col-0 in all three photoperiod regimens (data not shown). It has been reported that *sid2-1* flowers later than Col-0 (greater total leaf number at bolting; Martínez et al. 2004), however this is not observed in our experiments perhaps due to differences in plant growth conditions (day length, light quantity and humidity differences). Taken together, these data suggest that these SA-deficient mutants are developmentally similar to Col-0 in terms of leaf number, and the capacity to accumulate SA is required for ARR in *Arabidopsis* grown in long-day as well as short-day photoperiods.

Discussion

ARR competence is not associated with flowering in short- or long-day conditions

Previously we demonstrated that ARR competence is associated with the floral transition in Col-0 (Rusterucci et al. 2005). Here we sought to determine if the transition to flowering is responsible for initiating ARR competence by separating the transition to flowering from other developmental events that occur as plants age. To do this, the ARR phenotypes of mutants with three classes of flowering-time phenotype (early, late, and wild-type) were examined under short-day conditions. Overall there was no clear relationship between flowering time and the timing of ARR onset, with all ARR-competent plant lines displaying ARR between five and six wpg irrespective of flowering time. For example, late-flowering plant lines (*ld-1*, *FRI*$^{+}$, *and soc1-2*) displayed ARR at approximately the same time as Col-0 even though they did not flower during our experiments. This suggests that the floral transition is not required to initiate an ARR-competent state. Of the four plant lines that flowered early, *svp-31*, *svp-32*, and Ws-2 were defective for ARR and *tfl1-14* displayed a moderate ARR response. Even though *tfl1-14* had completed the floral transition by three wpg, ARR was not observed until six wpg, suggesting that early flowering does not initiate early ARR. The observation that *svp-31*, *svp-32*, and Ws-2 were ARR-defective further demonstrates that the floral transition is not involved in the initiation of ARR competence and led us to hypothesize that development of a minimum rosette leaf number is required to initiate ARR competence since *svp-31*, *svp-32*, and Ws-2 produced significantly fewer rosette leaves than either *tfl1-14* or Col-0. The fact that *tfl1-14* produced more rosette leaves than *svp-31*, *svp-32*, and Ws-2 is counter-intuitive since *tfl1-14* appeared to flower slightly earlier than *svp-31*, *svp-32*, and Ws-2 and would therefore be expected to have a lower maximum rosette leaf number. This difference could be explained by a higher leaf initiation rate in *tfl1-14* or a lower leaf initiation rate in *svp-31*, *svp-32*, and Ws-2 although it has previously been shown that *tfl1* mutants initiate leaves at a rate similar to Col-0 (Shannon and Meeks-Wagner 1991). Another explanation is that *tfl1-14* continued to produce rosette leaves after the transition to flowering, although this is inconsistent with the currently accepted model of organ development in reproductive-stage *Arabidopsis* which indicates that rosette leaves are not produced after the floral transition (Hempel and Feldman 1994).

To support the conclusion that the floral transition does not initiate ARR competence we looked at the ARR response of short-day-grown Col-0 that were forced to flower early by photoperiod-induced transient expression of *FT* (exposure to three long days). This treatment initiated the floral transition by four wpg as demonstrated by expression of *FT*, but did not elicit ARR competence suggesting that photoperiod-induced flowering is not sufficient for the onset of ARR competence in 4-week-old plants. This is consistent with the ARR defects observed in short-day-grown early-flowering plant lines and confirms that an early floral transition does not initiate ARR competence.

In *Arabidopsis* the floral transition occurs earlier in long days than in short days (Gregory and Hussey 1953). Since ARR onset also occurs earlier in long days and at approximately the same time as the transition to flowering, we suspected that the transition to flowering was the cue for ARR competence (Rusterucci et al. 2005). While this does not appear to be true for short-day-grown plants, we tested whether this might be the case for long-day-grown plants. Long-day-grown *co-9* mutants are delayed in photoperiod-induced flowering (Koornneef et al. 1991; Putterill et al. 1995) and remained vegetative at four wpg but still displayed a robust ARR response, similar to long-day-grown Col-0. This suggests that photoperiod-induced flowering is not required for the onset of ARR competence in long-day-grown plants. While it appears that development of a minimum rosette leaf number may initiate ARR competence in short-day-grown plants, the same relationship was not observed for long-day-grown plants since long-day-grown Col-0 displayed ARR at a rosette leaf number similar to short-day-grown, ARR-defective *svp-31*, *svp-32*, and Ws-2. This could indicate that the minimum leaf number requirement for ARR competence is lower in long-day-grown plants or that ARR in long-day-grown plants is regulated by a different mechanism altogether.

Vegetative phase change and ARR competence

Another consideration is that the vegetative phase change could be involved in the regulation of ARR competence. The central regulator of the vegetative phase change, miRNA156, targets members of the *SQUAMOSA PROMOTER BINDING PROTEIN-LIKE* (*SPL*) family, which have been shown to contribute to the onset of adult and reproductive phase characteristics (Schwarz et al. 2008; Usami et al. 2009; Wang et al. 2008; Wu et al. 2009; Wu and Poethig 2006). In wild-type plants *miR156* levels decrease over time, leading to a gradual de-repression of *SPL* genes and transition to the adult vegetative phase. Overexpression of *miR156* in 35S:miR156 plants causes the juvenile phase to be dramatically prolonged; with plants producing 90 ± 1.3 juvenile leaves whereas Col-0 produces 7.5 ± 0.7 (Wu et al. 2009). Preliminary results from our lab indicate that short-day-grown *35S:miR156* plants exhibit ARR at six wpg (data not shown), suggesting that the prolonged manifestation of juvenile characteristics does not delay the onset of ARR competence.

Many mutations in flowering-time genes also affect the timing of the vegetative phase change. Alternatively, some mutations alter the timing of either the vegetative phase change or transition to flowering without affecting the other (Telfer et al. 1997; Willmann and Poethig 2005). Interestingly, ARR-defective *svp-31*, *svp-32*, and Ws-2 undergo an earlier vegetative phase change relative to Col-0 (Hartmann et al. 2000; Telfer et al. 1997) whereas ARR-positive *tfl1-14* undergoes the vegetative phase change normally (Telfer et al. 1997). Although this might suggest that an early vegetative phase change is associated with ARR incompetence, long-day-grown Col-0 also undergoes an early vegetative phase change (Chien and Sussex 1996), and this does not result in an ARR defect. This suggests that the timing of the vegetative phase change does not regulate ARR competence, however, a more detailed analysis is required to fully address this question.

Timing of ARR onset differs between some plant lines

While some plant lines showed early ARR responses, others exhibited delayed ARR, such that robust resistance was not observed until seven wpg (*ld-1*) or only moderate responses were observed at six or seven wpg (*tfl1-14*, *soc1-2*). These differences had no obvious relationship with flowering-time. Instead it may be that some of the mutations that affect flowering time have pleiotropic effects. For example, autonomous pathway genes such as *LD* are believed to be involved in processes such as chromatin modification and RNA metabolism, and as a result, likely function in aspects of plant development other than flowering-time (Amasino 2010). This proposition is supported by observations of lethality or severe growth and developmental defects in various autonomous pathway mutants (Henderson et al. 2005; Koornneef et al. 1998; Veley and Michaels 2008). Variation in the timing of ARR could also result from differences in the genetic background of various plant lines used in this study (i.e., polymorphisms that are independent of mutations in flowering-time genes). Although all mutants used were in the Columbia background, whole-genome resequencing studies have revealed that different strains of Columbia can harbour thousands of unique polymorphisms (Ossowski et al. 2008). While many of these observed differences could reflect errors in the reference genome, the same group later showed that the rate of spontaneous mutation accumulation is much higher than previously thought (Ossowski et al. 2010). This implies that in some cases mutant lines may possess many genetic differences from wild-type controls (Santuari and Hardtke 2010).

We have demonstrated that the floral transition can be separated from ARR competence in both short- and long-day-grown plants. Therefore, the floral transition is not the developmental cue for ARR competence. Instead, vegetative development of a minimum numbers of leaves appears to be important for ARR competence in short-day grown *Arabidopsis*.

Acknowledgments This work was supported by a Natural Science and Engineering Research Council of Canada Discovery Grant to R. Cameron and growth chamber maintenance support from McMaster University. We would like to thank Jen Chin, who performed replicate experiments with *svp-31* and Ws-2. D. Wilson, M. Isaacs, and P. Carella were supported by Ontario Graduate Scholarships.

Conflict of interest The authors declare that they have no conflict of interest.

References

Abe M, Kobayashi Y, Yamamoto S, Daimon Y, Yamaguchi A, Ikeda Y, Ichinoki H, Notaguchi M, Goto K, Araki T (2005) Integration of spatial and temporal information during floral induction in *Arabidopsis*. Science 309:1052–1056

Abreu ME, Munné-Bosch S (2009) Salicylic acid deficiency in *NahG* transgenic lines and *sid2* mutants increases seed yield in the annual plant *Arabidopsis thaliana*. J Exp Bot 60:1261–1271

Agrios GN (2005) Plant pathology, 5th edn. Elsevier Academic Press, London

Alonso JM, Stepanova AN, Leisse TJ, Kim CJ, Chen H, Shinn P, Stevenson DK, Zimmerman J, Barajas P, Cheuk R et al (2003) Genome-wide insertional mutagenesis of *Arabidopsis thaliana*. Science 301:653–657

Alvarez J, Guli CL, Yu X, Smyth DR (1992) *terminal flower:* a gene affecting inflorescence development in *Arabidopsis thaliana*. Plant J 2:103–116

Amasino R (2010) Seasonal and developmental timing of flowering. Plant J 61:1001–1013

An H, Roussot C, Suàrez-López P, Corbesier L, Vincent C, Piñeiro M, Hepworth S, Mouradov A, Justin S, Turnbull C, Coupland G (2004) CONSTANS acts in the phloem to regulate a systemic signal that induces photoperiodic flowering in *Arabidopsis*. Development 131:3615–3628

Ayre BG, Turgeon R (2004) Graft transmission of a floral stimulant derived from *CONSTANS*. Plant Physiol 135:2271–2278

Bastow R, Mylne JS, Lister C, Lippman Z, Martienssen RA, Dean C (2004) Vernalization requires epigenetic silencing of *FLC* by histone methylation. Nature 427:164–167

Borner R, Kampmann G, Chandler J, Gleiβner R, Wisman E, Apel K, Melzer S (2000) A MADS domain gene involved in the transition to flowering in *Arabidopsis*. Plant J 24:591–599

Cameron RK, Zaton K (2004) Intercellular salicylic acid accumulation is important for age-related resistance in *Arabidopsis* to *Pseudomonas syringae*. Physiol Mol Plant P 65:197–209

Carviel JL, Al-Daoud F, Neumann M, Mohammad A, Provart NJ, Moeder W, Yoshioka K, Cameron RK (2009) Forward and reverse genetics to identify genes involved in the age-related resistance response in *Arabidopsis thaliana*. Mol Plant Pathol 10:621–634

Chien CJ, Sussex IM (1996) Differential regulation of trichome formation on the adaxial and abaxial leaf surfaces by gibberellins and photoperiod in *Arabidopsis thaliana* (L.) Heynh. Plant Physiol 111:1321–1328

Corbesier L, Gadisseur I, Silvestre G, Jacqmard A, Bernier G (1996) Design in *Arabidopsis thaliana* of a synchronous system of floral induction by one long day. Plant J 9:947–952

Corbesier L, Vincent C, Jang S, Fornara F, Fan Q, Searle I, Giakountis A, Farrona S, Gissot L, Turnbull C, Coupland G (2007) FT protein movement contributes to long-distance signaling in floral induction of *Arabidopsis*. Science 316:1030–1033

Develey-Rivière M, Galiana E (2007) Resistance to pathogens and host developmental stage: a multifaceted relationship within the plant kingdom. New Phytol 175:405–416

Fornara F, de Montaigu A, Coupland G (2010) Snapshot: control of flowering in *Arabidopsis*. Cell 141(550–550):e2

Giakountis A, Cremer F, Sim S, Reymond M, Schmitt J, Coupland G (2010) Distinct patterns of genetic variation alter flowering responses of *Arabidopsis* accessions to different daylengths. Plant Physiol 152:177–191

Gregory FG, Hussey GG (1953) Photoperiodic responses of *Arabidopsis thaliana*. Proc Linn Soc Lond 164:137–139

Hartmann U, Höhmann S, Nettesheim K, Wisman E, Saedler H, Huijser P (2000) Molecular cloning of *SVP*: a negative regulator of the floral transition in *Arabidopsis*. Plant J 21:351–360

Helliwell CA, Wood CC, Robertson M, Peacock WJ, Dennis ES (2006) The *Arabidopsis* FLC protein interacts directly in vivo with *SOC1* and *FT* chromatin and is part of a high-molecular-weight protein complex. Plant J 46:183–192

Hempel FD, Feldman LJ (1994) Bi-directional inflorescence development in *Arabidopsis thaliana:* acropetal initiation of flowers and basipetal initiation of paraclades. Planta 192:276–286

Henderson IR, Liu F, Drea S, Simpson GG, Dean C (2005) An allelic series reveals essential roles for FY in plant development in addition to flowering-time control. Development 132:3597–3607

Hugot K, Aimé S, Conrod S, Poupet A, Galiana E (1999) Developmental regulated mechanisms affect the ability of a fungal pathogen to infect and colonize tobacco leaves. Plant J 20:163–170

Imaizumi T, Tran HG, Swartz TE, Briggs WR, Kay SA (2003) FKF1 is essential for photoperiod-specific light signaling in *Arabidopsis*. Nature 426:302–306

Irish VF, Sussex IM (1990) Function of the apetala-1 gene during *Arabidopsis* floral development. Plant Cell 2:741–753

Jaeger KE, Wigge PA (2007) FT protein acts as a long-range signal in *Arabidopsis*. Curr Biol 17:1050–1054

Jang S, Torti S, Coupland G (2009) Genetic and spatial interactions between *FT*, *TSF and SVP* during the early stages of floral induction in *Arabidopsis*. Plant J 60:614–625

Jin JB, Jin YH, Lee J, Miura K, Yoo CY, Kim W, Oosten MV, Hyun Y, Somera DE, Lee I, Yun D, Bresan RA, Hasegawa PM (2008) The SUMO E3 ligase, *AtSIZ1*, regulates flowering by controlling a salicylic acid-mediated floral promotion pathway and through affects on *FLC* chromatin structure. Plant J 53:530–540

Johanson U, West J, Lister C, Michaels S, Amasino R, Dean C (2000) Molecular analysis of *FRIGIDA*, a major determinant of natural variation in *Arabidopsis* flowering-time. Science 290:344–347

Kardailsky I, Shukla VK, Ahn JH, Dagenais N, Christensen SK, Nguyen JT, Chory J, Harrison MJ, Weigel D (1999) Activation tagging of the floral inducer *FT*. Science 286:1962–1965

Kobayashi Y, Kaya H, Goto K, Iwabuchi M, Araki T (1999) A pair of related genes with antagonistic roles in mediating flowering signals. Science 286:1960–1962

Koornneef M, Hanhart CJ, van der Veen JH (1991) A genetic and physiological analysis of late flowering mutants in *Arabidopsis thaliana*. Mol Gen Genet 229:57–66

Koornneef M, Alonso-Blanco C, Blankestijn-de Vries H, Hanhart CJ, Peeters AJM (1998) Genetic interactions among late-flowering mutants of *Arabidopsis*. Genetics 148:885–892

Kus JV, Zaton K, Sarkar R, Cameron RK (2002) Age-related resistance in *Arabidopsis* is a developmentally-regulated defense response to *Pseudomonas syringae*. Plant Cell 14:479–490

Lee I, Amasino RM (1995) Effect of vernalization, photoperiod, and light quality on the flowering phenotype of *Arabidopsis* plants containing the *FRIGIDA* gene. Plant Physiol 108:157–162

Lee I, Blecker A, Amasino R (1993) Analysis of naturally occurring late flowering in *Arabidopsis thaliana*. Mol Gen Genet 237:171–176

Lee J, Nam J, Park HC, Na G, Miura K, Jin JB, Yoo CY, Baek D, Kim DH, Jeong JC, Kim D, Lee SY, Salt DE, Mengiste T, Gong Q, Ma S, Bohnert HJ, Kwak S, Bressan RA, Hasegawa PM, Yun D (2006) Salicylic acid-mediated innate immunity in *Arabidopsis* is regulated SIZ1 SUMO E3 ligase. Plant J 49:79–90

Lee JH, Yoo SJ, Park SH, Hwang I, Lee JS, Ahn JH (2007) Role of *SVP* in the control of flowering-time by ambient temperature in *Arabidopsis*. Gene Dev 21:397–402

Lee J, Oh M, Park H, Lee I (2008) SOC1 translocated to the nucleus by interaction with AGL24 directly regulates *LEAFY*. Plant J 55:832–843

Lee S, Han S, Sririyanum M, Park C, Seo Y, Ronald P (2009) A type I-secreted, sulfated peptide triggers XA21-mediated innate immunity. Science 326:850–853

Li D, Liu C, Shen L, Wu Y, Chen H, Robertson M, Helliwell CA, Ito T, Meyerowitz E, Yu H (2008) A repressor complex governs the integration of flowering signals in *Arabidopsis*. Dev Cell 15:110–120

Liljegren SJ, Gustafson-Brown C, Pinyopich A, Ditta GS, Yanofsky MF (1999) Interactions among *APETALA1*, *LEAFY*, and *TERMINAL FLOWER1* specify meristem fate. Plant Cell 11:1007–1018

Liu C, Chen H, Er HL, Soo HM, Kumar PP, Han J, Liou YC, Yu H (2008) Direct interaction of *AGL24* and *SOC1* integrates flowering signals in *Arabidopsis*. Development 135:1481–1491

Liu J, Li W, Ning Y, Shirsekar G, Cai Y, Wang X, Dai L, Wang Z, Liu W, Wang GL (2012) The U-box E3 ligase SPL11/PUB13 is

a convergence point of defense and flowering signaling in plants. Plant Physiol 160:28–37

Martínez C, Pons E, Prats G, León J (2004) Salicylic acid regulates flowering time and links defense responses and reproductive development. Plant J 37:209–217

Mazzola M, Leach JE, Nelson R, White FF (1994) Analysis of the interaction between *Xanthomonas oryzae* pv. *oryzae* and the rice cultivars IR24 and IRBB21. Phytopathology 84:392–397

McDaniel CN, Singer SR, Smith SME (1992) Developmental states associated with the floral transition. Dev Biol 153:59–69

Michaels SD, Amasino RM (1999) *FLOWERING LOCUS C* encodes a novel *MADS* domain protein that acts as a repressor of flowering. Plant Cell 11:949–956

Michaels SD, Amasino RM (2001) Loss of *FLOWERING LOCUS C* activity eliminates the late-flowering phenotype of *FRIGIDA* and autonomous pathway mutations but not responsiveness to vernalization. Plant Cell 13:935–941

Michaels SD, Himelblau E, Kim SY, Schomburg FM, Amasino RM (2005) Integration of flowering signals in winter-annual *Arabidopsis*. Plant Physiol 137:149–156

Ossowski S, Schneeberger K, Clark RM, Lanz C, Warthmann N, Weigel D (2008) Sequencing of natural strains of *Arabidopsis thaliana* with short reads. Genome Res 18:2024–2033

Ossowski S, Schneeberger K, Lucas-Lledó JI, Warthmann N, Clark RM, Shaw RG, Weigel D, Lynch M (2010) The rate and molecular spectrum of spontaneous mutations in *Arabidopsis thaliana*. Science 327:92–94

Poethig SR (1990) Phase change and the regulation of shoot morphogenesis in plants. Science 250:923–930

Putterill J, Robson F, Lee K, Simon R, Coupland G (1995) The *CONSTANS* gene of *Arabidopsis* promotes flowering and encodes a protein showing similarities to zinc finger transcription factors. Cell 80:847–857

Rèdei GP (1962) Supervital mutants of *Arabidopsis*. Genetics 47:443–460

Rivas-San Vicente M, Plasencia J (2011) Salicylic acid beyond defence: its role in plant development. J Exp Bot 62:3321–3338

Rusterucci C, Zhao Z, Haines K, Mellersh D, Neumann M, Cameron RK (2005) Age-related resistance to *Pseudomonas syringae pv. tomato* is associated with the transition to flowering in *Arabidopsis* and is effective against *Peronospora parasitica*. Physiol Mol Plant P 66:222–231

Samach A, Onouchi H, Gold SE, Ditta GS, Schwarz-Sommer Z, Yanofsky MF, Coupland G (2000) Distinct roles of CONSTANS target genes in reproductive development of *Arabidopsis*. Science 288:1613–1616

Santuari L, Hardtke CS (2010) The case for resequencing studies of *Arabidopsis thaliana* accessions: mining the dark matter of natural genetic variation. F1000 Rep 2:85

Schultz EA, Haughn GW (1993) Genetic analysis of the floral initiation process (FLIP) in *Arabidopsis*. Development 119:745–765

Schwarz S, Grande AV, Bujdoso N, Saedler H, Huijser P (2008) The microRNA regulated SBP-box genes SPL9 and SPL15 control shoot maturation in *Arabidopsis*. Plant Mol Biol 67:183–195

Searle I, He Y, Turck F, Vincent C, Fornara F, Kröber S, Amasino RA, Coupland G (2006) The transcription factor FLC confers a flowering response to vernalization by repressing meristem competence and systemic signaling in *Arabidopsis*. Gene Dev 20:898–912

Shannon S, Meeks-Wagner DR (1991) A mutation in the *Arabidopsis TFL1* gene affects inflorescence meristem development. Plant Cell 3:877–892

Shannon S, Meeks-Wagner DR (1993) Genetic interactions that regulate inflorescence development in *Arabidopsis*. Plant Cell 5:639–655

Sheldon CC, Burn JE, Perez PP, Metzger J, Edwards JA, Peacock J, Dennis ES (1999) The *FLF* MADS box gene: a repressor of flowering in *Arabidopsis* regulated by vernalization and methylation. Plant Cell 11:445–458

Simpson GG, Dean C (2002) *Arabidopsis*, the rosetta stone of flowering time? Science 296:285–289

Suárez-López P, Wheatley K, Robson F, Onouchi H, Valverde F, Coupland G (2001) *CONSTANS* mediates between the circadian clock and the control of flowering in *Arabidopsis*. Nature 410:1116–1120

Telfer A, Bollman KM, Poethig SR (1997) Phase change and the regulation of trichome distribution in *Arabidopsis thaliana*. Development 124:645–654

Usami T, Horiguchi G, Yano S, Tsukaya H (2009) The *more and smaller cells* mutants of *Arabidopsis* identify roles for *SQAMOSA PROMOTER BINDING PROTEIN-LIKE* genes in the control of heteroblasty. Development 136:955–964

Veley KM, Michaels SD (2008) Functional redundancy and new roles for genes of the autonomous floral promotion pathway. Plant Physiol 147:682–695

Vlot CA, Dempsey DA, Klessig DF (2009) Salicylic acid, a multifaceted hormone to combat disease. Annu Rev Phytopathol 47:177–206

Wang J, Schwab R, Czech B, Mica E, Weigel D (2008) Dual effects of miR156-targeted *SPL* genes and *CYP78A5/KLUH* on plastochron length and organ size in *Arabidopsis thaliana*. Plant Cell 20:1231–1243

Wang G, Seabolt S, Hamdoun S, Ng G, Park J, Lu H (2011) Multiple roles of WIN3 in regulating disease resistance, cell death, and flowering-time in *Arabidopsis*. Plant Physiol 156:1508–1519

Weigel D, Alvarez J, Smyth DR, Yanofsky MF, Meyerowitz EM (1992) *LEAFY* controls floral meristem identity in *Arabidopsis*. Cell 69:843–859

Whalen MC (2005) Host defense in a developmental context. Mol Plant Pathol 6:347–360

Wigge PA, Kim MC, Jaeger KE, Busch W, Schmid M, Lohmann JU, Weigel D (2005) Integration of spatial and temporal information during floral induction in *Arabidopsis*. Science 309:1056–1059

Willmann MR, Poethig SR (2005) Time to grow up: the role of smallRNAs in plants. Curr Opin Plant Biol 8:548–552

Wu G, Poethig S (2006) Temporal regulation of shoot development in *Arabidopsis thaliana* by *miR156* and its target *SPL3*. Development 133:3539–3547

Wu G, Park MY, Conway SR, Wang J, Weigel D, Poethig SR (2009) The sequential action of miR156 and miR172 regulates developmental timing in *Arabidopsis*. Cell 138:750–759

Yanovsky MJ, Kay SA (2002) Molecular basis of seasonal time measurement in *Arabidopsis*. Nature 419:308–312

Yoo SK, Chung KS, Kim J, Lee JH, Hong SM, Yoo SJ, Yoo SY, Lee JS, Ahn JH (2005) *CONSTANS* activates *SUPPRESSOR OF OVEREXPRESSION OF CONSTANS 1* through *FLOWERING LOCUS T* to promote flowering in *Arabidopsis*. Plant Physiol 139:770–778

2.8 Supplementary material

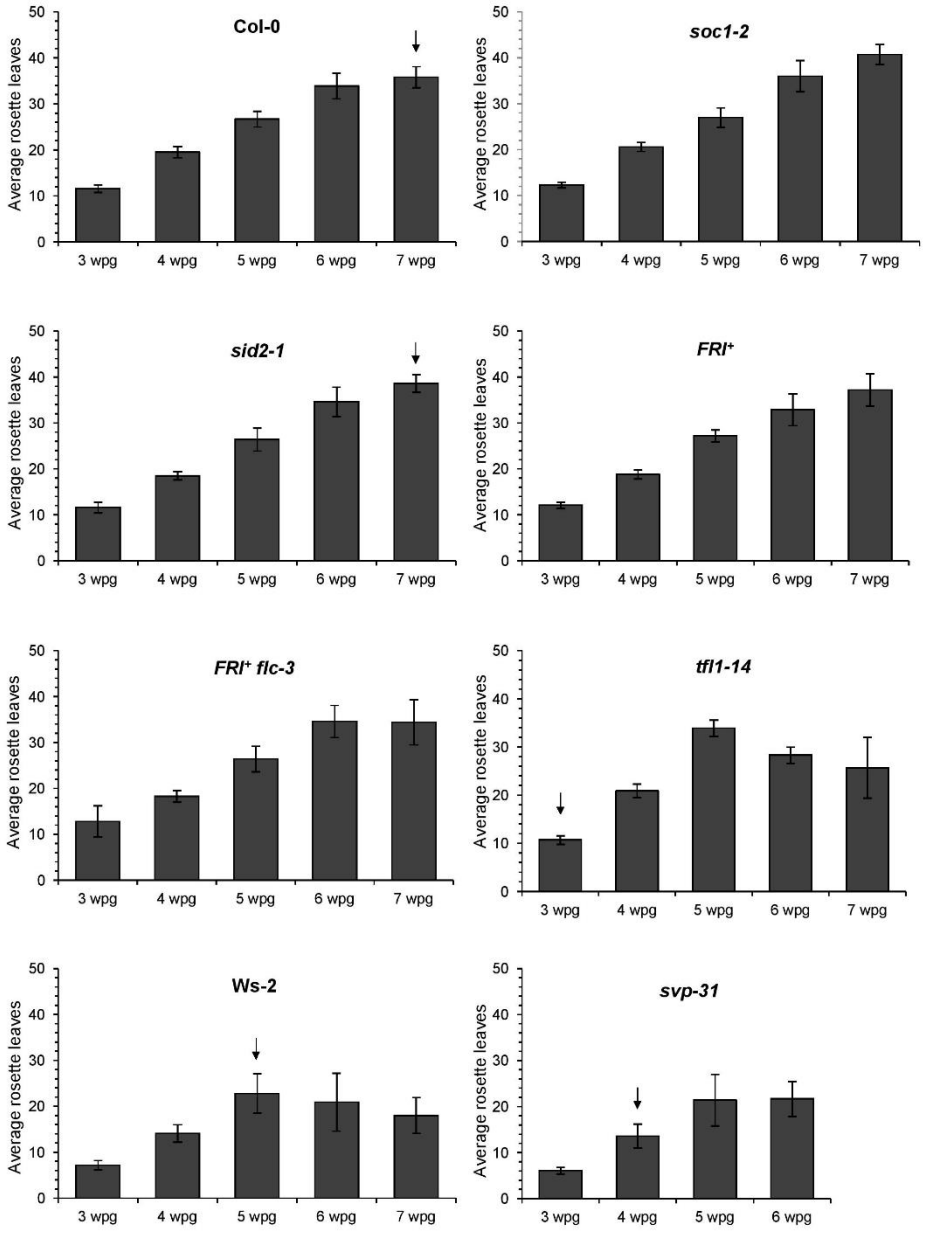

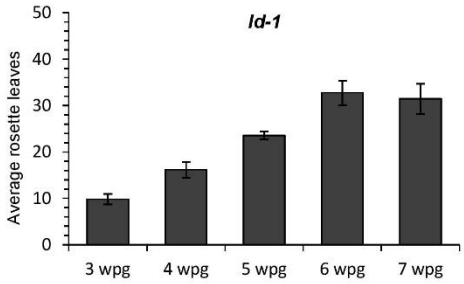

Supplementary Fig. 1 Average rosette leaf number between three and seven wpg. Each week a group of nine short-day-grown plants (Col-0, *sid2-1*, *FRI*$^{+}$ *flc-3*, *FRI*$^{+}$, Ws-2, *soc1-2*, *svp-31, tfl1-14*, *Id-1*) were analyzed for average rosette leaf number. For two of the three early-flowering lines (*svp-31*, *tfl1-14*) we observed that rosette leaf number continued to increase even after 100% of plants showed inflorescence stems. This is probably because the rosette leaf number values presented are an underestimate since only those leaves large enough to be resolved without magnification were counted at a given time. Therefore, several of the last rosette leaves were produced before the floral transition but were too small to count until one or two weeks after the floral transition. Arrows above bars mark the time at which 100% of plants showed inflorescence meristems.

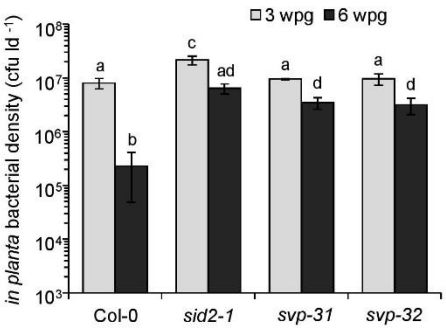

Percent inflorescence stems				
	Col-0	*sid2-1*	*svp-31*	*svp-32*
3 wpg	0	0	100	100
6 wpg	33	33	100	100

Average rosette leaf number				
	Col-0	*sid2-1*	*svp-31*	*svp-32*
3 wpg	13.8 ± 0.7	13.8 ± 0.8	9.8 ± 2.0	7.4 ± 0.7
6 wpg	36.4 ± 1.3	35.9 ± 1.2	14.1 ± 2.4	13.9 ± 2.6

Supplementary Fig. 2 *svp* mutants are defective for ARR. Col-0, *sid2-1, svp-31, and svp-32* were grown in short days and tested for ARR at three and six wpg. Plants were inoculated with 10^6 cfu ml^{-1} virulent *Pst* (DC3000) and bacterial levels were quantified three days later. Data are presented as the mean of three biological replicates. Error bars indicate standard deviation. Different letters indicate significant differences (Tukey's HSD [$p<0.01$]). Visible inflorescence stems and average rosette leaf number were scored at 3 and 6 wpg. Rosette leaf number values are presented as the average ± standard deviation (n=9). This experiment was performed twice with similar results.

Chapter 3 – Investigation of intercellular salicylic acid accumulation during compatible and incompatible *Arabidopsis-Pseudomonas syringae* interactions using a fast neutron-generated mutant allele of *EDS5* identified by genetic mapping and whole-genome sequencing

PREFACE

This chapter consists of a published research article which investigates intercellular SA accumulation during PTI and ETI in young plants. Specifically, wild-type plants accumulated intercellular SA in response *Pst(avrRpt2)*, which triggers ETI, suggesting that intercellular SA accumulation is a component of RPS2-mediated ETI. Intercellular SA also accumulated in plants responding to a COR-deficient strain of *P. syringae*, suggesting that COR suppresses intercellular SA accumulation and that intercellular SA accumulation is a component of PTI. This article also describes the identification of the causal mutation in the ARR-defective *iap1-1* mutant by map-based cloning and whole-genome sequencing. This approach, combined with other supporting evidence (complementation testing, gel electrophoresis and sequencing of the mutated region) showed that *iap1-1* has a complex mutation in *EDS5,* a gene that codes for the chloroplast SA transporter. This chapter also includes an addendum to the original article in which the results are discussed further.

Author contributions

DW, JC, PC, and MI performed the experiments. JC performed the disease resistance, electrolyte leakage, and SA quantification experiments shown in Figures 3.1 and 3.2, as well as the trypan blue staining shown in Figure S3.1. PC and MI performed the SA quantification experiments shown in Figure 3.3 and assisted with the electrolyte leakage assays shown in Figure 3.4. DW performed the disease resistance, electrolyte leakage, SA quantification, and other experiments shown in Figures 3.4-3.6, and prepared Table S3.1. JC performed the map-based cloning and DW performed the whole-genome sequencing with help from the Farncombe Institute staff for library preparation, and VC for data analysis. DW and RC wrote the manuscript and addendum with assistance from the other authors. RC, JC, and DW conceived and designed the experiments.

Citation and copyright information

Citation: Carviel, J.L., Wilson, D.C., Isaacs, M., Carella, P., Catana, V., Golding, B., Weretilnyk, E.A., Cameron, R.K. (2014). Investigation of intercellular salicylic acid accumulation during compatible and incompatible *Arabidopsis-Pseudomonas syringae* interactions using a fast neutron-generated mutant allele of *EDS5* identified by genetic mapping and whole-genome sequencing. PLoS ONE, 9: e88608. DOI: 10.1371/journal.pone.0088608.

Citation: Wilson, D.C., Carella, P., Cameron, R.K. (2014). Intercellular salicylic acid accumulation during compatible and incompatible *Arabidopsis-Pseudomonas syringae* interactions. Addendum in Plant Signaling & Behavior, 9: e29362. DOI: dx.doi.org/10.4161/psb.29362.

OPEN ACCESS Freely available online

PLOS ONE

Investigation of Intercellular Salicylic Acid Accumulation during Compatible and Incompatible *Arabidopsis-Pseudomonas syringae* Interactions Using a Fast Neutron-Generated Mutant Allele of *EDS5* Identified by Genetic Mapping and Whole-Genome Sequencing

Jessie L. Carviel[•], Daniel C. Wilson[•], Marisa Isaacs[¶], Philip Carella[¶], Vasile Catana, Brian Golding, Elizabeth A. Weretilnyk, Robin K. Cameron*

McMaster University, Department of Biology, Hamilton, Ontario, Canada

Abstract

A whole-genome sequencing technique developed to identify fast neutron-induced deletion mutations revealed that *iap1-1* is a new allele of *EDS5* (*eds5-5*). RPS2-AvrRpt2-initiated effector-triggered immunity (ETI) was compromised in *iap1-1/eds5-5* with respect to *in planta* bacterial levels and the hypersensitive response, while intra- and intercellular free salicylic acid (SA) accumulation was greatly reduced, suggesting that SA contributes as both an intracellular signaling molecule and an antimicrobial agent in the intercellular space during ETI. During the compatible interaction between wild-type Col-0 and virulent *Pseudomonas syringae* pv. *tomato* (*Pst*), little intercellular free SA accumulated, which led to the hypothesis that *Pst* suppresses intercellular SA accumulation. When Col-0 was inoculated with a coronatine-deficient strain of *Pst*, high levels of intercellular SA accumulation were observed, suggesting that *Pst* suppresses intercellular SA accumulation using its phytotoxin coronatine. This work suggests that accumulation of SA in the intercellular space is an important component of basal/PAMP-triggered immunity as well as ETI to pathogens that colonize the intercellular space.

Citation: Carviel JL, Wilson DC, Isaacs M, Carella P, Catana V, et al. (2014) Investigation of Intercellular Salicylic Acid Accumulation during Compatible and Incompatible *Arabidopsis-Pseudomonas syringae* Interactions Using a Fast Neutron-Generated Mutant Allele of *EDS5* Identified by Genetic Mapping and Whole-Genome Sequencing. PLoS ONE 9(3): e88608. doi:10.1371/journal.pone.0088608

Editor: Maeli Melotto, University of Texas, United States of America

Received October 31, 2013; **Accepted** January 10, 2014; **Published** March 4, 2014

Funding: This research was funded by a Natural Sciences and Engineering Research Council of Canada grant to RKC, an Ontario Research Excellence Fund grant to EAW, Ontario Graduate Scholarships to DW and MI, and McMaster University for growth chamber maintenance. The funders had no role in study design, data collection and analysis, decision to publish, or preparation of the manuscript.

Competing Interests: The authors have declared that no competing interests exist.

* E-mail: rcamero@mcmaster.ca

• These authors contributed equally to this work.

¶ These authors also contributed equally to this work.

Introduction

In response to pathogens *Arabidopsis* relies on various induced defenses. Basal resistance or PTI (PAMP-Triggered Immunity) is a defense response elicited by the recognition of conserved pathogen- or microbe-associated molecular patterns (PAMPs or MAMPs) by pattern recognition receptors [1]. Some bacteria, for example, certain pathovars of *Pseudomonas syringae*, are able to suppress PTI by delivering effector proteins into plant cells using a type-three secretion system [1]. Several of these effectors interfere with various stages of PTI, contributing to the pathogen's ability to cause disease on host plants [2–6]. In response, many plants possess resistance genes (R genes) that recognize effectors either directly or indirectly, leading to R gene-mediated resistance or Effector-Triggered Immunity (ETI) [7]. Some of the defense mechanisms associated with ETI are thought to overlap with those of PTI although they seem to occur more rapidly and with greater strength during ETI [1]. These defenses include extensive transcriptional reprogramming resulting in cellular changes such as expression of defense genes (e.g., *PR [PATHOGENESIS-RELATED]* genes), production of phytoalexins, salicylic acid (SA) biosynthesis, and cell-wall modifications [8–10]. In addition, ETI is often associated with the hypersensitive response (HR), a form of programmed cell death thought to contribute to inhibition of pathogen spread [11].

Many R genes encode NB-LRR (nucleotide-binding leucine-rich repeat) proteins which can be subdivided into two groups; those possessing N-terminal coiled-coil domains (CC-NB-LRR) and those with N-terminal TIR (Toll and Interleukin-1 receptor) domains (TIR-NB-LRR) [7]. CC- and TIR- type R genes are generally thought to function using separate pathways defined by their requirement for either *NDR1 (NON-RACE-SPECIFIC DISEASE RESISTANCE1)* or *EDS1 (ENHANCED DISEASE SUSCEPTIBILITY1)* respectively [12]. For example, *RPS2* encodes a CC-NB-LRR resistance protein that confers resistance to strains of *P. syringae* expressing *avrRpt2* [13,14]. Similarly, the TIR-NB-LRR resistance protein RPS4 confers resistance to strains of *P. syringae* expressing *avrRps4* [15,16].

Another form of induced disease resistance is the developmentally regulated Age-Related Resistance (ARR) response (reviewed in [17,18]). In *Arabidopsis*, ARR results in enhanced resistance to certain pathogens with increasing plant age [19]. Specifically, 6-week-old Col-0 plants grown in short days limit the growth of *P. syringae* pv. *tomato (Pst)* to levels that are 10- to 100-fold lower than in 3-week-old plants. Unlike PTI and ETI, the molecular mechanisms underpinning ARR in *Arabidopsis* are only beginning to be understood.

A common player in many disease resistance pathways is the phytohormone SA (reviewed in [20,21]). Wild-type *Arabidopsis* accumulates SA in response to inoculation with both virulent and avirulent *Pst* [22]. The importance of SA accumulation for different disease resistance responses is typically tested using transgenic and mutant plants with a reduced ability to accumulate SA. *NahG* plants expressing a bacterial salicylate hydroxylase gene convert SA to catechol and consequently accumulate very little SA [23]. *ICS1/SID2 (ISOCHORISMATE SYNTHASE1/SALICYLIC ACID INDUCTION DEFICIENT2)* encodes a key enzyme in the biosynthetic pathway responsible for most pathogen-responsive SA production in *Arabidopsis* [24,25]. *EDS5/SID1 (ENHANCED DISEASE SUSCEPTIBILITY5)* encodes a multidrug and toxin extrusion (MATE) family protein that localizes to the chloroplast envelope and transports SA from its site of synthesis into the cytoplasm [26–29]. Both *sid2* and *eds5/sid1* mutants accumulate little SA in response to pathogens [22]. *NahG*, *sid2*, and *eds5* support higher growth of virulent strains of *P. syringae* compared to wild-type plants suggesting that SA accumulation is important in limiting pathogen growth even in a compatible (susceptible) interaction [22,23,30,31]. ETI is compromised in *NahG* [8,23,32–34], *sid2*, and *eds5* [22,32,35] when initiated by several R genes (*RPS2*, *RPS4*, *RPM1*) interacting with their corresponding effectors. In experiments using type-three secretion system mutants or PAMPs (flg22) to initiate PTI in wild-type Col-0 or *sid2*, Tsuda et al. [36] demonstrated that SA accumulation is required for a successful PTI response. Thus, in *Arabidopsis*, SA accumulation is important in numerous ETI and PTI pathways.

SA accumulation is also required for the *Arabidopsis* ARR response to *Pst* as demonstrated by the ARR-defective phenotypes of *NahG*, *sid2-1*, and *sid1/eds5-3* [19,37]. Examination of mature plants responding to *Pst* revealed 6-fold higher SA levels in intercellular washing fluids (IWFs) relative to young plants [38]. Anti-microbial activity was often observed in the IWFs of mature plants inoculated with *Pst* as demonstrated by inhibition of *in vitro Pst* growth [38]. Preventing SA accumulation in the intercellular space by pressure-infiltrating ARR-competent plants with salicylate hydroxylase disrupted their ability to undergo ARR. Conversely, adding exogenous SA to the intercellular space rescued ARR-defective mutants and enhanced ARR in wild-type Col-0 [38]. Taken together this data led to the hypothesis that SA may act as an antimicrobial agent in the intercellular space during ARR.

A classical mutant screen for mature plants with defects in ARR was used to identify genes involved in the ARR response, including *iap1-1 (important for the ARR pathway1-1)*. Along with their ARR-defective phenotype, mature *iap1-1* plants accumulate little SA [37]. In this work, a combination of genetic mapping, whole-genome sequencing, and complementation analysis was used to identify *iap1-1* as a mutant allele of *EDS5*. While mapping the *iap1-1* mutation, we investigated the role of IAP1 in RPS2- and RPS4-mediated ETI by measuring bacterial levels and monitoring HR cell death using trypan staining and electrolyte leakage. Intercellular SA accumulation is important during ARR and requires functional IAP1, therefore we investigated both inter- and intracellular SA accumulation during ETI (incompatible interaction) and during a compatible interaction with virulent *Pst* in young Col-0 and *iap1-1*. Our results suggest that inter- and intracellular SA accumulation is important during both compatible and incompatible interactions.

Results

The *iap1-1* mutant is partially compromised in resistance to *Pst(avrRpt2)* and *Pst(avrRps4)*

The *iap1-1* mutant is defective for ARR to virulent *Pst* [37]. To determine whether *IAP1* is also required during NDR1- or EDS1-dependent ETI/incompatible interactions, young plants at 3 weeks post-germination (wpg) were inoculated with 10^6 cfu (colony-forming units) ml^{-1} *Pst*, *Pst(avrRpt2)*, or *Pst(avrRps4)* and *in planta* bacterial density was measured 3 days post-inoculation (dpi). *Pst(avrRpt2)* grew to significantly lower levels than *Pst* in both Col-0 and *iap1-1* indicating that an ETI response occurred (Figure 1A). However, *Pst(avrRpt2)* levels were significantly higher in *iap1-1* compared to Col-0 indicating that NDR1-dependent ETI to *Pst(avrRpt2)* is partially compromised by the *iap1-1* mutation. Similar results were obtained when Col-0 and *iap1-1* were inoculated with *Pst(avrRps4)* which indicates that EDS1-dependent ETI to *Pst(avrRps4)* is also partially compromised by the *iap1-1* mutation (Figure 1B). Therefore, *IAP1* is required for a full and robust ETI response to *Pst* carrying effectors recognized by two distinct classes of resistance proteins.

The hypersensitive response is partially compromised in *iap1-1*

Since the hypersensitive response (HR) is a common component of ETI elicited by both AvrRpt2 and AvrRps4 effectors [13,14,16] we investigated whether the *iap1-1* ETI defect was accompanied by a reduced HR. Four-week-old Col-0 and *iap1-1* were inoculated with 10^7 cfu ml^{-1} *Pst(avrRpt2)* or 10 mM $MgCl_2$ (mock-inoculated) and leaves were collected at 24 hours post-inoculation (hpi) and stained with trypan blue. Trypan blue does not pass through intact cell membranes of live cells therefore it selectively stains dying or dead cells and can be used to measure HR-associated cell death [47]. Visual analysis revealed little staining in mock-inoculated leaves whereas intense staining was observed in leaves inoculated with *Pst(avrRpt2)* (Figure S1). There was no obvious difference in the intensity of staining between Col-0 and *iap1-1* leaves suggesting that *iap1-1* undergoes a wild-type HR. By floating treated leaf tissue in a solution and measuring conductance, electrolyte leakage from dead or damaged cells can be quantified and used to track the progression of HR cell death over time [48]. Electrolyte leakage was monitored in tissue collected from 4-week-old Col-0 and *iap1-1* that were either mock-inoculated or inoculated with 10^7 cfu ml^{-1} *Pst(avrRpt2)* (Figure 1C). Mock-inoculated leaves showed little change in electrolyte leakage over time. Electrolyte leakage from leaves inoculated with *Pst(avrRpt2)* increased substantially between 7 and 13 hpi. By 13 hpi, electrolyte leakage from Col-0 leaves inoculated with *Pst(avrRpt2)* was approximately 4-fold higher than mock-inoculated tissue, while the increase in electrolyte leakage from *iap1-1* leaves was more modest (2.7-fold increase compared to mock-inoculated tissue). Electrolyte leakage from *iap1-1* leaves was significantly less than from wild-type leaves between 10 and 13 hpi with *Pst(avrRpt2)* (T-test $P<0.01$) suggesting that HR-mediated cell death is compromised in *iap1-1*.

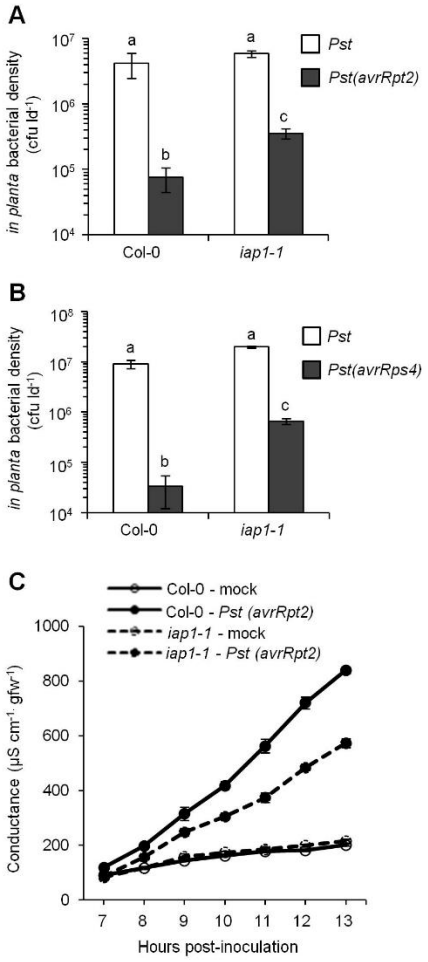

Figure 1. Effector-triggered immunity and the hypersensitive response in *iap1-1*. Three-week-old Col-0 and *iap1-1* were inoculated with 10^6 cfu ml^{-1} *Pseudomonas syringae* pv. *tomato (Pst)* and *Pst(avrRpt2)* (A) or *Pst(avrRps4)* (B). *In planta* bacterial levels (colony-forming units per leaf disc [cfu ld^{-1}]) were determined at 3 days post-inoculation and are presented as the mean ± standard deviation of three sample replicates. Different letters indicate significant differences (ANOVA, Duncan's MRT, $P<0.05$). Both experiments were repeated at least three times with similar results. (C) Electrolyte leakage was monitored in tissue collected from plants inoculated with 10^7 cfu ml^{-1} *Pst(avrRpt2)* or 10 mM $MgCl_2$ (mock) and is presented as the mean ± standard deviation of three samples. This experiment was repeated twice with similar results.
doi:10.1371/journal.pone.0088608.g001

Intracellular SA accumulation in response to *Pst* and *Pst(avrRpt2)*

SA is required for RPS2- and RPS4-mediated immunity [8,22,23,32–34]. If young *iap1-1* plants accumulate little SA like mature *iap1-1* [37], this could explain the compromised ETI response observed in young *iap1-1*. To test this hypothesis, an ADPWH_*lux* SA biosensor [42] was used to measure SA levels in both intercellular (IWFs) and intracellular (leaves minus IWFs) compartments of young (4 wpg) Col-0 and *iap1-1* plants that were untreated, mock-inoculated, or inoculated with 10^6 cfu ml^{-1} *Pst* or *Pst(avrRpt2)* (Figure 2). Intra- and intercellular SA results are discussed in this section and the next section respectively. Col-0 and *iap1-1* had similar levels of intracellular free SA in both untreated and mock-inoculated tissues at 12, 24, and 48 hpi (<100 ng gfw^{-1}) (Figure 2A). Col-0 inoculated with *Pst* accumulated 199 ng gfw^{-1} intracellular free SA by 48 hpi, significantly more than mock-inoculated controls (T-test $P<0.01$), whereas intracellular free SA levels in *iap1-1* were similar to mock-inoculated controls at all time points. In response to *Pst(avrRpt2)*, Col-0 accumulated 546–682 ng gfw^{-1} intracellular free SA at 12, 24, and 48 hpi, whereas *iap1-1* accumulated very little intracellular free SA (109–164 ng gfw^{-1}). This suggests that *iap1-1* accumulates little intracellular free SA in response to *Pst* or *Pst(avrRpt2)*. In addition, Col-0 accumulated higher levels of intracellular free SA in response to *Pst(avrRpt2)* compared to *Pst* (T-test $P<0.01$). Similar results were observed for intracellular total SA (free SA+SA-glucosides) with the exception that *iap1-1* accumulated high levels of total SA at 48 hpi with both *Pst* and *Pst(avrRpt2)*(Figure 2B).

Intercellular SA accumulation in response to *Pst* and *Pst(avrRpt2)*

Intercellular SA accumulation is essential for ARR to *Pst*, and intercellular SA addition and subtraction experiments suggest that SA acts as an anti-microbial agent in the intercellular space during ARR [38]. To determine if SA accumulates in a similar manner in young plants undergoing ETI, SA levels were measured in IWFs collected from leaf tissue of young (4 wpg) Col-0 and *iap1-1* that were untreated, mock-inoculated, or inoculated with 10^6 cfu ml^{-1} *Pst* or *Pst(avrRpt2)* (Figure 2C,D). IWFs from untreated and mock-inoculated Col-0 and *iap1-1* had similar levels of intercellular free SA at 12, 24, and 48 hpi (<200 ng ml IWF^{-1}). Intercellular free SA levels in IWFs collected from Col-0 inoculated with *Pst* were similar to mock-inoculated controls. This is consistent with previous findings that young Col-0 accumulates little intercellular SA in response to *Pst* [38]. IWFs collected from *iap1-1* plants inoculated with *Pst* contained similar free SA levels relative to mock-inoculated controls. IWFs from Col-0 inoculated with *Pst(avrRpt2)* contained high levels of free SA at 12, 24, and 48 hpi (522–1226 ng ml IWF^{-1}), whereas IWFs from *iap1-1* inoculated with *Pst(avrRpt2)* had similar levels as mock-inoculated controls (<200 ng ml IWF^{-1}). Similar results were observed for total SA levels in IWFs with the exception that Col-0 accumulated a modest level of intercellular total SA in response to *Pst* at 48 hpi (262 ng ml IWF^{-1} compared to 60 ng ml IWF^{-1} in mock-treated plants, T-test $P<0.01$). Therefore, *iap1-1* accumulated little intercellular SA in response to *Pst* or *Pst(avrRpt2)*. In addition, wild-type Col-0 accumulated high levels of intercellular SA in response to *Pst(avrRpt2)*, and modest levels in response to virulent *Pst*.

SA accumulation in response to *Pst(avrRpt2)* is RPS2-dependent

SA accumulates (3- to 7-fold, Figure 2) both intra- and intercellularly in young Col-0 during ETI to *Pst(avrRpt2)*. If this response is specific to ETI, SA accumulation should be reduced in the *rps2-201* resistance gene receptor mutant in response to

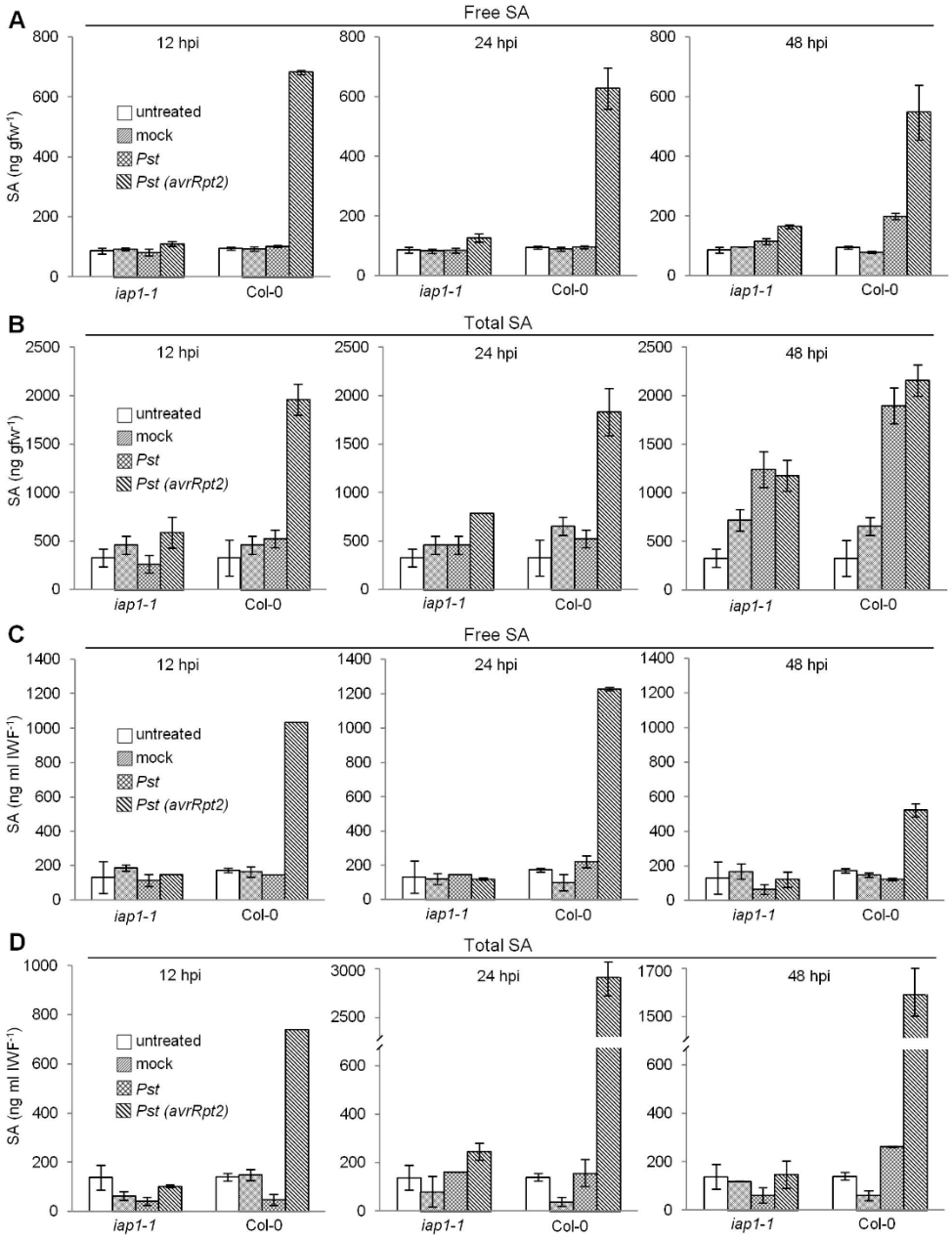

Figure 2. Salicylic acid accumulation in response to *Pst* and *Pst(avrRpt2)*. Four-week-old Col-0 and *iap1-1* were left untreated, mock-inoculated, or inoculated with 10^6 cfu ml^{-1} *Pseudomonas syringae* pv. *tomato (Pst)* or *Pst(avrRpt2)*. Levels of intracellular free salicylic acid (SA) (A) and total SA (free SA+SA glucosides) (B) were determined in leaves from which intercellular washing fluids (IWFs) had been removed. Intercellular levels of free SA (C) and total SA (D) were determined using IWFs collected from the same leaves as in (A) and (B). The mean ± standard deviation of three

replicate samples is shown. T-tests were performed to test for significant differences between means (see results section). This experiment was repeated twice with similar results.
doi:10.1371/journal.pone.0088608.g002

Pst(avrRpt2) [13]. Reduced SA accumulation has been observed in whole leaves of *rps2-201* [49], however, inter- and intracellular SA accumulation were not measured. To determine if SA accumulation is specific to the RPS2-AvrRpt2 pathway, intracellular and intercellular SA levels were measured in leaf tissue collected from Col-0 and *rps2-201* mutants that were untreated, mock-inoculated, or inoculated with 10^6 cfu ml^{-1} *Pst(avrRpt2)* (Figure 3). Untreated and mock-inoculated Col-0 and *rps2-201* leaves contained little intracellular SA (<80 ng gfw^{-1}). Col-0 inoculated with *Pst(avrRpt2)* accumulated substantial intracellular SA (3131 ng gfw^{-1}) whereas *rps2-201* accumulated 6-fold less (504 ng gfw^{-1}). IWFs from untreated and mock-inoculated Col-0 and *rps2-201* contained little SA (<80 ng ml IWF^{-1}). IWFs from Col-0 inoculated with *Pst(avrRpt2)* contained high levels of SA (838 ng ml IWF^{-1}) whereas IWFs from *rps2-201* contained 2-fold lower SA (346 ng ml IWF^{-1}). With respect to both intracellular and intercellular SA levels, *rps2-201* inoculated with *Pst(avrRpt2)* accumulated more SA than mock-inoculated controls but less than Col-0 inoculated with *Pst(avrRpt2)*. Little total SA accumulated in *rps2-201* leaves inoculated with *Pst(avrRpt2)* or in Col-0 inoculated with *Pst* (Figure 2B,D) at 24 hpi, therefore the majority of intracellular and intercellular SA accumulation induced in response to *Pst(avrRpt2)* is dependent on the RPS2-AvrRpt2 pathway.

Intercellular SA accumulated concurrently with cell death during ETI

As indicated above, elevated intercellular SA levels were observed by 12 hpi with *Pst(avrRpt2)* in wild-type Col-0 (Figure 2C,D). How SA reaches the intercellular space is not known, however, it is possible that SA leaks from dead or damaged cells during the HR that accompanies ETI. To test this hypothesis, electrolyte leakage was measured in Col-0 and *rps2-201* controls. To make it possible to associate SA accumulation and cell death, plants were inoculated with the same concentration of *Pst(avrRpt2)* that was used for the SA accumulation experiments (10^6 cfu ml^{-1}, Figure 4A). Use of a smaller and more sensitive conductivity meter made it possible to use small, standardized units of leaf tissue (leaf discs), which increased the accuracy of electrolyte leakage measurements. Since a lower bacterial inoculum concentration was used, fewer cells would undergo the HR, therefore cell death was monitored over 32 hours. If cell death occurs before and/or concurrently with SA accumulation, then SA may access the intercellular space from dying and dead cells. Bacterial density measured at 3 dpi demonstrated that *Pst(avrRpt2)* grew to significantly higher levels in *rps2-201* mutants than in Col-0 indicating that an ETI response occurred in Col-0 and was defective in the *rps2-201* mutant (Figure 4B). Electrolyte leakage from Col-0 inoculated with *Pst(avrRpt2)* was significantly greater than in mock-inoculated controls by 10 hpi (T-test, $P<0.05$) suggesting that cell death was occurring by this time (Figure 4A). Thus, the possibility that SA accesses the intercellular space by leaking out of dead cells during ETI could not be ruled out.

Electrolyte leakage was also measured in *iap1-1* to confirm the results of our first set of electrolyte leakage experiments which were carried out with higher inoculum concentrations and a different technique (see materials and methods). *Pst(avrRpt2)* levels supported by *iap1-1* at 3 dpi were significantly higher than in Col-0, consistent with an ETI defect in *iap1-1* (Figure 4B). In this set of experiments electrolyte leakage from *iap1-1* inoculated with

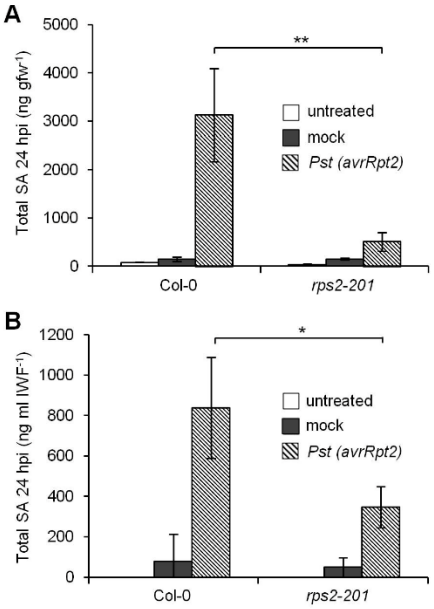

Figure 3. Salicylic acid accumulation in response to *Pst(avrRpt2)* is RPS2-dependent. Intracellular total salicylic acid (SA) levels (A) and intercellular total SA levels (B) were measured at 24 hpi in leaves collected from 4-week-old plants that were untreated, mock-inoculated, or inoculated with 10^6 cfu ml^{-1} *Pseudomonas syringae* pv. *tomato* carrying *avrRpt2* [*Pst(avrRpt2)*]. The mean ± standard deviation of three replicate samples is shown. Asterisks indicate significant differences between means (T-test, * $P<0.05$, ** $P<0.01$). This experiment was repeated twice with similar results.
doi:10.1371/journal.pone.0088608.g003

Pst(avrRpt2) was lower than Col-0 between 14 and 18 hpi, supporting previous evidence for a less robust HR in *iap1-1* relative to Col-0 (Figure 4A). It is interesting to note that electrolyte leakage was greater in *iap1-1* compared to Col-0 from 26 to 32 hpi with *Pst(avrRpt2)*, perhaps due to the fact that *iap1-1* is more susceptible to *Pst* than Col-0, and *Pst* switches to necrotrophy at the end of the infection cycle [50].

Coronatine suppresses SA accumulation during the compatible *Arabidopsis-Pst* interaction

Since young Col-0 accumulates little intercellular SA during the compatible interaction with *Pst* ([38], Figure 2C,D) we hypothesized that intercellular SA accumulation could be an important part of PTI/basal defense that is suppressed by virulent *Pst*. Work done by other groups demonstrated that the *Pseudomonas* phytotoxin coronatine suppresses SA accumulation in whole leaves [51,52]. To test whether coronatine suppresses intra- and/or intercellular SA accumulation, young (4 wpg) wild-type Col-0 were inoculated with *Pst* (strain DC3000) or coronatine-deficient

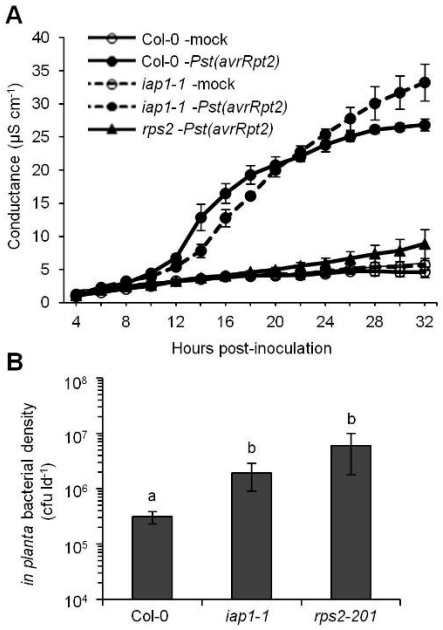

Figure 4. Electrolyte leakage in response to *Pst(avrRpt2)*. (A) Electrolyte leakage was measured in tissue collected from 4-week-old plants inoculated with 10 mM $MgCl_2$ (mock) or 10^6 cfu ml^{-1} *Pseudomonas syringae* pv. *tomato* carrying *avrRpt2* [*Pst(avrRpt2)*]. Values represent the mean ± standard deviation of three sample replicates (B) Four-week-old plants were inoculated with 10^6 cfu ml^{-1} *Pst(avrRpt2)* and bacterial density (colony-forming units per leaf disc [cfu ld^{-1}]) was measured at 3 days post-inoculation. Values represent the mean ± standard deviation of three sample replicates. Different letters indicate significant differences (ANOVA, Tukey's HSD, $P<0.05$). This experiment was repeated once with similar results.
doi:10.1371/journal.pone.0088608.g004

Pst cor$^-$ (strain DC3661) followed by intra- and intercellular SA quantification at 12, 24, and 48 hpi (Figure 5A,B). *Pst cor*$^-$ grew to lower levels than *Pst* by 3 dpi (Figure 5C). As seen previously, Col-0 accumulated modest levels of intracellular free SA by 48 hpi with *Pst* (410 ng gfw^{-1}) relative to untreated controls (144 ng gfw^{-1}, T-test $P<0.01$). In contrast, higher levels of intracellular free SA accumulated in response to *Pst cor*$^-$ at 24 and 48 hpi. A similar trend was observed for intracellular total SA levels. Moreover, Col-0 also accumulated higher levels of intercellular SA in response to *Pst cor*$^-$ relative to *Pst* at 48 hpi (~1400 ng ml IWF^{-1} compared to ~200 ng ml IWF^{-1} respectively). These results suggest that *Pst* suppresses both intra- and intercellular SA accumulation in a coronatine-dependent manner during the compatible interaction in young plants.

Map-based cloning and whole-genome sequencing to identify *iap1-1*

The *iap1-1* mutant was isolated from a screen for ARR-defective plants performed on a population of fast neutron mutants [37]. As demonstrated in this work *iap1-1* is partially compromised in ETI. To identify the causal mutation in *iap1-1* we began with a typical map-based cloning approach. A mapping population was generated and approximately 160 putative homozygous mutant F2s were used to map the *iap1-1* mutation close to marker 461250 (Monsanto Arabidopsis Polymorphism Collection) at 18,087,180 base-pairs (bp) on the long arm of chromosome four. The necessity of screening individual mature plants for an ARR-defective phenotype made the reliable identification of homozygous individuals difficult and time-consuming for fine mapping, therefore we sequenced the *iap1-1* genome in order to locate the mutation.

DNA isolated from a homozygous *iap1-1* individual was used to create a DNA library that was sequenced using an Illumina HiSeq 1500. This generated roughly 68 million paired-end reads which were then mapped to the Col-0 reference genome (TAIR 10) using BWA software [46] resulting in approximately 50-fold coverage of the genome. Since the majority of fast neutron-generated mutations are deletions [53–55] we reasoned that *iap1-1* was likely a deletion mutant. To identify deletions in the *iap1-1* genome we compiled a list of positions in the reference genome that had zero coverage by *iap1-1* reads. A region of zero coverage might indicate that the corresponding sequence is deleted in *iap1-1*. Genome-wide, 814 regions of zero coverage were identified, 244 of which were located on chromosome four. Based on the mapping data, zero-coverage regions located near marker 461250 on chromosome four were investigated. Two zero-coverage regions were found within 500 kb of the marker (Table S1), one of which was located in an intergenic region and was therefore unlikely to represent the causal mutation. Intergenic regions are defined as regions between genes not including recognizable promoters or untranslated regions. The other zero-coverage region was 65 bp within the first exon of *EDS5* (Figure 6A), a gene known to be required for SA accumulation [22] and ARR [19]. Gel electrophoresis of *EDS5* RT-PCR products from *iap1-1* and Col-0 showed a size difference that was consistent with a deletion in the *iap1-1* product (Figure 6B). Sequencing these products confirmed the 65 bp deletion in *iap1-1* and also revealed a 6 bp insertion between the nucleotides flanking the deleted region (Figure 6C). When the Col-0 reference genome was modified to contain this insertion/deletion mutation in *EDS5*, the Illumina reads generated from *iap1-1* mapped continuously across the modified *EDS5* locus, confirming that *iap1-1* harbours the insertion/deletion mutation depicted in Figure 6C. This mutation results in the net loss of 59 nucleotides from the first exon of *EDS5* and causes a frame-shift that produces a premature stop codon after the 52nd amino acid (Figure 6D).

The *iap1-1* and *eds5-3* mutations are allelic

Both *iap1-1* and *eds5-3* mutants have been shown to be required for ARR and pathogen-induced SA accumulation [19,22]. To confirm that *iap1-1* is an allele of *EDS5*, homozygous *iap1-1* mutants carrying the *gl1* marker were crossed with *eds5-3* and the F1 progeny were tested for ARR competence at 6 wpg. If the two mutations are not allelic then ARR should be restored in the F1 generation (complementation) but if *iap1-1* and *eds5-3* are allelic then the F1 generation should remain ARR-defective. Wild-type Col-0 supported low *Pst* levels (5×10^4 cfu ld^{-1}) characteristic of ARR whereas *iap1-1*, *eds5-3*, and *iap1-1*×*eds5-3* F1 plants supported high *Pst* levels (at least 50-fold higher than Col-0) indicating that they are compromised for the ARR response (Figure 6E). Therefore, *iap1-1* and *eds5-3* failed to complement each other indicating that these two mutations are allelic and *iap1-1* is a new mutant allele of *EDS5*.

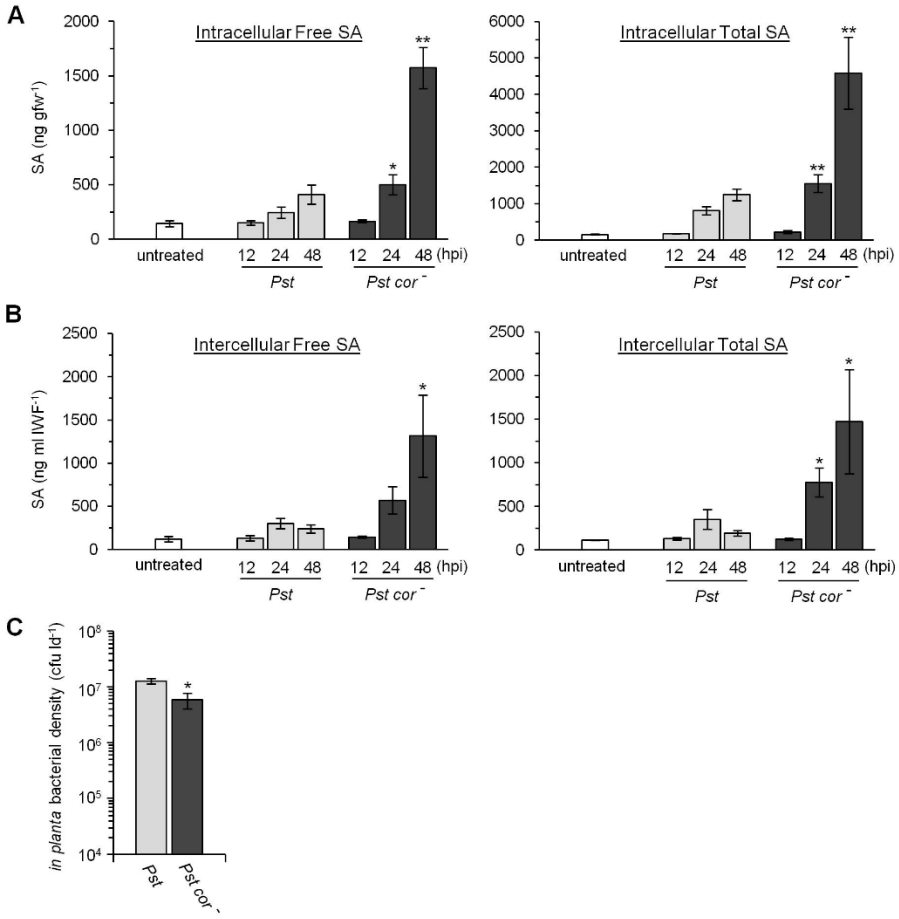

Figure 5. Coronatine suppresses salicylic acid accumulation. Intracellular (A) and intercellular (B) free and total salicylic acid (SA) levels were measured in leaves collected from 4-week-old Col-0 that were untreated or inoculated with 10^6 cfu ml^{-1} *Pseudomonas syringae* pv. *tomato (Pst)* strain DC3000 or the coronatine-deficient strain DC3661 *(Pst cor⁻)*. The mean ± standard deviation of three replicate samples is shown. Asterisks indicate a significant difference compared to plants inoculated with *Pst* at the corresponding time point (T-test, * $P<0.05$, ** $P<0.01$). (C) Bacterial density (colony-forming units per leaf disc [cfu ld^{-1}]) measured at 3 days post-inoculation. Values represent the mean ± standard deviation of three sample replicates. The asterisk indicates a significant difference (T-test $P<0.01$). These experiments were repeated once with similar results.
doi:10.1371/journal.pone.0088608.g005

Discussion

During ARR IAP1 is required for SA accumulation in the intercellular space where SA is thought to act as an antimicrobial agent [37]. This led us to investigate the role of IAP1 and intercellular SA accumulation during ETI. At the same time, map-based cloning, whole-genome sequencing, and complementation analysis identified *iap1-1* as a mutant allele of *EDS5*. In examining the literature, four *eds5* alleles already exist, therefore we propose that *iap1-1* be referred to as *eds5-5* in subsequent publications.

To avoid the time-consuming process of fine mapping, several approaches have been developed that combine the principles of genetic mapping with next-generation sequencing to identify EMS-generated mutations in *Arabidopsis* [56–61]. Most of these approaches involve sequencing pools of homozygous mutants selected from an F2 mapping population (reviewed in [62]). This step can be problematic if the mutant phenotype is difficult to score and homozygous individuals cannot be selected reliably. For example, heterozygous *iap1-1/eds5-5* plants display an ARR phenotype that is intermediate to that of homozygous mutants and wild-type plants, and can occasionally be misclassified as homozygous [37]. An alternative approach to avoid this issue is to directly sequence the mutant genome. Unfortunately, EMS mutants usually possess thousands of mutations making it difficult or impossible to identify the causal mutation by direct sequencing alone [62]. This problem can be solved by rough mapping the

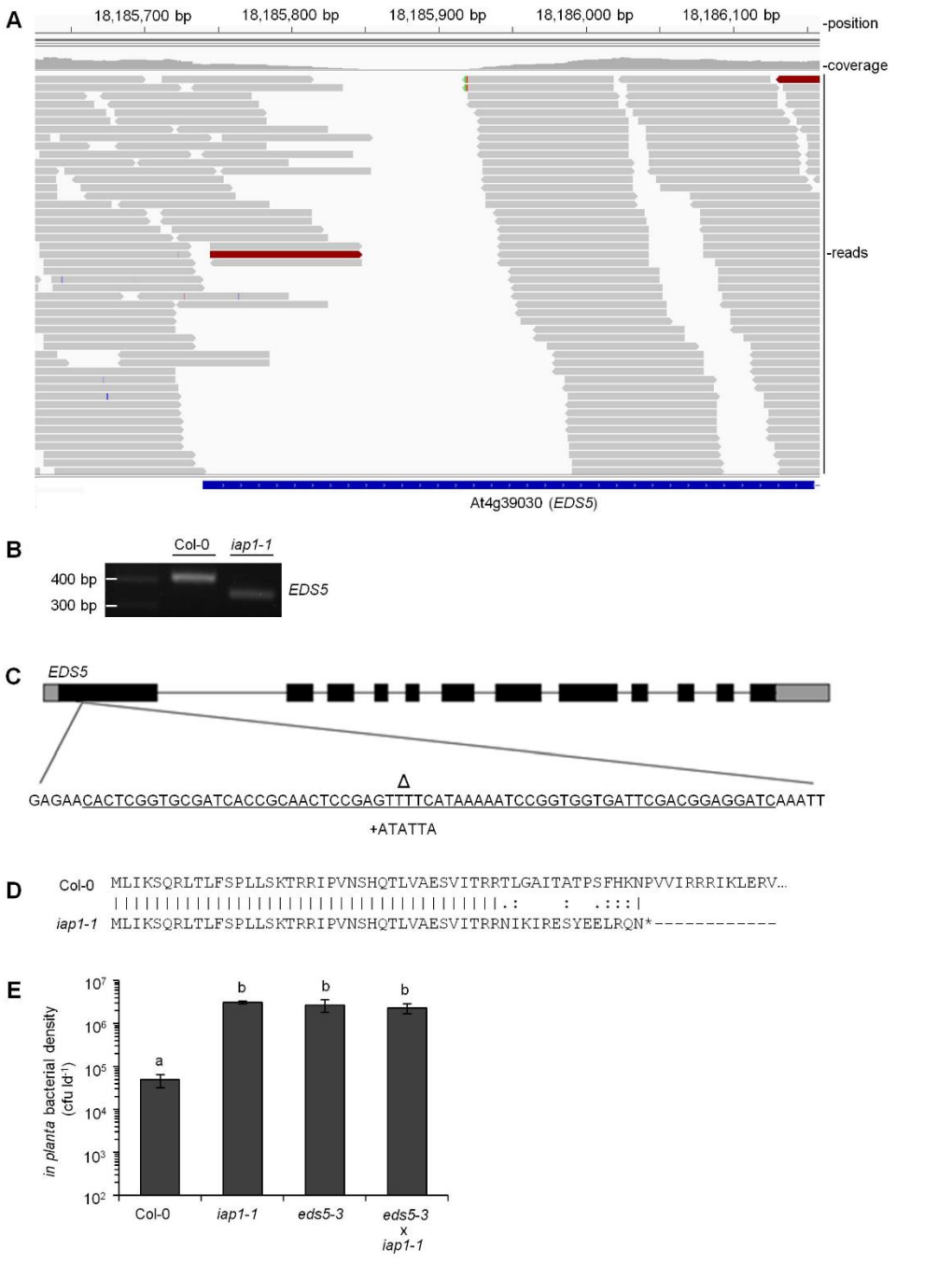
A
18,185,700 bp
18,185,800 bp
18,185,900 bp
18,186,000 bp
18,186,100 bp
-position
-coverage
-reads
At4g39030 (EDS5)
B
Col-0
iap1-1
400 bp
300 bp
EDS5
C
EDS5
Δ
GAGAACACTCGGTGCGATCACCGCAACTCCGAGTTTTCATAAAAATCCGGTGGTGATTCGACGGAGGATCAAATT
+ATATTA
D
Col-0 MLIKSQRLTLFSPLLSKTRRIPVNSHQTLVAESVITRRTLGAITATPSFHKNPVVIRRRIKLERV…
iap1-1 MLIKSQRLTLFSPLLSKTRRIPVNSHQTLVAESVITRRNIKIRESYEELRQN*----------
E
in planta bacterial density (cfu id-1)
a
b
b
b
Col-0
iap1-1
eds5-3
eds5-3 x iap1-1

Figure 6. *iap1-1* is an *eds5* mutant. (A) Integrated genome viewer screenshot showing *iap1-1* reads aligned to the Col-0 reference genome. The region of zero-coverage is located in the first exon of *EDS5*. (B) RT-PCR products generated from Col-0 and *iap1-1* using primers that flank the *iap1-1* mutation. (C) *EDS5* gene model including untranslated regions (thick grey lines) exons (thick black lines) and introns (thin black lines). The inset shows the nucleotides that are deleted (marked by Δ and underlined) and inserted (+ATATTA) in *iap1-1* relative to Col-0. (D) Predicted amino acid sequences of Col-0 and *iap1-1* EDS5. A premature stop in the *iap1-1* sequence is indicated by an asterisk. The full Col-0 EDS5 sequence is not shown. (E) Six-week-old Col-0, *iap1-1*, *eds5-3*, and *iap1-1*×*eds5-3* F1s were inoculated with 10^6 cfu ml^{-1} *Pseudomonas syringae* pv. *tomato* and bacterial density (colony-forming units per leaf disc [cfu ld^{-1}]) was determined at 3 days post-inoculation. Values represent the mean ± standard deviation of three sample replicates. Different letters indicate significant differences (ANOVA, Tukey's HSD, $P<0.05$). This experiment was repeated twice with similar results.
doi:10.1371/journal.pone.0088608.g006

mutation (to exclude most irrelevant mutations by determining the approximate position of the causal mutation) or backcrossing (to physically remove irrelevant mutations). Ashelford et al. [63] used both techniques followed by whole-genome sequencing to identify the *early bird* (*ebi-1*) EMS mutant. While successful, this effort was complicated by more than 30 non-synonymous mutations that were linked to the causal *ebi1* mutation that were not removed by backcrossing [63]. We used a similar approach combining genetic mapping and whole-genome sequencing to identify the fast neutron mutant *iap1-1/eds5-5*. Ashelford et al. [63] performed four backcrosses to eliminate irrelevant mutations from the *ebi1* mutant, whereas *iap1-1/eds5-5* was backcrossed only twice since the mutation load in fast neutron mutants is typically lower than in EMS mutants [64–66]. Therefore, fewer irrelevant mutations will be linked to the causal mutation, making it easier to identify. Based on this information we suggest that identifying fast neutron mutants using a combination of rough mapping and direct sequencing can be done rapidly and efficiently in comparison to EMS mutant identification.

Once the genome sequence data for *iap1-1/eds5-5* was obtained and the reads were aligned to the Col-0 reference genome, identification of potential deletion mutations was straightforward. Instead of generating a list of SNPs as would be done for an EMS-generated mutant, we compiled and assessed regions of the reference genome that were not covered by reads generated from the *iap1-1/eds5-5* mutant genome. A region of zero coverage could indicate that the corresponding sequence is deleted or highly polymorphic in *iap1-1/eds5-5* or could represent an error in the reference genome [67]. Regions of low coverage also occur for other reasons, including the difficulty of sequencing some genomic regions (e.g., low GC areas). Since we did not sequence the wild-type parent of *iap1-1/eds5-5* we cannot differentiate between these possibilities. Therefore, while 814 regions of zero coverage were identified, this is probably an overestimate of the fast neutron-induced mutations in *iap1-1/eds5-5*. Fast neutron mutant genomes are estimated to harbour deletions in approximately 10 genes [66]. Our bioinformatics strategy did not detect the co-localized insertion mutation present in *iap1-1/eds5-5*. The insertion was discovered later by Sanger sequencing demonstrating the necessity of confirming the molecular basis of fast neutron-generated mutations. Although not as common as deletions, other instances of co-localized insertion-deletion mutations resulting from fast neutron mutagenesis have been described [68,69].

To identify IAP1, we began by genetically mapping it to chromosome four and turned to whole-genome sequencing because it became available and additional mapping became unfeasible. Based on this experience, we propose a more rapid approach for gene identification in which rough mapping and sequencing are performed at the same time. As soon as the causal mutation is mapped to one chromosomal region, the sequencing data can be used to obtain a list of zero-coverage regions in this area. Zero-coverage regions in introns or intergenic sequences can be excluded as they are unlikely to affect gene function. The list of candidate zero-coverage regions in exons, promoters, and untranslated regions would be assessed to determine if mutations in any of these genes makes sense based on the mutant phenotype. If there are too many zero-coverage regions (>10), then further mapping may be required to reduce the number of candidate genes. If as expected for fast neutron-induced mutants, there are only a few zero-coverage regions in candidate genes, complementation analysis can be performed to confirm the identity of the gene. If whole-genome/next-generation sequencing had been available when we started to map *iap1-1/eds5-5*, we would have mapped it near one or two markers on chromosome four, then realized that there was just one zero-coverage region in one gene near these markers making us confident that this was the mutation responsible for the *iap1-1/eds5-5* phenotype. Moreover, this gene encoded EDS5, a SA transporter important for defense and therefore made sense with respect to the ARR-defective phenotype of *iap1-1/eds5-5*. Many years of challenging mapping would have been avoided if this method (simultaneous mapping and whole-genome sequencing) had been available.

Plants that are heterozygous for the *iap1-1/eds5-5* mutation display an ARR phenotype that is intermediate to that of homozygous mutants and wild-type plants, suggesting that *iap1-1/eds5-5* is a semidominant mutation [37]. Other mutant alleles of *eds5* have been classified as recessive (*eds5-1* [30] and *eds5-3* [22]). We believe this difference reflects the nature of assessing dominance in disease resistance mutants. For example, small changes in humidity may affect the growth of *Pst* in plants [70] such that heterozygotes may exhibit phenotypes that are similar to homozygous mutants or wild-type plants. Therefore during heterozygote analysis, if enough heterozygotes are classified with a wild-type phenotype, a semidominant mutation will be classified as recessive. It is also possible that *iap1-1/eds5-5* is a unique semidominant allele. Since *EDS5* transcripts are detectable in *iap1-1/eds5-5* mutants, a truncated EDS5 protein may be produced in *iap1-1/eds5-5* as 52 amino acids precede the premature stop codon in the *iap1-1/eds5-5* mutant. If the mutant peptide has a dominant negative effect on the wild-type protein this could explain the semidominant phenotype observed in heterozygous *iap1-1/eds5-5*. Other *eds5* mutant alleles that have been studied have been classified as recessive and also have premature stop codons and may produce truncated proteins [27]. However, the stop codons in *eds5-1*, *eds5-3*, and *iap1-1/eds5-5* occur at different positions suggesting that distinct peptides could be produced. Future studies to investigate whether these mutant alleles produce different peptides may shed light on the importance of the functional domains of the EDS5 MATE transporter. It is also possible that the semidominant phenotype of *iap1-1/eds5-5* is the result of an additional, unknown mutation.

We do not usually observe a difference in disease susceptibility between young Col-0 and *iap1-1/eds5-5* during the compatible interaction with virulent *Pst* [37, this study]. In some of our experiments young *iap1-1* is slightly more susceptible than Col-0, however, the difference is not always statistically significant. This observation conflicts with other studies of *eds5* mutants [22,30,31]. We propose that this difference may result from our use of a 10-

fold higher inoculum concentration (10^6 cfu ml^{-1}) during bacterial growth assays. Indeed, Glazebrook et al. [30] indicate that the enhanced disease susceptibility phenotype of *eds* mutants is more easily observed when lower inoculum concentrations are used.

Although *IAP1* is *EDS5*, a gene already known to be required for SA-mediated defense responses, both confirmatory and novel results were obtained during our investigation of compatible and incompatible (ETI) responses to *P. syringae* in *iap1-1/eds5-5*. Bacterial levels were modestly enhanced in *iap1-1/eds5-5* compared to Col-0 in response to both *Pst(avrRpt2)* and *Pst(avrRps4)* indicating that the ETI response was reduced, but not abolished in *iap1-1/eds5-5*, suggesting that IAP1/EDS5 contributes to ETI. Similar results were also observed in *eds5-3/sid1* in response to *Pst(avrRpt2)* [22]. In addition, Venugopal and colleagues [35] found that SA-deficient *sid2* mutants are also partially compromised for ETI. ETI was fully compromised in *sid2 eds1* double mutants suggesting that SA and EDS1 function redundantly during ETI. A macroscopic HR was observed in *NahG*, other *eds5* alleles [8,32], and *iap1-1/eds5-5*, and trypan blue staining detected similar levels of cell death in *iap1-1/eds5-5* and Col-0 (this study). Neither of these techniques is sensitive or quantitative, therefore electrolyte leakage assays were used to carefully examine the HR in *iap1-1/eds5-5*. Electrolyte leakage was modestly reduced in *iap1-1/eds5-5* compared to Col-0 inoculated with 10^6 or 10^7 cfu ml^1 *Pst(avrRpt2)* at several time points. Like the trypan blue assays, the electrolyte leakage assays confirm that HR cell death occurs in *iap1-1/eds5-5*, however, this sensitive assay indicates that the HR response was modestly reduced. We confirm that IAP1/EDS5 contributes to bacterial growth restriction during ETI and demonstrate that the HR is also partially dependent on functional IAP1/EDS5. In other words, it appears that IAP1/EDS5-dependent SA accumulation is required for a full HR and the bacterial growth restriction that takes place during RPS2-AvrRpt2-mediated ETI. In addition, electrolyte leakage assays revealed that cell death and intercellular SA accumulation occurred concurrently, suggesting that SA may gain access to the intercellular space from dead and dying cells during the HR. Consistent with this idea, the highest levels of intercellular SA accumulation were typically observed at 24 or 48 hpi with *Pst(avrRpt2)*, once extensive cell death had occurred. The timing of maximal intercellular SA accumulation varied between experiments, potentially because the timing and strength of the HR can be affected by variations in humidity that occur even within growth chambers.

SA accumulates in the intercellular space during ARR where it is thought to function as an antimicrobial agent. The idea that SA might act as an antimicrobial agent in the intercellular space in other defense responses has not been examined, therefore we measured both inter- and intracellular SA accumulation during ETI initiated by *Pst(avrRpt2)* and in response to virulent *Pst* (compatible interaction). Wild-type Col-0 accumulated intercellular SA in response to *Pst(AvrRpt2)* in the same range as observed during ARR (153 to 400 ng ml IWF^{-1}) [37,38] providing evidence for the importance of intercellular SA accumulation during ETI. Additionally, SA accumulation was reduced in *rps2-201* mutants indicating that the intercellular SA produced was specific to the RPS2-AvrRpt2 ETI pathway. In comparison, intercellular SA levels in *iap1-1/eds5-5* inoculated with *Pst(avrRpt2)* were similar to background levels observed in untreated and mock-inoculated controls demonstrating that *iap1-1/eds5-5* accumulates little SA during ETI as would be expected of an *eds5* mutant [22]. Although intercellular SA accumulation was reduced to background levels in *iap1-1/eds5-5*, RPS2-AvrRpt2-initiated ETI modestly reduced bacterial levels, suggesting that inter- and intracellular SA accumulation, as well as SA-independent constituents contribute to ETI.

During the response to virulent *Pst* over 48 hpi, *iap1-1/eds5-5* accumulated low levels of inter- (free and total) and intracellular (free) SA, similar to untreated or mock-inoculated plants, demonstrating that both intra- and intercellular SA accumulation is reduced by the *iap1-1/ed5-5* mutation. We also observed that total intracellular SA accumulation in Col-0 and *iap1-1* was low at early times after inoculation with virulent *Pst* (12 and 24 hpi), however, by 48 hpi, total intracellular SA levels increased to ~1000 ng gfw^{-1} in *iap1-1/eds5-5* and to ~1800 ng gfw^{-1} in Col-0, similar to SA levels induced by *Pst(avrRpt2)*. In Col-0 responding to virulent *Pst*, both intracellular and intercellular free SA levels were similar to background levels (untreated or mock-inoculated plants) with the exception of a modest increase in intracellular free SA levels at 48 hpi. One explanation for these observations is that PTI-associated SA accumulation is suppressed by virulent *Pst*. Support for this hypothesis comes from two studies in which the *Pseudomonas* phytotoxin coronatine was shown to inhibit whole-leaf SA accumulation in *Arabidopsis* in response to virulent *Pst* and *Ps maculicola* [51,52]. In addition, SA accumulates during PTI/basal resistance in response to the PAMP flg22 [36]. These investigations suggest that coronatine is important in suppressing SA accumulation during the PTI response and this produces a compatible environment for *Pseudomonas* infection. In this study we demonstrated that coronatine-producing *Pst* suppress both intracellular and intercellular SA accumulation. These data support the idea that intercellular SA accumulation is an important component of the PTI response.

Serrano et al. [28] speculate that *eds5* mutants do not accumulate SA because the EDS5 MATE transporter is not functional such that SA remains trapped in the chloroplast leading to high SA levels and feedback inhibition of SA biosynthesis. It is interesting to note that at the later 48 hpi time point, *iap1-1/eds5-5* accumulated elevated levels of total intracellular SA (free+−conjugated) in response to both virulent and avirulent *Pst*. Since little intracellular free SA accumulated at 48 hpi, the conjugated form of SA must be accumulating. We speculate that free SA is quickly converted to its conjugated form at 48 hpi with *Pst* and therefore little free SA is present for feedback inhibition of SA biosynthesis, allowing intracellular conjugated SA levels to rise. Also of note, both *iap1-1/eds5-5* and Col-0 were similarly susceptible to *Pst* even though *iap1-1/eds5-5* accumulated ~500 ng gfw^{-1} less intracellular total SA at 48 hpi compared to Col-0. Although free SA is generally regarded as the active form, studies on mutants in which enhanced disease susceptibility corresponds primarily with a reduced capacity to accumulate conjugated SA suggest that conjugated SA could be an important part of a successful defense response [71–74]. However, we speculate that by 48 hpi, suppression of PTI defense by *Pst* is waning such that intracellular conjugated SA accumulates in wild-type Col-0, however it is too late to mount a successful defense as bacteria have multiplied to high levels. It is also possible that the absence of accumulation of free SA in the intercellular space is responsible for the unsuccessful defense response in Col-0 and *iap1-1/eds5-5* to virulent *Pst*.

Conclusions

By developing a whole-genome/next-generation sequencing technique to identify deletion mutations, we identified a new mutant allele of *EDS5*. This technique will be useful for other researchers as it allows rapid identification of a deletion mutant by whole-genome sequencing once the mutation is roughly mapped.

Our studies of *iap1-1/eds5-5* revealed that SA accumulates in both the inter- and intracellular spaces during the RPS2-AvrRpt2-initiated ETI response. This suggests that SA contributes as both an intracellular signaling molecule and an antimicrobial agent in the intercellular space. We also demonstrated that intercellular SA accumulation is suppressed in a coronatine-dependent manner by virulent *Pst*. Therefore, SA may act as an antimicrobial agent in the intercellular space during PTI/basal resistance in *Arabidopsis*.

Materials and Methods

Plant growth conditions

The *iap1-1* [37], *rps2-201* [13], and *eds5-3/sid1* [22] mutants were used in conjunction with wild-type Columbia (Col-0). *iap1-1* was isolated from 5000 M2 fast neutron-mutagenized seeds (Lehle Seeds, Texas, USA) [37]. Seeds were surface-sterilized in 70% ethanol for 2 minutes and in sterilization solution (1.6% bleach, 0.1% Tween 20) for 10 minutes then washed with sterile water 5 times. Seeds were stratified at 4°C for at least 2 days before they were left to germinate on Murashige and Skoog (1962) medium for 5–7 days under continuous light. Seedlings were transferred to soil at the cotyledon stage (Sunshine Mix No. 1 [JVK]) and watered with 1 g L^{-1} 20-20-20 fertilizer. Temperature was maintained between 22°C and 24°C during a 9-hour photoperiod with an average light intensity of 150 µE m^{-2}·scc^{-1}. Humidity ranged between 75% (winter) and 85% (summer).

Disease resistance assays

Pseudomonas syringae pv. tomato (Pst) strain DC3000 (rifampicin and kanamycin resistant) and Pst(avrRpt2) were obtained from Dr. A. Bent (University of Wisconsin at Madison; [39]). Pst(avrRps4) was obtained from Dr. R. Subramaniam (Agriculture Canada). Pst cor^{-} (strain DC3661) was obtained from Dr. D. Cuppels (Agriculture Canada; [40]). Bacteria were shaken overnight at room temperature (22–24°C) in King's B media and kanamycin (50 µg ml^{-1}) to mid-log phase then resuspended in 10 mM $MgCl_2$ at a concentration of 10^6 or 10^7 cfu ml^{-1}. Plants were inoculated by pressure infiltration and in planta bacterial levels were determined as previously described [19,41].

Trypan staining and electrolyte leakage assays

Plants were inoculated with *Pst(avrRpt2)* (10^7 or 10^6 cfu ml^{-1}) or mock-inoculated with 10 mM $MgCl_2$. For trypan staining leaves were harvested at 24 hours post-inoculation (hpi) and immediately submersed in staining solution (0.02 g trypan blue, 8% phenol, 8% glycerol, 8% lactic acid, 8% water, 67% 95% ethanol). Leaves were boiled for 1 minute in the staining solution and left overnight followed by destaining in 70% ethanol. Images were captured using a digital camera (Nikon DXM1200F) mounted on a Nikon eclipse TE2000-S microscope at 10× magnification. For the first set of electrolyte leakage assays (Figure 1C) leaves were collected at 2 hpi, weighed, and rinsed in distilled water. 48 leaves per treatment were added to 80 ml of distilled water in triplicate and conductance was measured using a YSI environmental model 556 conductivity meter. For the second set of electrolyte leakage assays (Figure 4A) leaf discs were collected at 1 hpi, rinsed in nanopure water for 1 hour, then transferred to vials containing 10 ml nanopure water (9 plants per treatment, 10 leaf discs per vial, 3 vials per treatment). Conductance was measured periodically using a Jenway model 4070 portable conductivity meter.

IWF collection and SA measurement

IWF (intercellular washing fluid) collections were performed as described previously [19,38]. Briefly, Col-0 and *iap1-1* (4 weeks-old) were untreated, mock-inoculated (10 mM $MgCl_2$) or inoculated with 10^6 cfu ml^{-1} virulent *Pst*, avirulent *Pst(avrRpt2)*, or coronatine-deficient *Pst*. Leaves were harvested at 12, 24, and 48 hpi then surface-sterilized (50% ethanol and 0.05% bleach) and vacuum infiltrated with sterile water. Leaves were then blotted dry and centrifuged at 1000×g for 30 minutes in 50 ml syringes fitted into microcentrifuge tubes. The IWFs were filter-sterilized to remove *Pst*. ADPWH_*lux* is a non-pathogenic soil bacterium that has been modified to produce luciferase proportional to the amount of SA present [42] and was used to measure free SA and total SA (free SA plus SA-glucosides) as described previously [43]. Briefly, ADPWH_*lux* was grown overnight in LB media with shaking at 37°C and then diluted to an OD_{600} of 0.4 with fresh LB followed by incubation with IWFs or leaf tissue minus IWFs for 1 hour at 37°C in an opaque 96-well plate (Corning no.:3915). Luminescence was measured on a Biotek plate reader at 490 nm and used to calculate SA concentrations.

Map-based cloning

iap1-1 (Col-0 background) was crossed to Landsberg erecta (Ler) and the cross was confirmed in the F1 generation using InDel molecular markers [44]. Screening for homozygous *iap1-1 or IAP1* in the F2 generation was done by inoculating mature plants with virulent *Pst* (10^6 cfu ml^{-1}) and determining *in planta* bacterial levels after 3 days. Plants were classified ARR-incompetent if bacterial levels were $\geq 10^7$ cfu ld^{-1} and ARR-competent if bacterial levels were $\leq 10^5$ cfu ld^{-1}. InDel and CAPS molecular markers [44] were used to map the *iap1-1* mutation to the long arm of chromosome four [45]. Primers for significantly linked markers include AGAGGCAAGTGAATCAACCGT, ACTTC-GCAGCTCTCTGTTTTG (461250); GGGCAAGGTAATT-GATCGTCT, GCTTCTATAATCCGTGATCCG (461266); and GCACAAGGGAGAGAGATTCAA, GGATTCGAGAAT-TTCGGCA (460755). Primers for CAPS markers include GGAGATTGTTGAATACACTTGCTAC, GGCTAAGTTAT-GCAATATATTTCTCTT (18,268,815 bp); and TGCCGA-GAAAATCAGAGACA, CGACCTGAAAGACGTTAAATCC (18,111,371 bp) digested with PstI and RsaI, respectively.

Whole-genome sequencing

DNA was isolated from leaf tissue of an *iap1-1* plant using a modified phenol-chloroform extraction method. Briefly, tissue was ground in liquid nitrogen, incubated with DNA extraction buffer (200 mM Tris-HCL [pH 7.5], 250 mM NaCl, 25 mM EDTA, 0.5% SDS [w/v]), extracted with phenol-chloroform, and precipitated in isopropanol. The pellet was re-suspended and treated with RNase Cocktail (Life Technologies) followed by extraction with phenol-chloroform and again with chloroform alone. The DNA was then precipitated in ethanol. Library preparation was carried out according to manufacturer instructions (Nextera) and sequencing was performed on an Illumina HiSeq 1500 (high output mode) using approximately one third of a lane. Reads were aligned to the *Arabidopsis* Col-0 reference genome (TAIR 10) using BWA software [46].

RT-PCR

Leaf tissue was harvested, flash-frozen in liquid nitrogen, and stored at −80°C. RNA was isolated using Sigma TRI Reagent according to the manufacturer's instructions. Residual DNA was degraded using TURBO DNA-free (Life Technologies) prior to

RNA quantification. First-strand cDNA synthesis was carried out using M-MLV Reverse Transcriptase (Life Technologies). PCR primers used to amplify the *iap1-1* polymorphism were: 5′- ATGCTAATCAAATCCCAAAGATTGAC (F) and 5′- CAGCGAGTTCGATGGAGC (R) at 29 cycles. Products were visualized on a 2% agarose gel stained with ethidium bromide.

Supporting Information

Figure S1 Trypan blue staining for hypersensitive response cell death. Four-week-old Col-0 and *iap1-1* were inoculated with 10 mM $MgCl_2$ (mock) or 10^7 cfu ml^{-1} *Pseudomonas syringae* pv. *tomato (Pst)* carrying *avrRpt2*. Leaves were stained with trypan blue at 24 hours post-inoculation.
(TIF)

Table S1 Positions on the Col-0 reference genome near marker 461250 (18,087,180 bp) that were not covered by *iap1-1* Illumina sequencing reads.
(PDF)

Acknowledgments

We thank Barbara Kunkel (Washington University in St. Louis) for the *rps2-201* seeds and Dr. Marc Champigny for helpful discussions on whole-genome sequencing.

Author Contributions

Conceived and designed the experiments: RKC JC DW. Performed the experiments: JC DW MI PC. Analyzed the data: RKC JC DW MI PC VC BG EAW. Contributed reagents/materials/analysis tools: RKC EAW BG. Wrote the paper: RKC DW JC. Performed mapping and optimized SA biosensor assay: JC. Performed bioinformatics: VC.

References

1. Jones JDG, Dangl JL (2006) The plant immune system. Nature 444: 323–329.
2. de Torres M, Mansfield JW, Grabov N, Brown IR, Ammouneh H, et al. (2006) *Pseudomonas syringae* effector AvrPtoB suppresses basal defence in *Arabidopsis*. Plant J 47: 368–382.
3. Hauck P, Thilmony R, He SY (2003) A *Pseudomonas syringae* type III effector suppresses cell wall-based extracellular defense in susceptible *Arabidopsis* plants. Proc Natl Acad Sci USA 100: 8577–8582.
4. He P, Shan L, Lin NC, Martin GB, Kemmerling B, et al. (2006) Specific bacterial suppressors of MAMP signaling upstream of MAPKKK in *Arabidopsis* innate immunity. Cell 125: 563–575.
5. Li X, Lin H, Zhang W, Zou Y, Zhang J, et al. (2005) Flagellin induces innate immunity in nonhost interaction that is suppressed by *Pseudomonas syringae* effectors. Proc Natl Acad Sci USA 102: 12990–12995.
6. Zhang J, Shao F, Li Y, Cui H, Chen L, et al. (2007) A *Pseudomonas syringae* effector inactivates MAPKs to suppress PAMP-induced immunity in plants. Cell Host Microbe 1: 175–185.
7. Dangl JL, Jones JD (2001) Plant pathogens and integrated defense responses to infection. Nature 411: 826–833.
8. Tao Y, Xie Z, Chen W, Glazebrook J, Chang HS, et al. (2003) Quantitative nature of *Arabidopsis* responses compatible and incompatible interactions with the bacterial pathogen *Pseudomonas syringae*. Plant Cell 15: 317–330.
9. Thilmony R, Underwood W, He SY (2006) Genome-wide transcriptional analysis of the *Arabidopsis thaliana* interaction with the plant pathogen *Pseudomonas syringae* pv. *tomato* DC3000 and the human pathogen *Escherichia coli* O157:H7. Plant J 46: 34–53.
10. Truman W, de Zabala MT, Grant M (2006) Type III effectors orchestrate a complex interplay between transcriptional networks to modify basal defence responses during pathogenesis and resistance. Plant J 46: 14–33.
11. Mur LA, Kenton P, Lloyd AJ, Ougham H, Prats E (2008) The hypersensitive response; the centenary is upon us but how much do we know? J Exp Bot 59: 501–520.
12. Aarts N, Metz M, Holub E, Staskawicz BJ, Daniels MJ, et al. (1998) Different requirements for *EDS1* and *NDR1* by disease resistance genes define at least two R gene-mediated signaling pathways in *Arabidopsis*. Proc Natl Acad Sci USA 95: 10306–10311.
13. Kunkel BN, Bent AF, Dahlbeck D, Innes RW, Staskawicz BJ (1993) RPS2, an *Arabidopsis* disease resistance locus specifying recognition of *Pseudomonas syringae* strains expressing the avirulence gene avrRpt2. Plant Cell 5: 865–875.
14. Yu GL, Katagiri F, Ausubel FM (1993). *Arabidopsis* mutations at the *RPS2* locus result in loss of resistance to *Pseudomonas syringae* strains expressing the avirulence gene *avrRpt2*. Mol Plant Microbe Interact 6: 434–443.
15. Gassmann W, Hinsch ME, Staskawicz BJ (1999) The *Arabidopsis RPS4* bacterial-resistance gene is a member of the TIR-NBS-LRR family of disease resistance genes. Plant J 20: 265–277.
16. Hinsch M, Staskawicz B (1996) Identification of a new *Arabidopsis* disease resistance locus, *RPs4*, and cloning of the corresponding avirulence gene, *avrRps4*, from *Pseudomonas syringae* pv. *pisi*. Mol Plant Microbe Interact 1: 55–61.
17. Develey-Rivière MP, Galiana E (2007) Resistance to pathogens and host developmental stage: a multifaceted relationship within the plant kingdom. New Phytol 175: 405–416.
18. Whalen MC (2005) Host defense in a developmental context. Mol Plant Pathol 6: 347–360.
19. Kus JV, Zaton K, Sarkar R, Cameron RK (2002) Age-Related Resistance in *Arabidopsis* is a developmentally regulated defense response to *Pseudomonas syringae*. Plant Cell 14: 479–490.
20. Dempsey DA, Vlot CA, Wildermuth MC, Klessig DF (2011) Salicylic acid biosynthesis and metabolism. The Arabidopsis Book 9: e0156. doi: 10.1199/tab.0156.
21. Vlot CA, Dempsey DA, Klessig DF (2009) Salicylic acid, a multifaceted hormone to combat disease. Annu Rev Phytopathol 47:177–206.
22. Nawrath C, Métraux JP (1999) Salicylic acid induction-deficient mutants of *Arabidopsis* express *PR-2* and *PR-5* and accumulate high levels of camalexin after pathogen inoculation. Plant Cell 11: 1393–1404.
23. Delaney TP, Uknes S, Vernooij B, Friedrich L, Weymann K, et al. (1994) A central role of salicylic acid in plant disease resistance. Science 266: 1247–1250.
24. Garcion C, Lohmann A, Lamodière E, Catinot J, Buchala A, et al. (2008) Characterization and biological function of the *ISOCHORISMATE SYNTHASE2* gene of *Arabidopsis*. Plant Physiol 147: 1279–1287.
25. Wildermuth MC, Dewdney J, Wu G, Ausubel FM (2001) Isochorismate synthase is required to synthesize salicylic acid for plant defence. Nature 414: 562–571.
26. Fragnière C, Serrano M, Abou-Mansour E, Métraux JP, L'Haridon F (2011) Salicylic acid and its location in response to biotic and abiotic stress. FEBS Lett 585:1847–1852.
27. Nawrath C, Heck S, Parinthawong N, Métraux JP (2002) EDS5, an essential component of salicylic acid-dependent signaling for disease resistance in *Arabidopsis*, is a member of the MATE transporter family. Plant Cell 14: 275–286.
28. Serrano M, Wang B, Aryal B, Garcion C, Abou-Mansour E, et al. (2013) Export of salicylic acid from the chloroplast requires the MATE-like transporter EDS5. Plant Physiol 4: 1815–1821.
29. Yamasaki K, Motomura Y, Yagi Y, Nomura H, Kikuchi S, et al. (2013) Chloroplast envelope localization of EDS5, an essential factor for salicylic acid biosynthesis in *Arabidopsis thaliana*. Plant Signal Behav 8: e23603.
30. Glazebrook J, Rogers EE, Ausubel FM (1996) Isolation of *Arabidopsis* mutants with enhanced disease susceptibility by direct screening. Genetics 143: 973–982.
31. Rogers EE, Ausubel FM (1997) *Arabidopsis* enhanced disease susceptibility mutants exhibit enhanced susceptibility to several bacterial pathogens and alterations in PR-1 gene expression. Plant Cell 9: 305–316.
32. Clarke JD, Volko SM, Ledford H, Ausubel FM, Dong X (2000) Roles of salicylic acid, jasmonic acid, and ethylene in *cpr*-induced resistance in *Arabidopsis*. Plant Cell 12: 2175–2190.
33. Feys BJ, Moisan LJ, Newman MA, Parker JE (2001) Direct interaction between the *Arabidopsis* disease resistance signaling proteins, EDS1 and PAD4. EMBO J 20: 5400–5411.
34. Rairdan GJ, Delaney TP (2002) Role of salicylic acid and NIM1/NPR1 in race-specific resistance in *Arabidopsis*. Genetics 161: 803–811.
35. Venugopal SC, Jeong RD, Mandal MK, Zhu S, Chandra-Shekara AC, et al. (2009) Enhanced Disease Susceptibility 1 and salicylic acid act redundantly to regulate resistance gene-mediated signaling. PLOS Genet 5:e1000545.
36. Tsuda K, Sato M, Glazebrook J, Cohen JD, Katagiri F (2008) Interplay between MAMP-triggered and SA-mediated defense responses. Plant J 53: 763–775.
37. Carviel JL, Al-Daoud F, Neumann M, Mohammad A, Provart NJ, et al. (2009) Forward and reverse genetics to identify genes involved in the age-related resistance response in *Arabidopsis thaliana*. Mol Plant Pathol 10: 621–634.
38. Cameron RK, Zaton K (2004) Intercellular salicylic acid accumulation is important for age-related resistance in *Arabidopsis* to *Pseudomonas syringae*. Physiol Mol Plant Pathol 65: 197–209.
39. Whalen MC, Innes RW, Bent AF, Staskawicz BJ (1991) Identification of *Pseudomonas syringae* pathogens of *Arabidopsis* and a bacterial locus determining avirulence on both *Arabidopsis* and soybean. Plant Cell 3: 49–59.
40. Ma SW, Morris VL, Cuppels DA (1991) Characterization of a DNA region required for production of the phytotoxin coronatine by *Pseudomonas syringae* pv. *tomato*. Mol Plant Microbe Interact 4: 69–74.
41. Wolfe J, Hutcheon CJ, Higgins VJ, Cameron RK (2000) A functional gene-for-gene interaction is required for the production of an oxidative burst in response to infection with avirulent *Pseudomonas syringae* pv. *tomato* in *Arabidopsis thaliana*. Physiol Mol Plant Pathol 56: 253–261.

42. Huang WE, Huang L, Preston GM, Naylor M, Carr JP, et al. (2006) Quantitative in situ assay of salicylic acid in tobacco leaves using a genetically modified biosensor strain of Acinetobacter sp. ADP1. Plant J 46: 1073–1083.
43. DeFraia CT, Schmelz EA, Zhonglin M (2008) A rapid biosensor-based method for quantification of free and glucose-conjugated salicylic acid. Plant Methods 4: 28.
44. Jander G, Norris SR, Rounsley SD, Bush DF, Levin IM, et al. (2002) *Arabidopsis* map-based cloning in the post-genome era. Plant Physiol 129: 440–450.
45. Konieczny A, Ausubel FM (1993) A procedure for mapping *Arabidopsis* mutations using co-dominant ecotype-specific PCR based markers. Plant J 4: 403–410.
46. Li H, Durbin R (2009) Fast and accurate short read alignment with Burrows-Wheeler transform. Bioinformatics 25: 1754–1760.
47. van Wees S (2008) Phenotypic analysis of *Arabidopsis* mutants: trypan blue stain for fungi, oomycetes, and dead plant cells. CSH Protoc doi: 10.1101/pdb.prot4982.
48. Pike SM, Zhang XC, Gassmann W (2005) Electrophysiological characterization of the *Arabidopsis* avrRpt2-specific hypersensitive response in the absence of other bacterial signals. Plant Physiol 138: 1009–1017.
49. Cameron RK, Paiva NL, Lamb CJ, Dixon RA (1999) Accumulation of salicylic acid and *PR-1* gene transcripts in relation to the systemic acquired resistance (SAR) response induced by *Pseudomonas syringae* pv. *tomato* in *Arabidopsis*. Physiol Mol Plant Pathol 55: 121–130.
50. Glazebrook J (2005) Contrasting mechanisms of defense against biotrophic and necrotrophic pathogens. Annu Rev Phytopathol 43: 205–227.
51. de Torres Zabala M, Bennett MH, Truman WH, Grant MR (2009) Antagonism between salicylic acid and abscisic acid reflects early host-pathogen conflict and moulds plant defense responses. Plant J 59: 375–386.
52. Zheng XY, Spivey NW, Zeng W, Liu PP, Fu ZQ, et al. (2012) Coronatine promotes *Pseudomonas syringae* virulence in plants by activating a signaling cascade that inhibits salicylic acid accumulation. Cell Host Microbe 11: 587:596.
53. Bruggemann E, Handwerger K, Essex C, Storz G (1996) Analysis of fast neutron-generated mutants at the *Arabidopsis thaliana HY4* locus. Plant J 10: 755–760.
54. Li X, Song Y, Century K, Straight S, Ronald P, et al. (2001) A fast neutron deletion mutagenesis-based reverse genetics system for plants. Plant J 27: 235–242.
55. Rogers C, Wen J, Chen R, Oldroyd G (2009) Deletion-based reverse genetics in *Medicago truncatula*. Plant Physiol 151: 1077–1086.
56. Austin RS, Vidaurre D, Stamatiou G, Breit R, Provart NJ, et al. (2011) Next-generation mapping of *Arabidopsis* genes. Plant J 67: 715–725.
57. Cuperus JT, Montgomery TA, Fahlgren N, Burke RT, Townsend T, et al. (2010) Identification of *MIR390a* precursor processing-defective mutants in *Arabidopsis* by direct genome sequencing. Proc Natl Acad Sci USA 107: 466–471.
58. Jing B, Xu S, Xu M, Li Y, Li S, et al. (2011) Brush and spray: a high-throughput systemic acquired resistance assay suitable for large-scale genetic screening. Plant Physiol 157: 973–980.
59. Schneeberger K, Ossowski S, Lanz C, Juul T, Petersen AH, et al. (2009) SHOREmap: simultaneous mapping and mutation identification by deep sequencing. Nat Met 6: 550–551.
60. Uchida N, Sakamoto T, Kurata T, Tasaka M (2011) Identification of EMS-induced causal mutations in a non-reference *Arabidopsis thaliana* accession by whole genome sequencing. Plant Cell Physiol 52: 716–722.
61. Zhu Y, Mang HG, Sun Q, Qian J, Hipps A, et al. (2012) Gene discovery using mutagen-induced polymorphisms and deep sequencing: application to plant disease resistance. Genetics 192: 139–146.
62. Schneeberger K, Weigel D (2011) Fast-forward genetics enabled by new sequencing technologies. Trends Plant Sci 16: 282–288.
63. Ashelford K, Eriksson ME, Allen CM, D'Amore R, Johansson M, et al. (2011) Full genome re-sequencing reveals a novel circadian clock mutation in *Arabidopsis*. Genome Biol 12: R28.
64. Comai L, Henikoff S (2006) TILLING: practical single-nucleotide mutation discovery. Plant J 45: 684–694.
65. Henikoff S, Comai L (2003) Single-nucleotide mutations for plant functional genomics. Annu Rev Plant Bio 54: 375–401.
66. Koornneef M, Dellaert LW, van der Veen JH (1982) EMS- and radiation-induced mutation frequencies at individual loci in *Arabidopsis thaliana* (L.) Heynh. Mutat Res 93: 109–123.
67. Ossowski S, Schneeberger K, Clark RM, Lanz C, Warthmann N, et al. (2008) Sequencing of natural strains of *Arabidopsis thaliana* with short reads. Genome Res 18: 2024–2033.
68. Harper RM, Stowe-Evans EL, Luesse DR, Muto H, Tatematsu K, et al. (2000) The NPH4 locus encodes the auxin response factor ARF7, a conditional regulator of differential growth in aerial *Arabidopsis* tissue. Plant Cell 12: 757–770.
69. Hunter CA, Aukerman MJ, Sun H, Fokina M, Poethig SR (2003) *PAUSED* encodes the *Arabidopsis* exportin-t ortholog. Plant Physiol 132: 2135–2143.
70. Agrios GN (2005) Plant Pathology, 5th edition. Elsevier, Academic Press. 628 p.
71. Jagadeeswaran G, Raina S, Acharya BR, Maqbool SB, Mosher SL, et al. (2007) Arabidopsis *GH3-LIKE DEFENSE GENE 1* is required for accumulation of salicylic acid, activation of defense responses and resistance to *Pseudomonas syringae*. Plant J 51:234–246.
72. Lee MW, Lu H, Jung HW, Greenberg JT (2007) A key role for the Arabidopsis WIN3 protein in disease resistance triggered by *Pseudomonas syringae* that secrete AvrRpt2. Mol Plant Microbe Interact 20:1192–1200.
73. Nobuta K, Okrent RA, Stoutemyer M, Rodibaugh N, Kempema L, et al. (2007) The GH3 acyl adenylase family member PBS3 regulates salicylic acid-dependent defense responses in *Arabidopsis*. Plant Physiol 144:1144–1156.
74. Zheng Z, Qualley A, Fan B, Dudareva N, Chen Z (2009) An important role of a BAHD acyl transferase-like protein in plant innate immunity. Plant J 57:1040–1053.

3.9 Supplementary material

Table S1. Positions on the Col-0 reference genome near marker 461250 (18,087,180 bp) that were not covered by *iap1-1* Illumina sequencing reads.

Position (chromosome 4)	Size (bp)	Region	Description
18,585,053 - 18,585,056	4	intergenic	
18,185,855 - 18,185,919	65	exon	At4G39030 (*EDS5)*
17,405,532	1	intergenic	
17,362,499 - 17,362,513	15	intergenic	
17,357,652	1	intergenic	
17,357,246 - 17,357,356	12	intergenic	
17,317,390 - 17,317,401	12	intergenic	
17,317,380	1	intergenic	
17,315,542	1	intron	AT4G36740
17,315,483 - 17,315,494	12	intron	AT4G36740
17,313,889 - 17,313,894	6	intergenic	
17,276,554 - 17,276,587	34	5' UTR	AT4G36630
17,261,784 - 17,261,803	20	intron	AT4G36590

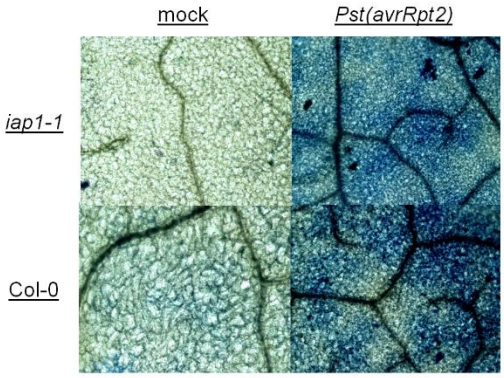

Figure S1. Trypan blue staining for hypersensitive response cell death. Four-week-old Col-0 and *iap1-1* were inoculated with 10mM $MgCl_2$ (mock) or 10^7 cfu ml^{-1} *Pseudomonas syringae* pv. *tomato (Pst)* carrying *avrRpt2*. Leaves were stained with trypan blue at 24 hours post-inoculation.

3.10 Addendum

ARTICLE ADDENDUM

Plant Signaling & Behavior 9, e29362; May; © 2014 Landes Bioscience

Intercellular salicylic acid accumulation during compatible and incompatible *Arabidopsis-Pseudomonas syringae* interactions

Daniel C Wilson, Philip Carella, and Robin K Cameron*

McMaster University; Department of Biology; Hamilton, ON Canada

The phytohormone salicylic acid (SA) plays an important role in several disease resistance responses. During the Age-Related Resistance (ARR) response that occurs in mature *Arabidopsis* responding to *Pseudomonas syringae* pv *tomato* (*Pst*), SA accumulates in the intercellular space where it may act as an antimicrobial agent. Recently we measured intracellular and intercellular SA levels in young, ARR-incompetent plants responding to virulent and avirulent strains of *Pst* to determine if intercellular SA accumulation is a component of additional defense responses to *Pst*. In young plants virulent *Pst* suppressed both intra- and intercellular SA accumulation in a coronatine-dependent manner. In contrast, high levels of intra- and intercellular SA accumulated in response to avirulent *Pst*. Our results support the idea that SA accumulation in the intercellular space is an important component of multiple defense responses. Future research will include understanding how mature plants counteract the effects of coronatine during the ARR response.

Keywords: *Arabidopsis*, *Pseudomonas syringae*, age-related resistance, effector-triggered immunity, salicylic acid, intercellular space, EDS5, whole-genome sequencing

*Correspondence to: Robin K Cameron; Email: rcamero@mcmaster.ca

Submitted: 05/22/2014

Accepted: 05/26/2014

Published Online: 05/29/2014

Citation: Wilson DC, Carella P, Cameron RK. Intercellular salicylic acid accumulation during compatible and incompatible Arabidopsis-Pseudomonas syringae interactions. Plant Signaling & Behavior 2014; 9:e29362; PMID: 24874267; http://dx.doi.org/10.4161/psb.29362

Addendum to: Carviel JL, Wilson DC, Isaacs M, Carella P, Catana V, Golding B, Weretilnyk EA, Cameron RK. Investigation of intercellular salicylic acid accumulation during compatible and incompatible arabidopsis-pseudomonas syringae interactions using a fast neutron-generated mutant allele of EDS5 identified by genetic mapping and whole-genome sequencing. PLoS One 2014; 9:e88608; http://dx.doi.org/10.1371/journal.pone.0088608; PMID:24594657

Plants and the pathogens that attack them have evolved numerous mechanisms to thwart each other in what is often described as an evolutionary arms race. Resistant host plants are able to effectively recognize and respond to pathogens, whereas successful pathogens have developed strategies to suppress plant defense. In *Arabidopsis*, disease resistance is developmentally regulated such that mature plants are resistant to a variety of pathogens that cause disease in young plants.[1,2] This phenomenon, known as Age-Related Resistance (ARR), is a pathogen-induced response in *Arabidopsis* characterized by accumulation of the phytohormone salicylic acid (SA), particularly in the intercellular space.[3] A large body of evidence indicates that SA acts as an intracellular signal for the induction of defense gene expression (reviewed in ref. 4), however, a number of experiments in *Arabidopsis* suggest that SA also acts as an antimicrobial compound in the intercellular space.[3] In a recent study[5] we investigated intra- and intercellular SA accumulation in young plants during compatible (virulent pathogen) and incompatible (avirulent pathogen) interactions with *Pseudomonas syringae* pv *tomato* (*Pst*). We also demonstrated the use of whole-genome sequencing to identify a fast neutron-generated mutant affected in SA accumulation and the ARR response.

Salicylic Acid Accumulation During a Compatible Interaction with *Pst*

The hemibiotrophic pathogen *Pst* DC3000 is highly virulent in young *Arabidopsis*, growing to high concentrations and causing severe disease symptoms. Consistent with previous results, young plants inoculated with virulent *Pst* accumulated modest levels of intracellular free SA and little intercellular free SA. Since *Pst* produces coronatine, a phytotoxin that has been shown to suppress SA accumulation (by experiments that measured whole-leaf SA levels in young plants),[6,7] we wondered whether

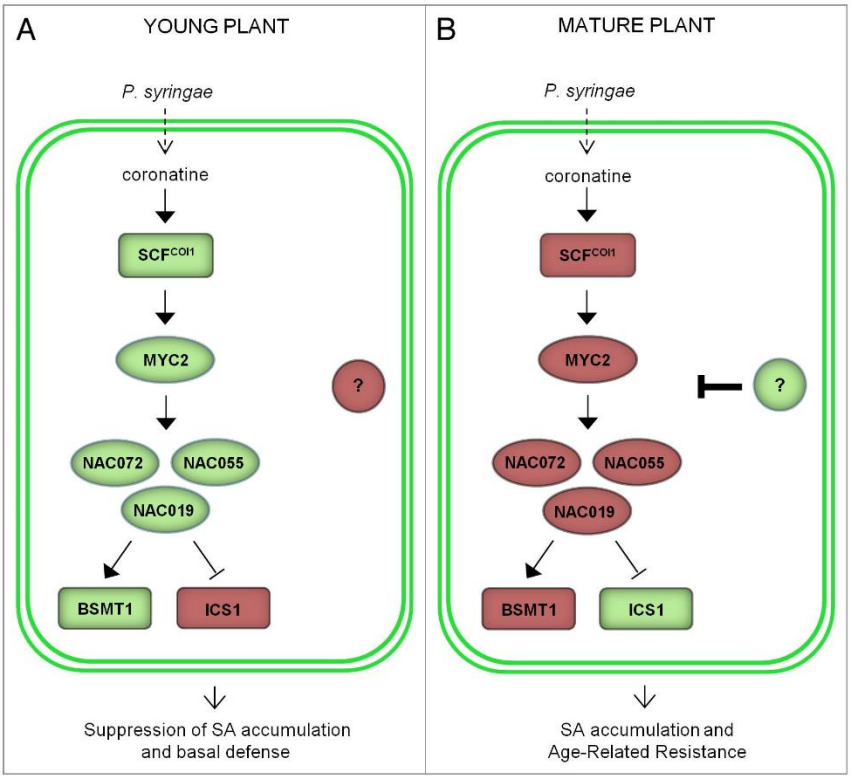

Figure 1. A model of coronatine-mediated suppression of salicylic acid (SA) accumulation in young and mature plants. In young plants **(A)** coronatine produced by virulent *P. syringae* binds to the SCF^{COI1} receptor complex and activates a signaling cascade that results in the MYC2-dependent upregulation of three NAC transcription factors (NAC019, NAC055, NAC072). The NACs downregulate the expression of genes that function in SA biosynthesis (*ICS1*), and upregulate the expression of genes that function in SA metabolism (*BSMT1*). The end result is suppression of SA accumulation in young plants, which contributes to pathogen virulence or host susceptibility.[7] In mature plants **(B)** we postulate that one or more developmentally regulated gene products interferes with this signaling cascade to prevent coronatine-mediated suppression of SA accumulation. As a result, mature plants responding to virulent *P. syringae* accumulate high levels of free SA and respond in a resistant manner. Components shown in green are active, components shown in red are inactive or repressed.

coronatine also suppresses intercellular SA accumulation. Indeed, young plants inoculated with coronatine-deficient *Pst* accumulated higher levels of both intra- and intercellular free SA, suggesting that *Pst* suppresses intra- and intercellular SA accumulation in a coronatine-dependent manner. These findings suggest that SA accumulation in the intercellular space is a component of the basal defense response that is suppressed by *Pst* in young plants.

A recent study demonstrated that coronatine suppresses SA accumulation in young plants by activating the jasmonic acid signaling pathway resulting in the upregulation of three NAC transcription factors (NAC019, NAC055, NAC072) that regulate SA biosynthesis and metabolism[7] (**Fig. 1A**). We hypothesize that suppression of SA accumulation by *Pst* is alleviated in mature plants, leading to the high levels of intra- and intercellular SA characteristic of the ARR response (**Fig. 1B**). Future research will focus on understanding the developmental events that allow mature plants to counteract the effects of coronatine.

Salicylic Acid Accumulation during the *RPS2-avrRpt2* Incompatible Interaction

Recognition of bacterial effectors by plant resistance proteins initiates a defense response known as Effector-Triggered Immunity (ETI, reviewed in ref. 8). Since ETI generally results in restriction of bacterial growth, pathogens expressing effectors that are recognized by resistance proteins are considered avirulent. In our study, we determined whether SA accumulates in

the intercellular space during ETI using an avirulent strain of *Pst* expressing the avrRpt2 effector, which is recognized by the RPS2 resistance protein.[9,10] We found that young plants inoculated with *Pst(avrRpt2)* accumulated high levels of intra- and intercellular free SA, suggesting that SA accumulation in the intercellular space may be an important component of ETI. In support of this idea, SA-deficient *eds5–5* (*enhanced disease susceptibility5–5*) mutants were partially compromised for RPS2- and RPS4-mediated ETI. SA accumulated to high levels in plants inoculated with *Pst(avrRpt2)* compared with those inoculated with virulent *Pst*, suggesting that coronatine-mediated suppression of SA accumulation is ineffective during RPS2-mediated ETI. This is consistent with the idea that the ETI response is recalcitrant to manipulation by pathogens.[11]

Whole-Genome Sequencing for Mutant Identification

The *iap1–1* mutant (*important for the ARR pathway1–1*) was isolated from a genetic screen for ARR-defective mutants.[12] To identify the causal fast neutron-generated mutation in *iap1–1* we performed rough mapping followed by whole-genome sequencing of the mutant. After sequencing the *iap1–1* genome, potential deletions were identified as regions of zero coverage when *iap1–1* reads were aligned to the wild-type reference genome. Information obtained from rough mapping was highly useful in that only a small subset of the deletions identified were reasonable candidates for the causal mutation. In fact, only two potential deletions were found within 500 kb of the marker to which *iap1–1* showed linkage. While one was a small deletion located in an intergenic region, the other consisted of a 65 bp deletion (plus a 6 bp insertion) in the first exon of *EDS5*, making it the obvious candidate for the causal mutation in *iap1–1*. We subsequently demonstrated that *iap1–1* was allelic to the *eds5–3* mutant, confirming that *iap1–1* (renamed *eds5–5*) is an *eds5* mutant. In our experience, rough mapping combined with whole-genome sequencing is a fast and effective means of mutant identification that is well suited for fast neutron mutants.

Conclusions

Our results suggest that intercellular SA accumulation is a common component of several disease resistance responses, and is a target of suppression by *Pst*. Whether or not pathogen-induced suppression of SA accumulation is successful depends on the genotypes of the plant and pathogen (i.e., whether the resulting interaction is compatible or incompatible), as well as the developmental stage of the plant.

Disclosure of Potential Conflicts of Interest

No potential conflicts of interest were disclosed.

References

1. Kus JV, Zaton K, Sarkar R, Cameron RK. Age-related resistance in Arabidopsis is a developmentally regulated defense response to Pseudomonas syringae. Plant Cell 2002; 14:479-90; PMID:11884688; http://dx.doi.org/10.1105/tpc.010481
2. Rusterucci C, Zhao Z, Haines K, Mellersh D, Neumann M, Cameron RK. Age-related resistance to *Pseudomonas syringae* pv. *tomato* is associated with the transition to flowering in *Arabidopsis* and is effective against *Peronospora parasitica*. Physiol Mol Plant Pathol 2005; 66:222-31; http://dx.doi.org/10.1016/j.pmpp.2005.08.004
3. Cameron RK, Zaton K. Intercellular salicylic acid accumulation is important for age-related resistance in Arabidopsis to *Pseudomonas syringae*. Physiol Mol Plant Pathol 2004; 65:197-209; http://dx.doi.org/10.1016/j.pmpp.2005.02.002
4. Vlot AC, Dempsey DA, Klessig DF. Salicylic Acid, a multifaceted hormone to combat disease. Annu Rev Phytopathol 2009; 47:177-206; PMID:19400653; http://dx.doi.org/10.1146/annurev.phyto.050908.135202
5. Carviel JL, Wilson DC, Isaacs M, Carella P, Catana V, Golding B, Weretilnyk EA, Cameron RK. Investigation of intercellular salicylic acid accumulation during compatible and incompatible arabidopsis-*pseudomonas syringae* interactions using a fast neutron-generated mutant allele of *EDS5* identified by genetic mapping and whole-genome sequencing. PLoS One 2014; 9:e88608; http://dx.doi.org/10.1371/journal.pone.0088608; PMID:24594657
6. de Torres Zabala M, Bennett MH, Truman WH, Grant MR. Antagonism between salicylic and abscisic acid reflects early host-pathogen conflict and moulds plant defence responses. Plant J 2009; 59:375-86; PMID:19392690; http://dx.doi.org/10.1111/j.1365-313X.2009.03875.x
7. Zheng XY, Spivey NW, Zeng W, Liu PP, Fu ZQ, Klessig DF, He SY, Dong X. Coronatine promotes *Pseudomonas syringae* virulence in plants by activating a signaling cascade that inhibits salicylic acid accumulation. Cell Host Microbe 2012; 11:587-96; PMID:22704619; http://dx.doi.org/10.1016/j.chom.2012.04.014
8. Dodds PN, Rathjen JP. Plant immunity: towards an integrated view of plant-pathogen interactions. Nat Rev Genet 2010; 11:539-48; PMID:20585331; http://dx.doi.org/10.1038/nrg2812
9. Kunkel BN, Bent AF, Dahlbeck D, Innes RW, Staskawicz BJ. RPS2, an *Arabidopsis* disease resistance locus specifying recognition of *Pseudomonas syringae* strains expressing the avirulence gene avrRpt2. Plant Cell 1993; 5:865-75; PMID:8400869; http://dx.doi.org/10.1105/tpc.5.8.865
10. Yu GL, Katagiri F, Ausubel FM. Arabidopsis mutations at the *RPS2* locus result in loss of resistance to *Pseudomonas syringae* strains expressing the avirulence gene *avrRpt2*. Mol Plant Microbe Interact 1993; 6:434-43; PMID:8400373; http://dx.doi.org/10.1094/MPMI-6-434
11. Tsuda K, Sato M, Stoddard T, Glazebrook J, Katagiri F. Network properties of robust immunity in plants. PLoS Genet 2009; 5:e1000772; http://dx.doi.org/10.1371/journal.pgen.1000772; PMID:20011122
12. Carviel JL, Al-Daoud F, Neumann M, Mohammad A, Provart NJ, Moeder W, Yoshioka K, Cameron RK. Forward and reverse genetics to identify genes involved in the age-related resistance response in *Arabidopsis thaliana*. Mol Plant Pathol 2009; 10:621-34; PMID:19694953; http://dx.doi.org/10.1111/j.1364-3703.2009.00557.x

Chapter 4 – Age-Related Resistance in *Arabidopsis thaliana* involves the MADS-domain transcription factor SHORT VEGETATIVE PHASE and direct action of salicylic acid on *Pseudomonas syringae*

PREFACE

This chapter consists of a research article (prepared for submission to Molecular Plant-Microbe Interactions) in which the role of SVP during ARR was investigated. Analysis of *svp* mutants showed that SVP contributes to SA accumulation during ARR. Analysis of *svp-32 soc1-2* double mutants suggests that *SOC1* is a downstream target of SVP during ARR. *SOC1* overexpressors are ARR-defective and fail to accumulate intercellular SA, consistent with SOC1 contributing negatively to ARR, upstream of intercellular SA accumulation. Lastly, in vitro antibacterial and antibiofilm assays, estimation of in vivo SA concentrations, and visualization of *P. syringae* in the intercellular space, all provide evidence that SA acts directly on pathogens in the intercellular space during ARR.

Author contributions

Authors: Wilson, D.C., Kempthorne, C.J., Carella, P., Liscombe, D.K., Cameron, R.K. DW performed the experiments with help from CK, who assisted with the disease resistance assays shown in Figure 4.2, scoring of bacterial cell types in the intercellular space (Figure 4.5), and inoculation and IWF collection for the

experiment shown in Figure 4.7. DW and RC wrote the manuscript with assistance from the other authors, and conceived and designed the experiments.

4.1 Abstract

Arabidopsis thaliana exhibits a developmentally regulated disease-resistance response known as Age-Related Resistance (ARR), a process that requires intercellular accumulation of salicylic acid (SA), which is thought to act as an antimicrobial agent. ARR is characterized by enhanced resistance to some pathogens at the late adult-vegetative and reproductive stages. While the transition to flowering does not cause the onset of ARR, both processes involve the MADS-domain transcription factor SHORT VEGETATIVE PHASE (SVP). In this study, ARR-defective *svp* mutants were found to accumulate reduced levels of intercellular SA compared to wild type in response to *P. syringae* pv. *tomato* (*Pst*). Double mutant and overexpression analyses suggest that SVP and SOC1 (SUPPRESSOR OF OVEREXPRESSION OF CO 1) act antagonistically, such that SVP is required for ARR to alleviate the negative effects of SOC1 on SA accumulation. In vitro, SA exhibited antibacterial and antibiofilm activity at concentrations similar to those measured in the intercellular space during ARR. In vivo, *Pst* formed biofilm-like aggregates in young susceptible plants, while this was drastically reduced in mature ARR-competent plants, which accumulate intercellular SA. Collectively, these results reveal a novel role for the floral

regulators SVP and SOC1 in disease resistance and provide evidence that SA acts directly on pathogens as an antimicrobial agent.

4.2 Introduction

Many plants exhibit enhanced resistance to disease at later developmental stages (Develey-Rivière and Galiana 2007, Whalen 2005). This phenomenon is often referred to as Age-Related Resistance (ARR). The model plant *Arabidopsis thaliana* displays ARR to *Pseudomonas syringae*, resulting in reduced bacterial growth in the leaf intercellular space of mature plants compared to young plants (Kus et al. 2002). ARR is a salicylic acid (SA)-dependent process, as several SA-deficient mutants are ARR-defective (Cameron and Zaton 2004, Carviel et al. 2009, Kus et al. 2002). However, SA signaling mutants are ARR-competent, suggesting that SA-mediated defense signaling is not essential for ARR (Carella et al. 2015, Kus et al. 2002). Instead, it is thought that SA acts directly on the pathogen as an antimicrobial agent during ARR. Evidence supporting this hypothesis includes the observation that antibacterial activity and SA are both detected in intercellular washing fluids (IWFs) of mature plants after inoculation with *P. syringae* pv. *tomato* (*Pst*) DC3000, but not in IWFs of untreated or young plants inoculated with *Pst* (Cameron and Zaton 2004, Kus et al. 2002). Moreover, addition of SA to the intercellular space of SA-deficient mutants restores ARR, and reduction of intercellular SA levels in wild-type plants by pressure-infiltrating with SA hydroxylase, compromises ARR (Cameron and Zaton 2004). Finally, SA

exhibits antimicrobial activity against a variety of phytopathogens in vitro (Amborabé et al. 2002, Brown 2007, Cameron and Zaton 2004, El-Mougy 2002, Georgiou et al. 2000, Martín et al. 2010, Prithiviraj et al. 1997, Lowe-Power et al. 2016, Yuan et al. 2007), however, concentrations greater than 1 mM are often required, and it is unclear whether these concentrations are reached in planta.

ARR coincides with the transition to flowering in both short-day (9 h light) and long-day (16 h light) photoperiods (Rusterucci et al. 2005). Despite the co-occurrence of these developmental events, analysis of flowering-time mutants and wild-type plants that were induced to flower early by transient exposure to long days demonstrated that the transition to flowering is neither sufficient nor required for the onset of ARR (Wilson et al. 2013). Interestingly, the same study also revealed that SVP (SHORT VEGETATIVE PHASE) plays a role in both processes, since mutants for this well-known flowering-time regulator were found to be ARR-defective.

The transition to flowering is a highly regulated process affected by numerous environmental and endogenous signals (Amasino 2010, Fornara et al. 2010). A few key genes act to integrate these signals, including *SVP*, a major negative regulator of flowering (Hartmann et al. 2000). SVP is a MADS-domain transcription factor that delays flowering in the absence of inductive signals through direct repression of positive regulators of flowering such as *SOC1* (*SUPPRESSOR OF OVEREXPRESSION OF CO 1*) (Gregis et al. 2013, Li et al. 2008). SOC1 functions primarily at the shoot apical meristem, where it activates

the floral meristem identity gene *LFY* (*LEAFY*) to initiate flowering in response to inductive signals such as long days, gibberellic acid, and ageing (Lee et al. 2008, Liu et al. 2008, Moon et al. 2005). SVP also represses *SOC1* in leaves (Li et al. 2008), however, the biological significance of this interaction is unclear.

In this study, investigation of SVP's role during ARR revealed that SVP is required for intercellular SA accumulation, and identified SOC1 as an additional MADS-domain transcription factor that affects both flowering and ARR. The potential for direct action of SA on *Pst* was assessed by antibacterial and biofilm assays in minimal medium that reflects the conditions in the intercellular space. Low concentrations of SA (≥ 2 µM) reduced biofilm formation, while higher concentrations (≥ 100 µM) reduced bacterial growth. Moreover, accumulation of SA in the intercellular space during ARR was associated with reduced formation of biofilm-like aggregates of *Pst*, suggesting that intercellular SA directly impacts pathogen growth and/or biofilm formation in mature *Arabidopsis*.

4.3 Results

SA accumulation is reduced in svp mutants responding to P. syringae

We first became interested in SVP upon discovering that mutants for this gene were ARR-defective (Wilson et al. 2013, Fig. 4.1A). Given that SA accumulation is a key component of the ARR response, we hypothesized that SVP might regulate SA accumulation, in which case *svp* mutants should be compromised in

their ability to accumulate SA. Therefore, SA was measured in mature Col-0 and *svp-41* before and after inoculation with *Pst*. Specifically, SA levels were measured in IWFs and leaf tissue (with IWFs removed) to assess intercellular and intracellular fractions of SA, respectively. As expected, Col-0 accumulated intracellular free and glucose-conjugated SA (SAG) in response to *Pst* (Fig. 4.1B,D). The *svp-41* mutant also accumulated intracellular free SA, albeit with a small but statistically significant 1.2-fold reduction relative to Col-0 at 24 h postinoculation (hpi). Intracellular SAG accumulation was noticeably reduced in *svp-41* relative to Col-0 at 24 and 48 hpi (2- to 4-fold reduction). While little to no intercellular SAG accumulates in response to *Pst* (Carviel et al. 2014), free SA accumulated to 2093 ng ml^{-1} in Col-0 IWFs at 24 hpi, but was reduced to 711 ng ml^{-1} in svp-41 (3-fold reduction, Fig. 4.1C). These data suggest that SVP function contributes to intracellular and intercellular SA accumulation during ARR.

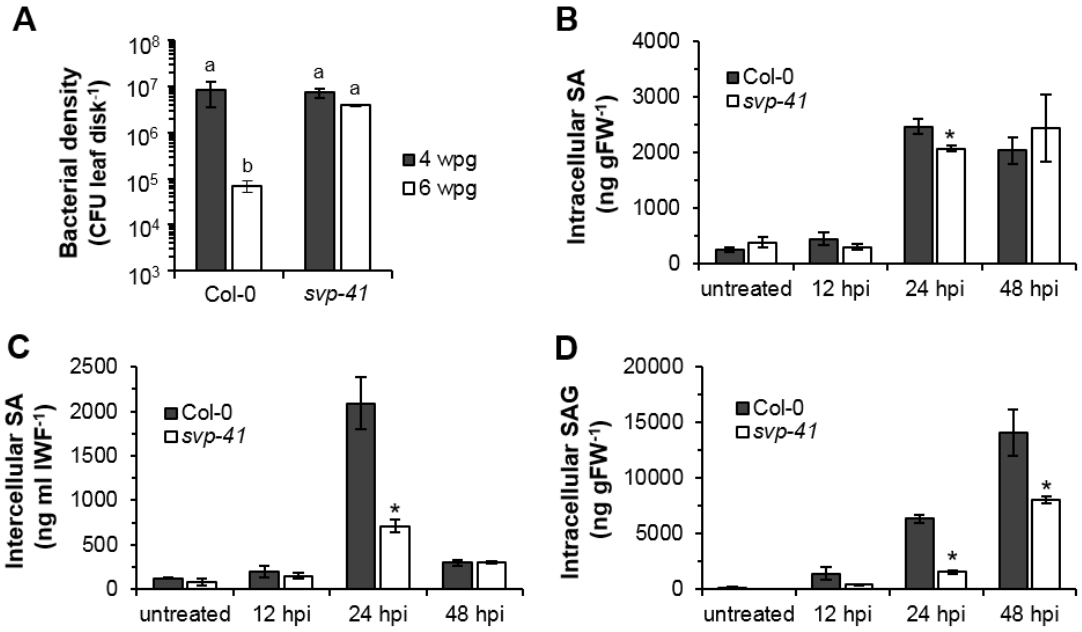

Figure 4.1 – ARR-defective *svp-41* mutants have reduced SA accumulation in response to *P. syringae*. **A,** Plants were inoculated with 10^6 CFU ml^{-1} *Pst* at either 4 or 6 weeks postgermination (wpg) and bacterial levels were quantified 3 days later. Different letters indicate significant differences (ANOVA followed by Tukey's HSD test, $P < 0.05$). **B-D,** SA and SA glucosides (SAG) were measured in intercellular washing fluid (IWF) (**C**) and the corresponding leaves (from which IWFs had been removed) (**B,D**) of plants that were either untreated or inoculated with 10^6 CFU ml^{-1} *Pst*. Asterisks indicate significant differences between genotypes at the same time point (T-test, $P < 0.05$). Each bar shows the mean of 3 sample replicates, and error bars show standard deviation. These experiments were performed 3 times with similar results.

Addition of SA to the intercellular space restores ARR to svp mutants

If the ARR-defective phenotype of svp mutants is caused by reduced intercellular SA accumulation, then adding exogenous SA to the intercellular space should restore ARR in *svp* mutants. To test this, 0.1 mM SA or a mock solution was pressure-infiltrated into the leaves of mature plants either 4 or 24 h before inoculation with *Pst*. Bacterial levels were then measured at 3 days postinoculation (dpi). Col-0 served as a positive control for ARR, and the SA-deficient *sid2-2* mutant was included as a negative control for ARR and because

application of exogenous SA restores ARR to *sid2* mutants (Cameron and Zaton 2004). Mock-treated *svp-32* and *sid2-2* supported higher bacterial levels than Col-0, consistent with the ARR-defective phenotypes of both mutants (Fig. 4.2). When SA was applied 4 h before inoculation with *Pst*, *svp-32* and *sid2-2* both supported lower bacterial levels relative to their mock-treated counterparts, whereas resistance was not enhanced in ARR-competent Col-0 as observed previously (Cameron and Zaton 2004). In contrast, when SA was applied 24 h before inoculation with *Pst*, all three genotypes supported similar bacterial levels relative to their mock-treated counterparts. Similar results were observed with the *svp-41* mutant (Fig. S4.1). Previous work has shown that leaves pressure-infiltrated with 0.1 mM SA contain elevated SA in IWFs after 5 h, with a return to untreated levels after 24 h (Cameron and Zaton 2004). Together these data suggest that exogenous intercellular SA restores ARR in *svp* mutants. These data link the ARR-defective phenotype of *svp* mutants to reduced intercellular SA accumulation and further demonstrate the importance of intercellular SA for ARR.

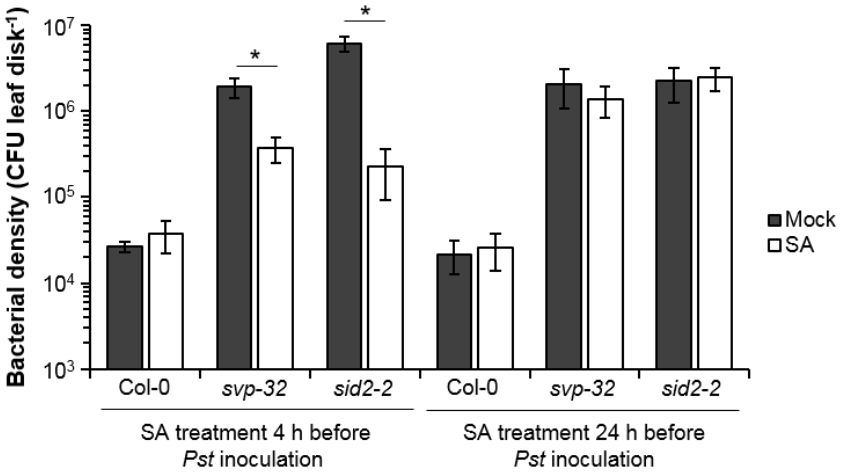

Figure 4.2 – Exogenous intercellular SA restores ARR to *svp-32* mutants. Mature plants (7 weeks postgermination) were pressure-infiltrated with 0.1 mM SA or water (mock) either 4 or 24 h before inoculation with 10^6 CFU ml^{-1} *Pst*. Bacterial levels were quantified 3 days later. Each bar shows the mean of 3 sample replicates, and error bars show standard the deviation. Asterisks indicate significant differences (ANOVA followed by Tukey's HSD test, $P < 0.05$). This experiment was performed 3 times with similar results.

Direct action of salicylic acid on P. syringae

In rich medium (King's B) *Pst* growth is reduced at SA concentrations of ≥ 1 mM (Cameron and Zaton 2004) and ≥ 2 mM (Fig. 4.3A). Since characteristics of the growth medium (e.g., pH) can influence bacterial growth rate, metabolism, and physiology (Kim et al. 2010), as well as the activity of antimicrobial agents (Amborabé et al. 2002), the antibacterial activity of SA was assessed in conditions similar to those found in the leaf intercellular space. To accomplish this, antibacterial assays were conducted using hrp-inducing minimal (HIM) medium (Huynh et al. 1989), which more closely resembles the composition of the leaf intercellular space. In HIM medium, the growth of *Pst* was reduced at 100-200 µM SA, and completely inhibited at 1 mM (Fig. 4.3B). At ≥ 2 mM SA, no colonies were observed when the culture was transferred to solid KB medium

without SA, suggesting that SA had bactericidal activity (Fig. S4.2). Therefore, SA is a stronger antibacterial agent under conditions that better represent the intercellular space. It has been suggested that acidification of the culture medium by SA accounts for its toxic effects (Van Duy et al. 2007), however, in our experiments SA had little effect on pH at the concentrations tested (Fig. S4.3). Since some plant pathogens degrade SA and use it as a carbon source (Lowe-Power et al. 2016, Rabe et al. 2013), we speculated that *Pst* may also have this ability. However, *Pst* was unable to grow in HIM medium with SA as the sole carbon source, suggesting that *Pst* DC3000 lacks the ability to degrade SA (Fig. S4.4).

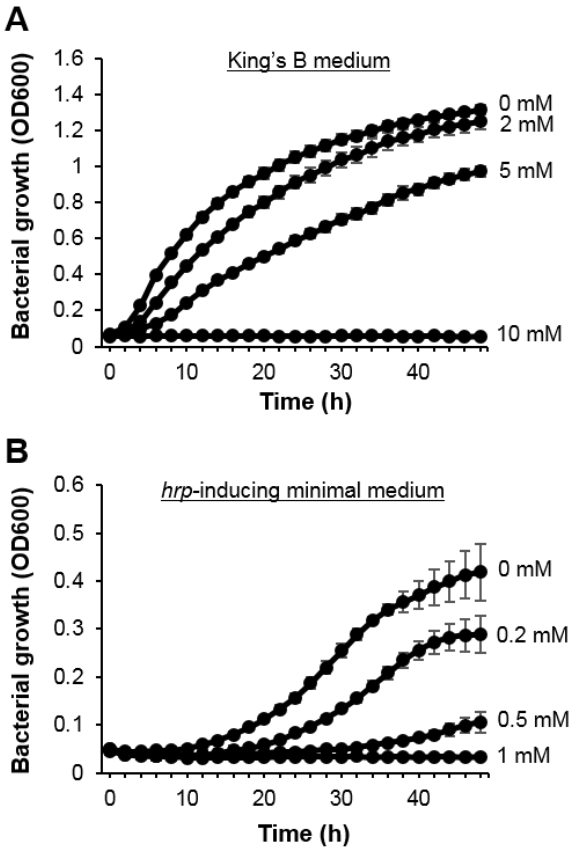

Figure 4.3 – Antibacterial activity of SA in vitro. *Pst* was grown in **A,** King's B medium, or **B,** *hrp*-inducing minimal medium along with the indicated concentrations of SA in a 96-well plate with shaking. Each data point shows the mean of 4 wells, and error bars indicate standard deviation. These experiments were performed at least 3 times with similar results.

Several studies suggest that biofilm formation contributes to the virulence of *P. syringae* on various hosts including *Arabidopsis* (Aslam et al. 2008, Schenk et al. 2008, Yu et al. 2008). This led us to speculate that elevated intercellular SA levels during ARR may reduce *Pst* biofilm formation, therefore we examined whether treatment with SA reduces *Pst* biofilm formation in vitro. The ability of *Pst* to form biofilms in vitro was assessed using a spectrophotometric microplate assay in which staining of surface-adherent cells with crystal violet allows for

quantification of biofilm formation (O'Toole 2011). In KB medium, *Pst* biofilm formation was negligible (Fig. S4.5), whereas extensive biofilm formation was observed beginning at 24 h in HIM medium (Fig. 4.4A). Interestingly, biofilm formation was reduced by SA in a concentration-dependent manner, as shown by quantitative assays (Fig. 4.4A) and qualitative assays performed with test tubes instead of microplates (Fig. 4.4B). The effect was most dramatic at 24 h and onwards, once extensive biofilm formation had occurred in the SA-free controls. At the lowest effective concentrations of SA (2-5 µM), biofilm formation was reduced by 1.3- to 2.3-fold. At higher concentrations (50-100 µM), similar to the levels estimated to accumulate in the intercellular space during ARR (Fig. 4.1C), biofilm formation was reduced by 2.1- to 7.1-fold. Concentrations greater than 100 µM were not tested as they were observed to reduce the growth of *Pst* (Fig. 4.3B).

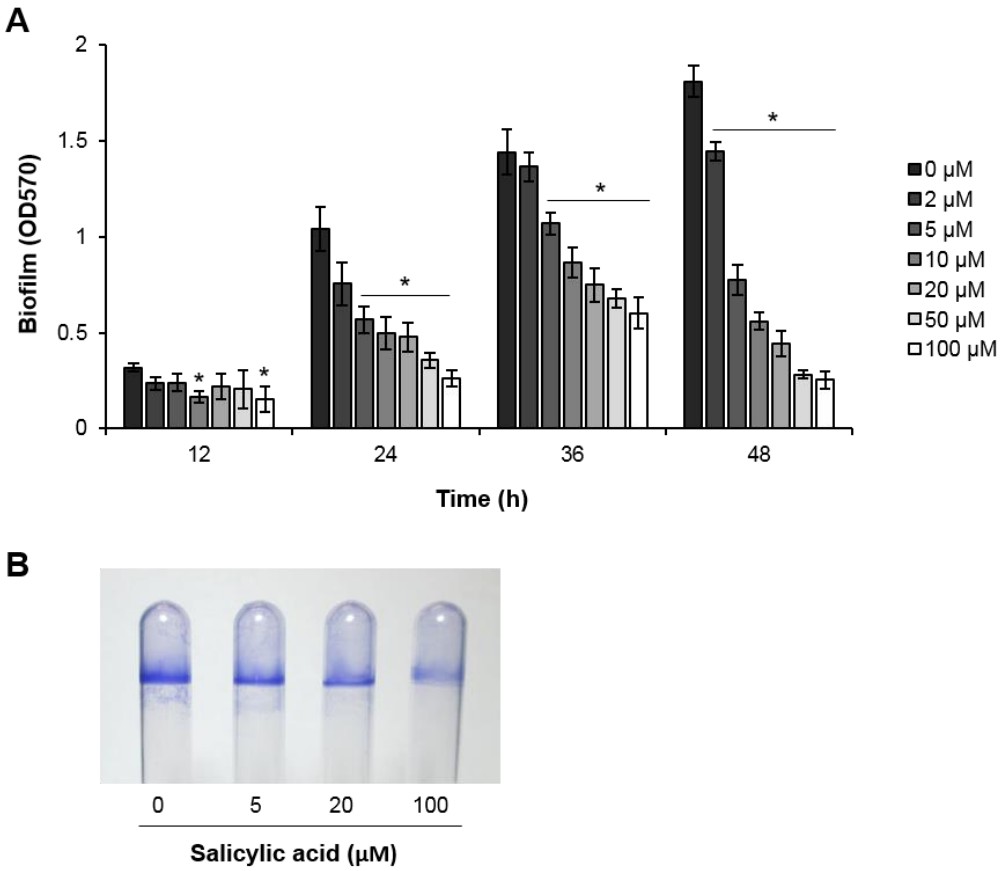

Figure 4.4 – SA reduces biofilm formation in vitro. **A,** *Pst* was cultured in *hrp*-inducing minimal medium along with with the indicated concentration of SA at room temperature without shaking in a 96-well plate. At the indicated time points plates were rinsed to remove unattached planktonic cells and biofilms were quantified by staining with crystal violet. Each bar shows the mean of 4 wells and error bars show standard deviation. Asterisks indicate significant differences relative to the 0 µM control at the corresponding time point (ANOVA followed by Tukey's HSD test, $P < 0.05$). **B,** Similar assays were conducted in test tubes that were photographed after staining with crystal violet following 30 h of incubation. These experiments were performed 3 times with similar results.

To determine whether intercellular SA accumulation during ARR plays a role in inhibiting biofilm formation in planta, a GFP-expressing strain of *Pst* DC3000 (carrying plasmid pDSK-GFPuv, Wang et al. 2007) was used to monitor the formation of biofilm-like aggregates (groups of densely packed, stationary bacterial cells) in leaf tissue of young and mature Col-0 and *svp-32* via

fluorescence microscopy. Aggregates were not observed in leaves immediately after inoculation, nor in the inoculum itself (Fig. S4.6). At 24 hpi, aggregates and individual free-swimming (planktonic) bacterial cells were visible in the spaces between mesophyll cells with autofluorescent chloroplasts (Fig. 4.5A-B, S4.7). For young Col-0 and *svp* mutants, most fields of view contained both free-swimming and aggregated cells (Fig. 4.5C). In contrast, most fields of view contained only free-swimming cells (66%) for mature Col-0 leaves, whereas most fields of view for mature *svp* leaves contained both free-swimming and aggregated cells (77%), similar to young plants. Taken together, these data support the hypothesis that mature, ARR-competent plants reduce the formation of biofilm-like aggregates through intercellular SA accumulation.

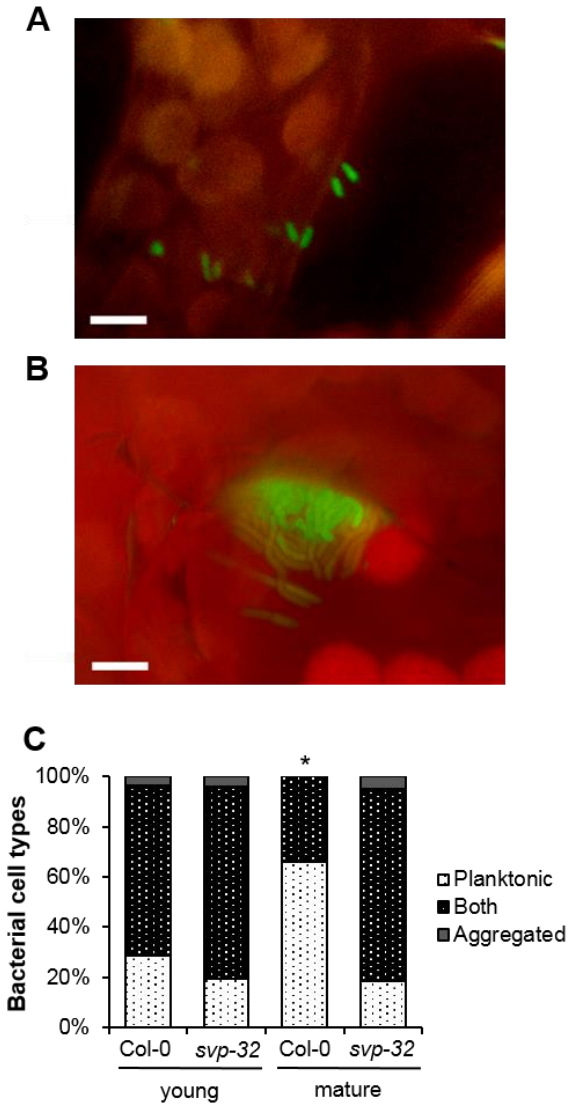

Figure 4.5 – Formation of bacterial aggregates in the leaf intercellular space. Twenty-four hours after inoculation with 10^6 CFU ml^{-1} *Pst* carrying pDSK-GFPuv, the lower epidermis was removed from the leaves and bacterial cells (green) were imaged by epifluoresence microscopy. Individual, free-swimming (planktonic) cells **(A)** and stationary aggregates **(B)** were observed. **C,** The proportion of bacterial cell types in plants of different ages (4 and 7 weeks postgermination) and genotypes was scored by assessing 8-10 fields of view from at least 6 plants for the presence of free-swimming cells, aggregated cells, or a mixture of both. The asterisk indicates a significant difference (Kruskal-Wallis test followed by Dunn's test). This experiment was performed 3 times with similar results. Scale bars = 5 µm.

SA reduces growth and biofilm formation of *Pst* in a concentration-dependent manner in vitro. To gain insight into whether SA might function similarly in the intercellular space during ARR, it would be useful to know the concentration of SA in planta. While collection and examination of IWFs makes it possible to detect intercellular compounds, dilution of intercellular contents is a consequence of the collection procedure. To account for this, a dilution correction factor was calculated for mature Col-0 according to the indigo carmine method described by Husted and Schoerring (1995). The dilution correction factor (6.73 ± 3.42, average ± standard deviation of three independent experiments) was applied to the concentrations of SA measured in IWFs, and suggests that SA is present at 40-100 µM in mature Col-0 at 24 hpi with *Pst*. At these concentrations SA has little effect on *Pst* growth in vitro (Fig. 4.3B), but significantly reduces biofilm formation (Fig. 4.4).

The ARR-defective phenotype of svp is not related to early flowering

It is possible that morphological changes associated with early flowering contribute to the *svp* ARR defect. To examine this idea, *KNAT1:SVP/svp-41* plants were assessed for ARR, since *SVP* expression from the meristem-specific *KNAT1* promoter delays flowering, while SVP is non-functional in the leaves (Andrés et al. 2014). Col-0 did not flower during the experiment and showed a strong ARR response (119-fold reduction in bacterial levels in mature plants relative to young plants, Fig. 4.6). The two *KNAT1:SVP/svp-41* lines did not

flower during the experiment, and both lines displayed an ARR-defective phenotype similar to the *svp-41* parental line. Furthermore, this corresponded to reduced intercellular SA accumulation compared to wild type (Fig. S4.8). Thus, the ARR-defective phenotype of *svp* mutants can be separated from early flowering, suggesting that the requirement of functional SVP for ARR is not an indirect effect of its role in flowering-time control.

A

	Col-0	*KNAT1:SVP/svp-41* line 2	*KNAT1:SVP/svp-41* line 5	*svp-41*
2 wpg	0	0	0	0
3 wpg	0	0	0	0
4 wpg	0	0	0	32
5 wpg	0	0	0	91
6 wpg	0	0	0	100

B

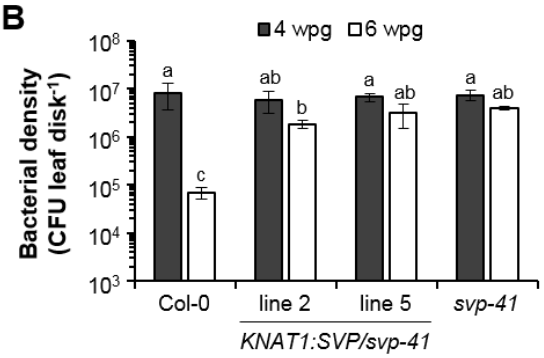

Figure 4.6 – The early-flowering and ARR-defective phenotypes of *svp-41* are not linked. **A,** Percentage of plants with visible infloresence stems was scored each week starting at 2 weeks postgermination (wpg, n ≥ 9). **B,** Plants were inoculated with 10^6 CFU ml^{-1} *Pst* at either 4 or 6 wpg and bacterial levels were quantified 3 days later. Each bar shows the mean of 3 sample replicates, and error bars show standard deviation. Different letters indicate significant differences (ANOVA followed by Tukey's HSD test, $P < 0.05$). This experiment was performed 3 times with similar results. This experiment was part of the experiment shown in Figure 1A.

Under long-day conditions, the onset of ARR is accelerated such that it occurs at 4 weeks postgermination (wpg, Rusterucci et al. 2005). To determine whether SVP is required for ARR in long days, the *KNAT1:SVP/svp-41* lines were used since they flower later and produce more rosette leaves than *svp-41*, making them more amenable to disease resistance assays performed with long-day-grown plants. While Col-0 showed a 15-fold decrease in bacterial levels between 3 and 4 wpg, the *KNAT1:SVP/svp-41* lines supported similarly high bacterial levels at 3 and 4 wpg (Fig. S4.9). Therefore, meristem-specific expression of *SVP* does not rescue the ARR defect of *svp-41* under long or short days, suggesting that functional SVP in leaves is required for the ARR response.

SOC1 negatively influences ARR

SVP directly represses expression of *SOC1* in both the meristem and leaves (Li et al. 2008). To test whether SVP function during ARR is associated with its repression of *SOC1*, *svp-32 soc1-2* double mutants were created and assayed for ARR. As shown previously (Wilson et al. 2013), *soc1-2* single mutants display wild-type ARR (Fig. 4.7A). Interestingly, the *svp-32 soc1-2* double mutant was ARR-competent, indicating that SVP function is not required for ARR in a *soc1-2* mutant background, and thus, the requirement of SVP for ARR may be due to its repression of *SOC1*. This suggested that SOC1 may have a negative impact on ARR, and indeed, the *SOC1*-overexpressing plant line *soc1-101D* (Lee et al. 2000, Moon et al. 2005) was ARR defective and failed to accumulate intercellular

SA (Fig. 4.7A-B). To further assess the potential involvement of SOC1 in ARR, transgenic plants with β-estradiol-inducible overexpression of *SOC1* were created (*XVE:SOC1/soc1-2*, see materials and methods). Maximum *SOC1* expression levels were reached by 24 h after treatment with β-estradiol, and were sustained for at least 3 days thereafter (Fig. 4.7E). To determine whether overexpression of *SOC1* impedes the ARR response, mature plants were pressure-infiltrated with β-estradiol or a mock solution 24 h before inoculation with *Pst*, and bacterial levels were measured at 3 dpi. ARR was observed in the *soc1-2* parental line and β-estradiol treatment had no effect on bacterial levels in *soc1-2*. In contrast, two independent *XVE:SOC1/soc1-2* lines consistently supported higher bacterial levels after β-estradiol treatment, although the difference was not always statistically significant (Fig. 4.7D). Together these data suggest that SOC1 negatively impacts the ARR response downstream of SVP, and upstream of intercellular SA accumulation. SOC1 was recently identified in a yeast one-hybrid screen for transcription factors that interact with the promoter of the SA biosynthesis gene *ICS1* (Zheng et al. 2015). To test whether the negative impact of SOC1 on ARR could be explained by repression of *ICS1*, expression of *ICS1* was measured in mature Col-0 and *soc1-101D* plants before and after inoculation with *Pst*. While Col-0 displayed a 5.5-fold induction of *ICS1* expression at 24 hpi with *Pst*, induction of *ICS1* expression was not observed in *soc1-101D* (Fig. 4.7C). Together these data suggest that SOC1 negatively impacts ARR by repression of *ICS1* expression and SA accumulation. A proposed model for the

contribution of SVP and SOC1 to intercellular SA accumulation during ARR is presented in Figure 8.

Since *soc1-101D* plants also displayed enhanced susceptibility compared to wild type at the young-plant stage (Fig. 4.7A), *XVE:SOC1/soc1-2* plants were used to further assess the possibility that *SOC1* overexpression negatively impacts disease-resistance in young plants. Young plants pressure-infiltrated with β-estradiol or a mock solution 24 h before inoculation with *Pst* supported similar in planta bacterial levels at 3 dpi (Fig. S4.10), suggesting that *SOC1* overexpression has a greater impact on disease resistance in mature compared to young plants.

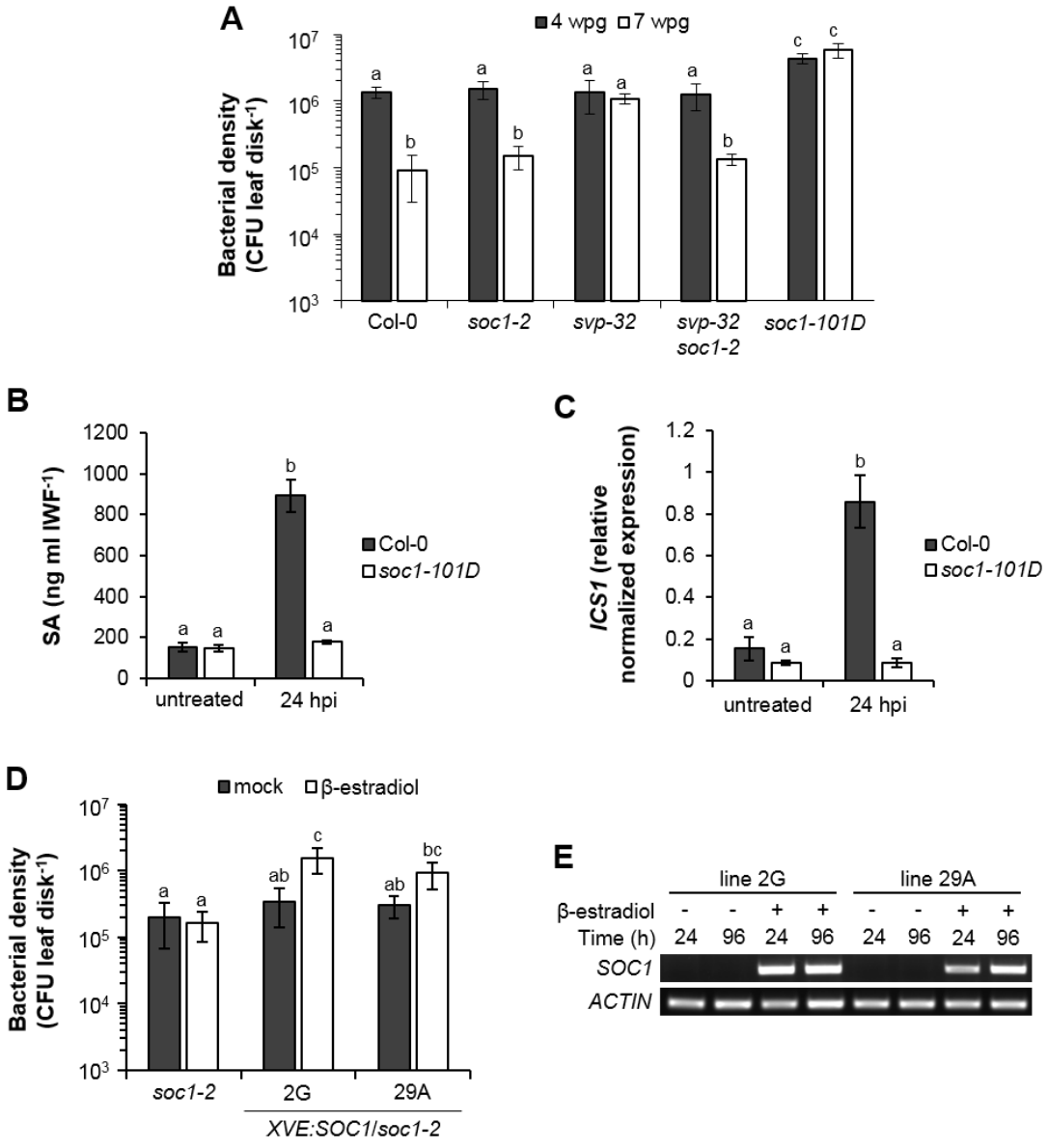

Figure 4.7 – SOC1 negatively impacts ARR. **A,** Plants were inoculated with 10^6 CFU ml^{-1} *Pst* at either 4 or 7 weeks postgermination (wpg) and bacterial levels were quantified 3 days later. Each bar shows the mean of 3 sample replicates, and error bars show standard deviation. Different letters indicate significant differences (ANOVA followed by Tukey's HSD test, $P < 0.05$). **B-C,** Plants were inoculated with 10^6 CFU ml^{-1} *Pst* at 6.5 wpg and SA levels were quantified in IWFs (B) and *ICS1* expression was quantified in leaf tissue (C) collected from untreated or inoculated plants at 24 h postinoculation (hpi)**. D,** Plants were pressure-infiltrated with 50 µM β-estradiol or a mock solution at 7 wpg, then inoculated with 10^6 CFU ml^{-1} *Pst* 24 h later. Bacterial levels were quantified 3 days after inoculation. Different letters indicate significant differences (ANOVA followed by Tukey's HSD test, $P < 0.05$). **E,** *SOC1* expression was measured by RT-PCR in leaf tissue of *XVE:SOC1/soc1-2* plants at 24 and 96 hpi with 50 µM β-estradiol (+) or a mock solution (-). These experiments were performed at least twice with similar results.

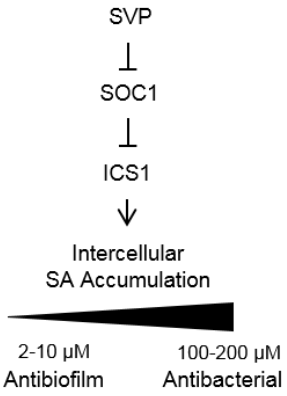

Figure 4.8 – Proposed model for the effect of SVP and SOC1 on intercellular SA accumulation during ARR. SVP is required for ARR to suppress expression of *SOC1*, which codes for a MADS-domain transcription factor that negatively impacts ARR through repression of the SA biosynthesis gene *ICS1*. In the presence of functional SVP, mature plants accumulate intercellular SA, which limits biofilm formation and/or bacterial growth.

4.4 Discussion

SVP and SOC1 contribute to ARR

Consistent with the hypothesis that SVP regulates SA accumulation during ARR, the ARR-defective phenotype of *svp* mutants is associated with a reduced ability to accumulate intercellular free SA in response to *Pst* (3-fold reduction relative to Col-0). Moreover, exogenous SA applied to the intercellular space 4 h before pathogen inoculation restored ARR in *svp* mutants, however, no effect on ARR was observed when SA was applied 24 h before inoculation, since it has been demonstrated that SA is taken up by cells by 24 h after SA application (Cameron and Zaton 2004).

Since SVP directly represses *SOC1* expression in seedlings (Gregis et al. 2013, Li et al. 2008), the ARR phenotype of *svp-32 soc1-2* mutants was tested to determine whether the function of SVP in ARR is associated with its repression of *SOC1*. The ARR-competent phenotype of *svp-32 soc1-2* mutants suggested that SOC1 acts downstream of SVP during ARR, and that the requirement of SVP for ARR is related to its repression of *SOC1*. In support of this idea, constitutive *SOC1* overexpressors were fully ARR-defective and failed to accumulate intercellular SA. β-estradiol-inducible *SOC1* overexpression lines displayed a modest ARR-defective phenotype, which may be explained by higher *SOC1* expression levels in constitutive overexpressors, as supported by the dose-dependent effect of *SOC1* on flowering time (Lee et al. 2000).

The negative impact of SOC1 on ARR appears to be due to repression of *ICS1* expression since constitutive *SOC1* overexpressors are defective for pathogen-induced *ICS1* expression and intercellular SA accumulation. Furthermore, repression of *ICS1* expression by SOC1 may be direct since SOC1 interacts with the *ICS1* promoter in yeast one-hybrid experiments (Zheng et al. 2015). Young and mature wild-type plants express *ICS1* to similar levels in response to *Pst* (Rusterucci et al. 2005), suggesting that SVP and SOC1 do not regulate the onset of ARR competence in wild-type plants. Perhaps SOC1 only inhibits ARR when expressed at the high levels found in *svp* mutants or *SOC1* overexpressors (Lee et al. 2000, Li et al. 2008).

The ARR-defective phenotype of *svp* mutants is not related to their early-flowering phenotype since *KNAT1:SVP/svp-41* plants expressing functional SVP only in the meristem did not flower during short-day ARR experiments, but remained ARR-defective. Similarly, the early-flowering and ARR-defective phenotypes associated with constitutive *SOC1* overexpression could be separated by inducible overexpression of *SOC1* during infection, which did not accelerate flowering but still negatively impacted ARR. Consistent with these results, the altered disease-resistance phenotypes of several late-flowering mutants were unchanged by mutations or treatments that accelerated flowering (Lyons et al. 2015, Singh et al. 2013). Therefore, rather than the timing of flowering affecting disease resistance, some flowering-time regulators appear to have distinct effects on disease-resistance responses such as Systemic Acquired Resistance (FLD, Singh et al. 2013), resistance to Fusarium oxysporum (FVE and FPA, Lyons et al. 2015), and ARR (SVP and SOC1, this work).

Antibacterial activity of salicylic acid

Many studies have shown that SA exhibits antimicrobial activity against phytopathogens in vitro (Amborabé et al. 2002, Brown 2007, Cameron and Zaton 2004, El-Mougy 2002, Georgiou et al. 2000, Martín et al. 2010, Prithiviraj et al. 1997, Lowe-Power et al. 2016, Yuan et al. 2007), with the range of effective concentrations spanning several orders of magnitude, probably due in large part to the different organisms and experimental conditions used. We found that SA

displayed ~10-fold greater antibacterial activity in minimal medium, which is a better representation of the conditions in the leaf intercellular space compared to rich media. This difference in SA antibacterial activity could be due to differential effects of these media on bacterial growth rate, physiology, and metabolism (Kim et al. 2010), or alternatively, on SA itself. For example, HIM medium has a pH of 5.7, similar to intercellular fluids (Jia and Davies 2007), whereas KB medium has a pH of 7.2. At lower pH, a greater proportion of SA exists in its protonated, lipophilic form, enhancing its ability to cross cell membranes, which may be a prerequisite for its antimicrobial activity. In support of this idea, Amborabé et al. (2002) showed that antifungal activity of SA against *Eutypa lata* increased at lower pH and was associated with increased SA uptake by fungal hyphae. The mechanism of action of SA as an antimicrobial agent is not fully understood, however, several studies suggest that it may dissipate the transmembrane proton gradient required for ATP production (Gutknecht 1990, Jörgensen et al. 1976, Smith 1959, Norman et al. 2004, Stenlid and Saddik 1962) or inhibit respiration (Norman et al. 2004) or catalase activity (Chen et al. 1993). In HIM medium *Pst* growth was reduced at SA concentrations as low as 100-200 µM, suggesting that SA may be effective at similar concentrations in planta. Application of an experimentally determined dilution correction factor to SA levels measured in IWFs suggested that SA accumulates to 40-100 µM in the intercellular space of mature plants 24 hpi with *Pst*, similar to the levels that accumulate in the intercellular space of tobacco in response to tobacco mosaic virus (Huang et al.

2006). These results suggest that SA may indeed act as an antimicrobial agent during ARR, especially given the possibility that SA is incompletely recovered during IWF collection, and may also reach higher concentrations in microenvironments of the leaf intercellular space, which cannot be assessed using currently available techniques. Moreover, it is possible that other antimicrobials act together with SA during ARR.

Biofilm formation by P. syringae and antibiofilm activity of salicylic acid

Many *P. syringae* genes that are expressed in planta are also expressed in minimal but not rich media (Boch et al. 2002, Huynh et al. 1989, Rahme et al. 1992). Similarly, we found that *Pst* formed biofilms in intercellular space-mimicking minimal medium, but not rich medium, leading to the idea that biofilm formation might also occur in planta. Indeed, fluorescence microscopy of leaves inoculated with *GFP*-expressing *Pst* revealed the presence of biofilm-like aggregates in the intercellular space at 24 hpi. Intriguingly, SA reduced *Pst* biofilm formation in vitro, at concentrations that were insufficient to affect growth and were estimated to exist in the intercellular space of mature wild-type plants. Furthermore, reduced formation of bacterial aggregates was observed in mature wild-type plants compared to young plants and mature *svp* mutants, both of which are impaired in intercellular SA accumulation. In young plants *Pst* suppresses intercellular SA accumulation using the phytotoxin coronatine (Carviel et al. 2014), which contributes to bacterial growth and disease. On the

other hand, mature ARR-competent plants accumulate intercellular SA in response to the same pathogen, leading us to speculate that ARR-competent plants circumvent coronatine-mediated suppression of intercellular SA accumulation. Taken together these data suggest that SA accumulation in the intercellular space reduces *Pst* growth and/or biofilm formation during ARR (Fig. 4.8).

Biofilms are usually described as surface-adherent aggregates of cells embedded in an extracellular matrix. These structures have been observed in several plant-pathogen interactions, are thought to provide protection against environmental stresses such as desiccation and antimicrobials, and have been linked to several virulence strategies (Danhorn and Fuqua 2007, Ichinose et al. 2013). In *P. syringae*, biofilms are largely studied in the context of epiphytic populations, although the kiwi pathogen *P. syringae* pv. *actinidiae* forms biofilms on both the leaf surface and within the intercellular space (Renzi et al. 2012). *Pst* biofilm formation is not well described, however, in leaves of Arabidopsis, *Pst* was shown to express algA and algD (Boch et al. 2002, Keith et al. 2003), genes involved in the biosynthesis of alginate, the major extracellular polysaccharide produced by *Pst* in tomato (Fett and Dunn 1989). Intriguingly, *Pst* algD mutants exhibited reduced growth in *Arabidopsis* compared to wild-type *Pst* (~10-fold, Aslam et al. 2008), suggesting that biofilm formation contributes to *Pst* virulence.

Interestingly, SA treatment at concentrations that are insufficient to affect bacterial growth also reduce in vitro biofilm formation and virulence factor production in animal pathogens such as *Pseudomonas aeruginosa* and *Staphylococcus aureus* (Prithiviraj et al. 2005ab, Yang et al. 2009). Similarly, in vitro SA treatment has been shown to suppress hrpA promoter activity in the plant pathogen *Erwinia amylovora* (Khokhani et al. 2013), the virA/G regulon of *Agrobacterium tumefaciens* (Yuan et al. 2007), and virulence gene expression in *Ralstonia solanacearum* (Lowe-Power et al. 2016). Yang et al. (2009) demonstrated that SA treatment interferes with multiple quorum sensing systems in *P. aeruginosa*. Furthermore, SA treatment activated the attKLM operon involved in degradation of quorum sensing signals in *A. tumefaciens* (Khokhani et al. 2013). Given that quorum sensing mediates many virulence strategies including production of toxins, virulence effectors, and biofilm formation (Danhorn and Fuqua 2007, Ichinose et al. 2013), the ability of SA to suppress virulence in a wide range of pathogens may be due to an ability to interfere with quorum sensing.

Pathogens have evolved several strategies to resist the toxic effects of SA including degradation of SA or its precursors (Tanaka et al. 2015). For example, *R. solanacearum* can degrade SA and use it as a carbon source (Lowe-Power et al. 2016). This ability confers enhanced SA tolerance in vitro and increased virulence on tobacco compared to strains that cannot use SA as a carbon source

(Lowe-Power et al. 2016). This ability does not appear to exist in *Pst* DC3000, which was unable to grow on SA as the sole carbon source.

Under biologically relevant conditions, SA concentrations in the micromolar range exhibit direct effects on pathogens, reducing their growth, virulence, or a combination of the two. We provide evidence that during ARR in Arabidopsis, SA accumulates in the intercellular space and contributes to suppression of *Pst* growth and biofilm formation. Furthermore, our data support the idea that the MADS-domain transcription factors SVP and SOC1 act antagonistically during flowering-time control and ARR, such that SVP is required for ARR to alleviate the negative impact of SOC1 on *ICS1* expression and SA accumulation. A better understanding of the interplay between development and defense, as well as the mechanisms of action of compounds that reduce growth and virulence of pathogens, will be useful for optimizing crop performance in the future.

4.5 Materials and methods

Plant lines and growth conditions

All plant lines used are in the Col-0 background and have been described previously: *sid2-2* (Nawrath and Métraux, 1999), *svp-32* and *svp-31* (Lee et al. 2007), *svp-41* (Hartmann et al. 2000), *soc1-2* and *soc1-101D* (Lee et al. 2000), *KNAT1:SVP/svp-41* (Andrés et al. 2014). Initial experiments used the *svp-32* allele, but later experiments with *KNAT1:SVP/svp-41* plants required that the *svp-*

41 allele be used. Similar results were obtained with both alleles (compare Figs. 4.1 and S4.11, and Figs. 4.2 and S4.1). The *svp-32 soc1-2* mutant was created by crossing the corresponding single mutants. Seeds were surface-sterilized, stratified for 2 days in darkness at 4°C, then plated on Murashige and Skoog medium. Approximately 1 week later, cotyledon-stage seedlings were transplanted to soil (Sunshine Mix #1) hydrated with 1 g L^{-1} all-purpose 20-20-20 fertilizer. Growth conditions were 22 ± 2°C, 80 ± 10% relative humidity, and 9 h of light unless otherwise specified in the figure legend (mixed fluorescent and incandescent, 120-150 µE m^{-1} s^{-1}).

To generate *XVE:SOC1/soc1-2* the *SOC1* coding sequence was PCR amplified from Col-0 cDNA using primers 5'-TAAGCAGGCGCGCCATGGTGAGGGGCAAAACTC (F) and 5'-TGCTTATTAATTAATCACTTTCTTGAAGAACAAGGTAAC (R) and cloned into the pER8 binary vector (Zuo et al. 2000) by restriction-ligation (*Asc*I and *Sac*I sites). The resulting construct was transformed into *A. tumefaciens* GV3101, *soc1-2* mutants were transformed via the floral dip method (Clough and Bent, 1998), and transformants were selected on the basis of hygromycin resistance (25 µg ml^{-1}). β-estradiol (SIGMA, E8875) was dissolved in DMSO and a 50 µM solution (0.5% DMSO) was applied by pressure-infiltration with a needle-less syringae.

Disease resistance assays

Overnight cultures of *Pst* DC3000 were grown in King's B (KB) medium to exponential phase. Cells were collected by centrifugation, resuspended in 10 mM $MgCl_2$ to 10^6 CFU ml^{-1}, and pressure-infiltrated into fully expanded leaves using a needle-less syringe. For quantification of in planta bacterial levels, 3 sets of 8 leaf disks (4 mm diameter) were collected and shaken at 200 rpm for 1 h in 10 mM $MgCl_2$ with 0.1% Silwet L-77. Serial dilutions were plated on KB medium with kanamycin (50 µg ml^{-1}) and rifampicin (100 µg ml^{-1}), and colonies were counted 2 days later.

Intercellular washing fluid collection and dilution correction factor determination

The technique for infiltration of leaves and collection of IWFs was adapted from Baker et al. (2012) and O'Leary et al. (2014) – see this reference for a video demonstration of the technique. Three pools of 8-12 leaves (or 30-40 leaves for *soc1-101D* plants, to account for their smaller size) were cut at the petiole and vacuum-infiltrated with water inside a 60 ml syringe until they appeared completely water-soaked. Leaves were then blotted dry, stacked between parafilm sheets, rolled around a 1 ml pipette tip, secured with a twist-tie, and placed inside the bottom third of a 60 ml syringe fitted to a 1.5 ml centrifuge tube with the petioles facing up. Leaves were then centrifuged using a swinging bucket rotor at 600 x g for 15 minutes at room temperature to collect the IWFs. In some cases leaves were subsequently frozen in liquid nitrogen and stored at -80°C for SA quantification. IWFs were centrifuged for an additional 5 minutes at 13,000 x

g, transferred to fresh tubes, weighed, and stored at -80°C. The remaining chlorophyll pellets (sometimes visible) were resuspended in 1 ml of ethanol and measured spectrophotometrically at 664 and 700 nm to assess contamination of IWFs with cellular contents (Baker et al. 2012). In a representative experiment, the chlorophyll levels in IWFs were 0.0085 percent of the corresponding leaf tissue, indicating that the IWFs had minimal cellular contamination.

The dilution correction factor was determined according to the method described by Husted and Schjoerring (1995), where dilution correction factor = $V_{air} + V_{water} / V_{water}$. IWFs were collected as described above except that leaves were vacuum-infiltrated with 50 µM indigo carmine in 50 mM sodium phosphate (pH 6.2). The volume of intercellular air space (V_{air}) was estimated by calculating the difference in leaf weight before and after infiltration, and the volume of intercellular water (V_{water}) was calculated according to the equation: $V_{water} = D_{dye} \times V_{air} / 1 - D_{dye}$, where D_{dye} is the dilution of the dye after IWF collection. Indigo carmine was measured spectrophotometrically at 608 nm.

SA quantification

SA was quantified using the ADPWH_lux SA biosensor (DeFraia et al. 2008) as described previously (Carviel et al. 2014). Similar results were obtained when SA was quantified by gas chromatography-mass spectrometry (Fig. S4.11).

Antibacterial assays

For antibacterial assays with pure SA, overnight cultures of *Pst* DC3000 were grown in KB medium to exponential phase, cells were collected by centrifugation, washed twice with fresh KB (20 g L^{-1} proteose peptone, 10 ml L^{-1} glycerol, 8.6 mM K_2HPO_4, 6 mM $MgSO_4$) or HIM (50 mM potassium phosphate buffer, 10 mM fructose, 7.6 mM $(NH_4)_2SO_4$, 3.6 mM $MgCl_2$, 1.7 mM NaCl, pH 5.7) medium, then resuspended in KB or HIM medium to an OD600 of 0.05. Aliquots of 160 µl were added to a 96-well microplate (Corning, C351172) containing 3.2 µl SA (Sigma, 247588) or ethanol (the solvent used for SA stock solutions, 0.02% final concentration). Plates were incubated with shaking at room temperature in a Tecan Sunrise with absorbance (600 nm) measured every 15 min. To determine bactericidal concentrations at the end of the experiment well contents were transferred to microcentrifuge tubes and cells were collected by centrifugation, resuspended in 10 mM $MgCl_2$, then plated on KB medium with kanamycin (50 µg ml^{-1}) and rifampicin (100 µg ml^{-1}). Bactericidal activity was assumed if no growth was visible after at least 3 days.

Biofilm assays

In vitro biofilm assays were performed essentially as described by O'Toole (2011). Overnight cultures of *Pst* DC3000 were grown to exponential phase in KB medium, diluted with fresh KB or HIM medium (1:100), and 150 µl aliquots were

added to a 96-well microplate (Corning, C351172) containing SA or ethanol. The cultures were then incubated at room temperature and stained at the indicated times. Prior to staining, microplates were inverted and rinsed twice with water to remove non-adherent cells. Each well was stained with 180 µl of 0.1% crystal violet for 10 min, followed by 4 washes with water to remove residual stain. For quantification of the stained biofilms, 200 µl of 30% acetic acid was added to each well and incubated for 15 min, then absorbance was measured at 570 nm. For qualitative assays a similar procedure was followed using a 500 µl culture volume in polypropylene tubes which were photographed after the staining step.

Imaging of Pst in the intercellular space by epifluorescence microscopy

Plants were inoculated with 10^6 CFU ml^{-1} *Pst* carrying pDSK-GFPuv (Wang et al. 2007). After 24 h leaves were cut at the petiole and sections of the lower epidermis were removed using invisible tape. Sections without the lower epidermis were isolated using a razor blade and mounted in water on a glass slide with coverslip with the epidermis-less surface facing upwards. Slides were imaged immediately using a Nikon Eclipse E800 microscope fitted with a Nikon DS-Fi1 camera head and DS-U3 control unit using 60X or 100X oil immersion lenses and a B-2A filter cube. For comparing the proportion of cell types between young and mature plants of different genotypes tissue preparation and imaging were performed by different individuals so that the scoring was blind.

Gene expression analysis

RNA extraction and cDNA synthesis were performed as described previously (Carviel et al. 2014) except that M-MLV Reverse Transcriptase (SIGMA, M1302) was used. qRT-PCR was performed using a BioRad CFX-96 Touch Real-Time PCR Detection System with 20 µl reactions consisting of 2 µl template (cDNA diluted 2-fold with water), 400 nM of each primer (annealing temperature 61ºC), and Advanced qPCR Mastermix (1X final concentration, Wisent Bioproducts, 800-4310-UL). For each sample, three biological replicates and two technical replicates were analyzed. Data analysis was performed using the BioRad CFX Manger 3.0 software and CUL4 (AT5G46210) and SEC5A (AT1G76850) were used as reference genes. The identity of each qRT-PCR product was confirmed by sequencing. RT-PCR was performed using Taq DNA Polymerase (ABM, G008). Annealing temperatures and cycle numbers were 60ºC and 28 cycles for ACTIN, and 53ºC and 32 cycles for SOC1. Table S4.1 lists the primers used.

4.6 Acknowledgements

For sharing materials we thank George Coupland (*KNAT1:SVP/svp-41*), Illha Lee (*soc1-2* and *soc1-101D*), and Kirankumar Mysore (*Pst* pDSK-GFPuv).

4.7 Literature cited

Amasino, R. (2010). Seasonal and developmental timing of flowering. Plant J. 61: 1001-1013.

Amborabé, B., Fleurat-Lessard, P., Chollet, J., Roblin, G. (2002). Antifungal effects of salicylic acid and other benzoic acid derivatives towards *Eutypa lata*: structure–activity relationship. *Plant Physiol. Biochem.* 40: 1051–1060.

Andrés, F., Porri, A., Torti, S., Mateos, J., Romera-Branchat, M., Garcia-Martínez, J. L., Fornara, F., Gregis, V., Kater, M. M., Coupland, G. (2014). SHORT VEGETATIVE PHASE reduces gibberellin biosynthesis at the *Arabidopsis* shoot apex to regulate the floral transition. Proc. Natl. Acad. Sci. U. S. A. 111: E2760-E2769.

Aslam, S. N., Newman, M.-A., Erbs, G., Morrissey, K. L., Chinchilla, D., Boller, T., Jensen, T. T., Castro, C. D., Ierano, T., Molinaro, A., Jackson, R. W., Knight, M. R., and Cooper, R. M. (2008). Bacterial polysaccharides suppress induced innate immunity by calcium chelation. Curr. Biol. 18: 1078-1083.

Baker, J. C., Kovalskaya, N. Y., Mock, N. M., Owens, R. A., Deahl, K. L., Whitaker, B.D., Roberts, D. P., Hammond, R. W., and Aver'yanov, A. A. (2012). An internal standard technique for improved quantitative analysis of apoplastic metabolites in tomato leaves. Physiol. Mol. Plant Pathol. 78: 31-37.

Boch, J., Joardar, V., Gao, L., Robertson, T. L., Lim, M., Kunkel, B. N. (2002). Identification of *Pseudomonas syringae* pv. *tomato* genes induced during infection of *Arabidopsis thaliana.* Mol. Microbiol. 44: 73-88.

Brown, D. G., Swanson, J. K., Allen, C. (2007). Two host-induced *Ralstonia solanacearum* genes, *acrA* and *dinF*, encode multidrug efflux pumps and contribute to bacterial wilt virulence. Appl. Environ. Microbiol. 73: 2777-2786.

Cameron, R. K., and Zaton, K. (2004). Intercellular salicylic acid accumulation is important for age-related resistance in arabidopsis to *Pseudomonas syringae*. Physiol. Mol. Plant Pathol. 65: 197:209.

Carella, P., Wilson, D. C., Cameron, R. K. (2015). Some things get better with age: differences in salicylic acid accumulation and defense signaling in young and mature *Arabidopsis.* Front. Plant Sci. 5: article 775.

Carviel, J. L., Al-Daoud, F., Neumann, M., Mohammad, A., Provart, N. J., Moeder, W., Yoshioka, K., Cameron, R. K. (2009). Forward and reverse genetics to identify genes involved in the age-related resistance response in *Arabidopsis thaliana.* Mol. Plant Pathol. 10: 621-634.

Carviel, J. L., Wilson, D. C., Isaacs, M., Carella, P., Catana, V., Golding, B., Weretilnyk, E. A., Cameron, R. K. (2014). Investigation of intercellular salicylic acid accumulation during compatible and incompatible *Arabidopsis-Pseudomonas syringae* interactions using a fast neutron-generated mutant allele of *EDS5* identified by genetic mapping and whole-genome sequencing. PLoS One 9: e88608.

Chen, Z., Silva, H., Klessig, D.F. (1993). Active oxygen species in the induction of plant systemic acquired resistance by salicylic acid. Science, 262: 1883-1886.

Clough, S. J., Bent, A. F. (1998). Floral dip: a simplified method for Agrobacterium-mediated transformation of Arabidopsis thaliana. Plant J. 16: 735-743.

Danhorn, T., Fuqua, C. (2007). Biofilm formation by plant-associated bacteria. Annu. Rev. Microbiol. 61: 401-422.

DeFraia, C., Schmelz, E. A., Mou, Z. (2008). A rapid biosensor-based method for quantification of free and glucose-conjugated salicylic acid. Plant Methods 4: 28.

Develey-Rivière, M-P., Galiana, E. (2007). Resistance to pathogens and host developmental stage: a multifaceted relationship within the plant kingdom. New Phytol. 175: 405-416.

El-Mougy, N. S. (2002). In vitro studies on antimicrobial activity of salicylic acid and acetyl salicylic acid as pesticidal alternatives against some soilborne plant pathogens. *Egypt. J. Phytopathol.* 30: 41–55.

Fett, W. F., Dunn, M. F. (1989). Exopolysaccharides produced by phytopathogenic *Pseudomonas syringae* pathovars in infected leaves of susceptible hosts. Plant Physiol. 89: 5-9.

Fornara, F., de Montaigu, A., Coupland, G. (2010). SnapShot: control of flowering in *Arabidopsis*. Cell 141: 550-550e.2.

Georgiou, C. D., Tairis, N., Sotiropoulou, A. (2000). Hydroxyl radical scavengers inhibit lateral-type sclerotial differentiation and growth in phytopathogenic fungi. Mycologia 95: 825–834.

Gregis, V., Andrés, F., Sessa, A., Guerra, R. F., Simonini, S., Mateos, J. L., Torti, S., Zambelli, F., Prazzoli, G. M., Bjerkan, K. M., Grini, P. E., Pavesi, G., Colombo, L., Coupland, G., Kater, M. M. (2013). Identification of pathways directly regulated by SHORT VEGETATIVE PHASE during vegetative and reproductive development in *Arabidopsis*. Genome Biol. 14: R56.

Gutknecht, J. (1990). Salicylates and proton transport through lipid bilayer membranes: a model for salicylate-induced uncoupling and swelling in mitochondria. J. Membr. Biol. 115: 253-260.

Hartmann, U., Höhmann, S., Nettesheim, K., Wisman, E., Saedler, H., Huijser, P. (2000). Molecular cloning of *SVP*: a negative regulator of the floral transition in *Arabidopsis*. Plant J. 21: 351-360.

Huang, W. E., Huang, L., Preston, G. M., Naylor, M., Carr, J. P., Li, Y., Singer, A. C., Whiteley, A. S., and Wang H. (2006). Quantitative *in situ* assay of salicylic acid in tobacco leaves using a genetically modified biosensor strain of *Acinetobacter* sp. ADP1. Plant J. 46: 1073-1083.

Husted, S., and Schjoerring, J. K. (1995). Apoplastic pH and ammonium concentration in leaves of *Brassica napus* L. Plant Physiol. 109: 1453-1460.

Huynh, T. V., Dahlbeck, D., Staskawicz, B. J. (1989). Bacterial blight of soybean: regulation of a pathogen gene determining host cultivar specificity. Science 245: 1374-1377.

Ichinose, Y., Taguchi, F., Mukaihara, T. (2013). Pathogenicity and virulence factors of *Pseudomonas syringae.* J. Gen. Plant Pathol. 79: 285-296.

Jaeger, K. E., Wigge, P. A. (2007). FT protein acts as a long-range signal in Arabidopsis. Curr. Biol. 17: 1050–1054.

Jia, W., Davies, W. J. (2007). Modification of leaf apoplastic pH in relation to stomatal sensitivity to root-sourced abscisic acid signals. Plant Physiol. 143: 68-77.

Jörgensen, T. G., Weis-Fogh, U. S., Nielsen, H. H., Olesen, H. P. (1976). Salicylate-and aspirin-induced uncoupling of oxidative phosphorylation in mitochondria isolated from the mucosal membrane of the stomach. Scand. J. Clin. Lab. Invest. 36: 659-664.

Keith, R. C., Keith, L. M. W., Hernandez-Guzman, G., Uppalapati, S. R., Bender, C. L. (2003). Alginate gene expression by *Pseudomonas syringae* pv. *tomato* DC3000 in host and non-host plants. Microbiology 149: 1127-1138.

Kim, B. J., Schneider, D. J., Cartinhour, S. W., Shuler, M. L. (2010). Complex responses to culture conditions in *Pseudomonas syringae* pv. *tomato* DC3000 continuous cultures: the role of iron in cell growth and virulence factor production. Biotechnol. Bioeng. 105: 995-964.

Khokhani, D., Zhang, C., Li, Y., Wang, Q., Zeng, Q., Yamazaki, A., Hutchins, W., Zhou, S-S., Chen, X., Yang, C-H. (2013). Discovery of plant phenolic compounds that act as type III secretion system inhibitors or inducers of the fire blight pathogen, *Erwinia amylovora.* Appl. Environ. Microbiol. 79: 5424-5436.

Kus, J. V., Zaton, K., Sarkar, R., Cameron, R. K. (2002). Age-Related-Resistance in Arabidopsis is a developmentally regulated defense response to *Pseudomonas syringae.* Plant Cell 14: 479-490.

Lee, H., Suh, S-S., Park, E., Cho, E., Ahn, J. H., Kim, S-G., Lee, J. S., Kwon, Y. M., Lee, I. (2000). The AGAMOUS-LIKE 20 MADS domain protein integrates floral inductive pathways in *Arabidopsis.*

Lee, J. H., Yoo, S. J., Park, S. H., Hwang, I., Lee, J.S., Ahn, J. H. (2007). Role of SVP in the control of flowering-time by ambient temperature in Arabidopsis. Genes Dev. 21: 397–402.

Lee, J., Oh, M., Park, H., Lee, I. (2008). SOC1 translocated to the nucleus by interaction with AGL24 directly regulates LEAFY. Plant J 55: 832–843.

Li, D., Liu, C., Shen, L., Wu, Y., Chen, H., Robertson, M., Helliwell, C. A., Ito, T., Meyerowitz, E., Yu, H. (2008). A repressor complex governs the integration of flowering signals in Arabidopsis. Dev. Cell 15: 110–120.

Liu, C., Chen, J., Er, H. L., Soo, H. M., Kumar, P. P., Han, J-H., Liou, Y. C., Yu, H. (2008). Direct interaction of *AGL24* and *SOC1* integrates flowering signals in *Arabidopsis*. Development 135: 1481-1491.

Lowe-Power, T. M., Jacobs, J. M., Ailloud, F., Fochs, B., Prior, P., Allen, C. (2016). Degradation of the plant defense signal salicylic acid protects *Ralstonia solanacearum* from toxicity and enhances virulence on tobacco. mBio 7: e00656-16.

Lyons, R., Rusu, A., Stiller, J., Powell, J., Manners, J. M., Kazan, K. (2015). Investigating the association between flowering time and defense in the *Arabidopsis thaliana-Fusarium oxysporum* interaction. PLoS ONE 10: e0127699.

Martín, J. A., Solla, A., Witzell, J., Gil, L., García-Vallejo, M. C. (2010). Antifungal effect and reduction of *Ulmus minor* symptoms to *Ophiostoma novo-ulmi* by carvacrol and salicylic acid. *Eur. J. Plant Pathol.* 127: 21–32.

Moon, J., Lee, H., Kim, M., Lee, I. (2005). Analysis of flowering pathway integrators in *Arabidopsis*. Plant Cell Physiol. 46: 292-299.

Nawrath, C., Métraux, J-P. (1999). Salicylic acid induction-deficient mutants of Arabidopsis express *PR-2* and *PR-5* and accumulate high levels of camalexin after pathogen inoculation. Plant Cell 11: 1393-1404.

Norman, C., Howell, K. A., Millar, H. A., Whelan, J. M., Day, D. A. (2004). Salicylic acid is an uncoupler and inhibitor of mitochondrial electron transport. Plant Physiol. 134: 492-501.

O'Leary, B. M., Rico, A., McCraw, S., Fones, H. N., Preston, G. M. (2014). The infiltration-centrifugation technique for extraction of apoplastic fluid from plant leaves using *Phaseolus vulgaris* as an example. J. Visualized Exp. 94: e52113.

O'Toole, G. A. (2011). Microtiter dish biofilm formation assay. JoVE 47.

Prithiviraj, B., Manickam, M., Singh, U. P., Ray, A. B. (1997). Antifungal activity of anacardic acid a naturally occurring derivative of salicylic acid. *Can. J. Bot.* 75: 207–211.

Prithiviraj, B., Bais, H. P., Jha, A. K., Vivanco, J. M. (2005a). *Staphylococcus aureus* pathogenicity on *Arabidopsis thaliana* is mediated either by a direct effect of salicylic acid on the pathogen of by SA-dependent, NPR1-independent host responses. Plant J. 43: 417-432.

Prithiviraj, B., Bais, H. P., Weir, T., Suresh, B., Najarro, E. H., Dayakar, B. V., Schweizer, H. P., Vivanco, J. M. (2005b). Down regulation of virulence factors of *Pseudomonas aeruginosa* by salicylic acid attenuates its virulence on *Arabidopsis thaliana* and *Caenorhabditis elegans.* Infect. Immun. 73: 5319-5328.

Rabe, F., Rashidi-Ajami, Z., Doehlemann, G., Kahmann, R., Djamei, A. (2013). Degradation of the plant defense hormone salicylic acid by the biotrophic fungus *Ustilago maydis*. Mol. Microbiol. 89: 179-188.

Rahme, L. G., Mindrinos, M. N., Panopoulos, N. J. (1992). Plant and environmental sensory signals control the expression of *hrp* genes in *Pseudomonas syringae* pv. *phaseolicola.* J. Bacteriol. 174: 3499-3507.

Renzi, M., Copini, P., Taddei, A. R., Rossetti, A., Gallipoli, L., Mazzaglia, A., Balestra, G. M. (2012). Bacterial canker on kiwifruit in Italy: anatomical changes in the wood and in the primary infection sites. Phytopathology 102: 827-840.

Rusterucci, C., Zhao, Z., Haines, K., Mellersh, D., Neumann, M., Cameron, R. K.

(2005). Age-related resistance to *Pseudomonas syringae* pv. *tomato* is associated with the transition to flowering in Arabidopsis and is effective against *Peronospora parasitica*. Physiol. Mol. Plant Pathol. 66: 222-231.

Schenk, A., Weingart, H., and Ullrich, M. S. (2008). The alternative sigma factor AlgT, but not alginate synthesis, promotes in planta multiplication of *Pseudomonas syringae* pv. *glycinea*. Microbiology 154: 413-421.

Singh, V., Roy, S., Giri M. K., Chaturvedi, R., Chowdhury, Z., Shah, J., Nandi, A. K. (2013). *Arabidopsis thaliana FLOWERING LOCUS D* is required for systemic acquired resistance. Mol. Plant Microbe Interact. 9: 1079-1088.

Smith, M. J. H. (1959). Salicylates and metabolism. J. Pharm. Pharmacol. 11: 705-720.

Stenlid, G., Saddik, K. (1962). The effect of some growth regulators and uncoupling agents upon oxidative phosphorylation in mitochondria of cucumber hypocotyls. Physiol. Plant. 15: 369-379.

Tanaka, S., Han, X., Kahmann, R. (2015). Microbial effectors target multiple steps in the salicylic acid production and signaling pathway. Front. Plant Sci. 6: 349.

Van Duy, N., Mäder, U., Tran, N. P., Cavin, J-F., Tam, L. T., Albrecht, D., Hecker, M., Antelmann, H. (2007). The proteome and transcriptome analysis of *Bacillus subtilis* in response to salicylic acid. Proteomics 7: 698-710.

Whalen, M. C. (2005). Host defence in a developmental context. Mol. Plant Pathol. 6: 347-360.

Wang, K., Kang, L., Anand, A., Lazorovits, G., and Mysore, K. S. (2007). Monitoring in planta bacterial infection at both cellular and whole-plant levels using the green fluorescent protein variant GFPuv. New Phytol. 174: 212-223.

Wilson, D. C., Carella, P., Isaacs, M., and Cameron, R. K. (2013). The floral transition is not the developmental switch that confers competence for the arabidopsis age-related resistance response to *Pseudomonas syringae* pv. *tomato*. Plant Mol. Biol. 83: 235:246.

Yang, L., Rybtke, M. T., Jakobsen, T. H., Hentzer, M., Bjarnsholt, T., Givskov, M., Tolker-Nielsen, T. (2009). Computer-aided identification of recognized drugs as *Pseudomonas aeruginosa* quorum-sensing inhibitors. Antimicrob. Agents Chemother. 53: 2432-2433.

Yu, J., Peñaloza-Vázquez, A., Chakrabarty, A. M., and Bender, C. L. (1999). Involvement of the exopolysaccharide alginate in the virulence and epiphytic fitness of *Pseudomonas syringae* pv. *syringae*. Mol. Microbiol. 33: 712-720.

Yuan, Z-C., Edlind, M. P., Liu, P., Saenkham, P., Banta, L. M., Wise, A. A., Ronzone, E., Binns, A. N., Kerr, K., Nester, E. W. (2007). The plant signal salicylic acid shuts down expression of the *vir* regulon and activates quormone quenching genes in *Agrobacterium*. Proc. Natl. Acad. Sci. U. S. A. 104: 11790-11795.

Zheng, X-Y., Zhou, M., Yoo, H., Pruneda-Paz, J.L., Spivey, N.W., Kay, S.A., Dong, X. (2015). Spatial and temporal regulation of biosynthesis of the plant immune signal salicylic acid. Proc. Natl. Acad. Sci. U. S. A. 112: 9166-9173.

Zuo, J., Niu, Q-W., Chua, N-H. (2000). An estrogen receptor-based transactivator XVE mediates highly inducible gene expression in transgenic plants. Plant J. 24: 265-273.

4.8 Supplementary materials

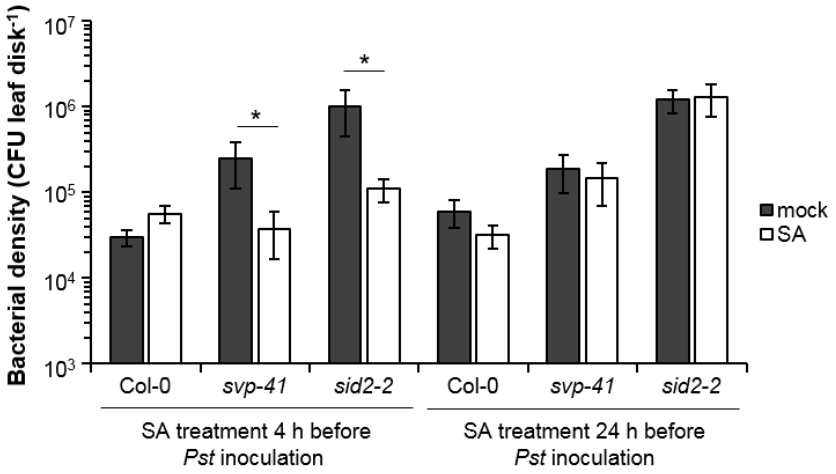

Figure S1 – Exogenous intercellular SA restores ARR to *svp-41* mutants. Mature plants (7 weeks postgermination) were pressure-infiltrated with 0.1 mM SA or water (mock) either 4 or 24 h before inoculation with 10^6 CFU ml^{-1} *Pst*. Bacterial levels were quantified 3 days later. Each bar shows the mean of 3 sample replicates, and error bars show standard the deviation. Asterisks indicate significant differences (ANOVA followed by Tukey's HSD test, $P < 0.05$).

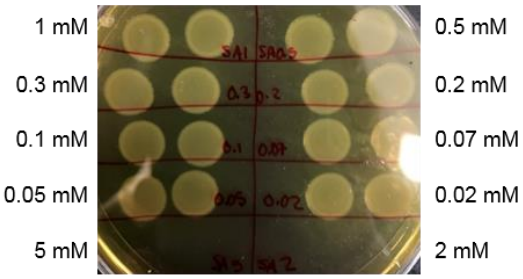

Figure S2 – Bactericidal activity of salicylic acid. After 72 h of growth in *hrp*-inducing minimal medium with various concentrations of SA (indicated beside the image), *Pst* cultures were centrifuged, pelleted cells were resuspended in 10 mM $MgCl_2$, and the suspensions were plated on King's B medium. SA was assumed to be bactericidal at concentrations for which no colonies were visible after at least 3 days. This experiment was performed at least three times.

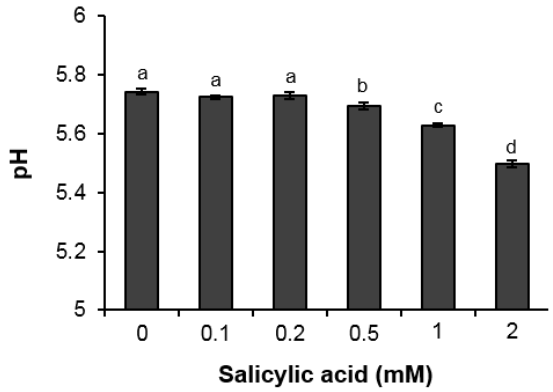

Figure S3 – The effect of salicylic acid on pH of *hrp*-inducing minimal medium. Each bar shows the mean of 3 sample replicates, error bars show standard the deviation, and different letters indicate statistically significant differences (ANOVA followed by Tukey's HSD test, $P < 0.05$).

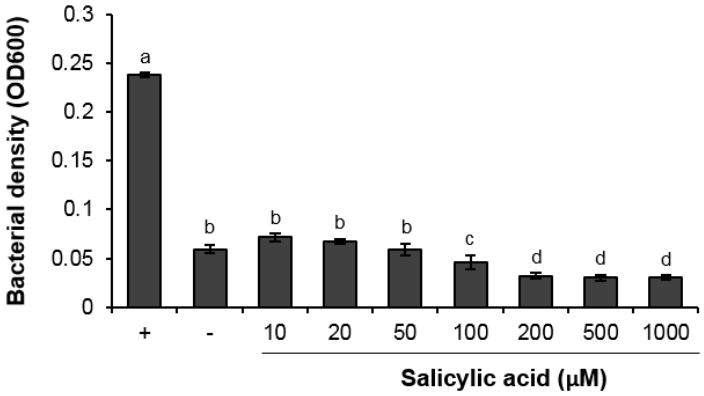

Figure S4 – *Pst* does not grow in *hrp*-inducing minimal medium with salicylic acid as the sole carbon source. *Pst* was grown overnight in King's B medium, washed twice with *hrp*-inducing minimal medium, then resuspended to an OD600 of 0.05 in the same medium. Cell suspensions were then incubated in triplicate with various concentrations of SA in a 96-well plate with shaking. Absorbance (OD600) was measured after 48 h. Medium with (+) and without (-) 10 mM fructose served as positive and negative controls respectively. Different letters indicate statistically significant differences (ANOVA followed by Tukey's HSD test, $P < 0.05$).

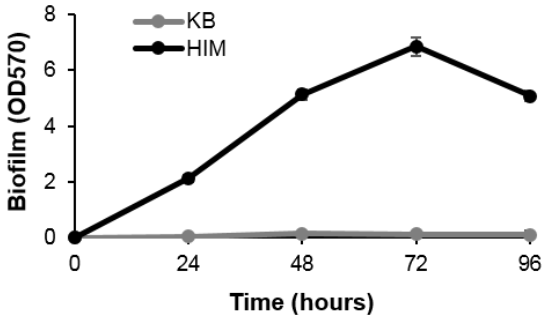

Figure S5 – Biofilm formation is greatly reduced in King's B (KB) medium compared to *hrp*-inducing minimal (HIM) medium. *Pst* was cultured in KB or HIM medium at room temperature without shaking in a 96-well plate. At the indicated time points plates were rinsed to remove unattached planktonic cells and biofilms were quantified by staining with crystal violet. Each data point shows the mean of 8 wells and error bars show standard deviation. This experiment was performed twice with similar results.

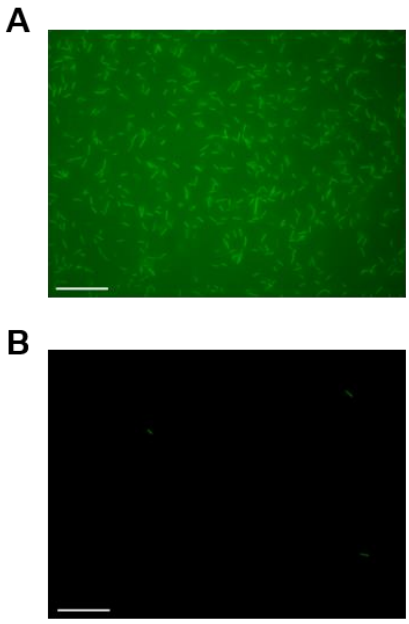

Figure S6 – Aggregates of stationary bacterial cells are not observed in undiluted overnight cultures ($4x10^8$ cfu ml^{-1}) **(A)** or freshly prepared inoculum ($1x10^6$ cfu ml^{-1}) **(B)**. Scale bars = 25 µm. Bacterial cells were too few to allow for observation in planta immediately following inoculation (100-1000 cfu leaf $disk^{-1}$).

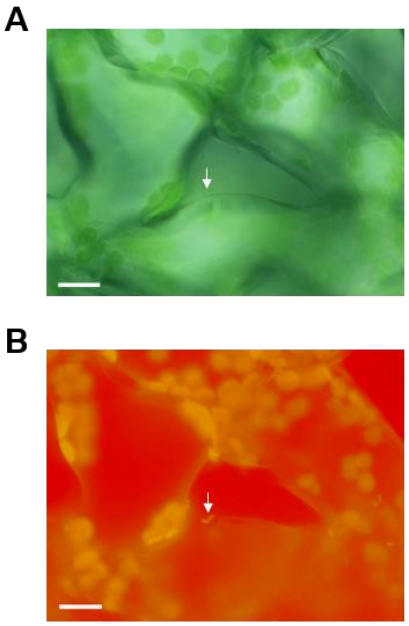

Figure S7 – *P. syringae* in the leaf intercellular space. Images were captured under **A,** bright field, or **B,** fluorescence mode. The arrows indicate a pair of bacterial cells in the intercellular space adjacent to a mesophyll cell. Scale bars = 25 µm.

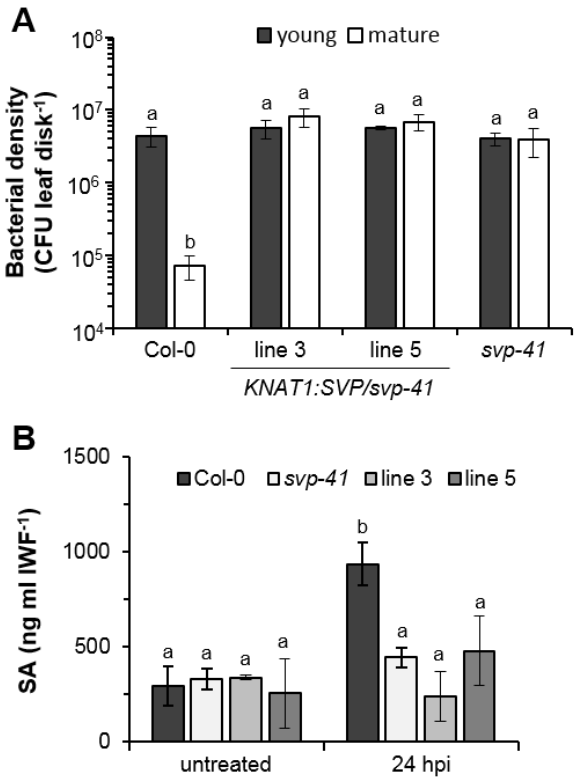

Figure S8 – ARR-defective *KNAT1:SVP/svp-41* plants have reduced SA accumulation in response to *P. syringae*. **A,** Plants were inoculated with 10^6 CFU ml^{-1} *Pst* at either 4 or 6 weeks postgermination and bacterial levels were quantified 3 days later. **B,** SA was measured in intercellular washing fluids (IWFs) collected from mature plants that were either untreated or inoculated with 10^6 CFU ml^{-1} *Pst*. Each bar shows the mean of 3 sample replicates, and error bars show standard deviation. Different letters indicate significant differences (ANOVA followed by Tukey's HSD test, $P < 0.05$). These experiments were performed 3 times with similar results.

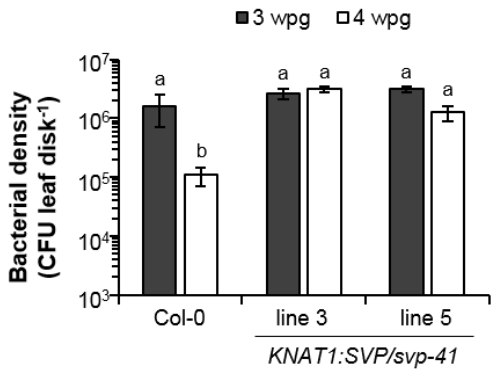

Figure S9 – SVP is required for ARR under long-day conditions. Long-day-grown plants (16 h light) were inoculated with 10^6 CFU ml^{-1} *Pst* at either 3 or 4 weeks postgermination (wpg) and bacterial levels were quantified 3 days later. Each bar shows the mean of 3 sample replicates, and error bars show standard deviation. Letters indicate significant differences (ANOVA followed by Tukey's HSD test, $P < 0.05$). This experiment was performed twice with similar results.

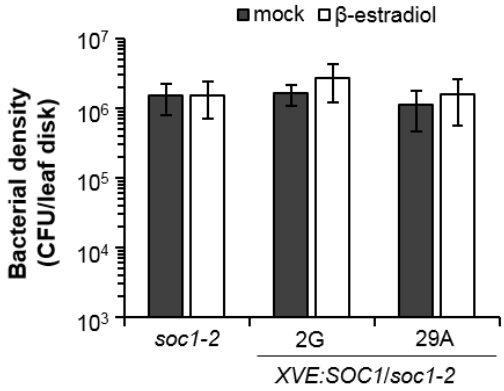

Figure S10 – β-estradiol-induced *SOC1* overexpression does not affect resistance to *Pst* in young plants. Three-week-old plants were pressure-infiltrated with 50 μM β-estradiol or a mock solution, then inoculated with 10^6 CFU ml^{-1} *Pst* 24 h later. Bacterial levels were quantified 3 days after inoculation. There are no significant differences between the means (ANOVA, $P > 0.05$). This experiment was performed 3 times with similar results.

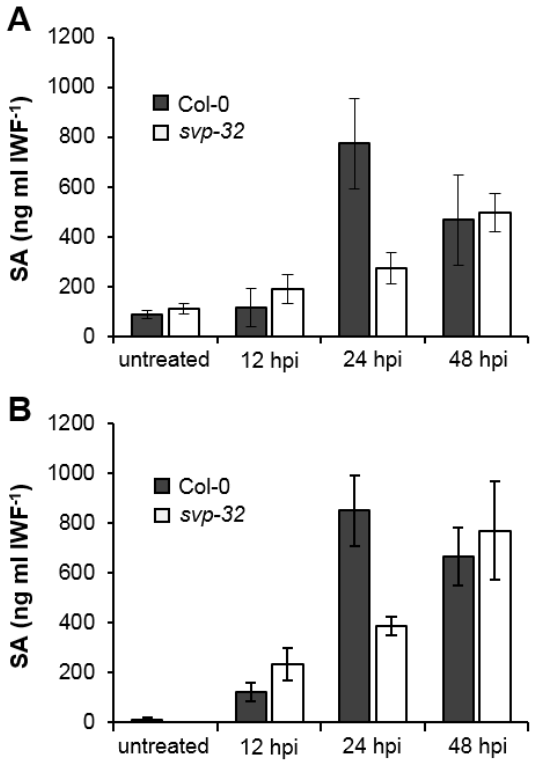

Figure S11 – ARR-defective *svp-32* mutants have reduced intercellular SA accumulation in response to *P. syringae*. SA levels in intercellular washing fluids (IWFs) of 6-week-old plants that were either untreated or inoculated with 10^6 CFU ml^{-1} *Pst* were measured using the ADPWH_lux biosensor **(A)** or gas chromatography-mass spectrometry (GC-MS) **(B)**. The samples used for A and B were from the same experiment. Each bar shows the mean of 3 sample replicates, and error bars show standard deviation. For GC-MS quantification of SA, 30 µl of IWF was extracted by sonication for 10 min in 300 µl 1-propanol:water:HCl (2:1:0.005) and 300 µl dichloromethane. Following phase separation by centrifugation (10 min at 20,000 rcf), the organic phase was transferred to a 4 ml glass vial and dried at 70ºC under a stream of nitrogen gas. The dried organic phase was derivatized by adding 50 µl *N*-methyl-*N*-(trimethylsilyl)trifluoroacetamide (SIGMA 69479) and incubating at 80ºC for 45 min. Derivitization products were run on a Bruker 436 GC equipped with a split/splitless injector (injector port 250ºC) and coupled to a SCION SQ MS operated in electron ionization mode (positive polarity, 70 eV). Compounds were separated on a Bruker B-5ms column (60 m, 0.25 mm ID) held at 60ºC for 5 min after injection then increased to160ºC (at 20ºC min^{-1}) then 260ºC (at 6ºC min^{-1}). For each sample, the peak area for SA was divided by the peak area of the internal standard (500 ng SA-d_6 [CDN isotopes, D-1156] added before extraction) and fitted to a standard curve generated by GC-MS analysis of various concentrations of pure SA dissolved in dichloromethane.

Table S1 – PCR primers used in this study.

Primer	Sequence (5' to 3')
qRT-PCR	
ICS1-F	TGGCAGGGAGACTTACGAAGG
ICS1-R	CCAATAGGTCCCGCATACATTCC
SEC5A-F	ACACTCTTGTAGCTGTCCATGC
SEC5A-R	TGTCGATTAGACCTTCGATCAGC
CUL4-F	AAGGAGCTGGCTGTTTCCC
CUL4-R	TGTCCTCTATGCTGGTGGAATC
RT-PCR	
ACT-F	GGCGATGAAGCTCAATCCAAACG
ACT-R	GGTCACGACCAGCAAGATCAAGACG
SOC1-F	ATGGTGAGGGGCAAAACTCAG
SOC1-R	TCTCGTTTTCTGCAGCTAGAGC

Chapter 5 – Discussion

5.1 The developmental cue for ARR competence

An important goal of this thesis was to uncover the developmental cue that leads to ARR competence. In many cases the onset of ARR is associated with a particular developmental transition (Develey-Rivière and Galiana, 2007; Whalen, 2005). In *Arabidopsis*, ARR is associated with the transition to flowering (Rusterucci et al., 2005). However, upon further investigation, the transition to flowering was determined not to be the developmental cue for ARR competence. That is to say, the transition to flowering is not required for ARR, nor is it sufficient to induce ARR, so although the two events occur at a similar time in the plant life cycle, they are not causally linked (Wilson et al., 2013).

Although there is no evidence for a causal link between ARR and the transition to flowering, their cooccurrence may not be purely coincidental. It is well known that there is an antagonistic relationship between growth and defense, although the underlying mechanisms are not fully understood (Huot et al., 2014). For example, most mutants that constitutively produce SA have dwarf phenotypes, whereas SA-deficient mutants and transgenics exhibit greater vegetative biomass and seed production compared to wild type (Abreu and Munné-Bosch, 2009; Janda and Ruelland, 2015). Therefore, there appears to be a tradeoff between growth and SA-mediated disease resistance, or at least SA biosynthesis. In *Arabidopsis*,

rosette leaf production ceases after the transition to flowering (Hempel and Feldman, 1994), so it seems that at this stage of development, prioritization of defense (i.e., onset of ARR competence) would incur minimal growth-related fitness costs. Although SA accumulation during ARR is pathogen-induced (Cameron and Zaton, 2004), in some cases inducible defense responses still appear to have fitness costs (Heil and Baldwin, 2002). For example, plants possessing the R protein RPM1, which confers ETI to pathogens carrying the AvrB or AvrRpm1 effectors, produced 9% fewer seeds compared to plants lacking RPM1 (Tian et al., 2003). Therefore, delaying resistance onset until later developmental stages could be advantageous if the resistance response has a large impact on growth. Parniske et al. (1997) put forth another reason why disease resistance might be developmentally regulated, proposing that susceptible young plants function similarly to a refuge crop by reducing selection for pathogen strains that can circumvent the defense responses deployed by mature plants.

At least two transcription factors have been proposed to control the balance between growth and disease resistance. DEL1 (DP-E2F-LIKE 1) is highly expressed in expanding leaves and directly represses *EDS5* (SA transporter gene), presumably to ameliorate the growth-limiting effects of SA (Chandaran et al., 2014). TBF1 (TL1-BINDING FACTOR 1) appears to repress genes associated with growth-related functions, and activate those associated with

defense-related functions, during PTI and SAR (Pajerowska-Mukhtar et al., 2012). Future studies of *tbf1* mutants may reveal a role for TBF1 in ARR as well.

ARR occurs in both short- and long-day-grown plants, however, the onset of ARR competence occurs several weeks earlier in long days (Rusterucci et al., 2005). This raises the possibility that there are mechanistically distinct ARR responses in short and long days. However, SA accumulation mutants are ARR-defective in both short and long days, demonstrating that SA accumulation is required for ARR in both photoperiods (Wilson et al., 2013). Similarly, SVP is required for ARR in both photoperiods (Chapter 4, unpublished). These shared genetic requirements argue against the idea of distinct ARR responses in short and long days. Moreover, the earlier onset of ARR in long days may reflect the accelerated development of long-day-grown plants. Indeed, in both photoperiods onset of ARR competence occurs at a similar developmental stage, i.e., near the transition to flowering (Rusterucci et al., 2005), and therefore, the developmental cue for ARR competence is likely the same in short and long days. On a practical note, this raises the possibility that ARR assays in the lab could be routinely carried out in long days for faster completion of experiments. The tradeoff, however, is that long-day-grown plants produce fewer leaves and larger inflorescences, so leaf tissue is less abundant and more difficult to work with during inoculation and collection procedures.

5.2 SVP and SOC1 contribute to ARR

5.2.1 SVP and SOC1 function upstream of intercellular salicylic acid accumulation

Investigating the relationship between ARR and the transition to flowering led to the discovery that mutants for the floral repressor SVP were ARR-defective (Wilson et al., 2013). Given that SA accumulation is a key component of the ARR response, we hypothesized that SVP might regulate SA accumulation. Consistent with this hypothesis, *svp* mutants were compromised in their ability to accumulate SA in response to *Pst*. Specifically, the ARR-defective phenotype of *svp* mutants is associated with a reduced ability to accumulate intercellular SA. This conclusion is based on experiments that provide evidence for the importance of intercellular SA during ARR (Kus et al., 2002; Cameron and Zaton, 2004), and experiments in which exogenous SA application only restores ARR to *svp* mutants when SA is present in the intercellular space at the time of inoculation with *Pst* (Chapter 4, unpublished). These observations are consistent with the hypothesis that SA acts directly on *Pst* as an antibacterial agent during ARR (Cameron and Zaton, 2004).

Since SVP is a transcription factor, I hypothesized that it influences ARR through transcriptional activation or repression of one or more of its target genes. A well-known target gene of SVP is *SOC1*, which SVP represses in both meristem and leaf tissues of seedlings (Li et al., 2008). Surprisingly, the *soc1-2* mutation fully

restored ARR to the *svp-32* mutant, i.e., *svp-32* mutants are ARR-defective, whereas *svp-32 soc1-2* mutants are ARR-competent, suggesting that SVP is only required for ARR in plants with functional SOC1 (Chapter 4, unpublished). In other words, it appears that *SOC1* is a downstream target of SVP during ARR, and the requirement of SVP during ARR is related to its repression of *SOC1*. This provided the first evidence that SOC1 might act as a negative regulator of ARR, since SVP contributes positively to ARR (Wilson et al., 2013). In support of this idea, constitutive *SOC1* overexpressors were fully ARR-defective and failed to accumulate intercellular SA. Moreover, inducible *SOC1* overexpressors were partially compromised for ARR as demonstrated by enhanced susceptibility (2- to 7-fold) of mature plants induced to overexpress *SOC1* (Chapter 4, unpublished). Together these data suggest that the MADS-domain transcription factors SVP and SOC1 act antagonistically during ARR, upstream of intercellular SA accumulation.

5.2.2 How does SVP regulate SOC1 function during ARR?

To test whether SVP contributes to the onset of ARR competence by repressing *SOC1* expression in mature plants, *SVP* and *SOC1* expression was measured in leaf tissue of young and mature plants responding to *Pst* (Chapter 4, unpublished). *SVP* expression was higher in mature plants compared to young plants (in both mock- and *Pst*-inoculated plants), consistent with SVP contributing to the onset of ARR competence. *SOC1* expression was expected to show the

opposite trend since SVP directly represses *SOC1* expression in seedlings (Gregis et al., 2013; Li et al., 2008), double mutant analysis suggests that SOC1 functions downstream of SVP during ARR, and the ARR-defective phenotype of *SOC1* overexpressors suggests that SOC1 negatively impacts ARR (Chapter 4, unpublished). Unexpectedly, *SOC1* was expressed at similar levels in young and mature plants. Therefore, the requirement of SVP for ARR and its apparent action upstream of *SOC1* cannot be explained by transcriptional repression of *SOC1* by SVP. In the following paragraphs two alternative explanations for these observations are discussed.

One possibility is that SVP regulates SOC1 at the post-translational level. Yeast-2-hybrid studies show that SVP and SOC1 interact with each other, and also share multiple interaction partners (de Folter et al., 2005, Immink et al., 2009). In several cases the nuclear localization or DNA-binding specificity of MADS-domain transcription factors is influenced by their protein-protein interaction partners (Lee et al., 2008; Mateos et al., 2015; Posé et al., 2013; Shen et al., 2011). Therefore, it seems plausible that SVP may regulate SOC1 activity either by interacting with SOC1 itself, or a shared interaction partner. Assessing SVP and SOC1 protein abundance, sub-cellular localization, and DNA-binding profiles in young and mature plants responding to *Pst* would help to address whether SVP contributes to the onset of ARR by negatively regulating SOC1 at the post-translational level.

It is also possible that SVP, although required for ARR, does not regulate the onset of ARR competence, and this regulation occurs through an unknown SVP-independent mechanism. Perhaps, for example, SOC1 inhibits ARR by suppressing an SA biosynthesis gene, but only when expressed at high levels that occur in *SOC1* overexpressors and *svp* mutants (both ARR-defective). If this is the case, the requirement of SVP for ARR is explained by the necessity to keep *SOC1* expression levels low, but since *SOC1* expression is not different between young and mature wild-type plants, there is no evidence that SVP is involved in regulating onset of ARR competence. In either case, the data show that SVP is required for ARR and suggest that SVP contributes positively to ARR through negative regulation of SOC1. Further work is required to determine the mechanism through which this occurs, as well as the downstream targets of SOC1 that are relevant to ARR.

5.2.3 How does SOC1 negatively impact ARR?

SOC1 influences a number of processes other than the transition to flowering. It is possible that the role of SOC1 during one or more of these processes could be linked to its role during ARR. SOC1 negatively influences the cold-tolerance response by directly repressing cold-response genes such as *CBFs* (*CRT/DRE-BINDING FACTORS*; Seo et al., 2009), however, there is no obvious link between cold tolerance and ARR. SOC1 also delays dark-induced senescence by directly repressing *PPH*, which codes for PHEOPHYTINASE, an enzyme

involved in chlorophyll degradation. Whether SOC1 plays a similar role in developmentally regulated senescence is unclear (Chen et al., 2017), and in any case, ARR precedes visible signs of senescence and expression of senescence marker genes (Kus et al., 2002). Finally, SOC1 positively influences stomatal opening by an unknown mechanism (Kimura et al., 2015), however, inoculation by pressure-infiltration, the technique used in our ARR studies, bypasses stomatal immunity. Therefore, existing evidence suggests that there is no functional link between the role of SOC1 during ARR and its involvement in other processes like the cold-tolerance response, senescence, and stomatal opening.

One of the genes that SOC1 activates to initiate flowering is the floral meristem identity gene *LFY* (Lee and Lee, 2010). Interestingly, LFY appears to act as a negative regulator of resistance to *P. syringae* by repressing genes required for callose deposition in the cell wall (Winter et al., 2011). However, this effect was only evident in the cauline leaves, probably because in wild-type plants *LFY* is only expressed in the meristem and in the leaf primordia of cauline leaves especially (Blazquez et al., 1997; Lee et al., 2000). Moreover, callose deposition in response to *Pst* was not enhanced in mature plants compared to young plants (Figure A1). Therefore, if SOC1 contributes to regulating the onset of ARR, it probably does so independently of LFY.

Since SOC1 negatively impacts ARR and appears to act upstream of intercellular SA accumulation (Chapter 4, unpublished), it may negatively regulate genes involved in SA biosynthesis. Intriguingly, SOC1 was recently identified in a yeast

one-hybrid screen for transcription factors that associate with the promoter of the SA biosynthesis gene *ICS1* (Zheng et al., 2015). The interaction of SOC1 with the *ICS1* promoter was not further investigated by Zheng et al. (2015), nor is there supporting evidence from transcriptome or genome-wide DNA-association studies of SOC1 (Immink et al., 2012; Seo et al., 2009; Tao et al., 2012). However, compared to wild type, mature *svp-32* mutants (in which *SOC1* expression is elevated) exhibit reduced *ICS1* expression after inoculation with *Pst* (Figure A2), providing evidence that SOC1 negatively regulates *ICS1* expression. Future analysis of *ICS1* expression in mutants and overexpressors of *SOC1* may provide more direct evidence for a SOC1-*ICS1* regulatory relationship.

A genome-wide approach such as RNA-seq could also be used to identify genes regulated by SOC1 during ARR. Given the modest ARR-defective phenotype of inducible *SOC1* overexpressors, it would probably be better to use constitutive overexpressors for these experiments. At a minimum these experiments should compare mature wild-type plants with *SOC1* overexpressors responding to *Pst*. Including mock-inoculated plants would allow for the identification of genes that are differentially expressed between the two genotypes specifically in response to *Pst* (as opposed to genes that are differentially expressed between the two genotypes in healthy plants). However, given the possibility that SOC1 is not involved in regulating ARR, as mentioned in the above paragraph, a better approach might be to compare young and mature wild-type plants, both mock-inoculated and responding to *Pst*.

5.2.4 SVP and SOC1 have distinct roles in ARR and flowering-time control

SVP and SOC1 are well-known regulators of flowering time, with SVP acting as a floral repressor, and SOC1 as a floral activator (Amasino, 2010; Fornara et al., 2010; Figure 1.2). However, the ARR-defective phenotypes of *svp* mutants and *SOC1* overexpressors are not related to their early-flowering phenotypes (Chapter 4, unpublished). Plants expressing *SVP* specifically in the meristem (in the *svp-41* background) did not flower during short-day ARR experiments, but remained ARR-defective. Similarly, the early-flowering and ARR-defective phenotypes associated with constitutive *SOC1* overexpression could be separated by inducible overexpression of *SOC1* during infection, which did not accelerate flowering but still negatively impacted ARR. This was not unexpected, since another early-flowering mutant, *tfl1-14,* was previously shown to be ARR-competent (Wilson et al., 2013). Consistent with these results, the altered disease-resistance phenotypes of several late-flowering mutants remained unchanged by mutations or treatments that accelerated flowering (Lyons et al., 2015; Singh et al., 2013). Therefore, rather than the timing of flowering affecting disease resistance, some flowering-time regulators appear to play distinct roles in disease resistance (Kazan et al., 2015). This list now includes SVP and SOC1, whose function during ARR appears to be independent of either protein's role during flowering-time control.

5.2.5 FLC may contribute to ARR

The MADS-domain transcription factor FLC (FLOWERING LOCUS C) is a floral repressor (Michaels and Amasino, 1999), similar to SVP. Indeed, the two proteins interact and can associate with DNA as a complex or independent of one another (Mateos et al., 2015). Consequently, SVP and FLC regulate partially overlapping sets of genes, including *SOC1* (Deng et al., 2011; Gregis et al., 2013; Mateos et al., 2015). This raises the possibility that FLC also plays a role during ARR. In the summer-annual accession Col-0, *FLC* expression is low because its positive regulator FRI (FRIGIDA) is non-functional. Therefore, FLC contributes little to flowering-time control in Col-0 (Michaels and Amasino, 1999; Sheldon et al., 1999), and probably makes little to no contribution to ARR, although this has not been tested directly (i.e., assessing the ARR phenotype of an *flc* mutant). However, in *FRI*+ Col-0, a strain in which a functional allele of *FRI* was introgressed from the winter-annual accession SF-2 (Michaels and Amasino, 1999), *FLC* is expressed at much higher levels, and ARR was stronger than in wild-type Col-0 (10.1-fold lower bacterial levels at 7 weeks of age; Wilson et al., 2013). Furthermore, when *FLC* was mutated in this strain, the stronger ARR phenotype was almost completely lost (1.3-fold lower bacterial levels at 7 weeks of age). These data hint that *FLC* contributes to ARR, especially in winter-annual accessions in which it is more highly expressed.

5.2.6 Natural variation in SVP and SOC1 activity may contribute to natural variation in disease resistance

There is extensive variation in disease resistance within natural accessions of *Arabidopsis* (Weigel, 2012). In some cases this may be associated with variation in SVP or SOC1 activity between accessions. A study that analyzed over 80 accessions of *Arabidopsis* found that enhanced resistance to the hemibiotrophic fungal pathogen *Fusarium oxysporum* was positively correlated with late flowering (Lyons et al., 2015). In addition, some late-flowering mutants, including *fve* (full name, not an abbreviation) displayed enhanced resistance compared to wild type. Although the contribution of SVP and SOC1 was not investigated in the study by Lyons et al. (2015), it is possible that differential SVP and SOC1 activity in these accessions and mutants could account for at least some of the observed variation in disease resistance. For example, *SVP* expression was upregulated in long-day-grown *fve* seedlings (Lee et al., 2007; Li et al., 2008), and *fve* mutants grown in short days for 4 weeks then moved to long days for the 2-week infection period showed enhanced resistance to *F. oxysporum* (Lyons et al., 2015). Additionally, some accessions of *Arabidopsis* possess non-functional *SVP* alleles (Méndez-Vigo et al., 2013), although they were not included in the *F. oxysporum* study (Lyons et al., 2015), so whether they exhibit enhanced disease susceptibility is unknown. Assessing ARR in *Arabidopsis* accessions with non-functional *SVP* alleles would shed light on the extent to which natural variation in SVP activity contributes to natural variation in disease resistance. Moreover,

since *SVP* and *SOC1* are widely conserved (Lee and Lee, 2010; Méndez-Vigo et al., 2013) and may be involved in disease resistance in a variety of other plants, this strategy could also be applied to crop plants. For example, *JOINTLESS* is the tomato ortholog of *SVP*, and several *jointless* tomato varieties exist (Hileman et al., 2006; Mao et al., 2000; Zahara and Scheuerman, 1988) and could be compared to *JOINTLESS* varieties for their ability to exhibit ARR. Interestingly, transcriptomics analysis of natural populations of European ash trees revealed a 56-gene network that was significantly correlated with resistance to the fungal pathogen *Hymenoscyphus fraxineus* (Harper et al., 2015). This network included putative orthologs of *SVP* and *SOC1*, suggesting that *SVP* and *SOC1* orthologs influence disease resistance.

There is considerable interest in controlling flowering time in crop plants, for example, in their patent “Means and Methods for Controlling Flowering in Plants”, Nielsen et al. (2012) describe the inducible expression of floral activators, including *SOC1*, as a potential strategy to induce flowering. However, given that our work (Wilson et al., 2013; Chapter 4, unpublished) and the work of others (Kazan et al., 2015) has shown that some flowering-time regulators have roles in other processes such as disease resistance, such a strategy could have adverse effects. For example, inducing high levels of *SOC1* expression could cause enhanced disease susceptibility. This underscores the importance of understanding the interplay between disease resistance and developmental

processes if we are to successfully design strategies to obtain high-yielding, disease-resistant crops.

5.3 SA as an antimicrobial agent during ARR

During PTI and ETI SA appears to act a signal for defense-gene expression, whereas during ARR (i.e., in mature plants) SA plays an important but different role (Carella et al., 2015b). Evidence from earlier studies suggested that this role involved the direct action of SA against pathogens in the intercellular space but high amounts (at least 1 mM) were required for antibacterial activity in vitro and it was not known how much SA accumulated in vivo (Cameron and Zaton, 2004; Kus et al., 2002). Therefore, I sought to answers two questions: 1) At what range of concentrations does SA have antibacterial activity under biologically relevant conditions? 2) Are these concentrations of SA present in the intercellular space during ARR? To answer the first question, antibacterial assays were performed in *hrp*-inducing minimal (HIM) medium (Huynh et al., 1989), which is a better representation of the conditions in the leaf intercellular space (e.g., pH, type and abundance of nutrients) compared to rich media. In support of this proposition, many *P. syringae* genes that are expressed during infection of plants are also expressed in minimal media, but are expressed at much lower levels or not at all in rich media (Boch et al., 2002; Huynh et al., 1989; Rahme et al., 1992). For example, Boch et al. (2002) isolated over 300 *Pst* genes that were expressed during infection of *Arabidopsis* but not during growth on solid KB medium (King's

B, a rich medium; King et al., 1954), and found that the majority (~85%) were also expressed during growth on solid minimal media. The antibacterial activity of SA was enhanced ~10-fold in HIM medium compared to KB medium, reducing *Pst* growth at concentrations as low as 100-200 µM (Chapter 4, unpublished). Therefore, SA exhibits antibacterial activity at 100-200 µM under biologically relevant conditions.

To determine the level to which SA accumulates in the intercellular space during ARR, an experimentally determined dilution correction factor was applied to SA concentrations measured in IWFs. This was necessary as the contents of the intercellular space become diluted during IWF collection (Husted and Schoerring,1995). This analysis suggests that SA accumulates to 40-100 µM in the intercellular space of mature plants 24 hours after inoculation with *Pst* (Chapter 4, unpublished). Therefore, it is possible that SA accumulates to sufficient levels in the intercellular space to have antibacterial activity, especially considering that SA might be incompletely extracted from the intercellular space during IWF collection. This could result from incomplete vacuum infiltration of the leaf intercellular space, incomplete removal of IWFs from the leaves by centrifugation, or cross-linking of SA to the cell wall, as has been seen to occur with the structurally similar compound 4-hydroxybenzoic acid (Tan et al., 2004; Veit et al., 2001). In addition, SA may reach higher concentrations in microenvironments of the leaf intercellular space, a possibility that cannot be assessed using the IWF collection technique. In an interesting study by Huang et

al. (2006), the authors used an SA biosensor (the same one used in our studies; described in DeFraia et al., 2008 and Huang et al., 2005) to monitor intercellular SA accumulation in vivo, specifically in tobacco plants responding tobacco mosaic virus (TMV) with ETI. They found that SA accumulated to 100-150 µM in many sections of the leaf, and up to 380 µM in a few small sections, although the imaging technique that was used did not allow for the resolution of individual cells. Finally, it is likely that other antimicrobials accumulate in the intercellular space and contribute to bacterial growth reduction during ARR (Cameron lab, unpublished data). Together, the antibacterial activity of SA under conditions that mimic the leaf intercellular space, and the conservative estimate of intercellular SA concentrations in vivo, make a strong case for the hypothesis that SA acts as an antibacterial agent in the intercellular space during ARR.

The difference in SA antibacterial activity in HIM medium and KB medium could be due to differential effects of these media on bacterial growth rate, physiology, and metabolism (Kim et al., 2010), or alternatively, effects of the different media on SA itself. For example, HIM medium has a pH of 5.7, similar to intercellular fluid (Husted and Schjoerring, 1995; Jia and Davies, 2007), whereas KB medium has a pH of 7.2. At lower pH a greater proportion of SA exists in its protonated, lipophilic form, enhancing SA's ability to cross cell membranes, which may be necessary for SA to exert its toxic effects. In support of this idea, Amborabé et al. (2002) showed that antifungal activity of SA against *Eutypa lata* was greater at lower pH, and was associated with increased SA uptake by fungal hyphae.

Bosmund (1960) reported similar findings from experiments where *Proteus vulgaris* and *Saccharomyces cerevisiae* were treated with benzoic acid. Many studies have shown that SA has antimicrobial effects on phytopathogens in vitro (Amborabé et al., 2002; Brown, 2007; Cameron and Zaton, 2004; El-Mougy, 2002; Georgiou et al., 2000; Martín et al., 2010; Prithiviraj et al., 1997; Lowe-Power et al., 2016; Yuan et al., 2007), with the range of effective concentrations spanning several orders of magnitude (~10 µM to 10 mM). Our findings suggest that at least some of this variation could be due to the use of different growth media, and that this is an important variable to consider when designing antimicrobial assays.

The antimicrobial activity of SA extends well beyond phytopathogens. SA also exhibits antimicrobial activity against a variety of animal pathogens and is a common treatment for acne and warts, which are associated with bacterial and viral infections, respectively (Himejima and Kubo, 1991; Raman and Levitt, 2014). Regarding SA's mode of action as an antimicrobial agent, several possibilities have been put forth. One of the most often invoked is that SA is an uncoupling agent. Uncouplers transport protons across plasma membranes, dissipating the transmembrane proton gradient required for the production of ATP (Pelczar et al., 2010). Several studies suggest that SA acts as an uncoupling agent in mitochondria isolated from animals (Gutknecht, 1990; Jörgensen et al., 1976; Smith, 1959) and plants (Norman et al., 2004; Stenlid and Saddik, 1962). Bacteria also rely on a proton gradient (across the cytoplasmic membrane) for

ATP production (Pelczar et al., 2010), and therefore are also susceptible to uncouplers (Lewis et al., 1994). The antimicrobial activity of SA may also stem from its ability to inhibit catalase, an enzyme important for detoxification of reactive oxygen species (Chen et al., 1993), inhibit respiration (Norman et al., 2004), or increase membrane permeability (McDonnell and Russell, 1999). It is also quite possible that SA has multiple modes of action, with some occurring only at higher concentrations. For example, Norman et al. (2004) found that treatment of tobacco cells or mitochondria with 0.01 or 0.10 mM SA stimulated respiration, consistent with uncoupling, whereas treatment with 1 mM SA inhibited respiration. As well as affecting microbial viability or growth, as has been discussed so far, there is also evidence that SA acts as an antivirulence agent (discussed in section 5.4).

Pathogens have evolved numerous strategies to resist the toxic effects of SA including degradation or modification of SA or its precursors (Tanaka et al., 2015). For example, *R. solanacearum* can degrade SA and use it as a carbon source (Lowe-Power et al., 2016). This ability confers enhanced SA tolerance in vitro and enhanced virulence on tobacco compared to strains that cannot use SA as a carbon source. This strategy does not appear to be used by *Pst* DC3000*,* which was unable to grow on SA as the sole carbon source (Chapter 4, unpublished). If SA acts directly on *Pst* as an antimicrobial agent during ARR, then SA-resistant *Pst* strains would be expected to exhibit enhanced growth in mature, ARR-competent *Arabidopsis* compared to wild-type *Pst*. To test this

hypothesis, attempts were made to isolate SA-resistant *Pst* strains but unfortunately they proved unsuccessful (D. Wilson, unpublished observations). Instead, *Pst* strains carrying the SA-degrading enzyme NahG could be used in a similar manner.

5.4 SA as an antivirulence agent during ARR

Antivirulence agents reduce the ability of pathogens to cause disease without directly reducing their growth or survival (Clatworthy et al., 2007). I hypothesized that SA acts as an antivirulence agent by limiting the ability of *Pst* to form biofilms in the intercellular space during ARR. This idea arose from studies which demonstrated that in vitro biofilm formation by animal pathogens is reduced by SA concentrations that are insufficient to affect pathogen growth (Prithiviraj et al., 2005ab; Yang et al., 2009). Moreover, biofilm formation occurs during multiple plant-pathogen interactions and seems to contribute to pathogen virulence (Danhorn and Fuqua, 2007; Ichinose et al., 2013). Based on this information I set out to test whether *Pst* forms biofilms in vitro and in the leaf intercellular space, and whether exposure to SA affects this process.

Just as many bacterial genes that are expressed in planta are expressed in minimal media but not rich media (Boch et al., 2002; Huynh et al., 1989; Rahme et al., 1992), *Pst* formed biofilms in HIM medium but not KB medium (Chapter 4, unpublished), hinting that *Pst* forms biofilms in planta. Intriguingly, treatment with

SA reduced the ability of *Pst* to form biofilms in vitro by as much as 86% at the highest concentration that did not affect growth (50 µM). An effect could be seen at concentrations as low as 2 µM, 20-fold less than the lowest amount estimated to accumulate in the intercellular space of mature, ARR-competent plants (40 µM). In *Arabidopsis* leaves imaged 24 hours after inoculation with *GFP*-expressing *Pst,* both free-swimming bacterial cells and stationary biofilm-like aggregates were observed in the intercellular space, suggesting that *Pst* forms biofilms in planta. Furthermore, young plants and mature *svp* mutants had a larger proportion of bacterial aggregates (71-82% of fields of view contained aggregates) compared to mature, wild-type plants (32% of fields of view contained aggregates; Chapter 4, unpublished). Therefore, the ability of mature plants with functional SVP to accumulate intercellular SA corresponded with a reduction in the proportion of biofilm-like aggregates in the intercellular space, supporting the initial hypothesis that SA limits biofilm formation during ARR.

Biofilms are usually described as surface-adherent groups of cells embedded in an extracellular matrix (Danhorn and Fuqua, 2007). These structures are thought to provide protection against environmental stresses such as desiccation and antimicrobials (Danhorn and Fuqua, 2007; Ichinose et al., 2013). The extracellular polysaccharides associated with biofilms also bind calcium, preventing calcium influx into the plant cell and thereby suppressing this important signal for the activation of disease-resistance responses (Aslam et al., 2008). In addition, biofilm formation is associated with increased expression of

effector genes, although the mechanistic basis for this phenomenon is not known (Ichinose et al., 2011). Alginate is the main extracellular polysaccharide produced by several pathovars of *P. syringae* in planta (Fett and Dunn, 1989; Osman et al., 1986) and it contributes to in vitro biofilm formation in *P. syringae* pv. *glycinea* (Laue et al., 2006). Alginate-deficient mutants of *P. syringae* pv. *syringae* and *P. syringae* pv. *glycinea* exhibited reduced growth and caused fewer disease symptoms compared to wild-type strains on bean and soybean, respectively (Schenk et al., 2008; Yu et al., 1999). Similarly, *Pst algD* mutants exhibited reduced growth and caused fewer disease symptoms compared to the wild-type strain in *Arabidopsis* (Aslam et al., 2008). Moreover, *Pst* expresses alginate biosynthesis genes in various plants including *Arabidopsis* and tomato (Boch et al., 2002; Keith et al., 2003), and produces alginate in tomato (Fett and Dunn, 1989). Electron microscopy revealed that *P. syringae* pv. *actinidiae* forms biofilms on both the leaf surface and within the intercellular space of kiwi plants (Renzi et al., 2012). Together with our results these studies suggest that biofilm formation occurs in planta and contributes to the virulence of *P. syringae.* In the future, to assess the contribution of alginate to *Pst* biofilm formation, *algD* mutants should be compared to wild type for their ability to form biofilms in vitro and in planta.

Consistent with our findings that treatment with SA reduces the ability of *Pst* to form biofilms in vitro, other studies have observed similar phenomena with different phytopathogens. At concentrations that did not affect growth, in vitro SA treatment repressed *hrpA* promoter activity in *Erwinia amylovora* (Khokhani et al.,

2013), the *virA/G* regulon of *Agrobacterium tumefaciens* (Yuan et al., 2007), and virulence gene expression in *Ralstonia solanacearum* (Lowe-Power et al., 2016). This raises the question of how SA affects biofilm formation and virulence gene expression in several different pathogens of both animals and plants. The answer may relate to the ability of SA to interfere with quorum sensing, the ability of bacteria to sense their population size and regulate various behaviors including biofilm formation and virulence factor production (Danhorn and Fuqua, 2007; Ichinose et al., 2013). Yang et al. (2009) identified SA in a screen for compounds predicted to bind to the *P. aeruginosa* quorum sensing regulator LasR. They also showed that treatment with concentrations of SA that did not affect growth reduced expression of a gene known to be upregulated by the LasR quorum sensing system. Therefore, SA may interfere with quorum sensing by binding to the LuxR-family protein LasR. The existence of LuxR-family proteins in several phytopathogens including *P. syringae* (Gray and Garey, 2001) suggests that this mechanism of action could explain the ability of SA to reduce biofilm formation and virulence factor production in a wide range of bacterial pathogens. Other groups have reported that SA interferes with quorum sensing, including Bandara et al. (2006) who found that treatment with SA inhibited synthesis of AHL (*N*-Acyl homoserine lactone) quorum sensing molecules in *P. aeruginosa*. Chang et al. (2014) reported similar findings using *E. coli* expressing *P. aeruginosa* AHL synthases. However, these studies either used concentrations of SA that reduced growth (Bandara et al., 2006) or did not test the effect of SA on growth (Chang et

al., 2014), so it is possible that the observed reduction in AHL synthesis was an indirect effect of reduced bacterial growth. There are many other examples of plant compounds that interfere with quorum sensing (Venturi and Fuqua, 2013), including rosmarinic acid produced by sweet basil (Corral-Lugo et al., 2016), and L-canavanine produced by *Medicago sativa* (Keshavan, et al., 2005). Although further work is required to determine whether SA interferes with quorum sensing in phytopathogens such as *P. syringae*, this possibility hints that SA may have effects on the virulence of *P. syringae* that extend beyond its demonstrated effect on biofilm formation.

5.5 A role for intercellular SA during PTI and ETI

The *iap1-1* mutant was isolated in a screen for ARR-defective mutants, and mature *iap1-1* plants were unable to accumulate intercellular SA in response to *Pst* (Carviel et al., 2009). It was also discovered that young *iap1-1* mutants had compromised ETI and accumulated little intercellular SA during this response (Carviel et al., 2014). Subsequently, map-based cloning and next-generation sequencing revealed that *iap1-1* is an *eds5* mutant, which is in line with the disease-resistance and SA-accumulation phenotypes mentioned above. During the course of our experiments with young *iap1-1* mutants, wild-type plants accumulated substantial amounts of intercellular SA during the ETI response to avirulent *Pst(avrRpt2)* (500-1200 ng ml IWF^{-1}, similar to the amount detected during ARR) (Carviel et al., 2014). This led us to speculate that intercellular SA

accumulation plays a role during ETI as well as ARR. In contrast, young plants responding to virulent *Pst*, which activates PTI but not ETI, accumulated little to no intercellular SA. However, *Pst* partially suppress PTI (Xin and He, 2013), therefore, if intercellular SA accumulation plays a role during PTI, it might be suppressed by *Pst*. Indeed, previous studies had shown that the *Pst* phytotoxin COR suppresses SA accumulation in whole leaves (de Torres Zabala et al., 2009; Zheng et al., 2012), and we found that young plants inoculated with a COR-deficient strain of *Pst* accumulated 2- to 5-fold more intercellular SA than plants inoculated with wild-type *Pst.* This suggests that intercellular SA accumulation is a component of PTI that is suppressed by wild-type *Pst* (Carviel et al., 2014), therefore, our results suggest that intercellular SA accumulation is a component of both PTI and ETI. Consistent with this idea, tobacco responding to TMV with ETI accumulated intercellular SA, whereas an ETI-defective genotype of tobacco did not (Huang et al., 2006). To further test this idea, intercellular SA accumulation could be monitored in *Arabidopsis* responding to treatments that activate PTI but do not suppress it, for example, non-host pathogens or MAMPs such as flg22.

Since mature plants accumulate higher levels of SA than young plants in response to virulent *Pst*, it is possible that mature plants overcome the COR-mediated suppression of SA accumulation that occurs in young plants. I hypothesized that SVP confers this ability because SVP is required for ARR (Wilson et al., 2013) and evidence suggests that SVP regulates genes required

for the COR-mediated suppression of SA accumulation. Specifically, SVP was shown to associate with the promoters of *NAC055*, *NAC072*, and *NAC019* by chromatin immunoprecipitation (ChIP)-chip using 9-day-old *35S:SVP* seedlings (Tao et al., 2012), and with the *COI1* promoter by ChIP-seq using 14-day-old *SVP:SVP-GFP/svp-41* seedlings (Gregis et al., 2013). In addition, *NAC055* and *NAC019* were upregulated in a microarray experiment comparing 14-day-old *svp-41* seedlings to wild type (Gregis et al., 2013). Indeed, in untreated plants the three *NAC* genes and *COI1* were more highly expressed in *svp-32* mutants compared to wild type, suggesting that SVP negatively regulates the expression of these genes (Figure A2). However, the significance of this is unclear since COR ultimately suppresses SA accumulation by downregulating *ICS1* expression and upregulating *BSMT1* expression (through COI1 and the NACs; Figure 1.1; Zheng et al., 2012), but *ICS1* and *BSMT1* expression were similar in young and mature wild-type plants (Figure A2). Therefore, increased SA accumulation in mature plants relative to young plants does not appear to be the result of mature plants exhibiting increased *ICS1* expression or reduced *BSMT1* expression compared to young plants.

As previous studies demonstrated that *nac055* mutants were partially ARR-defective (Al-Daoud and Cameron, 2011; Carviel et al., 2009), the ARR phenotype of a *nac072 nac055 nac019* triple mutant was tested to determine whether these highly similar genes contribute redundantly to ARR. Unexpectedly the triple mutant was ARR-competent (Figure A3). This is consistent with the

findings of Zheng et al. (2012), which suggest that these three NAC transcription factors are negative regulators of disease resistance, and more specifically, negative regulators of SA accumulation (Figure 1.1). It is possible that the partial ARR defect of the *nac055* single mutant resulted from elevated expression of *NAC072* and *NAC019* as part of a compensatory mechanism for the loss of *NAC055.*

5.6 How does SA access the intercellular space?

During ARR, SA accumulates in the intercellular space where our data strongly suggest that it acts directly on pathogens (Cameron and Zaton, 2004; Carviel et al., 2009; Chapter 4, unpublished). How SA accesses the intercellular space is unknown. While SA should be able to diffuse across the cell membrane, especially in its lipophilic protonated form (Gutknecht et al., 1990), several studies suggest that in some situations it is actively transported. In castor bean, exogenous SA applied to the leaf surface is eventually loaded into the phloem (Rocher et al., 2006). During this process SA must cross the plasma membranes of epidermal and companion cells, and Rocher et al. (2009) showed that this involves a combination of diffusion and the activity of an unknown transporter. In tobacco suspension cells treated with SA (20 or 200 µM), SA was taken up within minutes then excreted back into the culture medium over the next several hours (Chen et al., 2001). Treatment with the chelating agent EGTA or inhibitors of reactive oxygen species, protein kinases, or protein synthesis, all reduced the

ability of the cells to excrete SA, but only in the 200 µM SA treatment, suggesting the existence of an inducible form of SA transport that is active at high concentrations of SA. In cells treated with 20 µM SA, SA excretion was insensitive to the various inhibitors used and may have occurred by diffusion (Chen et al., 2001). Finally, in *Arabidopsis*, SA is transported out of chloroplasts by the MATE-family transporter EDS5 (Serrano et al., 2013). Based on these data we speculated that SA might be transported to the intercellular space by EDS5 or a similar transporter. EDS5 appears to localize to the chloroplast envelope, not the plasma membrane (Serrano et al., 2013; Yamasaki et al., 2013), however, a BLAST search revealed a protein with 72% sequence similarity to EDS5 which was designated ELM1 (EDS5-LIKE MATE TRANSPORTER; AT2G21340). Several T-DNA insertion mutants for *ELM1* were obtained and one was determined to be a null expression mutant (Figure A4). If ELM1 transports SA to the intercellular space, then *elm1* mutants should be ARR-defective. However, *elm1* mutants were fully ARR-competent (Figure A4), suggesting that ELM1 does not transport SA to the intercellular space. Soon after these experiments were performed, Parinthawong et al. (2015) demonstrated that ELM1 (which they named EDS5H) is localized to the chloroplast envelope but is not involved in pathogen-induced SA accumulation, and therefore, probably does not transport SA across the chloroplast or cytoplasmic membranes.

SA may also access the intercellular space by leaking out of dead or dying cells. This might be the case during ETI, which is often associated with HR cell death

(Luis et al., 2008). During RPS2-mediated ETI, SA accumulation in the intercellular space was detected at 12 hpi (the earliest time point analyzed), around the same time that electrolyte leakage, which is indicative of dead or damaged cells, began to increase (Carviel et al., 2014). This is consistent with the hypothesis that SA accesses the intercellular space by leaking out of dead or dying cells during ETI, although checking for intercellular SA accumulation at earlier time points, before the onset of cell death, could reveal whether cell death is required for SA to access the intercellular space during ETI. During ARR, no macroscopic cell death is observed, and little electrolyte leakage is detected (Figure A5), therefore, SA probably doesn't access the intercellular space from dead or dying cells during ARR.

Another possibility is that SA itself is not transported into the intercellular space, but rather its glucose conjugate SAG, which is then hydrolyzed back to free SA by intercellular β-glucosidase(s). This idea stems from the observations that 1) SAG pressure-infiltrated into the intercellular space of tobacco was rapidly converted to free SA, and 2) intercellular fluids of tobacco possessed β-glucosidase activity (Hennig et al., 1993; Seo et al., 1995). So while there is evidence that SAG is actively transported into the vacuole (Dean et al., 2004), in theory it could also be transported to the intercellular space then hydrolyzed to form free SA to act directly on pathogens. Inherent in this model is the assumption that SAG itself is not active against pathogens. This assumption has not been tested directly, however, SAG is less lipophilic than SA, and should

therefore have a reduced ability to enter bacterial or fungal cells. While mostly speculative, the idea that SAG is transported to the intercellular space fits with the SA accumulation phenotype of *svp* mutants, which accumulate very little intracellular SAG and intercellular SA, but accumulate intracellular SA similar to wild type (Chapter 4, unpublished). This is to say that reduced intracellular SAG accumulation in *svp* mutants may explain their reduced ability to accumulate intercellular SA. If SAG formation really is an intermediate step in the pathway to intercellular SA accumulation, this could explain the enhanced disease susceptibility phenotypes of other mutants affected primarily in SAG accumulation (e.g., *gdg1/win3/pbs3* [Jagadeeswaran et al., 2007; Lee et al., 2007; Nobuta et al., 2007] and *eps1* [Zheng et al., 2009]). Examining the localization of free SA in these mutants (i.e., intracellular vs. intercellular) would be one way to further test this hypothesis. For now the question of how SA accesses the intercellular space during plant disease-resistance responses remains unanswered, although it seems that a combination of diffusion (across either healthy or damaged membranes) and active transport are probably involved.

5.7 Conclusion

The work presented in this thesis significantly contributes to our understanding of ARR in the *Arabidopsis-Pseudomonas* pathosystem, and the involvement of salicylic acid in this and other disease-resistance responses. While

developmental transitions are often associated with changes in disease resistance, we have shown that in *Arabidopsis* the transition to flowering and ARR are not causally linked. Nevertheless, we identified two proteins, the MADS-domain transcription factors SVP and SOC1, that appear to play distinct roles in the transition to flowering and ARR. Both proteins were shown to act upstream of intercellular SA accumulation, a key component of ARR, although this work suggests that intercellular SA accumulation is involved in PTI and ETI as well. Finally, this work provides compelling evidence that SA acts directly on pathogens as an antimicrobial and antibiofilm agent in the intercellular space during ARR. These findings are likely applicable to other plant-pathogen interactions, where increased knowledge of the interplay between development and disease resistance will be important for designing strategies to obtain high-yielding disease-resistance crops.

References

Abreu, M.E., Munné-Bosch, S. (2009). Salicylic acid deficiency in *NahG* transgenic lines and *sid2* mutants increases seed yield in the annual plant *Arabidopsis thaliana.* Journal of Experimental Botany, 60: 1261-1271.

Afzal, A.J., da Cunha, L., Mackey, D. (2011). Separable fragments and membrane tethering of *Arabidopsis* RIN4 regulate its suppression of PAMP-triggered immunity. The Plant Cell, 23: 3798-3811.

Agrios, G.N. (2005). Plant Pathology, Fifth Edition. Burlington, MA, U.S.A.: Elsevier Academic Press.

Al-Daoud, F., Cameron, R.K. (2011). ANAC055 and ANAC092 contribute non-redundantly in an EIN2-dependent manner to Age-Related Resistance in *Arabidopsis*. Physiological and Molecular Plant Pathology, 76: 212-222.

Amasino, R. (2010). Seasonal and developmental timing of flowering. The Plant Journal, 61: 1001-1013.

Amborabé, B., Fleurat-Lessard, P., Chollet, J., Roblin, G. (2002). Antifungal effects of salicylic acid and other benzoic acid derivatives towards *Eutypa lata*: structure–activity relationship. Plant Physiology and Biochemistry, 40: 1051–1060.

Andrés, F., Coupland, G. (2012). The genetic basis of flowering responses to seasonal cues. Nature Reviews, 13: 627-639.

Andrés, F., Porri, A., Torti, S., Mateos, J., Romera-Branchat, M., Garcia-Martínez, J.L., Fornara, F., Gregis, V., Kater, M.M., Coupland, G. (2014). SHORT VEGETATIVE PHASE reduces gibberellin biosynthesis at the *Arabidopsis* shoot apex to regulate the floral transition. PNAS, 111: E2760-E2769.

Aslam, S.N., Newman, M-A., Erbs, G., Morrissey, K.L., Chinchilla, D., Boller, T., Jensen, T.T., Castro, C.D., Ierano, T., Molinaro, A., Jackson, R.W., Knight, M.R., and Cooper, R.M. (2008). Bacterial polysaccharides suppress induced innate immunity by calcium chelation. Current Biology, 18: 1078-1083.

Axtell, M.J., Chisholm, S.T., Dahlbeck, D., Staskawicz, B.J. (2003). Genetic and molecular evidence that the *Pseudomonas syringae* type II effector protein AvrRpt2 is a cysteine protease. Molecular Microbiology, 49: 1537-1546.

Axtell, M.J., Staskawicz, B.J. (2003). Initiation of *RPS2*-specified disease resistance in *Arabidopsis* is coupled to the AvrRpt2-directed elimination of RIN4. Cell, 112: 369-377.

Bartsch, M., Bednarek, P., Vivancos, P.D., Schneider, B., von Roepenack-Lahaye, E., Foyer, C.H., Kombrink, E., Scheel, D., Parker, J.E. (2010). Accumulation of isochorismate-derived 2,3-dihydroxybenzoic 3-*O*-β-$_{D}$-xyloside in *Arabidopsis* resistance to pathogens and ageing of leaves. The Journal of Biological Chemistry, 285: 25654-25665.

Battacharyya, M.K., Ward, E.W.B. (1986). Expression of gene-specific and age-related resistance and the accumulation of glyceollin in soybean leaves infected with *Phytophthora megasperma* f. sp. *glycinea*. Physiological and Molecular Plant Pathology, 29: 105-113.

Bauer, Z., Gómez-Gómez, L., Boller, T., Felix, G. (2001). Sensitivity of different ecotypes and mutants of *Arabidopis thaliana* toward the bacterial elicitor flagellin correlates with the presence of receptor-binding sites. Journal of Biological Chemistry, 276: 45669-45676.

Belkhadir, Y., Nimchuk, Z., Hubert, D.A., Mackey, D., Dangl, J.L. (2004). Arabidopsis RIN4 negatively regulates disease resistance mediated by RPS2 and RPM1 downstream or independent of the NDR1 signal modulator and is not required for the virulence functions of bacterial type III effectors AvrRpt2 or AvrRpm1. The Plant Cell, 16: 2822-2835.

Bigeard, J., Colcombet, J., Hirt, H. (2015). Signaling mechanisms in pattern-triggered immunity (PTI). Molecular Plant, 8: 521-539.

Blázquez, M.A., Soowal, L.N., Lee, I., Weigel, D. (1997). *LEAFY* expression and flower initiation in *Arabidopsis.* Development, 124: 3835-3844.

Boch, J., Joardar, V., Gao, L., Robertson, T.L., Lim, M., Kunkel, B.N. (2002). Identification of *Pseudomonas syringae* pv. *tomato* genes induced during infection of *Arabidopsis thaliana.* Molecular Microbiology, 44: 73-88.

Boller, T., Felix, G. (2009). A renaissance of elicitors: perception of microbe-associated molecular patterns and danger signals by pattern-recognition receptors. The Annual Review of Plant Biology, 60: 379-406.

Bosmund, I. (1960). The bacteriostatic action of benzoic and salicylic acids: influence of pH on the total uptake of benzoic acid by *Proteus vulgaris* and baker's yeast. Physiologia Plantarum, 13: 793-799.

Brown, D.G., Swanson, J.K., Allen, C. (2007). Two host-induced *Ralstonia solanacearum* genes, *acrA* and *dinF*, encode multidrug efflux pumps and contribute to bacterial wilt virulence. Applied and Environmental Microbiology, 73: 2777-2786.

Cameron, R.K., Zaton, K. (2004). Intercellular salicylic acid accumulation is important for age-related resistance in *Arabidopsis* to *Pseudomonas syringae*. Physiological and Molecular Plant Pathology, 65: 197-209.

Cao, H., Bowling, S.A., Gordon, S.A., Dong, X. (1994). Characterization of an Arabidopsis mutant that is nonresponsive to inducers of systemic acquired resistance. The Plant Cell, 6: 1583-1592.

Carella, P., Kempthorne, C.J., Wilson, D.C., Isaacs, M. (2017). Exploring the role of DIR1, DIR1-like and other lipid transfer proteins during systemic immunity in Arabidopsis. Physiological and Molecular Plant Pathology, 97: 49-57.

Carella, P., Merl-Pham, J., Wilson, D.C., Dey, S., Hauck, S.M., Vlot, C.A., Cameron, R.K. (2016a). Comparative proteomics analysis of phloem exudates collected during the induction of systemic acquired resistance. Plant Physiology, 171: 1495-1510.

Carella, P., Wilson, D.C., Kempthorne, C.J., Cameron, R.K. (2016b). Vascular sap proteomics: providing insight into long-distance signaling during stress. Frontiers in Plant Science, 7: 651.

Carella, P., Wilson, D.C., Cameron, R.K. (2015a). Mind the gap: signal movement through plasmodesmata is critical for the manifestation of SAR. Plant Signaling & Behavior, 10: e1075683.

Carella, P., Wilson, D.C., Cameron, R.K. (2015b). Some things get better with age: differences in salicylic acid accumulation and defense signaling in young and mature *Arabidopsis.* Frontiers in Plant Science, 5: 775.

Carviel, J.L., Al-Daoud, F., Neumann, M., Mohammad, A., Provart, N.J., Moeder, W., Yoshioka, K., Cameron, R.K. (2009). Forward and reverse genetics to identify genes involved in the age-related resistance response in *Arabidopsis thaliana.* Molecular Plant Pathology, 10: 621-634.

Carviel, J.L., Wilson, D.C., Isaacs, M., Carella, P., Catana, V., Golding, B., Weretilnyk, E.A., Cameron, R.K. (2014). Investigation of intercellular salicylic acid accumulation during compatible and incompatible *Arabidopsis-Pseudomonas syringae* interactions using a fast neutron-generated mutant allele of *EDS5* identified by genetic mapping and whole-genome sequencing. PLoS ONE, 9: e88608.

Chandaran, D., Rickert, J., Huang, Y., Steinwand, M.A., Marr, S.K., Wildermuth, M.C. (2014). Atypical E2F transcriptional repressor DEL1 acts at the intersection of plant growth and immunity by controlling the hormone salicylic acid. Cell Host & Microbe, 15: 506-513.

Chang, C-Y., Krishnan, T., Wang, H., Chen, Y., Yin, W-F., Chong, Y-M., Tan, L.Y., Chong, T.M., Chan, K-G. (2014). Non-antibiotic quorum sensing inhibitors acting against *N*-acyl homoserine lactone synthase as druggable targets. Scientific Reports, 4: 7245.

Chen, H-J., Hou, W-C., Kuć, J., Lin, Y-H. (2001). Ca^{2+}-dependent and Ca^{2+}-independent excretion modes of salicylic acid in tobacco cell suspension culture. Journal of Experimental Botany, 52: 1219-1226.

Chen, J., Zhu, X., Ren, J., Qui, K., Li, Z., Gao, J., Zhou, X., Kuai, B. (2017). Suppressor of overexpression of CO 1 negatively regulated dark-induced leaf degreening and senescence by directly repressing pheophytinase and other senescence-associated genes in Arabidopsis. Plant Physiol. 173: 1881-1891.

Chen, Z., Silva, H., Klessig, D.F. (1993). Active oxygen species in the induction of plant systemic acquired resistance by salicylic acid. Science, 262: 1883-1886.

Chinchilla, D., Bauer, Z., Regenass, M., Boller, T., Felix, G. (2006). The *Arabidopsis* receptor kinase FLS2 binds flg22 and determines the specificity of flagellin perception. The Plant Cell, 18: 465-476.

Chinchilla, D., Zipfel, C., Robatzek, S., Kemmerling, B., Nürnberger, T., Jones, J.D.G., Felix, G., Boller, T. (2007). A flagellin-induced complex of the receptor FLS2 and BAK1 initiates plant defence. Nature, 448: 497-501.

Chisholm, S.T., Dahlbeck, D., Krishnamurthy, N., Day, B., Sjolander, K., Staskawicz, B.J. (2004). Molecular characterization of proteolytic cleavage sites of the *Pseudomonas syringae* effector AvrRpt2. PNAS, 102: 2087-2092.

Clatworthy, A.E., Pierson, E., Hung, D.T. (2007). Targeting virulence: a new paradigm for antimicrobial therapy. Nature, 3: 541-548.

Coll, N.S., Epple, P., Dangl, J.L. (2011). Programmed cell death in the plant immune system. Cell Death and Differentiation, 18: 1247-1256.

Coupland, G., Kater, M.M. (2013). Identification of pathways directly regulated by SHORT VEGETATIVE PHASE during vegetative and reproductive development in *Arabidopsis.* Genome Biology, 14:R56.

Corral-Lugo, A., Daddaoua, A., Ortega, A., Espisona-Urgel, M., Drell, T. (2016). Rosmarinic acid is a homoserine lactone mimic produced by plants that activates a bacterial quorum-sensing regulator. Science Signaling, 409: ra1.

Cui, H., Tsuda, K., Parker, J.E. (2015). Effector-triggered immunity: from pathogen perception to robust defense. The Annual Review of Plant Biology, 66: 487-511.

Danhorn, T., Fuqua, C. (2007). Biofilm formation by plant-associated bacteria. The Annual Review of Microbiology, 61: 401-422.

de Folter, S., Immink, R. G. H., Kieffer, M., Pařenicová, L., Henz, S. R., Weigel, D., Busscher, M., Kooiker, M., Colombo, L., Kater, M. M., Davies, B., Angenent, G. C. (2005). Comprehensive interaction map of the Arabidopsis MADS box transcription factors. The Plant Cell 17: 1424-1433.

de Groot, R.S., Wilson, M.A., Boumans, R.M.J. (2002). A typology for the classification, description and valuation of ecosystem functions, goods, and services. Ecological Economics, 41: 393-408.

de Torres Zabala, M., Bennett, M.H., Truman, W.H., Grant, M.R. (2009). Antagonism between salicylic and abscisic acid reflects host-pathogen conflict and moulds plant defence responses. The Plant Journal, 59: 375-386.

Dean, J.V., Mills, J.D. (2004). Uptake of salicylic acid 2-*O*-*β*-$_D$-glucose in soybean tonoplast vesicles by an ATP-binding cassette transporter-type mechanism. Physiologia Plantarum, 120: 603-612.

Dean, J.V., Mohammed, L.A., Fitzpatrick, T. (2005). The formation, vacuolar localization, and tonoplast transport of salicylic acid glucose conjugates in tobacco cell suspension cultures. Planta, 221: 287-296.

Dean, J.V., Shah, R.P., Mohammed, L.A. (2003). Formation and vacuolar localization of salicylic acid conjugates in soybean cell suspension cultures. Physiologia Plantarum, 118: 328-336.

Dean, J.V., Delaney, S.P. (2008). Metabolism of salicylic acid in wild-type, *ugt74f1* and *ugt74f2* glucosyltransferase mutants of *Arabidopsis thaliana*. Physiologia Plantarum, 132: 417-425.

DeFraia, C., Schmelz, E.A., Mou, Z. (2008). A rapid biosensor-based method for quantification of free and glucose-conjugated salicylic acid. Plant Methods 4: 28.

Delaney, T.P., Friedrich, L., Ryals, J.A. (1995). *Arabidopsis* signal transduction mutant defective in chemically and biologically induced resistance. PNAS, 92: 6602-6606.

Dempsey, D.A., Klessig, D.F. (2017). How does the multifaceted plant hormone salicylic acid combat disease in plants and are similar mechanisms utilized in humans? BMC Biology, 15: 23.

Dempsey, D.A., Vlot, A.C., Wildermuth, M.C., Klessig, D.F. (2011). Salicylic acid biosynthesis and metabolism. The Arabidopsis Book 9: 1-24.

Deng, W., Ying, H., Helliwell, C.A., Taylor, J.M.., Peacock, W.J., Dennis, E.S. (2011). FLOWERING LOCUS C (FLC) regulates development pathways throughout the life cycle of *Arabidopsis*. PNAS, 108: 6680-6685.

Desveaux, D., Subramaniam, R., Després, C., Mess, J-N., Lévesque, C., Fobert, P.R., Dangl, J.L., Brisson, N. (2004). A “Whirly” transcription factor is required for salicylic acid-dependent disease resistance in *Arabidopsis*. Developmental Cell, 6: 229-240.

Develey-Rivière, M-P., Galiana, E. (2007). Resistance to pathogens and host developmental stage: a multifaceted relationship within the plant kingdom. New Phytologist, 175: 405-416.

Dodds, P.N., Rathjen, J.P. (2010). Plant immunity: towards an integrated view of plant-pathogen interactions. Nature, 11: 539-548.

Dong, X., Mindrinos, M., Davis, K.R., Ausubel, F.M. (1991). Induction of *Arabidopsis* defense genes by virulent and avirulent *Pseudomonas syringae* strains and by a cloned avirulence gene. The Plant Cell, 3: 61-72.

Dou, D., Zhou, J-M. (2012). Phytopathgen effectors subverting host immunity: different foes, similar battleground. Cell Host & Microbe, 12: 484-495.

El-Mougy, N.S. (2002). In vitro studies on antimicrobial activity of salicylic acid and acetyl salicylic acid as pesticidal alternatives against some soilborne plant pathogens. Egyptian Journal of Phytopathology, 30: 41–55.

Eriksson, S., Böhlenius, H., Moritz, T., Nilsson, O. (2006). GA4 is the active gibberellin in the regulation of *LEAFY* transcription and *Arabidopsis* floral initiation. The Plant Cell, 18: 2172-2181.

Fett, W.F., Dunn, M.F. (1989). Exopolysaccharides produced by phytopathogenic Pseudomonas syringae pathovars in infected leaves of susceptible hosts. Plant Physiology, 89: 5-9.

Fornara, F., de Montaigu, A., Coupland, G. (2010). SnapShot: control of flowering in *Arabidopsis*. Cell, 141: 550-550e.2.

Fu, Z.Q., Dong, X. (2013). Systemic acquired resistance: turning local infection into global defense. The Annual Review of Plant Biology, 64: 839-863.

Fu, Z.Q., Yan, S., Saleh, A., Wang, W., Ruble, J., Oka, N., Mohan, R., Spoel, S.H., Tada, Y., Zheng, N., Dong, X. (2012). NPR3 and NPR4 are receptors for the immune signal salicylic acid in plants. Nature, 486: 228-232.

Fragnière, C., Serrano, M., Abou-Mansour, E., Mètraux, J-P. (2011). Salicylic acid and its location in response to biotic and abiotic stress. FEBS Letters, 585: 1847-1852.

Gassmann, W. (2005). Natural variation in the *Arabidopsis* response to the avirulence gene hopPsyA uncouples the hypersensitive response from disease resistance. Molecular Plant Microbe Interactions, 18: 1054-1060.

Gassmann, W., Bhattacharjee, S. (2012). Effector-triggered immunity signaling: from gene-for-gene pathways to protein-protein interaction networks. Molecular Plant Microbe Interactions, 25: 862-868.

Geng, X., Jin, L., Shimada, M., Kim, M.G., Mackey, D. (2014). The phytotoxin coronatine is a multifunctional component of the virulence armament of *Pseudomonas syringae.* Planta, 240: 1149-1165.

Georgiou, C.D., Tairis, N., Sotiropoulou, A. (2000). Hydroxyl radical scavengers inhibit lateral-type sclerotial differentiation and growth in phytopathogenic fungi. Mycologia, 95: 825–834.

Glazebrook, J. (2005). Contrasting mechanisms of defense against biotrophic and necrotrophic pathogens. The Annual Review of Phytopathology, 43: 205-227.

Glazebrook, J., Rogers, E.E., Ausubel, F.M. (1996). Isolation of Arabidopsis mutants with enhanced disease susceptibility by direct screening. Genetics, 145: 973-982.

Gómez-Gómez, L., Boller, T. (2000). FLS2: an LRR receptor-like kinase involved in the perception of the bacterial elicitor flagellin in Arabidopsis. Molecular Cell, 6: 1003-1011.

Gray, K.M., Garey, J.R. (2001). The evolution of bacterial LuxI and LuxR quorum sensing regulators. Microbiology, 147: 2379-2387.

Gregis, V., Andrés, F., Sessa, A., Guerra, R.F., Simonini, S., Mateos, J.L., Torti, S., Zambelli, F., Prazzoli, G.M., Bjerkan, K.M., Grini, P.E., Pavesi, G., Colombo, L., Coupland, G., Kater, M.M. (2013). Identification of pathways directly regulated by SHORT VEGETATIVE PHASE during vegetative and reproductive development in *Arabidopsis*. Genome Biology 14: R56.

Gutknecht, J. (1990). Salicylates and proton transport through lipid bilayer membranes: a model for salicylate-induced uncoupling and swelling in mitochondria. Journal of Membrane Biology, 115: 253-260.

Harper, A.L., McKinney, L.V., Nielsen, L.R., Havlickova, L., Li, Y., Trick, M., Fraser, F., Wang, L., Fellgett, A., Sollars, E.S.A., Janacek, S.H., Downie, J.A.,

Buggs, R.J.A., Kjaer, E.D., Bancroft, I. (2015). Molecular markers for tolerance of European ash (*Fraxinus excelsior*) to dieback disease identified using associative transcriptomics. Scientific Reports, 6: 19335.

Hartmann, U., Höhmann, S., Nettesheim, K., Wisman, E., Saedler, H., Huijser, P. (2000). Molecular cloning of *SVP*: a negative regulator of the floral transition in *Arabidopsis*. The Plant Journal, 21: 351-360.

Heil, M., Baldwin, I.T. (2002). Fitness costs of induced resistance: emerging experimental support for a slippery concept. Trends in Plant Science, 7: 61-66.

Hempel, F.D., Feldman, L.J. (1994). Bi-directional inflorescence development in *Arabidopsis thaliana*: acropetal initiation of flowers and basipetal initiation of paraclades. Planta, 192: 276-286.

Hennig, J., Malamy, J., Grynkiewicz, G., Indulski, J., Klessig, D.F. (1993). Interconversion of the salicylic acid signal and its glucoside in tobacco. The Plant Journal, 4: 593-600.

Hileman, L.C., Sundstrom, J.F., Litt, A., Chen, M., Shumba, T., Irish, V.F. (2006). Molecular and phylogenetic analyses of the MADS-box gene family in tomato. Molecular Biology and Evolution, 23: 2245-2258.

Himejima, M., Kubo, I. (1991). Antimicrobial agents from cashew *Anacardium occidentale* (Anacardiaceae) nut shell oil. Journal of Agriculture and Food Chemistry, 39: 416-421.

Hogenhout, S.A., Van der Hoorn, R.A.L., Terauchi, R., Kamoun, S. (2009). Emerging concepts in effector biology of plant-associated organisms. Molecular Plant Microbe Interactions, 22: 115-122.

Huang, W.E., Wang, H., Zheng, H., Huang, L., Singer, A.C., Thompson, I., Whiteley, A.S. (2005). Chromosomally located gene fusions constructed in *Acinetobacter* sp. ADP1 for the detection of salicylate. Environmental Microbiology, 7: 1339-1348.

Huang, W.E., Huang, L., Preston, G.M., Naylor, M., Carr, J.P., Li, Y., Singer, A.C., Whiteley, A.S., Wang H. (2006). Quantitative in situ assay of salicylic acid in tobacco leaves using a genetically modified biosensor strain of *Acinetobacter* sp. ADP1. The Plant Journal, 46: 1073-1083.

Hugot, K., Aimé, S., Conrod, S., Poupet, A., Galiana, E. (1999). Developmental regulated mechanisms affect the ability of a fungal pathogen to infect and colonize tobacco leaves. The Plant Journal, 20: 163-170.

Hunter, R.E., Halloin, J.M., Veech, J.A., Carter, W.W. (1978). Terpenoid accumulation in hypocotyls of cotton seedlings during ageing and after infection by *Rhizoctonia solani*. Physiology and Biochemistry; 68: 347-350.

Huot, B., Yao, J., Montgomery, B.L., He, S.Y. (2014). Growth-defense tradeoffs in plants: a balancing act to optimize fitness. Molecular Plant, 7: 1267-1287.

Husted, S., Schjoerring, J.K. (1995). Apoplastic pH and ammonium concentration in leaves of *Brassica napus* L. Plant Physiology, 109: 1453-1460.

Huynh, T.V., Dahlbeck, D., Staskawicz, B.J. (1989). Bacterial blight of soybean: regulation of a pathogen gene determining host cultivar specificity. Science, 245: 1374-1377.

Hwang, B.K. (1995). Effects of age-related resistance and metalazyl on capsidiol production in pepper plants infected with *Phytophthora capsici*. In: Handbook of phytoalexin metabolism and action. New York, U.S.A.: Marcel Dekker.

Hyun, Y., Richter, R., Coupland, G. (2017). Competence to flower: age-controlled sensitivity to environmental cues. Plant Physiology, 173: 36-46.

Hyun, Y., Richter, R., Vincent, C., Martinez-Gallegos, R., Porri, A., Coupland, G. (2016). Multi-layed regulation of SPL15 and cooperation with SOC1 integrate endogenous flowering pathways at the *Arabidopsis* shoot meristem.

Ichinose, Y., Taguchi, F., Mukaihara, T. (2013). Pathogenicity and virulence factors of *Pseudomonas syringae.* Journal of General Plant Pathology, 79: 285-296.

Immink, R.G.H., Posé, D., Ferrario, S., Ott, F., Kaufmann, K., Valentim, F.L., de Folter, S., van der Wal, F., van Dijk, A.D.J., Schmid, M., Angenent, G.C. (2012). Characterization of SOC1's central role in flowering by the identification of its upstream and downstream regulators. Plant Physiology, 160: 433-449.

Jagadeeswaran, G., Raina, S., Acharya, B.R., Maqbool, S.B., Mosher, S.L., Appel, H.M., Schultz, J.C., Klessig, D.F., Raina, R. (2007). Arabidopsis *GH3-LIKE DEFENSE GENE 1* is required for accumulation of salicylic acid, activation of defense responses and resistance to *Pseudomonas syringae.* The Plant Journal, 51: 234-246.

Janda, M., Ruelland, E. (2015). Magical mystery tour: salicylic acid signaling. Environmental and Experimental Botany, 114: 117-128.

Jia, W., Davies, W.J. (2007). Modification of leaf apoplastic pH in relation to stomatal sensitivity to root-sourced abscisic acid signals. Plant Physiology, 143: 68-77.

Jones, J.G.D., Dangl, J.L. (2006). The plant immune system. Nature, 444: 323-329.

Jörgensen, T.G., Weis-Fogh, U.S., Nielsen, H.H., Olesen, H.P. (1976). Salicylate- and aspirin-induced uncoupling of oxidative phosphorylation in mitochondria isolated from the mucosal membrane of the stomach. Scandanavian Journal of Clinical and Laboratory Investigation, 36: 659-664.

Kazan, K., Lyons, R. (2015). The link between flowering time and stress tolerance. Journal of Experimental Botany, 67: 47-60.

Keith, R.C., Keith, L.M.W., Hernandez-Guzman, G., Uppalapati, S.R., Bender, C.L. (2003). Alginate gene expression by *Pseudomonas syringae* pv. *tomato* DC3000 in host and non-host plants. Microbiology 149: 1127-1138.

Keshavan, N.D., Chowdhary, P.K., Haines, D.C., Gonzalez, J.E. (2005). L-canavanine made by *Medicago sativa* interferes with quorum sensing in *Sinorhizobium meliloti*. Journal and Bacteriology, 187: 8427-8436.

Khan, M.I.R., Fatma, M., Per, T.S., Anjum, N.A., Khan, N.A. (2015). Salicylic acid-induced abiotic stress tolerance and underlying mechanisms in plants. Frontiers in Plant Science, 6: 462.

Khokhani, D., Zhang, C., Li, Y., Wang, Q., Zeng, Q., Yamazaki, A., Hutchins, W., Zhou, S-S., Chen, X., Yang, C-H. (2013). Discovery of plant phenolic compounds that act as type III secretion system inhibitors or inducers of the fire blight pathogen, *Erwinia amylovora*. Applied and Environmental Microbiology, 79: 5424-5436.

Kim, B.J., Schneider, D.J., Cartinhour, S.W., Shuler, M.L. (2010). Complex responses to culture conditions in *Pseudomonas syringae* pv. *tomato* DC3000 continuous cultures: the role of iron in cell growth and virulence factor production. Biotechnology and Bioengineering, 105: 995-964.

Kim, H-S., Desveaux, D., Singer, A.U., Patel, P., Sondek, J., Dangl, J.L. (2005). The *Pseudomonas syringae* effector AvrRpt2 cleaves its C-terminally acylated target, RIN4, from *Arabidopsis* membranes to block RPM1 activation. PNAS, 102: 6496-6501.

Kimura, Y., Aoki, S., Ando, E., Kitatsuji, A, Watanabe, A., Ohnishi, M., Takahashi, K., Inoue, S-I., Nakamichi, N., Tamada, Y., Kinoshita, T. (2015). A flowering integrator, SOC1, affects stomatal opening in *Arabidopsis thaliana.* Plant Cell Physiology. 56: 640-649.

King, E.O., Ward, M.K., Raney, D.E. (1954). Two simple media for the demonstration of pyocyanin and fluorescin. Journal of Laboratory and Clinical Medicine, 44: 301–307.

Klessig, D.F., Tian, M., Choi, H.W. (2016). Multiple targets of salicylic acid and its derivatives in plants and animals. Frontiers in Immunology, 7: 206.

Kus, J.V., Zaton, K., Sarkar, R., Cameron, R.K. (2002). Age-related resistance in *Arabidopsis* is a developmentally regulated defense response to *Pseudomonas syringae*. The Plant Cell, 14: 479-490.

Koo, Y.J., Kim, M.A., Kim, E.H., Song, J.T., Jung, C., Moon, J-K., Kim, J-H., Seo, H.S., Song, S.I., Him, J-K., Lee, J.S., Cheong, J-J., Choi, Y.D. (2007). Overexpression of salicylic acid carboxyl methyltransferase reduces salicylic acid-mediated pathogen resistance in *Arabidopsis thaliana.* Plant Molecular Biology, 64: 1-15.

Laue, H., Schenk, A., Li, H., Lambertsen, L., Neu, T.R., Molin, S., Ullrich, M.S. (2006). Contribution of alginate and levan production to biofilm formation by *Pseudomonas syringae.* Microbiology, 152: 2909-2918.

Lee, H., Suh, S-S., Park, E., Cho, E., Ahn, J.H., Kim, S.G., Lee, J.S., Kwon, Y.M., Lee, I. (2000). The AGAMOUS-LIKE 20 MADS domain protein integrates floral inductive pathways in *Arabidopsis*. Genes & Development, 14: 2366-2376.

Lee, J., Lee, I. (2010). Regulation and function of SOC1, a flowering pathway integrator. Journal of Experimental Botany, 61: 2247-2254.

Lee, J.H., Yoo, S.J., Park, S.H., Hwang, I., Lee, J.S., Ahn, J.H. (2007). Role of SVP in the control of flowering-time by ambient temperature in Arabidopsis. Genes and Development, 21: 397–402.

Lee, M.W., Lu, H., Jung, H.W., Greenberg, J.T. (2007). A key role for the *Arabidopsis* WIN3 protein in disease resistance triggered by *Pseudomonas syringae* that secrete AvrRpt2. Molecular Plant Microbe Interactions, 20: 1192-1200.

Lee-Jones, D. (2016). Kiwifruit sector report. USDA Foreign Agricultural Service Gain Report, NZ1601.

Lewis, K., Naroditskaya, V., Ferrante, A., Fokina, I. (1994). Bacterial resistance to uncouplers. Journal of Bioenergetics and Biomembranes. 20: 639-646.

Li, D., Liu, C., Shen, L., Wu, Y., Chen, H., Robertson, M., Helliwell, C.A., Ito, T., Meyerowitz, E., Yu, H. (2008). A repressor complex governs the integration of flowering signals in Arabidopsis. Developmental Cell, 15: 110–120.

Lim, E-K., Doucet, C.J., Li, Y., Elias, L., Worrall, D., Spencer, S.P., Ross, J., Bowles, D.J. (2002). The activity of *Arabidopsis* glycosyltransferases toward salicylic acid, 4-hydroxybenzoic acid, and other benzoates. The Journal of Biological Chemistry, 277: 686-692.

Liu, P-P., Yang, Y., Pichersky, E., Klessig, D.F. (2010). Altering expression of *Benzoic Acid/Salicylic Acid Carboxyl Methyltransferase 1* compromises systemic acquired resistance and PAMP-triggered immunity in *Arabidopsis.* Molecular Plant Microbe Interactions, 23: 82-90.

Lowe-Power, T.M., Jacobs, J.M., Ailloud, F., Fochs, B., Prior, P., Allen, C. (2016). Degradation of the plant defense signal salicylic acid protects *Ralstonia solanacearum* from toxicity and enhances virulence on tobacco. mBio 7: e00656-16.

Luis, M.A.J., Kenton, P., Lloyd, A.J., Ougham, H., Prats, E. (2008). The hypersensitive response; the centenary is upon us but how much do we know? Journal of Experimental Botany, 59: 501-520.

Lyons, R., Rusu, A., Stiller, J., Powell, J., Manners, J.M., Kazan, K. (2015). Investigating the association between flowering time and defense in the *Arabidopsis thaliana-Fusarium oxysporum* interaction. PLoS ONE, 10: e0127699.

Macho, A.P., Zipfel, C. (2014). Plant PRRs and the activation of innate immune signaling. Molecular Cell, 54: 263-272.

Mackey, D., Belkhadir, Y., Alonso, J.M., Ecker, J.R., Dangl, J.L. (2003). *Arabidopsis* RIN4 is a target of the type III virulence effector AvrRpt2 and modulates RPS2-mediated resistance. Cell, 112: 379-389.

Madan, R.K., Levitt, J. (2014). A review of toxicity from topical salicylic acid preparations. Journal of the American Academy of Dermatology, 70: 788-792.

Mao, L., Begum, D., Chuang, H-W., Budiman, M.A., Szymkowiak, E.J., Irish, E.E., Wing, R.A. (2000). *JOINTLESS* is a MADS-box gene controlling tomato flower abscission zone development. Nature, 406: 910-913.

Martín, J.A., Solla, A., Witzell, J., Gil, L., García-Vallejo, M.C. (2010). Antifungal effect and reduction of *Ulmus minor* symptoms to *Ophiostoma novo-ulmi* by carvacrol and salicylic acid. European Journal of Plant Pathology, 127: 21–32.

Mateos, J.L., Madrigal, P., Tsuda, K., Rawat, V., Richter, R., Romera-Branchat, M., Fornara, F., Schneeberger, K., Krajewski, P., Coupland, G. (2015). Combinatorial activities of SHORT VEGETATIVE PHASE and FLOWERING

LOCUS C define distinct modes of flowering regulation in *Arabidopsis.* Genome Biology, 16:31.

McDonnell, G., Russell, D.A. (1999). Antiseptics and disinfectants: activity, action, and resistance. Clinical Microbiology Reviews, 12: 147-179.

McDowell, J.M., Williams, S.G., Funderburg, N.T., Eulgem, T., Dangl, J.L. (2005). Genetic analysis of developmentally regulated resistance to downy mildew (*Hyaloperonospora parasitica*) in *Arabidopsis thaliana.* Molecular Plant-Microbe Interactions, 11: 1226-1234.

Méndez-Vigo, B., Martínez-Zapater, J.M., Alonso-Blanco, C. (2013). The flowering repressor *SVP* underlies a novel *Arabidopsis thaliana* QTL interacting with the genetic background. PLoS Genetics, 9: e1003289.

Michaels, S.D., Amasino, R.M. (1999). *FLOWERING LOCUS C* encodes a novel MADS domain protein that acts as a repressor of flowering. The Plant Cell, 11: 949-956.

Nabors, M.W. (2004). Introduction to Botany. San Francisco, CA, U.S.A.: Pearson Education Inc.

Nawrath, C., Mètraux, J-P. (1999). Salicylic acid induction-deficient mutants of Arabidopsis express *PR-2* and *PR-5* and accumulate high levels of camalexin after pathogen inoculation. The Plant Cell, 11: 1393-1404.

Nielsen, K.K., Andersen, C.H., Folling, M., Gao, C., Lenk, I., Didion, T., Jensen, C.S., Petersen, K., Storgaard, M. (2012). Means and methods for controlling flowering in plants. Google Patents, US8237013.

Nobuta, K., Okrent, R.A., Stoutemyer, M., Rodibaugh, N., Kempema, L., Wildermuth, M.C., Innes, R.W. (2007). The GH3 acyl adenylase family member PBS3 regulates salicylic acid-dependent defense responses in Arabidopsis. Plant Physiology, 144: 1144-1156.

Norman, C., Howell, K.A., Millar, H.A., Whelan, J.M., Day, D.A. (2004). Salicylic acid is an uncoupler and inhibitor of mitochondrial electron transport. Plant Physiology, 134: 492-501.

Oerke, E.C. (2006). Crop losses to pests. Journal of Agricultural Science, 144: 31-43.

Osman, S.F., Fett, W.F., Fishman, M.L. (1986). Exopolysaccharides of the phytopathogen *Pseudomonas syringae* pv. *glycinea*. Journal of Bacteriology, 166: 66-71.

Pajerowska-Mukhtar, K.M., Wang, W., Tada, Y., Oka, N., Tucker, C.L., Fonseca, J.P., Dong, X. (2012). The HSF-like transcription factor TBF1 is a major molecular switch for plant growth-to-defense transition. Current Biology, 22: 103-112.

Pajoro, A., Biewers, S., Dougali, E., Valentim, F.L., Mendes, M.A., Porri, A., Coupland, G., Van de Peer, Y., van Dijk, A.D.J., Colombo, L., Davies, B., Angenent, G.C. (2014). The (r)evolution of gene regulatory networks controlling *Arabidopsis* plant reproduction: a two-decade history. Journal of Experimental Botany, 65: 4731-4745.

Panter, S.N., Hammond-Kosack, K.E., Harrison, K., Jones, J.D.G., Jones, D.A. (2002). Developmental control of promoter activity is not responsible for mature onset of *Cf-9B*-mediated resistance to leaf mold in tomato. Molecular Plant Microbe Interactions, 15: 1099-1107.

Parinthawong, N., Cottier, S., Buchala, A., Nawrath, C., Mètraux, J-P. (2015). Localization and expression of EDS5H a homologue of the SA transporter EDS5. BMC Plant Biology, 15: 135.

Parniske, M., Hammon-Kosack, K.E., Golstein, C., Thomas, C.M., Jones, D.A., Harrison, K., Wulff, B.B.H., Jones, J.D.G. (1997). Novel disease resistance specificities result from sequence exchange between tandemly repeated genes at the *Cf-4/9* locus of tomato. Cell, 91: 821-832.

Pelczar, M.J., Chan, E.C.S., Krieg, N.R. (2010). Microbiology: an application-based approach. Naveen Shahdara, Delhi, India: Tata McGraw Hill

Prithiviraj, B., Manickam, M., Singh, U. P., Ray, A. B. (1997). Antifungal activity of anacardic acid a naturally occurring derivative of salicylic acid. Canadian Journal of Botany, 75: 207–211.

Prithiviraj, B., Bais, H.P., Jha, A.K., Vivanco, J.M. (2005a). *Staphylococcus aureus* pathogenicity on *Arabidopsis thaliana* is mediated either by a direct effect of salicylic acid on the pathogen of by SA-dependent, NPR1-independent host responses. The Plant Journal, 43: 417-432.

Prithiviraj, B., Bais, H.P., Weir, T., Suresh, B., Najarro, E.H., Dayakar, B.V., Schweizer, H.P., Vivanco, J.M. (2005b). Down regulation of virulence factors of *Pseudomonas aeruginosa* by salicylic acid attenuates its virulence on *Arabidopsis thaliana* and *Caenorhabditis elegans.* Infection and Immunity, 73: 5319-5328.

Rahme, L.G., Mindrinos, M.N., Panopoulos, N.J. (1992). Plant and environmental sensory signals control the expression of *hrp* genes in *Pseudomonas syringae* pv. *phaseolicola.* Journal of Bacteriology, 174: 3499-3507.

Renzi, M., Copini, P., Taddei, A.R., Rossetti, A., Gallipoli, L., Mazzaglia, A., Balestra, G.M. (2012). Bacterial canker on kiwifruit in Italy: anatomical changes in the wood and in the primary infection sites. Phytopathology 102: 827-840.

Rivière, M-P., Marais, A., Ponchet, M., Willats, W., Galiana, E. (2008). Silencing of acidic pathogenesis-related *PR-1* genes increases extracellular β-(1→3)-glucanase activity at the onset of tobacco defense reactions. Journal of Experimental Botany, 59: 1225-1239.

Rusterucci, C., Zhao, Z., Haines, K., Mellersh, D., Neumann, M., Cameron, R.K. (2005). Age-related resistance to *Pseudomonas syringae* pv. *tomato* is associated with the transition to flowering in *Arabidopsis* and is effective against *Peronospora parasitica.* Physiological and Molecular Plant Pathology, 66: 222-231.

Robatzek, S., Wirthmueller, L. (2013). Mapping FLS2 function to structure: LRRs, kinase and its working bits. Protoplasma, 250: 671-681.

Rocher, F., Chollet, J-F., Jousse, C., Bonnemain, J-L. (2006). Salicylic acid, an ambimobile molecule exhibiting a high ability to accumulate in the phloem. Plant Physiology, 141: 1684-1683.

Rocher, F., Chollet, J-F., Legros, S., Jousse, C., Lemoine, R., Faucher, M., Bush, D.R., Bonnemain, J-L. (2009). Salicylic acid transport in *Ricinus communis* involves a pH-dependent carrier system in addition to diffusion. Plant Physiology, 150: 2081-2091.

Schenk, A., Weingart, H., and Ullrich, M.S. (2008). The alternative sigma factor AlgT, but not alginate synthesis, promotes in planta multiplication of *Pseudomonas syringae* pv. *glycinea*. Microbiology, 154: 413-421.

Schulze, B., Mentzel, T., Jehle, A.K., Mueller, K., Beeler, S., Boller, T., Felix, G., Chinchilla, D. (2010). Rapid heteromerization and phosphorylation of ligand-activated plant transmembrane receptors and their associated kinase BAK1. The Journal of Biological Chemistry, 285: 9444-9451.

Senthil-Kumar, M., Mysore, K.S. (2013). Nonhost resistance against bacterial pathogens: retrospectives and prospects. The Annual Review of Phytopathology, 51: 407-427.

Seo, E., Lee, H., Jeon, J., Park, H., Kim, J., Noh, Y-S., Lee, I. (2009). Crosstalk between cold response and flowering in *Arabidopsis* is mediated through the flowering-time gene *SOC1* and its upstream negative regulator *FLC*. Plant Cell 21: 3185-3197.

Seo, S., Ishizuka, K., Ohashi, Y. (1995). Induction of salicylic acid β-glucosidase in tobacco leaves by exogenous salicylic acid. Plant Cell Physiology, 36: 447-453.

Serrano, M., Wang, B., Aryal, B., Garcion, C., Abou-Mansour, E., Heck, S., Geisler, M., Mauch, F., Nawrath, M., Mètraux, J-P. (2013). Export of salicylic acid from the chloroplast requires the multidrug and toxin extrusion-like transporter EDS5. Plant Physiology, 162: 1815-1821.

Shah, J., Tsui, F., Klessig, D.F. (1997). Characterization of a salicylic acid-insensitive mutant (*sai1*) of *Arabidopsis thaliana,* identified in a selective screen utilizing the SA-inducible expression of the *tms2* gene. Molecular Plant Microbe Interactions, 10: 69-78.

Sharabani, G., Shtienberg, D., Borenstein, M., Shulhani, R., Lofthouse, M., Sofer, M., Chalupowicz, L., Barel, V., Manulis-Sasson, S. (2013). Effects of plant age on disease development and virulence of *Clavibacter michiganensis* subsp. *michiganensis* on tomato. Plant Pathology, 62: 1114-1122.

Sheldon, C.C., Burn, J.E., Perez, P.P., Metzger, J., Edwards, J.A., Peacock, W.J., Dennis, E.S. (1999). The *FLF* MADS box gene: a repressor of flowering in Arabidopsis regulated by vernalization and methylation. The Plant Cell, 11: 445-458.

Shen, L., Kang, Y.G.G., Liu, L., Yu, H. (2011). The J-domain protein J3 mediates the integration of flowering signals in *Arabidopsis.* The Plant Cell, 23: 499-514.

Singh, V., Roy, S., Giri, M.K., Chaturvedi, R., Chowdhury, Z., Shah, J., Nandi, A.K. (2013). *Arabidopsis thaliana FLOWERING LOCUS D* is required for systemic acquired resistance. Molecular Plant Microbe Interactions, 9: 1079-1088.

Smith, M.J.H. (1959). Salicylates and metabolism. Journal of Pharmacy and Pharmacology, 11: 705-720.

Stenlid, G., Saddik, K. (1962). The effect of some growth regulators and uncoupling agents upon oxidative phosphorylation in mitochondria of cucumber hypocotyls. Physiologia Plantarum, 15: 369-379.

Strawn, M.A., Marr, S.K., Inoue, K., Inada, N., Zubeita, C., Wildermuth, M.C. (2007). *Arabidopsis* isochorismate synthase functional in pathogen-induced salicylate biosynthesis exhibits properties consistent with a role in diverse stress responses. The Journal of Biological Chemistry, 282: 5919-5933.

Song, J.T., Koo, Y.J., Seo, H.S., Kim, M.C., Choi, Y.D., Kim, J.H. (2008). Overexpression of AtSGT1, and Arabidopsis salicylic acid glucosyltransferase, leads to increased susceptibility to *Pseudomonas syringae.* Phytochemistry, 69: 1128-1134.

Song, J.T. (2006). Induction of a salicylic acid glucosyltransferase, AtSGT1, is an early disease resistance response in *Arabidopsis thaliana.* Molecules and Cells, 22: 233-238.

Sun, Y., Li, L., Macho, A.P., Han, Z., Hu, Z., Zipfel, C., Zhou, J-M., Chai, J. (2013). Structural basis for flg22-induced activation of the *Arabidopsis* FLS2-BAK1 immune complex. Science, 343: 624-628.

Tan, J., Bednarek, P., Liu, J., Schneider, B., Svatoš, A., Hahlbrock, K. (2004). Universally occurring phenylpropanoid and species-specific indolic metabolites in infected and uninfected *Arabidopsis thaliana* roots and leaves. Phytochemistry, 65: 691-699.

Tanaka, S., Han, X., Kahmann, R. (2015). Microbial effectors target multiple steps in the salicylic acid production and signaling pathway. Frontiers in Plant Science, 6: 349.

Tao, Z., Shen, L., Liu, C., Liu, L., Yan, Y., Yu, H. (2012). Genome-wide identification of SOC1 and SVP targets during the floral transition in Arabidopsis. The Plant Journal, 70: 549-561.

Tian, D., Traw, M.B., Chen, J.Q., Kreitman, M., Bergelson, J. (2003). Fitness costs of R-gene-mediated resistance in *Arabidopsis thaliana.* Nature, 423: 74-77.

Tsuda, K., Sato, M., Glazebrook, J., Cohen, J.D., Katagiri, F. (2008). Interplay between MAMP-triggered and SA-mediated defense responses. The Plant Journal, 53: 763-775.

Tsuda, K., Sato, M., Stoddard, T., Glazebrook, J., Katagiri F. (2009). Network properties of robust immunity in plants. PLoS Genetics, 5: e1000772.

Veit, S., Wörle, J.M., Nürnberger, T., Koch, W., Seitz, H.U. (2001). A novel protein elicitor (PaNie) from *Pythium aphanidermatum* induces multiple defense responses in carrot, *Arabidopsis*, and tobacco. Plant Physiology, 127: 832-841.

Venturi, V., Fuqua, C. (2013). Chemical signaling between plants and plant-pathogenic bacteria. The Annual Review of Phytopathology, 51: 17-37.

Vicente, M.R-S., Plasencia, J. (2011). Salicylic acid beyond defense: its role in plant growth and development. Journal of Experimental Botany, 62: 3321-3338.

Vlot, A.C.., Dempsey, D.A., Klessig, D.F. (2009). Salicylic acid, a multifaceted hormone to combat disease. The Annual Review of Phytopathology, 47: 177-206.

Wang, L., Tsuda, K., Truman, W., Sato, M., Nguyen, L.V., Katagiri, F., Glazebrook, J. (2011). CBP60g and SARD1 play partially redundant critical roles in salicylic acid signaling. The Plant Journal, 67: 1029-1041.

Weigel, D. (2012). Natural variation in Arabidopsis: from molecular genetics to ecological genomics. Plant Physiology, 158: 2-22.

Whalen, M.C. (2005). Host defence in a developmental context. Molecular Plant Pathology, 6: 347-360.

Whalen, M.C., Innes, R.W., Bent, A.F., Staskawicz, B.J. (1991). Identification of *Pseudomonas syringe* pathogens of *Arabidopsis* and a bacterial locus determining avirulence on both *Arabidopsis* and soybean. The Plant Cell, 3: 49-59.

Wildermuth, M.C., Dewdney, J., Wu, G., Ausubel, F.M. (2001). Isochorismate synthase is required to synthesize salicylic acid for plant defence. Nature, 414: 562-571.

Wilson, D.C., Carella, P., Cameron, R.K. (2014). Intercellular salicylic acid accumulation during compatible and incompatible *Arabidopsis-Pseudomonas syringae* interactions. Plant Signaling & Behavior, 9: e29362.

Wilson, D.C., Carella, P., Isaacs, M., Cameron, R.K. (2013). The floral transition is not the developmental switch that confers competence for the *Arabidopsis* Age-Related Resistance response to *Pseudomonas syringae* pv. *tomato*. Plant Molecular Biology, 83: 235-246.

Wilson, R.N., Heckman, J.W., Somerville, C.R. (1992). Gibberellin is required for flowering in *Arabidopsis thaliana* under short days. Plant Physiology, 100: 403-408.

Winter, C.M., Austin, R.S., Blanvillain-Baufumé, S., Reback, M.A., Monniaux, M., Wu, M-F., Sang, Y., Yamaguchi, A., Yamaguchi, N., Parker, J.E., Parcy, F., Jensen, S.T., Li, H., Wagner, D. (2011). LEAFY target genes reveal floral regulatory logic, *cis* motifs, and a link to biotic stimulus response. Developmental Cell, 20: 430-433.

Wu, G., Poethig, S. (2006). Temporal regulation of shoot development in *Arabidopsis thaliana* by *miR156* and its target SPL3. Development 133: 3539–3547

Wu, Y., Zhang, D., Chu, J.Y., Boyle, P., Wang, Y., Brindle, I.D., De Luca, V., Després, C. (2012). The *Arabidopsis* NPR1 protein is a receptor for the plant defense hormone salicylic acid. Cell Reports, 1: 639-647.

Wu, Y., Zhou, J-M. (2013). Receptor-like kinases in plant innate immunity. Journal of Investigative Plant Biology, 55: 1271-1286.

Xin, X-F., He, S.Y. (2013). *Pseudomonas syringae* pv. *tomato* DC3000: a model pathogen for probing disease susceptibility and hormone signaling in plants. The Annual Review of Phytopathology, 51: 473-498.

Yamasaki, K., Motomura, Y., Yagi, Y., Nomura, H., Shingo, K., Nakai, M., Shiina, T. (2013). Chloroplast envelope localization of EDS5, an essential factor for salicylic acid biosynthesis in *Arabidopsis thaliana.* Plant Signaling & Behavior, 8: e23603.

Yang, L., Rybtke, M.T., Jakobsen, T.H., Hentzer, M., Bjarnsholt, T., Givskov, M., Tolker-Nielsen, T. (2009). Computer-aided identification of recognized drugs as *Pseudomonas aeruginosa* quorum-sensing inhibitors. Antimicrobial Agents and Chemotherapy, 53: 2432-2433.

Yoshida, R., Fekih, R., Fujiwara, S., Oda, A., Miyata, K., Tomozoe, Y., Nakagawa, M., Niinuma, K., Hayashi, K., Ezura, H., Coupland, G., Mizoguchi, T. (2009). Possible role of EARLY FLOWERING 3 (ELF3) in clock-dependent floral regulation by SHORT VEGETATIVE PHASE (SVP) in *Arabidopsis thaliana.* New Phytologist, 182: 838-850.

Yuan, Z-C., Edlind, M.P., Liu, P., Saenkham, P., Banta, L.M., Wise, A.A., Ronzone, E., Binns, A.N., Kerr, K., Nester, E.W. (2007). The plant signal salicylic acid shuts down expression of the *vir* regulon and activates quormone quenching genes in *Agrobacterium*. PNAS, 104: 11790-11795.

Zahara, M.B., Scheuerman, R.W. (1988). Hand-harvesting jointless vs. jointed-stem tomatoes. California Agriculture, 43: 14.

Zhang, K., Halitschke, R., Yin, C., Liu, C-J., Gan, S-S. (2013). Salicylic acid 3-hydroxylase regulates *Arabidopsis* longevity by mediating salicylic acid catabolism. PNAS, 110: 14807-14812.

Zhang, Y., Xu, S., Ding, P., Wang, D., Cheng, Y.T., He, J., Gao, M., Xu, F., Li, Y., Zhu, Z., Li, X., Zhang, Y. (2010). Control of salicylic acid synthesis and systemic

acquired resistance by two members of a plant-specific family of transcription factors. PNAS, 107: 18220-18225.

Zheng, X-Y., Spivey, N.W., Zeng, W., Liu, P-P., Fu, Z.Q., Klessig, D.F., He, S.Y., Dong, X. (2012). Coronatine promotes *Pseudomonas syringae* virulence in plants by activating a signaling cascade that inhibits salicylic acid accumulation. Cell Host & Microbe, 11: 587-596.

Zheng, X-Y., Zhou, M., Yoo, H., Pruneda-Praz, J.L., Spivey, N.W., Kay, S.A., Dong, X. (2015). Spatial and temporal regulation of biosynthesis of the plant immune signal salicylic acid. PNAS, 112: 9166-9173.

Zheng, Z., Qualley, A., Fan, B., Dudareva, N., Chen, Z. (2009). An important role of a BAHD acyl transferase-like protein in plant innate immunity. The Plant Journal, 57: 1040-1053.

Zipfel, C., Kunze, G., Chinchilla, D., Caniard, A., Jones, J.D.G., Boller, T., Felix, G. (2006). Perception of the bacterial PAMP EF-Tu by the receptor EFR restricts *Agrobacterium*-mediated transformation. Cell, 125: 749-760.

Appendix

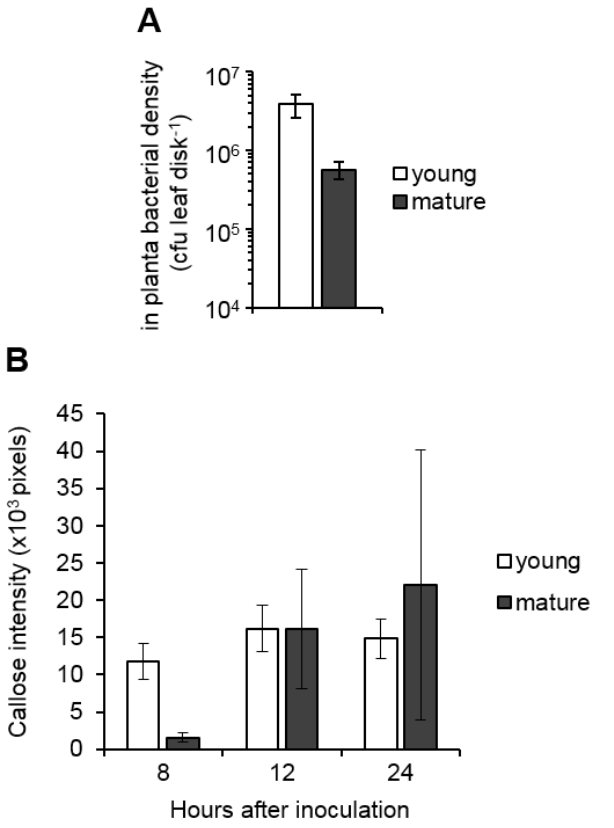

Figure A1 – Callose deposition in young and mature plants responding to *Pst.* Plants were inoculated with 10^6 cfu ml^{-1} *Pst* DC3000 at 3.5 or 6 weeks of age. A) Bacterial levels were quantified three days later. B) Leaves were stained for callose deposits at the indicated time points. This experiment was repeated by J. Doucet and M. Bragga with similar results.

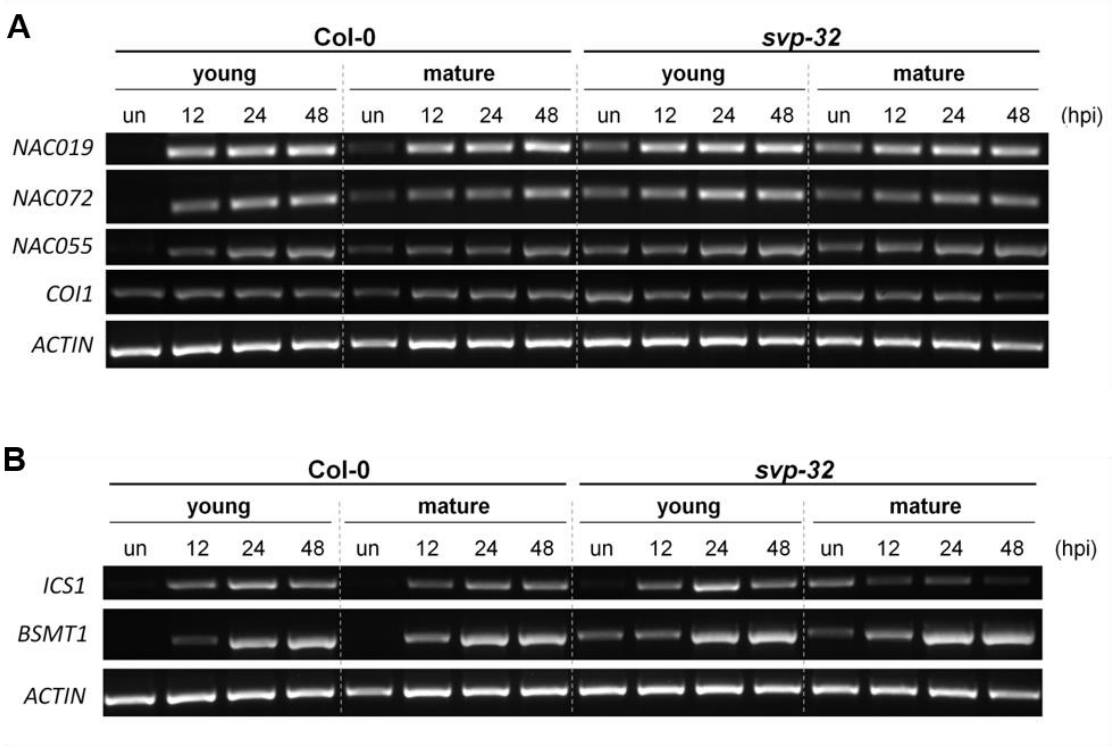

Figure A2 – Expression of genes involved in coranatine-mediated suppression of SA accumulation in young and mature Col-0 and *svp-32* mutants. Expression of *COI1, NAC072/055/019* (A), *ICS1,* and *BSMT1* (B) was measured via RT-PCR in leaf tissue collected from young and mature (3.5 and 6 weeks of age respectively) Col-0 and *svp-32* that were untreated (un) or inoculated with 10^6 cfu ml^{-1} *Pst* DC3000. Cycle numbers were: 28 (*NAC019*), 27 (*NAC072*), 29 (*NAC055*), 26 (*COI1*), 23 (ICS1), and 28 (*BSMT1* and *ACTIN*). This experiment was performed twice with similar results. The same samples were analysed in parts A and B but the figure was divided into two parts for clarity. Abbreviations: BSMT1, benzoic acid/salicylic acid carboxyl methyltransferase 1; COI1, coronatine-insensitive 1; ICS1, isochorismate synthase 1; NAC, NAM/ATAF1,2/CUC2.

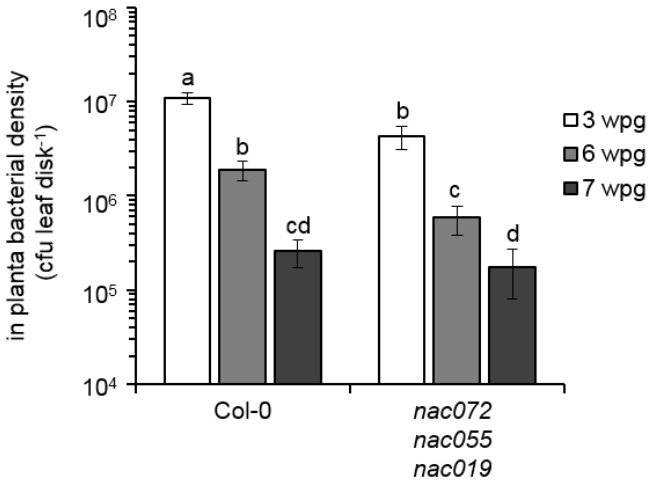

Figure A3 – Three functionally redundant *NAC* genes are not required for ARR. Plants were inoculated with 10^6 cfu ml^{-1} *Pst* DC3000 at 3, 6, or 7 weeks post-germination (wpg) and bacterial levels were quantified 3 days later. Each bar shows the mean of 3 sample replicates, and error bars show standard deviation. Different letters indicate significant differences (ANOVA followed by Tukey's HSD test, $P < 0.05$). This experiment was performed 3 times with similar results. The *nac* triple mutant was obtained from X. Dong (Zheng et al., 2012).

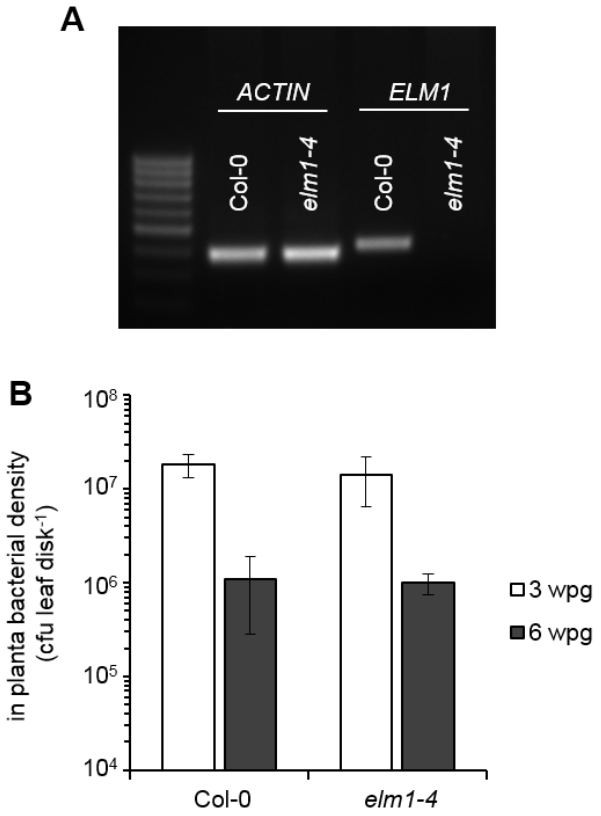

Figure A4 – The EDS5-like MATE transporter ELM1 is not required for ARR. A) Gene expression measured by RT-PCR in leaf tissue collected from Col-0 and *elm1-4.* Primers for *ELM1* were: 5'-TTCCCTCACTTTACGGTCATG (F), 5'-GAATGATAAACTGACCTGCCG (R); for *ACTIN* primer sequences see Wilson et al. 2013. The cycle number was 28 for both primer sets. B) Plants were inoculated with 10^6 cfu ml^{-1} *Pst* DC3000 at 3 or 6 weeks post-germination (wpg) and bacterial levels were quantified 3 days later. Each bar shows the mean of 3 sample replicates, and error bars show standard deviation. This experiment was performed twice with similar results. The *elm1-4* mutant was obtained from the ABRC (SAIL_341_E08/ CS815910).

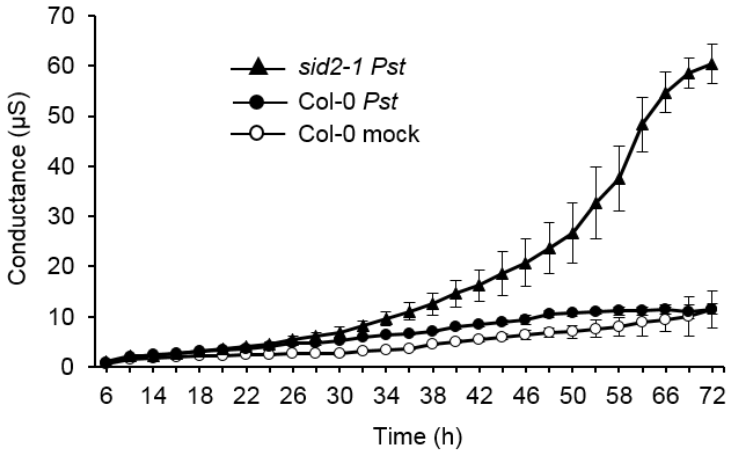

Figure A5 – Electrolyte leakage is reduced in ARR-competent plants. Electrolyte leakage (conductance in units of microseiemens) was measured in tissue collected from 6-week-old Col-0 or ARR-defective *sid2-1* as described in Carviel et al. (2014) for Figure 4A. Plants were inoculated with 10 mM $MgCl_2$ (mock) or 10^6 cfu ml^{-1} *Pst* DC3000. In this experiment Col-0 supported a 115-fold reduction in bacterial levels ($4.58x10^4$ cfu leaf $disk^{-1}$) relative to *sid2-1* ($5.25x10^6$ cfu/leaf $disk^{-1}$) at 3 days post-inoculation. This experiment was performed 3 times with similar results.